

***Structural and mechanistic studies on
deubiquitinating enzymes USP7 and USP40***

Robbert Q. Kim

ISBN: 978-94-6380-188-1

Publisher: het Nederlands Kanker Instituut - Antoni van Leeuwenhoekziekenhuis

Printing: ProefschriftMaken on 100% Recycled White Zero paper

Cover art: Dr. Hedwich C. Vlieg

Layout: Robbert Q. Kim

The research described in this thesis was supported by KWF (Koningin Wilhelmina Fonds).
This thesis was printed with financial support from Erasmus University Rotterdam and the
Netherlands Cancer Institute.

Copyright: © 2018 Robbert Q. Kim. All rights reserved.

***Studies naar de structuur en het mechanisme van
deubiquitinerende enzymen USP7 en USP40***

Structural and Mechanistic Studies on
Deubiquitinating Enzymes USP7 and USP40

Proefschrift

ter verkrijging van de graad van doctor aan de
Erasmus Universiteit Rotterdam
op gezag van de
rector magnificus

Prof.dr. R.C.M.E. Engels

en volgens besluit van het College voor Promoties.
De openbare verdediging zal plaatsvinden op

vrijdag **8 maart 2019** om **11:30** uur

door
Robbert Kim
geboren te Wageningen

Promotiecommissie:

Promotoren: Prof. dr. T.K. Sixma
Prof. dr. A. Perrakis

Overige leden: Prof. dr. C.P. Verrijzer
Dr.ir. J.H.G. Lebbink
Prof. dr. M. Vermeulen

Table of contents

<i>Chapter 0.</i> <i>General Introduction</i>
<i>Chapter 1.</i> <i>Regulation of USP7</i>
<i>Chapter 2.</i> <i>Structure of USP7 CD123</i>
<i>Chapter 3.</i> <i>USP7 activity mechanism</i>
<i>Chapter 4.</i> <i>USP40 activity</i>
<i>Chapter 5.</i> <i>General Discussion</i>
<i>Addenda.</i>

7	0
33	1
53	2
71	3
119	4
151	5
159	A

Chapter 0.
General Introduction

0

Chapter 0. General Introduction

Almost every process in the cell involves proteins, each serving their own particular function. This functionality can however be expanded by covalent attachments to their chain of amino acids: posttranslational modifications (PTMs). After transcription and folding the protein can be subjected to a wide variety of alterations, including the conjugation of hydroxyl-, methyl-, or phosphate groups with certain residues. The attachment of such a molecular identifier can have a very specific effect on the function of this protein, changing its cellular location and its ability to interact with other proteins amongst others¹.

Such PTMs not only broaden the functionality of proteins, it can also account for a layer of regulation. By controlling the target protein function, the modification can prevent the need for the target to be degraded and the need to synthesise a new protein with only a minor difference. Furthermore, the modification can alter the three-dimensional conformation of the target, mediate protein-protein interactions and change the intrinsic activity of the target. Through these functions, PTMs can activate and inhibit cell processes, allowing for quickly fine-tuning the delicate balance necessary at a certain stage in the cell's lifecycle^{2,3}.

Ubiquitin

One of these modifications is the conjugation of ubiquitin to the target protein (Fig. 1). Ubiquitin is a protein of 76 residues (Fig. 2a), identified in 1975 as "ubiquitous immunopoietic peptide"⁴. The peptide has been found in all eukaryotic cells with strong sequence conservation: between mammals, plants and yeast only three of the 76 amino acids change. After the discovery of ubiquitin as a PTM, a vast amount of research into the function has been published^{5,6}. Ubiquitination has since then been recognised to be critical for many cellular processes, ranging from DNA damage response to proteasomal degradation and from transcription to modulating protein activity^{6,7}. The findings resulted in a better understanding of how the cell controls biochemical processes such as the cell cycle. The importance of ubiquitin-driven proteolysis is underscored by the Nobel Prize in Chemistry awarded in 2004⁸.

Ubiquitination pathway

The conjugation of ubiquitin to a target protein (ubiquitination, or ubiquitylation) is the best studied part of the ubiquitin pathway (Fig. 1). Ubiquitin is attached to an amino group on the target with its C-terminus (Fig. 2b), and requires three successive enzyme activities for creating this covalent isopeptide bond (Fig. 1). The first step is executed by the ubiquitin-activating enzyme E1⁹. The enzyme activates the C-terminal glycine of ubiquitin, using ATP¹⁰. The adenylated ubiquitin then forms a thioester bond with a cysteine of the E1 enzyme, releasing AMP. In the second step the activated ubiquitin is transferred to a ubiquitin-conjugating enzyme, E2¹¹. In the third step the final transfer of ubiquitin from the active site cysteine to the amino group, most often the ϵ -amino group of a lysine, is carried out (Fig. 1). This transfer can occur directly from the E2 to the target, or through a covalent E3-ubiquitin intermediate¹². The latter case requires a ubiquitin ligase E3 with the HECT domain that takes over the active ubiquitin from the E2 and subsequently transfers it to the target protein¹³. Direct transfer, however, is catalysed by an E3 that contains a RING domain. This brings the E2 in close proximity to the target^{14,15} and catalyses the reaction^{16,17}. Some E3 classes display a mix of these two methods, as is seen for example in ubiquitin transfer mediated by Cullin-RING ligases^{18,19} or the RING-in-between RING family of E3s²⁰.

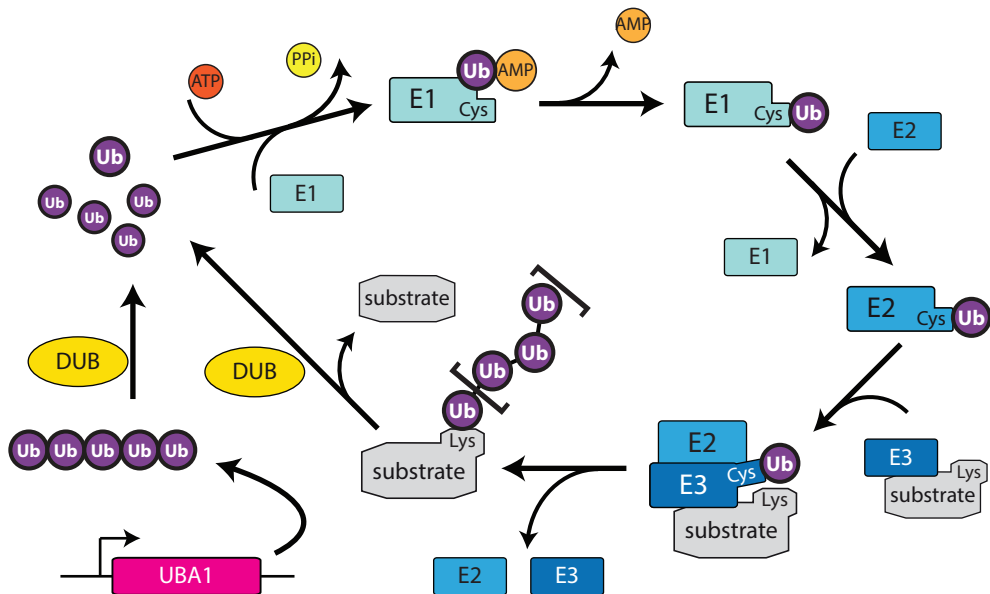


Figure 1. Ubiquitination pathway. Ubiquitination is carried out in an E1-E2-E3 enzyme cascade, requiring ATP in the process. DUBs can reverse this post-translational modification.

This last step, where the ubiquitin is attached to the target lysine, determines a change of fate for this target. Specificity can be achieved by the spatial arrangement of the target, E3 and E2, induced by their specific interactions²¹. This orients the ubiquitin and lysines within reach can all be ubiquitinated²². Whereas only two E1 enzymes have been found, the amount of E2s is in the dozens and so far about five hundred E3s are discovered²³. This large amount of ubiquitin ligases expands the targeted proteins greatly and makes sure various processes can be regulated specifically through the ubiquitination pathway^{24,25}.

Ubiquitin chains

The ubiquitination pathway is more versatile than just mono-ubiquitination, where ubiquitin is specifically attached to a target protein. Chains of ubiquitin, with various linkage types can be built onto the target-conjugated ubiquitin, as ubiquitin itself has multiple amino groups that can be ubiquitinated. There are seven lysines that can be modified and the N-terminus also has an amino group that can be targeted, resulting in linear ubiquitin chains (Fig. 2a). These eight ubiquitin attachment points allow for a variety of ubiquitin chains that can be formed (M1, K6, K11, K27, K29, K33, K48 and K63), and since mixed chains are possible²⁶⁻²⁸ a large variety of ubiquitin signals can be encoded onto a target protein^{29,30}. These individual modifications may assign a different fate to the protein targeted. Usage of chemically generated chains^{31,32} can help to identify their specific interactors³³ and investigate the effect of the linkage type. The effects of these different ubiquitin chains on proteins have been studied to various degrees³⁴. K48-linked ubiquitin chains have been found to be the most abundant type of chains and have been studied extensively³⁵. The K48 mark targets the substrate for proteasomal degradation, as the three-dimensional structure of these chains is recognised

Chapter 0. General Introduction

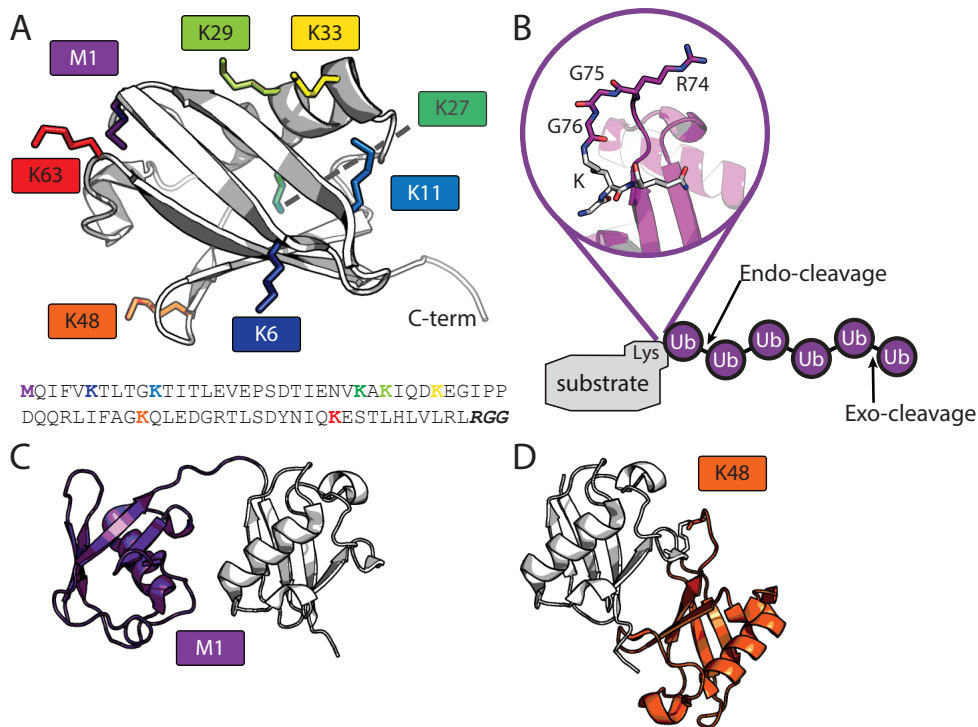


Figure 2. The ubiquitin structure in **A.** (from PDB: 1UBQ¹⁰⁹) shows the C-terminus that can get covalently linked to the target lysine (K) via an isopeptide bond. Figure **B.** depicts such an isopeptide bond, for clarity the C-terminal residues of Ub are marked as well. Ubiquitin itself has the N-terminus and 7 lysines available for ubiquitination (see colouring legend on the sequence at the bottom of **A.**) to generate ubiquitin chains. The different chain options can lead to different outcomes, based on the adopted three-dimensional architecture. In **C.** and **D.** the difference between a compacted chain (K63, PDB: 5GOK) and an extended one (K48, PDB: 3M3J) is visualised.

by the proteasome subunits Rpn10 and Rpn13^{36,37}. Other compacted ubiquitin chains (Fig. 2c), such as K11-linked ones³⁸, change the substrate's fate similarly^{39,40}, indicating that the downstream effect of these chains is dependent on the three-dimensional conformation^{41,42}. Ubiquitin chains that exhibit a more extended conformation (Fig. 2c) are recognised by different proteins, and therefore have a different effect³⁸. For instance linear chains (M1), that are recognised to act predominantly in the NF- κ B pathway⁴³. Or K63-linked chains which serve as a mark for signalling, is also important in this NF- κ B pathway⁴⁴, but is also important in the DNA damage response^{45,46}.

This variety of chains, with their specific outcomes, is further complicated by the existence of mixed chains^{26,47}. These chains can contain multiple ubiquitin molecules linked with different linkages, but can also be supplemented with other PTMs^{48,49} such as phosphorylation⁵⁰ or inclusion of ubiquitin-like modifiers⁵¹ like SUMO^{52,53}, FAT10⁵⁴ or ISG15⁵⁵.

Deubiquitination

Just like with other PTMs, proper regulation can only be performed if it is possible to remove the signal from the target protein. In the case of ubiquitination this is carried out by deubiquitinating enzymes (DUBs or deubiquitinases)^{56,57}. These enzymes hydrolyse the isopeptide bond between ubiquitin and the targeted protein (Fig. 1).

Some DUBs exhibit a strict target specificity^{56,58,59}, just like the E3 ligases. There are also more promiscuous DUBs and there are DUBs that recognise a specific ubiquitin chain type. These DUBs distinguish between the various linkages by observing the specifics of the (iso)peptide bond, such as distances and angles between two moieties in the chain (Fig. 2c) or the presence of an aiding residue on the substrate⁶⁰.

This specificity is narrowed down even more for deubiquitinases that only recognise and cleave off the last ubiquitin in a chain⁶¹. This cleaving of the distal ubiquitin, also known as exo-deubiquitination, depends greatly on the ubiquitin binding pocket and whether or not it can accommodate an extra ubiquitin linkage. Contrary to this mechanism is endo-deubiquitination which can only break the isopeptide bond within a ubiquitin chain, or to the substrate. This could allow for direct release of the whole ubiquitin chain.

Next to DUBs that only recognise poly-ubiquitin⁶², there are substrate-specific ones⁶³. These enzymes recognise the targeted protein with the ubiquitin attachment. The hydrolysis then often cleaves off an entire ubiquitin chain (if present), i.e. after the proximal ubiquitin^{28,64}. These latter enzymes need both the substrate and the attached ubiquitin moieties for recognition and subsequent hydrolysis to revert the substrate to a mono- or unubiquitinated one.

DUBs play a role similar to the phosphatases in pathways regulated by phosphorylation. They serve as a regulatory layer, making the ubiquitination pathway a reversible and more finely tuned process. However, the role of deubiquitinases is more than just antagonising the ubiquitination pathway, it is essential in the very first steps of ubiquitination as well. Ubiquitin is always expressed as an immature proprotein, a linear polyubiquitin that must be cleaved (Fig. 1) to yield the mature ubiquitin monomers. DUBs carry out this function and are therefore responsible for the pool of available ubiquitin⁶⁰. The deubiquitinases also supply to this pool by degrading ubiquitin chains, leaving the free ubiquitin monomers.

Furthermore, DUBs can rescue ubiquitin from aberrant covalent adducts. Along the ubiquitination pathway there are various points at which the thiol ester intermediates can get attacked by small nucleophiles. Some DUBs are able to recognise this aberration and rescue the trapped ubiquitin⁶⁵. With these described functions deubiquitination not only antagonises the ubiquitination pathway, it also maintains the available pool of ubiquitin monomers.

Ubiquitin and diseases: regulation of E3's and DUBs

Many cellular processes require spatial or temporal regulation, which can be achieved by posttranslational modification of the proteins involved. This also means that, if the fine regulatory balance of ubiquitination is disturbed, certain dependent pathways may be disturbed. Malfunction in the ubiquitin pathway itself could therefore lead to a plethora of dysregulated cellular pathways⁶⁶⁻⁶⁸. For instance, proteasomal degradation is heavily linked to ubiquitination and its dysregulation has been implied in various neurological disorders⁶⁹. As various pathways could lead to various diseases, ubiquitination can be involved in diseases linked to these processes.

Chapter 0. General Introduction

One way to keep these (de)ubiquitination enzymes in check is to regulate them. Deubiquitinating enzyme abundance can be tuned by increased transcription or degradation of the DUB, but interestingly ubiquitination of DUBs itself is not confirmed as a trigger for their proteasomal degradation⁷⁰. The post-translational modifications with ubiquitin, likewise to phosphorylation or SUMOylation, can have other effects on the DUB. It can change its localisation, allow for complex formation, or even adapt the intrinsic activity⁷¹. Other external factors that regulate DUB activity are binding partners that can help recruit a target or even the substrate itself. In **chapter 3** we investigate the effect of a ubiquitinated p53-substrate on the activity of USP7.

Some DUBs however also have intramolecular regulatory domains. Their three-dimensional build-up can be such that they possess a self-inhibiting or self-activating ability⁷². Such intrinsic self-regulation could allow for fine-tuning of the DUB activity, and have a potential for specific human intervention in the form of drugs^{73,74}. As the self-activation of DUBs is the main theme of this thesis we will discuss this in more detail.

Various families of DUBs

There are seven different classes of DUBs⁷², based on the ubiquitin protease domain (Fig. 3). Six of these classes are cysteine proteases, using the cysteine thiol group in the active site to mediate the hydrolysis of the ubiquitin bond⁷⁵, whilst the other class are metalloproteases. Below we discuss these separate classes and some of their hallmarks concisely. The main topic of this thesis, USP7, is a member of the Ubiquitin Specific Protease (USP) class, warranting a more extensive, separate description for the USP class.

The metalloprotease DUBs use Zn^{2+} in the interaction with the substrate^{56,59}, where a JAMM (JAB1/MPN/Mov34) domain (Fig. 3a) coordinates the Zn ion by an aspartic acid, histidine and serine residue⁷⁶. The zinc ion can activate a water molecule which subsequently performs a nucleophilic attack, breaking the peptide bond between the ubiquitin moiety and its target. So far about a dozen putative deubiquitinases of this family have been found, although not all zinc-coordinating amino acids are conserved between them. This could imply that some of them are inactive, awaiting experimental confirmation of their function⁷⁷.

The class of the Ubiquitin C-terminal Hydrolases (UCHs) (Fig. 3b) encompasses four members with an UCH domain containing the active site cysteine⁷⁸. In hydrolysis this cysteine is aided by an aspartic acid, a histidine and a glutamine⁷⁹. UCH enzymes seem unable to process diubiquitin conjugates⁸⁰ and are well-known for processing relatively small protein substrates⁸¹. This has long been attributed to its hallmark cross-over loop⁸², but since UCHs have been shown to cleave ubiquitin off of SUMO-(chains) the role of this loop is debated⁸¹.

The second smallest class are the Machado-Joseph Disease Protein Domain Proteases (MJDs) with five members. Although the domain fold differs from the other classes, the catalytic triad residues are still a cysteine, histidine and aspartate. The only protein of the family of which structural information is available⁸³, Ataxin-3 (Fig. 3c), is mutated in the Machado-Josephin disease, giving the class its name. The protein structure shows a misaligned catalytic triad, which transforms into an active conformation upon ubiquitin binding. An interesting feature found in this MJD structure is an α -helix that blocks access to the active site, but whether this is conserved throughout the class still needs experimental validation⁸⁴. It has been implied that this helix is stabilized in an open conformation when Ataxin-3 itself gets ubiquitinated, making the active site available⁸⁵.

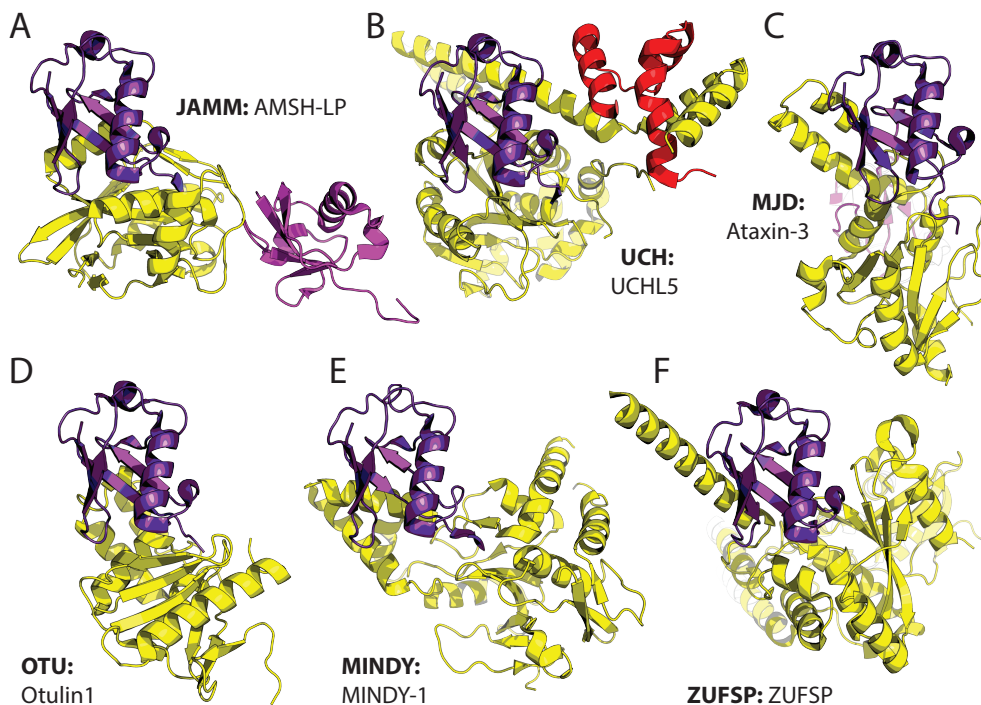


Figure 3. The structures of deubiquitinating enzyme types in complex with ubiquitin. The bound ubiquitin is coloured purple and kept in the same orientation, while the DUB is coloured yellow. Other ubiquitin molecules, members of a chain, are depicted in magenta and secondary, modulating proteins in red. For each class a representative is chosen: **A.** AMSH-LP in complex with a K63-linked diubiquitin (PDB: 2ZNV⁷¹), **B.** UCHL5 with an activating fragment of INO80G (4UF6⁸⁰), **C.** Ataxin-3 in complex with K48 diubiquitin (2JRI⁸³), **D.** Otulin-1 (3BY4⁸⁷), **E.** MINDY-1 (5JQS⁹²) and **F.** ZUFSP (6EI1⁹⁵)

For a third class of DUBs, Ovarian Tumour Proteases (OTUs), several structures (Fig. 3d) have been elucidated^{86–88}. These structures indicate that the active site residues are cysteine, histidine, aspartate or asparagine, and threonine. Further analysis of the OTU catalytic core indicates an unproductive conformation and remodelling of the site is necessary for actual isopeptidase activity, a feature that is shared with some other members of the cysteine-protease DUBs^{89,90}. Interestingly, some deubiquitinases already show a regulatory function independent of their protease activity. OTUB1, for instance, can inhibit the E2 UBC13 without performing a deubiquitination event⁹¹. This indicates non-canonical functions for deubiquitinating enzymes, adding to their functionality, even if the active site remains in an inactive configuration.

A relatively new class of cysteine protease DUBs is MINDY (motif interacting with ubiquitin (MIU) containing novel DUB family)⁹². This class (Fig. 3e) currently contains four members that share a MINDY domain with the active site cysteine helped by a histidine and a glutamate in catalysis. Again, for this DUB the triad is in an inactive conformation that rearranges upon binding of ubiquitin⁹². Inquiries into biological roles for MINDY DUBs are still ongoing, but these DUBs seem to be specific for K48 ubiquitin chains⁹³.

Chapter 0. General Introduction

The newest class of ZUFSP DUBs (Fig. 3f) was identified with activity-based profiling using a K63-specific probe^{94–97}. This class, with currently one confirmed member, share their fold with Ufm1 and Atg8 proteases⁹⁸ having an active site cysteine that is aided in catalysis by a histidine and aspartate. ZUFSP binds RPA and is involved in genomic stability, with its specificity for K63-linked ubiquitin chains induced by the ubiquitin-binding domain MIU.

Ubiquitin Specific Proteases (USPs)

The focus of this thesis is on USP7 and USP40, two members of the Ubiquitin Specific Protease (USP) family. This is the largest class of DUBs with currently over 60 identified members. This family is the best studied one, although many functions and substrates remain unknown. Nevertheless, both knowledge about USP structures as well as their functionality increases. The USP family is characterized by the papain-like USP domain (Fig. 4), which is responsible for binding the distal ubiquitin and subsequent hydrolysis of the isopeptide bond. The domain has a papain-like fold⁹⁰ and is structurally very well conserved, although inserts⁹⁹ can be present within the USP domain. Globally, the USP domain consists of a fingers region, a palm and a thumb region (Fig. 4a). The ubiquitin that gets hydrolysed can bind between the fingers and the thumb where a lot of acidic residues can accommodate the positively charged ubiquitin⁹⁰. Its C-terminal tail with which it is attached to a substrate, will then be positioned between the palm and thumb regions, close to the catalytic residues (Fig. 4c).

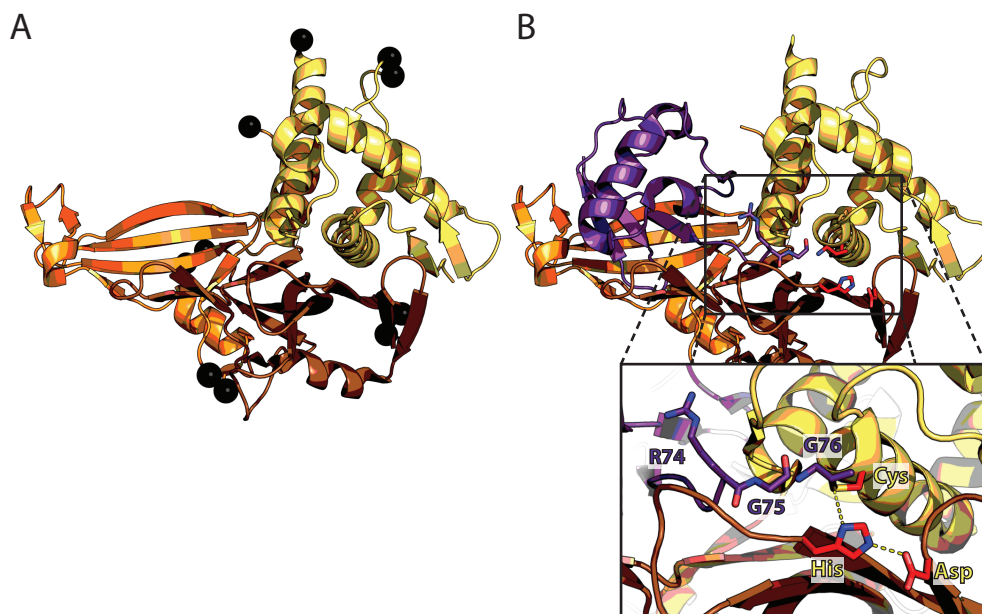


Figure 4. Structure of the USP domain of USP12 (PDB: 5L8W¹⁷²) reveals three separate subdomains: the Fingers region (orange), the Palm (brown) and the Thumb (yellow) in **A**. Furthermore, the five common insertions points, where the USP domain can have small loops or even domains inserted⁹⁹, are marked in black spheres. In **B**, the ubiquitin-bound structure is depicted, using the same colouring scheme with ubiquitin in purple, supplemented with a zoom of the active site (residues in red) where the catalytic cysteine is bound to the C-terminus of Ub.

The catalytic residues are cysteine, histidine and aspartate, although for some USPs asparagine substitutes the latter^{99,100}. The catalytic cysteine needs to be deprotonated in the catalysis¹⁰¹, which is carried out by the histidine that can act as a general base when it is coordinated by the aspartic acid (Fig. 5). Now the cysteine can perform a nucleophilic attack on the isopeptide bond that link the ubiquitin molecule to the substrate, forming a tetrahedral intermediate^{59,101}. This 'oxyanion' state will then collapse, resulting in the release of the substrate (Fig. 5) and a ubiquitin-bound protease. For the DUB to return to its basal state a second nucleophilic attack, this time performed by a water molecule, is necessary. This will generate a second oxyanion state that will collapse similarly, resulting in the release of the ubiquitin molecule and a regenerated enzyme⁵⁹ (Fig. 5).

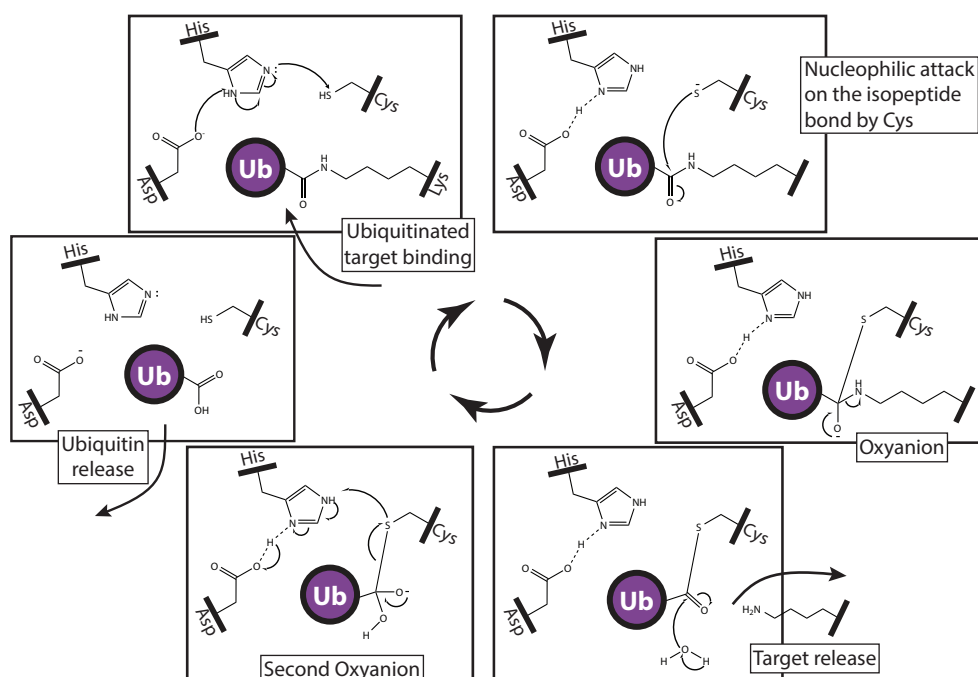


Figure 5. Reaction mechanism of cysteine DUBs, like USPs, shows how the active site residues need to be in close proximity to allow for an active state and start the hydrolysis cycle resulting in deubiquitination of the target lysine.

Structural analyses of various USP domains however have shown that these catalytic residues are, for some USPs, not in a catalytically competent configuration⁹⁰. Furthermore, biochemical assays indicate that most USP catalytic domains are able to digest any type of ubiquitin-chain linkage¹⁰², a feature that is not always valid in full-length and/or *in vivo* studies⁶². These apparent discrepancies indicate that the catalytic domain requires a secondary domain or protein interaction for full, physiological activity. As both the potential regulation and specificity of a deubiquitinating enzyme can provide insight into its biological function, research into the activation has gathered interest^{103,104}. On top of that, structural

Chapter 0. General Introduction

and mechanical insight on enzymes can allow for the development of more potent and more specific inhibitors leading to potential clinical drug development^{105–107}.

In this thesis we focus specifically on the activity mechanism of a subclass of USPs, containing both USP7 and USP40, and how this deubiquitinating activity can be modulated. USP7 has been described to have seven different domains. N-terminally of the catalytic domain, it has a TRAF domain (Fig. 6) that mediates many of its target interactions. On the C-terminus USP7 has five Ubiquitin-like (Ubl) domains that are important for full activity and can also serve as an interaction hotspot¹⁰⁸. These Ubl domains resemble the ubiquitin fold¹⁰⁹, having the β -grasp structure, but have very little sequence homology (<12% identity)¹¹⁰. They could be artefacts from the development of the pathway throughout evolution, or serve a direct role: the ubiquitin resemblance could be a way to inhibit the enzymes, or even enhance them^{102,111}. In this thesis we look specifically at the effect of the ancillary domains on the activity of USP7.

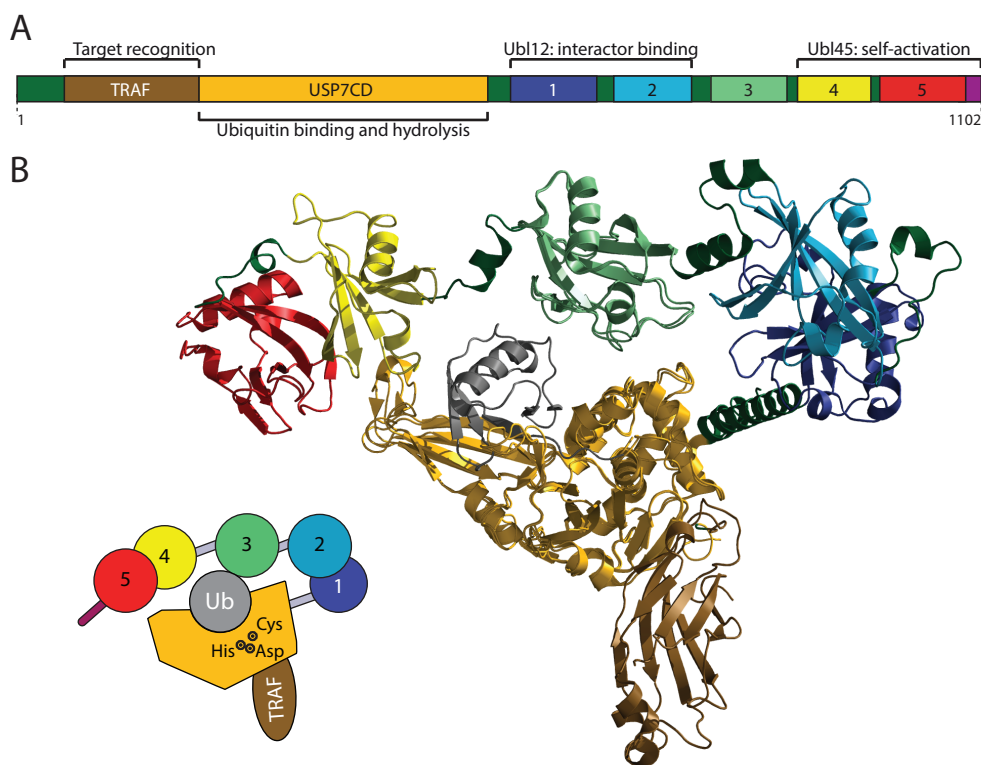


Figure 6. USP7 consists of seven different domains with each a different physiological function. In **A**, the protein is schematically depicted with the TRAF domain, Catalytic domain (CD) and the five Ubl domains marked (numbers). The very C-terminal tail (purple) is not a separate domain, but plays a major role in the self-activation. The colouring scheme of the domains is carried over in panel **B**, which depicts the structural model of full-length USP7. This model is built from various crystal structures (PDB: 1NBF, 2YLM and 5FWI), with bound ubiquitin in grey^{90,108,173}.

USP7 in disease

The main subject of this thesis is the enzyme USP7 (Fig. 6), and specifically its mode of action. The enzyme has originally been identified as ‘herpes virus associated ubiquitin specific protease’ (HAUSP) for its interaction with the herpes protein ICP0^{112,113}, but its multiple physiological roles and links to various diseases earned USP7 its medical attention.

USP7 is implicated in various cancers^{114–116}, and is frequently mutated in specific childhood leukaemias^{117,118}. In other cancers¹¹⁹ it is found to be rarely mutated, but rather up- or downregulated^{120,121}. This suggests that USP7 is essential for cell survival, as is further illustrated by the embryonic lethality of a full gene-loss¹²². Also, having only a single (working) allele can already have dramatic consequences for neurodevelopment¹²³. Haploinsufficiency causes a disease that stems from a dysfunctional interaction of USP7 with MAGE-L2 and TRIM27 in the cytosol, where only a small fraction of USP7 is found^{124,125}. Most USP7 is found in the nucleus¹²⁶, where it interacts with many proteins¹²⁷. It stabilises both the ‘guardian of the genome’ p53¹²⁸, as well as its E3 ligase MDM2, dictating the balance through its deubiquitinating activity^{122,129–131}. Furthermore, USP7 has also been described to bind DNMT1 and UHRF^{132,133} and PCNA and Rad18^{134,135}, illustrating a USP7 link to DNA maintenance and DNA damage repair as well. Through these various interactions, USP7 is involved in multiple pathways, ranging from transcription regulation and DNA replication^{136,137} to apoptosis¹³⁸. The plethora of USP7 functions makes the protein an important player and good material to further the understanding of the human cell¹³⁹.

At the same time, the broad spectrum of interacting proteins makes it difficult to define the full function of USP7. Causality relations are not always obvious, e.g. USP7 both stabilises p53 as well as mediating its ubiquitination through MDM2^{63,140}. The complexity of USP7 as a node in various pathways still remains elusive, although its individual interactions are becoming increasingly better mapped. In **chapter 1** we describe the biochemically validated interactions of USP7, through which domains these take place (Fig. 6a) and what role these may have in the cell¹⁴¹.

USP7 regulation: external factors

A high number of the described interactions are direct E3-USP7 complexes. In such a complex, the DUB can protect the associated E3 from auto-ubiquitination and subsequent proteasomal degradation^{142,143}. Such direct regulation has been found for USP9X which prevents the E3 Itch from becoming ubiquitinated¹⁴⁴. The direct interaction with E3s can also serve a second role. By associating with the E3 ligase, the DUB is able to directly deubiquitinate and stabilise the protein targeted by the E3. By forming such an ‘on/off’ switch, the targeted protein can be tightly regulated¹⁴⁵. In the review on regulation of the DUB USP7 in **chapter 1**¹⁴¹, we will discuss such interactions of USP7, sketching the importance and possible outcomes of USP7-E3 complexes¹²⁴.

Both E3 and other interactors often recruit USP7 for its main feature; the deubiquitinating activity. The recruitment of a DUB can protect the target from proteasomal degradation, but the DUB activity of USP proteins can also be influenced by secondary factors. The factors could be external factors, like these interacting proteins, or intramolecular factors, such as internal domains¹⁴⁶. By association with a USP these interactors can change the DUBs localisation, thereby influencing where it can perform its deubiquitinating activity, like in the case for USP14¹⁴⁷.

Chapter 0. General Introduction

Such interactors can also be substrates, as they possess affinity for their deubiquitinating enzyme. But substrates can do more than just recruiting; they may even aid in the ubiquitin hydrolysis as they can induce a catalytically competent conformation in the DUB^{90,148}, through so-called induced fit^{149,150}. Similarly, other external factors like PTMs or secondary binders (like e.g. in Fig. 3b) could influence the DUB activity. In **chapter 1**, we review interactors of USP7 and their potential effect on USP7 activity, while the activation mechanism of USP7 will be discussed in **chapters 2 and 3**.

Internal factors in USP7 activation

The main properties of a USP enzyme that can be affected by its internal domains are the intrinsic DUB activity and the recruitment of the target protein and binding of ubiquitin. For the selection of the right substrate, like a poly-ubiquitin chain, the USP can have a Ubiquitin-binding domain (UBD)¹⁵¹ or a loop insertion to distinguish specific chains¹⁵². For the recruitment of particular substrates the USP protein can have a separate domain with affinity for a specific target, like the DUSP-Ubl domain (Domain in USP - Ubiquitin-like domain) of USP15¹⁵³, which increases the chance to find this target. Both can increase the DUB activity on this particular substrate, also by aiding in substrate-induced rearrangement⁶⁰ of the catalytic core. For USP7 this function is carried out by the N-terminal TRAF domain (Fig. 6) as it recognises substrates p53¹⁴⁰, MDM2⁶³ and viral proteins^{154,155}. In **chapter 3** we show how the recognition of a ubiquitinated substrate by the TRAF domain affects the deubiquitinating activity of USP7.

The other ancillary domains of USP7 are located downstream of the catalytic domain (Fig. 6a) and can also affect the activity on a substrate¹⁵⁶. A crystal structure of USP7-CD123 (Fig. 6a) provided essential information to generate a full-length structural model of the protein (Fig. 6b (**Chapter 2**)) and also showed how the catalytic domain connects to the downstream Ubl domains and how the connection influences the activity. The final three-dimensional structure illustrates the possibilities of USP7 self-activation, in terms of steric hindrance, but also where the three Ubl domains fit in. These domains are an anchoring point for various interactors, for instance the allosteric activator GMPS (Guanosine monophosphate Synthetase) that can hyperactivate USP7¹⁰⁸.

The last two Ubl domains and the very C-terminal tail are essential for full activity of USP7 and both perform an important, but different function in the self-activation (**chapter 3**). Our findings, based on biophysical methods, NMR (Nuclear Magnetic Resonance) spectroscopy and molecular modelling, show that these domains fulfil a distinct part and collaborate to ensure effective hydrolysis of USP7 targets. Furthermore, we investigate the effects of the TRAF domain on USP7 activity using a realistic substrate. Our findings show that the ubiquitinated substrate can play a major role in the activity of the enzyme.

C-terminal Ubl domains in other USPs

USP7 is not the only protein containing integrated Ubl domains. Within the USP class of DUBs, various members harbour Ubl domains^{110,157} (Fig. 7). Our studies on USP7 indicated an interesting role for the Ubl domains located C-terminally of the catalytic domain, but thus far it is not known whether this is protein-specific. To investigate whether activity-regulation by C-terminal Ubl domains represents a general mechanism we look at one other member of this particular USP subgroup, USP40 (Fig. 7).

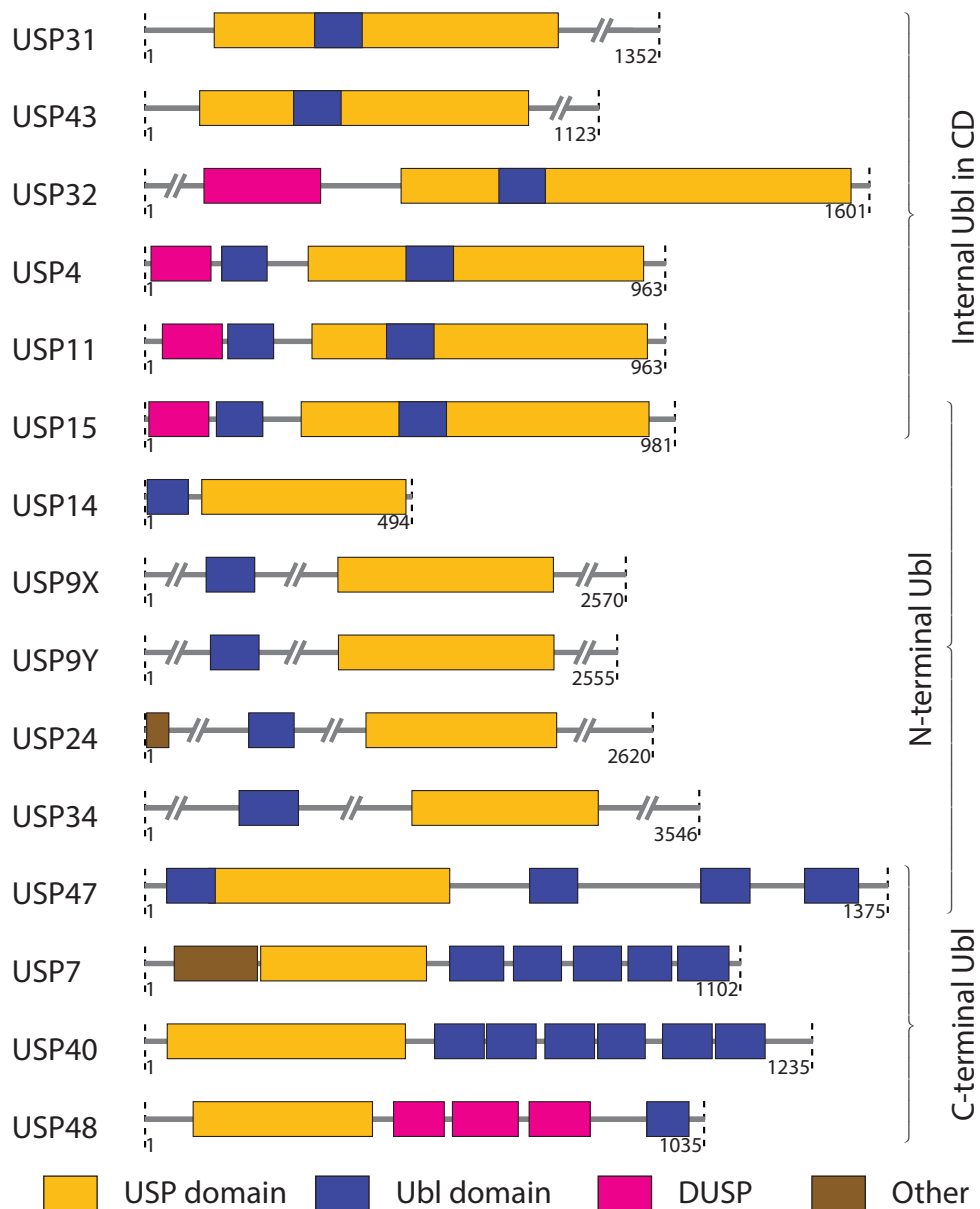


Figure 7. Ubl domains occur often in USPs. USP proteins (USP CD in yellow) that contain one or more Ubiquitin-like domains (Ubl domain in blue) can be grouped by the position of the Ubl in relation to the CD. The Ubl domains annotated here have been predicted¹¹⁰ and in few cases structurally confirmed. The other domains (in brown) such as the domain in USPs (DUSP; magenta) are depicted for completeness' sake and taken from UniProt annotation¹⁷⁴.

Chapter 0. General Introduction

Using sequence analysis with Phyre¹⁵⁸, four members could be identified that contain a Ubl domain located C-terminally of their catalytic domain: USP7, USP40, USP47 and USP48¹¹⁰. Apart from USP7 very little is known on the activation mechanisms of these proteins. Production of USP47 for *in vitro* assays has been described¹⁵⁹, but no in-depth studies have been undertaken. The fact that USP47 cross-reacts with inhibitors developed for USP7¹⁶⁰ could be a hint at a similar activity mechanism. USP48 is not closely related to USP7, although it seems to share the protective function of the E3 MDM2¹⁶¹ and it has a Ubl domain at its C-terminus¹⁶². Our lab described an H2A-specific role for this DUB¹⁶³, showing that deletion resulted in a decreased intrinsic activity of USP48.

For USP40 little is known about its activity or biological role. Next to USP40 binding to nestin¹⁶⁴ and a Single Nucleotide Polymorphism (SNP) possibly relating it to Parkinson's disease¹⁶⁵, a mass spectrometry (MS) screen has found the protein to interact specifically with K27-linked ubiquitin chains³⁵. In **chapter 4** we show that USP40 is a *bona fide* DUB and that its C-terminal Ubl domains have an activating role in the deubiquitinating activity. Next to biochemical characterisation of the enzyme, we investigate USP40 ubiquitin-linkage preference and present initial steps towards a mechanical and structural model of USP40.

Investigation of mechanisms of action

In this thesis we utilise structural biology, biochemistry and biophysics^{166,167} to gain insights into the mechanisms of the USP7 class of deubiquitinating enzymes. These efforts towards detailed understanding on the mode of action of USP7 and USP40 can aid to better comprehend their biological function and can provide essential insight into the development of specific inhibitors¹⁶⁸⁻¹⁷⁰.

In **chapter 1** we describe an overview of the structure of USP7 as well as a basic mechanism of action. Furthermore, we discuss the identified and verified interactors of this DUB and speculate on how their interaction affects USP7 activity.

Chapter 2 describes our structural studies on the CD123 construct (Fig. 6) of USP7. We show that a long, uncommon helix connects CD to the Ubl domains and that it has a function in the intrinsic activity, possibly by arranging the Ubl domains spatially.

In **chapter 3** we go deeper into the activation mechanism of USP7. We show that USP7 works *in cis* and has an induced fit mode of action with a major role for the Ubl45 domain. Furthermore, we extend our study from a minimal substrate to a more realistic one and show that the target recognition plays a major role in the deubiquitination cycle.

Chapter 4 then describes our biochemical analysis of USP40, a close paralogue of USP7. We show that it has a similar activation mechanism and has preferred binding to certain diubiquitin chains. Our studies also annotated six new Ubl domains and allow for the speculation of a new subgroup in the USP class of enzymes.

In **chapter 5** we will discuss the findings presented in this thesis and their implications for the future.

List of abbreviations

ADP	Adenosine diphosphate
AI	Auto-induction
AMP	Adenosine monophosphate
Asp	Aspartic acid, Aspartate
ATP	Adenosine triphosphate
Cys	Cysteine
DTT	Dithiothreitol
DUB	Deubiquitinating enzyme
EDTA	Ethylenediaminetetraacetic acid
FAT10	HLA-F-adjacent transcript 10
GMPS	Guanosine monophosphate Synthetase
GST	Glutathione S-transferase
HECT	Homologous to the E6-AP Carboxyl Terminus
His	Histidine
IEX	Ion exchange chromatography
ISG15	Interferon-stimulated gene 15
JAMM	Jab1/Mov34/Mpr1 protease
kDa	Kilodalton
MALLS	Multi-angle laser light scattering
MINDY	Motif interacting with ubiquitin domain
MIU	Motif interacting with ubiquitin
MJD	Machado-Josephin domain protease
MS	Mass Spectrometry
MX	Macromolecular X-ray crystallography
NMR	Nuclear Magnetic Resonance
o/n	overnight
OTU	Ovarian tumour protease
PDB	Protein Data Bank
PTM	Post-translational modification
RING	Really Interesting New Gene
SAXS	Small-angle X-ray scattering
SDS-PAGE	Sodium dodecyl sulphate polyacrylamide gel electrophoresis
SEC	Size-exclusion chromatography
SNP	Single Nucleotide Polymorphism
SUMO	Small Ubiquitin-like Modifier
TB	Terrific Broth
TCEP	tris(2-carboxyethyl)phosphine
TRAF	TNF receptor-associated factor
Ub	Ubiquitin
UBD	Ubiquitin-binding domain
Ubl	Ubiquitin-like
UCH	Ubiquitin C-terminal hydrolase
USP	Ubiquitin Specific Protease

Chapter 0. General Introduction

References

- [1] Csizmok, V. and Forman-Kay, J.D. Complex regulatory mechanisms mediated by the interplay of multiple post-translational modifications. *Current Opinion in Structural Biology* Elsevier Current Trends. **48** 2018, 58–67.
- [2] Deribe, Y.L., Pawson, T. and Dikic, I. Post-translational modifications in signal integration. *Nature Structural & Molecular Biology* **17** 2010, 666–72. <https://doi.org/10.1038/nsmb.1842>
- [3] Mann, M. and Jensen, O.N. Proteomic analysis of post-translational modifications. *Nature Biotechnology* **21** 2003, 255–61. <https://doi.org/10.1038/nbt0303-255>
- [4] Hershko, A. and Ciechanover, A. The ubiquitin system. *Annual Review of Biochemistry* **67** 1998, 425–79. <https://doi.org/10.1146/annurev.biochem.67.1.425>
- [5] Yau, R. and Rape, M. The increasing complexity of the ubiquitin code. *Nature Cell Biology* **18** 2016, 579–86. <https://doi.org/10.1038/ncb3358>
- [6] Komander, D. and Rape, M. The ubiquitin code. *Annual Review of Biochemistry* **81** 2012, 203–29. <https://doi.org/10.1146/annurev-biochem-060310-170328>
- [7] Kravtsova-Ivantsiv, Y. and Ciechanover, A. Non-canonical ubiquitin-based signals for proteasomal degradation. *Journal of Cell Science* **125** 2012, 539–48. <https://doi.org/10.1242/jcs.093567>
- [8] “The Nobel Prize in Chemistry 2004” [Internet]. Nobelprize.org.
- [9] Schulman, B.A. and Wade Harper, J. Ubiquitin-like protein activation by E1 enzymes: the apex for downstream signalling pathways. *Nature Reviews Molecular Cell Biology* **10** 2009, 319–31. <https://doi.org/10.1038/nrm2673>
- [10] Hershko, A., Ciechanover, A. and Rose, I.A. Resolution of the ATP-dependent proteolytic system from reticulocytes: a component that interacts with ATP. *Proceedings of the National Academy of Sciences of the United States of America* **76** 1979, 3107–10.
- [11] Ye, Y. and Rape, M. Building ubiquitin chains: E2 enzymes at work. *Nature Reviews Molecular Cell Biology* Nature Publishing Group. **10** 2009, 755–64. <https://doi.org/10.1038/nrm2780>
- [12] Buetow, L. and Huang, D.T. Structural insights into the catalysis and regulation of E3 ubiquitin ligases. *Nature Reviews Molecular Cell Biology* **17** 2016, 626–42. <https://doi.org/10.1038/nrm.2016.91>
- [13] Rotin, D. and Kumar, S. Physiological functions of the HECT family of ubiquitin ligases. *Nature Reviews Molecular Cell Biology* **10** 2009, 398–409. <https://doi.org/10.1038/nrm2690>
- [14] Deshaies, R.J. and Joazeiro, C.A.P. RING Domain E3 Ubiquitin Ligases. *Annual Review of Biochemistry* **78** 2009, 399–434. <https://doi.org/10.1146/annurev.biochem.78.101807.093809>
- [15] Budhidarmo, R., Nakatani, Y. and Day, C.L. RINGS hold the key to ubiquitin transfer. *Trends in Biochemical Sciences* **37** 2012, 58–65. <https://doi.org/10.1016/j.tibs.2011.11.001>
- [16] Dou, H., Buetow, L., Sibbet, G.J., Cameron, K. and Huang, D.T. Essentiality of a non-RING element in priming donor ubiquitin for catalysis by a monomeric E3. *Nature Structural & Molecular Biology* **20** 2013, 982–6. <https://doi.org/10.1038/nsmb.2621>
- [17] Metzger, M.B., Pruneda, J.N., Klevit, R.E. and Weissman, A.M. RING-type E3 ligases: Master manipulators of E2 ubiquitin-conjugating enzymes and ubiquitination. *Biochimica et Biophysica Acta (BBA) - Molecular Cell Research* **1843** 2014, 47–60. <https://doi.org/10.1016/j.bbamcr.2013.05.026>
- [18] Petroski, M.D. and Deshaies, R.J. Function and regulation of cullin–RING ubiquitin ligases. *Nature Reviews Molecular Cell Biology* **6** 2005, 9–20. <https://doi.org/10.1038/nrm1547>
- [19] Zheng, N., Schulman, B.A., Song, L., Miller, J.J., Jeffrey, P.D., Wang, P., Chu, C., Koepp, D.M., Elledge, S.J., Pagano, M., Conaway, R.C., Conaway, J.W., Harper, J.W. and Pavletich, N.P. Structure of the Cul1-Rbx1-Skp1-F boxSkp2 SCF ubiquitin ligase complex. *Nature* **416** 2002, 703–9. <https://doi.org/10.1038/416703a>
- [20] Wenzel, D.M., Lissounov, A., Brzovic, P.S. and Klevit, R.E. UBC7 reactivity profile reveals parkin and HHAR1 to be RING/HECT hybrids. *Nature* **474** 2011, 105–8. <https://doi.org/10.1038/nature09966>
- [21] Zheng, N. and Shabek, N. Ubiquitin Ligases: Structure, Function, and Regulation. *Annual Review of Biochemistry* **86** 2017, 129–57. <https://doi.org/10.1146/annurev-biochem-060815-014922>
- [22] Fischer, E.S., Scrima, A., Böhm, K., Matsumoto, S., Lingaraju, G.M., Faty, M., Yasuda, T., Cavadini, S., Wakasugi, M., Hanaoka, F., Iwai, S., Gut, H., Sugawara, K. and Thomä, N.H. The Molecular Basis of CRL4DDB2/CSA Ubiquitin Ligase Architecture, Targeting, and Activation. *Cell* **147** 2011, 1024–39. <https://doi.org/10.1016/j.cell.2011.10.035>
- [23] Clague, M.J., Heride, C. and Urbé, S. The demographics of the ubiquitin system. *Trends in Cell Biology* **25** 2015, 417–26. <https://doi.org/10.1016/j.tcb.2015.03.002>

- [24] Wright, J.D., Mace, P.D. and Day, C.L. Noncovalent Ubiquitin Interactions Regulate the Catalytic Activity of Ubiquitin Writers. *Trends in Biochemical Sciences* **41** 2016, 924–37. <https://doi.org/10.1016/j.tibs.2016.08.003>
- [25] Berndsen, C.E. and Wolberger, C. New insights into ubiquitin E3 ligase mechanism. *Nature Structural & Molecular Biology* **21** 2014, 301–7. <https://doi.org/10.1038/nsmb.2780>
- [26] Meyer, H.-J. and Rape, M. Enhanced Protein Degradation by Branched Ubiquitin Chains. *Cell* **157** 2014, 910–21. <https://doi.org/10.1016/j.cell.2014.03.037>
- [27] Emmerich, C.H., Ordureau, A., Strickson, S., Arthur, J.S.C., Pedrioli, P.G.A., Komander, D. and Cohen, P. Activation of the canonical IKK complex by K63/M1-linked hybrid ubiquitin chains. *Proceedings of the National Academy of Sciences of the United States of America* **110** 2013, 15247–52. <https://doi.org/10.1073/pnas.1314715110>
- [28] Hospenthal, M.K., Freund, S.M. V and Komander, D. Assembly, analysis and architecture of atypical ubiquitin chains. *Nature Structural & Molecular Biology* **20** 2013, 555–65. <https://doi.org/10.1038/nsmb.2547>
- [29] Husnjak, K. and Dikic, I. Ubiquitin-binding proteins: decoders of ubiquitin-mediated cellular functions. *Annual Review of Biochemistry* **81** 2012, 291–322. <https://doi.org/10.1146/annurev-biochem-051810-094654>
- [30] Xu, P., Duong, D.M., Seyfried, N.T., Cheng, D., Xie, Y., Robert, J., Rush, J., Hochstrasser, M., Finley, D. and Peng, J. Quantitative proteomics reveals the function of unconventional ubiquitin chains in proteasomal degradation. *Cell Elsevier Ltd.* **137** 2009, 133–45. <https://doi.org/10.1016/j.cell.2009.01.041>
- [31] El Oualid, F., Merckx, R., Ekkebus, R., Hameed, D.S., Smit, J.J., de Jong, A., Hilkmann, H., Sixma, T.K. and Ovaa, H. Chemical synthesis of ubiquitin, ubiquitin-based probes, and diubiquitin. *Angewandte Chemie (International Ed in English)* **49** 2010, 10149–53. <https://doi.org/10.1002/anie.201005995>
- [32] Oualid, F. El, Hameed, D.S., Atmioui, D. El, Hilkmann, H. and Ovaa, H. Synthesis of Atypical Diubiquitin Chains. *Methods in Molecular Biology (Clifton, NJ)* p. 597–609. https://doi.org/10.1007/978-1-61779-474-2_42
- [33] Zhao, X., Lutz, J., Höllmüller, E., Scheffner, M., Marx, A. and Stengel, F. Identification of Proteins Interacting with Ubiquitin Chains. *Angewandte Chemie - International Edition* **56** 2017, 15764–8. <https://doi.org/10.1002/anie.201705898>
- [34] Akutsu, M., Dikic, I. and Bremm, A. Ubiquitin chain diversity at a glance. *Journal of Cell Science* **129** 2016, 875–80. <https://doi.org/10.1242/jcs.183954>
- [35] Zhang, X., Smits, A.H., van Tilburg, G.B.A., Jansen, P.W.T.C., Makowski, M.M., Ovaa, H. and Vermeulen, M. An Interaction Landscape of Ubiquitin Signaling. *Molecular Cell* **65** 2017, 941–955.e8. <https://doi.org/10.1016/j.molcel.2017.01.004>
- [36] Schreiner, P., Chen, X., Husnjak, K., Randles, L., Zhang, N., Elsasser, S., Finley, D., Dikic, I., Walters, K.J. and Groll, M. Ubiquitin docking at the proteasome through a novel pleckstrin-homology domain interaction. *Nature* **453** 2008, 548–52. <https://doi.org/10.1038/nature06924>
- [37] Zhang, N., Wang, Q., Ehlinger, A., Randles, L., Lary, J.W., Kang, Y., Haririnia, A., Storaska, A.J., Cole, J.L., Fushman, D. and Walters, K.J. Structure of the S5a:K48-Linked Diubiquitin Complex and Its Interactions with Rpn13. *Molecular Cell* **35** 2009, 280–90. <https://doi.org/10.1016/j.molcel.2009.06.010>
- [38] Ziv, I., Matiuhiu, Y., Kirkpatrick, D.S., Erpapazoglou, Z., Leon, S., Pantazopoulou, M., Kim, W., Gygi, S.P., Haguenauer-Tsapis, R., Reis, N., Glickman, M.H. and Kleifeld, O. A Perturbed Ubiquitin Landscape Distinguishes Between Ubiquitin in Trafficking and in Proteolysis. *Molecular & Cellular Proteomics* **10** 2011, M111.009753. <https://doi.org/10.1074/mcp.M111.009753>
- [39] Matsumoto, M.L., Wickliffe, K.E., Dong, K.C., Yu, C., Bosanac, I., Bustos, D., Phu, L., Kirkpatrick, D.S., Hymowitz, S.G., Rape, M., Kelley, R.F. and Dixit, V.M. K11-linked polyubiquitination in cell cycle control revealed by a K11 linkage-specific antibody. *Molecular Cell* **39** 2010, 477–84. <https://doi.org/10.1016/j.molcel.2010.07.001>
- [40] Bremm, A., Freund, S.M. V and Komander, D. Lys11-linked ubiquitin chains adopt compact conformations and are preferentially hydrolyzed by the deubiquitinase Cezanne. *Nature Structural & Molecular Biology* **17** 2010, 939–47. <https://doi.org/10.1038/nsmb.1873>
- [41] Ronau, J.A., Beckmann, J.F. and Hochstrasser, M. Substrate specificity of the ubiquitin and Ubl proteases. *Cell Research* **26** 2016, 441–56. <https://doi.org/10.1038/cr.2016.38>
- [42] Varadan, R., Walker, O., Pickart, C. and Fushman, D. Structural properties of polyubiquitin chains in solution. *Journal of Molecular Biology* **324** 2002, 637–47.

Chapter 0. General Introduction

- [43] Iwai, K. Diverse ubiquitin signaling in NF- κ B activation. *Trends in Cell Biology* **22** 2012, 355–64. <https://doi.org/10.1016/j.tcb.2012.04.001>
- [44] Wang, Y., Shan, B., Liang, Y., Wei, H. and Yuan, J. Parkin regulates NF- κ B by mediating site-specific ubiquitination of RIPK1. *Cell Death & Disease* **9** 2018, 732. <https://doi.org/10.1038/s41419-018-0770-z>
- [45] Sato, Y., Yoshikawa, A., Mimura, H., Yamashita, M., Yamagata, A. and Fukai, S. Structural basis for specific recognition of Lys 63-linked polyubiquitin chains by tandem UIMs of RAP80. *The EMBO Journal* **28** 2009, 2461–8. <https://doi.org/10.1038/emboj.2009.160>
- [46] Trempe, J.-F. Reading the ubiquitin postal code. *Current Opinion in Structural Biology* **21** 2011, 792–801. <https://doi.org/10.1016/j.sbi.2011.09.009>
- [47] David, Y., Ternette, N., Edelmann, M.J., Ziv, T., Gayer, B., Sertchook, R., Dadon, Y., Kessler, B.M. and Navon, A. E3 Ligases Determine Ubiquitination Site and Conjugate Type by Enforcing Specificity on E2 Enzymes. *Journal of Biological Chemistry* **286** 2011, 44104–15. <https://doi.org/10.1074/jbc.M111.234559>
- [48] Swatek, K.N. and Komander, D. Ubiquitin modifications. *Cell Research* **26** 2016, 399–422. <https://doi.org/10.1038/cr.2016.39>
- [49] Morimoto, D. and Shirakawa, M. The evolving world of ubiquitin: transformed polyubiquitin chains. *Biomolecular Concepts* **7** 2016, 157–67. <https://doi.org/10.1515/bmc-2016-0009>
- [50] Swaney, D.L., Beltrao, P., Starita, L., Guo, A., Rush, J., Fields, S., Krogan, N.J. and Villén, J. Global analysis of phosphorylation and ubiquitylation cross-talk in protein degradation. *Nature Methods* **10** 2013, 676–82. <https://doi.org/10.1038/nmeth.2519>
- [51] van der Veen, A.G. and Ploegh, H.L. Ubiquitin-Like Proteins. *Annual Review of Biochemistry* **81** 2012, 323–57. <https://doi.org/10.1146/annurev-biochem-093010-153308>
- [52] Geoffroy, M.-C. and Hay, R.T. An additional role for SUMO in ubiquitin-mediated proteolysis. *Nature Reviews Molecular Cell Biology* **10** 2009, 564–8. <https://doi.org/10.1038/nrm2707>
- [53] Flotho, A. and Melchior, F. Sumoylation: A Regulatory Protein Modification in Health and Disease. *Annual Review of Biochemistry* **82** 2013, 357–85. <https://doi.org/10.1146/annurev-biochem-061909-093311>
- [54] Theng, S.S., Wang, W., Mah, W.-C., Chan, C., Zhuo, J., Gao, Y., Qin, H., Lim, L., Chong, S.S., Song, J. and Lee, C.G. Disruption of FAT10-MAD2 binding inhibits tumor progression. *Proceedings of the National Academy of Sciences of the United States of America* **111** 2014, E5282–91. <https://doi.org/10.1073/pnas.1403383111>
- [55] Hochstrasser, M. Origin and function of ubiquitin-like proteins. *Nature* **458** 2009, 422–9. <https://doi.org/10.1038/nature07958>
- [56] Komander, D., Clague, M.J. and Urbé, S. Breaking the chains: structure and function of the deubiquitinases. *Nature Reviews Molecular Cell Biology* Nature Publishing Group. **10** 2009, 550–63. <https://doi.org/10.1038/nrm2731>
- [57] Wilkinson, K.D. DUBs at a glance. *Journal of Cell Science* **122** 2009, 2325–9. <https://doi.org/10.1242/jcs.041046>
- [58] Reyes-Turcu, F.E., Shanks, J.R., Komander, D. and Wilkinson, K.D. Recognition of Polyubiquitin Isoforms by the Multiple Ubiquitin Binding Modules of Isopeptidase T. *Journal of Biological Chemistry* **283** 2008, 19581–92. <https://doi.org/10.1074/jbc.M800947200>
- [59] Komander, D. Mechanism, specificity and structure of the deubiquitinases. *Sub-Cellular Biochemistry* **54** 2010, 69–87. https://doi.org/10.1007/978-1-4419-6676-6_6
- [60] Keusekotten, K., Elliott, P.R., Glockner, L., Fiil, B.K., Damgaard, R.B., Kulathu, Y., Wauer, T., Hospenthal, M.K., Gyrd-Hansen, M., Krappmann, D., Hofmann, K. and Komander, D. OTULIN antagonizes LUBAC signaling by specifically hydrolyzing Met1-linked polyubiquitin. *Cell* **153** 2013, 1312–26. <https://doi.org/10.1016/j.cell.2013.05.014>
- [61] Schaefer, J.B. and Morgan, D.O. Protein-linked ubiquitin chain structure restricts activity of deubiquitinating enzymes. *The Journal of Biological Chemistry* **286** 2011, 45186–96. <https://doi.org/10.1074/jbc.M111.310094>
- [62] Ritorto, M.S., Ewan, R., Perez-Oliva, A.B., Knebel, A., Buhrlage, S.J., Wightman, M., Kelly, S.M., Wood, N.T., Virdee, S., Gray, N.S., Morrice, N.A., Alessi, D.R. and Trost, M. Screening of DUB activity and specificity by MALDI-TOF mass spectrometry. *Nature Communications* **5** 2014, 4763. <https://doi.org/10.1038/ncomms5763>
- [63] Sheng, Y., Saridakis, V., Sarkari, F., Duan, S., Wu, T., Arrowsmith, C.H. and Frappier, L. Molecular recognition of p53 and MDM2 by USP7/HAUSP. *Nature Structural & Molecular Biology* **13** 2006, 285–91. <https://doi.org/10.1038/nsmb1067>

- [64] Ye, Y., Akutsu, M., Reyes-Turcu, F., Enchev, R.I., Wilkinson, K.D. and Komander, D. Polyubiquitin binding and cross-reactivity in the USP domain deubiquitinase USP21. *EMBO Reports* **12** 2011, 350–7. <https://doi.org/10.1038/embor.2011.17>
- [65] Pickart, C.M. and Rose, I.A. Ubiquitin carboxyl-terminal hydrolase acts on ubiquitin carboxyl-terminal amides. *The Journal of Biological Chemistry* **260** 1985, 7903–10.
- [66] Wang, D., Ma, L., Wang, B., Liu, J. and Wei, W. E3 ubiquitin ligases in cancer and implications for therapies. *Cancer and Metastasis Reviews* **36** 2017, 683–702. <https://doi.org/10.1007/s10555-017-9703-z>
- [67] Atkin, G. and Paulson, H. Ubiquitin pathways in neurodegenerative disease. *Frontiers in Molecular Neuroscience* **7** 2014, 63. <https://doi.org/10.3389/fnmol.2014.00063>
- [68] Mansour, M.A. Ubiquitination: Friend and foe in cancer. *The International Journal of Biochemistry & Cell Biology* **101** 2018, 80–93. <https://doi.org/10.1016/j.biocel.2018.06.001>
- [69] Bustamante, H.A., González, A.E., Cerda-Troncoso, C., Shaughnessy, R., Otth, C., Soza, A. and Burgos, P. V. Interplay Between the Autophagy-Lysosomal Pathway and the Ubiquitin-Proteasome System: A Target for Therapeutic Development in Alzheimer's Disease. *Frontiers in Cellular Neuroscience* **12** 2018, 126. <https://doi.org/10.3389/fncel.2018.00126>
- [70] Haq, S. and Ramakrishna, S. Deubiquitylation of deubiquitylases. *Open Biology* The Royal Society. **7** 2017, <https://doi.org/10.1098/rsob.170016>
- [71] Pang, C.N.I., Hayen, A. and Wilkins, M.R. Surface Accessibility of Protein Post-Translational Modifications. *Journal of Proteome Research* **6** 2007, 1833–45. <https://doi.org/10.1021/pr060674u>
- [72] Mevissen, T.E.T. and Komander, D. Mechanisms of Deubiquitinase Specificity and Regulation. *Annual Review of Biochemistry* **86** 2017, 159–92. <https://doi.org/10.1146/annurev-biochem-061516-044916>
- [73] Lei, H., Shan, H. and Wu, Y. Targeting deubiquitinating enzymes in cancer stem cells. *Cancer Cell International* **17** 2017, 101. <https://doi.org/10.1186/s12935-017-0472-0>
- [74] Pinto-Fernandez, A. and Kessler, B.M. DUBbing Cancer: Deubiquitylating Enzymes Involved in Epigenetics, DNA Damage and the Cell Cycle As Therapeutic Targets. *Frontiers in Genetics* **7** 2016, 133. <https://doi.org/10.3389/fgene.2016.00133>
- [75] Eletr, Z.M. and Wilkinson, K.D. Regulation of proteolysis by human deubiquitinating enzymes. *Biochimica et Biophysica Acta* **1843** 2014, 114–28. <https://doi.org/10.1016/j.bbamcr.2013.06.027>
- [76] Shrestha, R.K., Ronau, J.A., Davies, C.W., Guenette, R.G., Strieter, E.R., Paul, L.N. and Das, C. Insights into the Mechanism of Deubiquitination by JAMM Deubiquitinases from Cocrystal Structures of the Enzyme with the Substrate and Product. *Biochemistry* **53** 2014, 3199–217. <https://doi.org/10.1021/bi5003162>
- [77] Ambroggio, X.I., Rees, D.C. and Deshaies, R.J. JAMM: a metalloprotease-like zinc site in the proteasome and signalosome. Hidde L. Ploegh, editor. *PLoS Biology* **2** 2004, E2. <https://doi.org/10.1371/journal.pbio.0020002>
- [78] Johnston, S.C., Larsen, C.N., Cook, W.J., Wilkinson, K.D. and Hill, C.P. Crystal structure of a deubiquitinating enzyme (human UCH-L3) at 1.8 Å resolution. *The EMBO Journal* **16** 1997, 3787–96. <https://doi.org/10.1093/emboj/16.13.3787>
- [79] Boudreaux, D.A., Maiti, T.K., Davies, C.W. and Das, C. Ubiquitin vinyl methyl ester binding orients the misaligned active site of the ubiquitin hydrolase UCHL1 into productive conformation. *Proceedings of the National Academy of Sciences of the United States of America* **107** 2010, 9117–22. <https://doi.org/10.1073/pnas.0910870107>
- [80] Sahtoe, D.D., van Dijk, W.J., El Oualid, F., Ekkebus, R., Ovaa, H. and Sixma, T.K. Mechanism of UCH-L5 Activation and Inhibition by DEUBAD Domains in RPN13 and INO80G. *Molecular Cell* **57** 2015, 887–900. <https://doi.org/10.1016/j.molcel.2014.12.039>
- [81] Bett, J.S., Ritorto, M.S., Ewan, R., Jaffray, E.G., Virdee, S., Chin, J.W., Knebel, A., Kurz, T., Trost, M., Tatham, M.H. and Hay, R.T. Ubiquitin C-terminal hydrolases cleave isopeptide- and peptide-linked ubiquitin from structured proteins but do not edit ubiquitin homopolymers. *Biochemical Journal* **466** 2015, 489–98. <https://doi.org/10.1042/BJ20141349>
- [82] Johnston, S.C., Riddle, S.M., Cohen, R.E. and Hill, C.P. Structural basis for the specificity of ubiquitin C-terminal hydrolases. *The EMBO Journal* **18** 1999, 3877–87. <https://doi.org/10.1093/emboj/18.14.3877>
- [83] Nicastro, G., Masino, L., Esposito, V., Menon, R.P., De Simone, A., Fraternali, F. and Pastore, A. Josephin domain of ataxin-3 contains two distinct ubiquitin-binding sites. *Biopolymers* **91** 2009, 1203–14. <https://doi.org/10.1002/bip.21210>

Chapter 0. General Introduction

- [84] Seki, T., Gong, L., Williams, A.J., Sakai, N., Todi, S. V. and Paulson, H.L. JosD1, a Membrane-targeted Deubiquitinating Enzyme, Is Activated by Ubiquitination and Regulates Membrane Dynamics, Cell Motility, and Endocytosis. *Journal of Biological Chemistry* **288** 2013, 17145–55. <https://doi.org/10.1074/jbc.M113.463406>
- [85] Todi, S. V, Winborn, B.J., Scaglione, K.M., Blount, J.R., Travis, S.M. and Paulson, H.L. Ubiquitination directly enhances activity of the deubiquitinating enzyme ataxin-3. *The EMBO Journal* **28** 2009, 372–82. <https://doi.org/10.1038/emboj.2008.289>
- [86] Mevissen, T.E.T.T., Hospenthal, M.K., Geurink, P.P., Elliott, P.R., Akutsu, M., Arnaudo, N., Ekkebus, R., Kulathu, Y., Wauer, T., El Oualid, F., Freund, S.M.V. V, Ovaa, H. and Komander, D. OTU Deubiquitinases Reveal Mechanisms of Linkage Specificity and Enable Ubiquitin Chain Restriction Analysis. *Cell Elsevier*. **154** 2013, 169–84. <https://doi.org/10.1016/j.cell.2013.05.046>
- [87] Messick, T.E., Russell, N.S., Iwata, A.J., Sarachan, K.L., Shiekhhattar, R., Shanks, J.R., Reyes-Turcu, F.E., Wilkinson, K.D. and Marmorstein, R. Structural basis for ubiquitin recognition by the Otu1 ovarian tumor domain protein. *The Journal of Biological Chemistry* **283** 2008, 11038–49. <https://doi.org/10.1074/jbc.M704398200>
- [88] Komander, D. and Barford, D. Structure of the A20 OTU domain and mechanistic insights into deubiquitination. *The Biochemical Journal* **409** 2008, 77–85. <https://doi.org/10.1042/BJ20071399>
- [89] Edelmann, M.J., Iphöfer, A., Akutsu, M., Altun, M., di Gleria, K., Kramer, H.B., Fiebigler, E., Dhe-Paganon, S. and Kessler, B.M. Structural basis and specificity of human otubain 1-mediated deubiquitination. *The Biochemical Journal* **418** 2009, 379–90. <https://doi.org/10.1042/BJ20081318>
- [90] Hu, M., Li, P., Li, M., Li, W., Yao, T., Wu, J.-W., Gu, W., Cohen, R.E. and Shi, Y. Crystal Structure of a UBP-Family Deubiquitinating Enzyme in Isolation and in Complex with Ubiquitin Aldehyde. *Cell* **111** 2002, 1041–54. [https://doi.org/10.1016/S0092-8674\(02\)01199-6](https://doi.org/10.1016/S0092-8674(02)01199-6)
- [91] Juang, Y.-C., Landry, M.-C., Sanches, M., Vittal, V., Leung, C.C.Y., Ceccarelli, D.F., Mateo, A.-R.F., Pruneda, J.N., Mao, D.Y.L., Szilard, R.K., Orlicky, S., Munro, M., Brzovic, P.S., Klevit, R.E., Sicheri, F. and Durocher, D. OTUB1 Co-opts Lys48-Linked Ubiquitin Recognition to Suppress E2 Enzyme Function. *Molecular Cell* **45** 2012, 384–97. <https://doi.org/10.1016/j.molcel.2012.01.011>
- [92] Abdul Rehman, S.A., Kristariyanto, Y.A., Choi, S.-Y., Nkosi, P.J., Weidlich, S., Labib, K., Hofmann, K. and Kulathu, Y. MINDY-1 Is a Member of an Evolutionarily Conserved and Structurally Distinct New Family of Deubiquitinating Enzymes. *Molecular Cell* **63** 2016, 146–55. <https://doi.org/10.1016/j.molcel.2016.05.009>
- [93] Kristariyanto, Y.A., Abdul Rehman, S.A., Weidlich, S., Knebel, A. and Kulathu, Y. A single MIU motif of MINDY-1 recognizes K48-linked polyubiquitin chains. *EMBO Reports* **18** 2017, 392–402. <https://doi.org/10.15252/embr.201643205>
- [94] Hewings, D.S., Heideker, J., Ma, T.P., AhYoung, A.P., El Oualid, F., Amore, A., Costakes, G.T., Kirchhofer, D., Brasher, B., Pillow, T., Popovych, N., Maurer, T., Schwerdtfeger, C., Forrest, W.F., Yu, K., Flygare, J., Bogoy, M. and Wertz, I.E. Reactive-site-centric chemoproteomics identifies a distinct class of deubiquitinase enzymes. *Nature Communications* **9** 2018, 1162. <https://doi.org/10.1038/s41467-018-03511-6>
- [95] Hermanns, T., Pichlo, C., Woiwode, I., Klopffleisch, K., Witting, K.F., Ovaa, H., Baumann, U. and Hofmann, K. A family of unconventional deubiquitinases with modular chain specificity determinants. *Nature Communications* **9** 2018, 799. <https://doi.org/10.1038/s41467-018-03148-5>
- [96] Haahr, P., Borgermann, N., Guo, X., Typas, D., Achuthankutty, D., Hoffmann, S., Shearer, R., Sixma, T.K. and Mailand, N. ZUFSP Deubiquitylates K63-Linked Polyubiquitin Chains to Promote Genome Stability. *Molecular Cell* **70** 2018, 165–174.e6. <https://doi.org/10.1016/j.molcel.2018.02.024>
- [97] Kwasna, D., Abdul Rehman, S.A., Natarajan, J., Matthews, S., Madden, R., De Cesare, V., Weidlich, S., Virdee, S., Ahel, I., Gibbs-Seymour, I. and Kulathu, Y. Discovery and Characterization of ZUFSP/ZUP1, a Distinct Deubiquitinase Class Important for Genome Stability. *Molecular Cell* **70** 2018, 150–164.e6. <https://doi.org/10.1016/j.molcel.2018.02.023>
- [98] Ha, B.H., Ahn, H.-C., Kang, S.H., Tanaka, K., Chung, C.H. and Kim, E.E. Structural Basis for Ufm1 Processing by UfSP1. *Journal of Biological Chemistry* **283** 2008, 14893–900. <https://doi.org/10.1074/jbc.M708756200>
- [99] Ye, Y., Scheel, H., Hofmann, K. and Komander, D. Dissection of USP catalytic domains reveals five common insertion points. *Molecular BioSystems The Royal Society of Chemistry*. **5** 2009, 1797–808. <https://doi.org/10.1039/b907669g>

- [100] Nijman, S.M.B., Luna-Vargas, M.P. a, Velds, A., Brummelkamp, T.R., Dirac, A.M.G., Sixma, T.K. and Bernards, R. A genomic and functional inventory of deubiquitinating enzymes. *Cell* **123** 2005, 773–86. <https://doi.org/10.1016/j.cell.2005.11.007>
- [101] Storer, A.C., Ménard, R., Cstorer, A. and Ménard, R. Catalytic mechanism in papain family of cysteine peptidases. *Methods in Enzymology* **244** 1994, 486–500. [https://doi.org/10.1016/0076-6879\(94\)44035-2](https://doi.org/10.1016/0076-6879(94)44035-2)
- [102] Faesen, A.C., Luna-Vargas, M.P.A., Geurink, P.P., Clerici, M., Merks, R., van Dijk, W.J., Hameed, D.S., El Oualid, F., Ovaa, H. and Sixma, T.K. The differential modulation of USP activity by internal regulatory domains, interactors and eight ubiquitin chain types. *Chemistry & Biology* **18** 2011, 1550–61. <https://doi.org/10.1016/j.chembiol.2011.10.017>
- [103] Fraile, J.M., Quesada, V., Rodríguez, D., Freije, J.M.P. and López-Otín, C. Deubiquitinases in cancer: new functions and therapeutic options. *Oncogene* **31** 2012, 2373–88. <https://doi.org/10.1038/onc.2011.443>
- [104] Love, K.R., Catic, A., Schlieker, C. and Ploegh, H.L. Mechanisms, biology and inhibitors of deubiquitinating enzymes. *Nature Chemical Biology* **3** 2007, 697–705. <https://doi.org/10.1038/nchembio.2007.43>
- [105] Farshi, P., Deshmukh, R.R., Nwankwo, J.O., Arkwright, R.T., Cvek, B., Liu, J. and Dou, Q.P. Deubiquitinases (DUBs) and DUB inhibitors: a patent review. *Expert Opinion on Therapeutic Patents* Informa Healthcare. **25** 2015, 1191–208. <https://doi.org/10.1517/13543776.2015.1056737>
- [106] Pfoh, R., Lacdao, I.K. and Saridakis, V. Deubiquitinases and the new therapeutic opportunities offered to cancer. *Endocrine-Related Cancer* **22** 2015, T35–54. <https://doi.org/10.1530/ERC-14-0516>
- [107] Colland, F. The therapeutic potential of deubiquitinating enzyme inhibitors. *Biochemical Society Transactions* **38** 2010, 137–43. <https://doi.org/10.1042/BST0380137>
- [108] Faesen, A.C., Dirac, A.M.G., Shanmugham, A., Ovaa, H., Perrakis, A. and Sixma, T.K. Mechanism of USP7/HAUSP activation by its C-terminal ubiquitin-like domain and allosteric regulation by GMP-synthetase. *Molecular Cell Elsevier Inc.* **44** 2011, 147–59. <https://doi.org/10.1016/j.molcel.2011.06.034>
- [109] Vijay-Kumar, S., Bugg, C.E. and Cook, W.J. Structure of ubiquitin refined at 1.8 Å resolution. *Journal of Molecular Biology* **194** 1987, 531–44.
- [110] Zhu, X., Ménard, R. and Sulea, T. High incidence of ubiquitin-like domains in human ubiquitin-specific proteases. *Proteins: Structure, Function, and Bioinformatics* **69** 2007, 1–7. <https://doi.org/10.1002/prot.21546>
- [111] Clerici, M., Luna-Vargas, M.P.A., Faesen, A.C. and Sixma, T.K. The DUSP–Ubl domain of USP4 enhances its catalytic efficiency by promoting ubiquitin exchange. *Nature Communications* **5** 2014, 5399. <https://doi.org/10.1038/ncomms6399>
- [112] Everett, R.D., Meredith, M., Orr, A., Cross, A., Kathoria, M. and Parkinson, J. A novel ubiquitin-specific protease is dynamically associated with the PML nuclear domain and binds to a herpesvirus regulatory protein. *The EMBO Journal* **16** 1997, 1519–30. <https://doi.org/10.1093/emboj/16.7.1519>
- [113] Pfoh, R., Lacdao, I.K., Georges, A.A., Capar, A., Zheng, H., Frappier, L. and Saridakis, V. Crystal Structure of USP7 Ubiquitin-like Domains with an ICP0 Peptide Reveals a Novel Mechanism Used by Viral and Cellular Proteins to Target USP7. *PLoS Pathogens* **11** 2015, e1004950. <https://doi.org/10.1371/journal.ppat.1004950>
- [114] Song, M.S., Salmena, L., Carracedo, A., Egia, A., Lo-Coco, F., Teruya-Feldstein, J. and Pandolfi, P.P. The deubiquitinylation and localization of PTEN are regulated by a HAUSP–PML network. *Nature* **455** 2008, 813–7. <https://doi.org/10.1038/nature07290>
- [115] Novellasdemunt, L., Foglizzo, V., Cuadrado, L., Antas, P., Kucharska, A., Encheva, V., Snijders, A.P. and Li, V.S.W. USP7 Is a Tumor-Specific WNT Activator for APC-Mutated Colorectal Cancer by Mediating β -Catenin Deubiquitination. *Cell Reports* **21** 2017, 612–27. <https://doi.org/10.1016/j.celrep.2017.09.072>
- [116] Masuya, D., Huang, C., Liu, D., Nakashima, T., Yokomise, H., Ueno, M., Nakashima, N. and Sumitomo, S. The HAUSP gene plays an important role in non-small cell lung carcinogenesis through p53-dependent pathways. *The Journal of Pathology* **208** 2006, 724–32. <https://doi.org/10.1002/path.1931>
- [117] Huether, R., Dong, L., Chen, X., Wu, G., Parker, M., Wei, L., Ma, J., Edmonson, M.N., Hedlund, E.K., Rusch, M.C., Shurtleff, S.A., Mulder, H.L., Boggs, K., Vadordaria, B., Cheng, J., Yergeau, D., Song, G., Becksfort, J., Lemmon, G. et al. The landscape of somatic mutations in epigenetic regulators across 1,000 paediatric cancer genomes. *Nature Communications* Nature Publishing Group. **5** 2014, 1–7. <https://doi.org/10.1038/ncomms4630>

Chapter 0. General Introduction

- [118] Ma, X., Liu, Y., Liu, Y., Alexandrov, L.B., Edmonson, M.N., Gawad, C., Zhou, X., Li, Y., Rusch, M.C., Easton, J., Huether, R., Gonzalez-Pena, V., Wilkinson, M.R., Hermida, L.C., Davis, S., Sioson, E., Pounds, S., Cao, X., Ries, R.E. et al. Pan-cancer genome and transcriptome analyses of 1,699 paediatric leukaemias and solid tumours. *Nature* **555** 2018, 371–6. <https://doi.org/10.1038/nature25795>
- [119] Gao, J., Aksoy, B.A., Dogrusoz, U., Dresdner, G., Gross, B., Sumer, S.O., Sun, Y., Jacobsen, A., Sinha, R., Larsson, E., Cerami, E., Sander, C. and Schultz, N. Integrative Analysis of Complex Cancer Genomics and Clinical Profiles Using the cBioPortal. *Science Signaling* **6** 2013, pl1-pl1. <https://doi.org/10.1126/scisignal.2004088>
- [120] Zhao, G.-Y., Lin, Z.-W., Lu, C.-L., Gu, J., Yuan, Y.-F., Xu, F.-K., Liu, R.-H., Ge, D. and Ding, J.-Y. USP7 overexpression predicts a poor prognosis in lung squamous cell carcinoma and large cell carcinoma. *Tumour Biology : The Journal of the International Society for Oncodevelopmental Biology and Medicine* **36** 2015, 1721–9. <https://doi.org/10.1007/s13277-014-2773-4>
- [121] Zhi, Y., ShouJun, H., Yuanzhou, S., Haijun, L., Yume, X., Kai, Y., Xianwei, L. and Xueli, Z. STAT3 repressed USP7 expression is crucial for colon cancer development. *FEBS Letters* **586** 2012, 3013–7. <https://doi.org/10.1016/j.febslet.2012.06.025>
- [122] Kon, N., Kobayashi, Y., Li, M., Brooks, C.L., Ludwig, T. and Gu, W. Inactivation of HAUSP in vivo modulates p53 function. *Oncogene* **29** 2010, 1270–9. <https://doi.org/10.1038/onc.2009.427>
- [123] Foundation for USP7-Related Diseases [Internet]. www.usp7.org.
- [124] Hao, Y.-H., Fountain, M.D., Fon Tacer, K., Xia, F., Bi, W., Kang, S.-H.L., Patel, A., Rosenfeld, J.A., Le Caignec, C., Isidor, B., Krantz, I.D., Noon, S.E., Pfotenhauer, J.P., Morgan, T.M., Moran, R., Pedersen, R.C., Saenz, M.S., Schaaf, C.P. and Potts, P.R. USP7 Acts as a Molecular Rheostat to Promote WASH-Dependent Endosomal Protein Recycling and Is Mutated in a Human Neurodevelopmental Disorder. *Molecular Cell* **59** 2015, 956–69. <https://doi.org/10.1016/j.molcel.2015.07.033>
- [125] Hao, Y.-H., Doyle, J.M., Ramanathan, S., Gomez, T.S., Jia, D., Xu, M., Chen, Z.J., Billadeau, D.D., Rosen, M.K. and Potts, P.R. Regulation of WASH-dependent actin polymerization and protein trafficking by ubiquitination. *Cell NIH Public Access*. **152** 2013, 1051–64. <https://doi.org/10.1016/j.cell.2013.01.051>
- [126] Fernández-Montalván, A., Bouwmeester, T., Joberty, G., Mader, R., Mahnke, M., Pierrat, B., Schlaeppi, J.-M., Worpenberg, S. and Gerhartz, B. Biochemical characterization of USP7 reveals post-translational modification sites and structural requirements for substrate processing and subcellular localization. *The FEBS Journal* **274** 2007, 4256–70. <https://doi.org/10.1111/j.1742-4658.2007.05952.x>
- [127] Sowa, M.E., Bennett, E.J., Gygi, S.P. and Harper, J.W. Defining the human deubiquitinating enzyme interaction landscape. *Cell Elsevier Ltd*. **138** 2009, 389–403. <https://doi.org/10.1016/j.cell.2009.04.042>
- [128] Brazhnik, P. and Kohn, K.W. HAUSP-regulated switch from auto- to p53 ubiquitination by Mdm2 (in silico discovery). *Mathematical Biosciences* **210** 2007, 60–77. <https://doi.org/10.1016/j.mbs.2007.05.005>
- [129] Kon, N., Zhong, J., Kobayashi, Y., Li, M., Szabolcs, M., Ludwig, T., Canoll, P.D. and Gu, W. Roles of HAUSP-mediated p53 regulation in central nervous system development. *Cell Death and Differentiation* **18** 2011, 1366–75. <https://doi.org/10.1038/cdd.2011.12>
- [130] Cummins, J.M., Rago, C., Kohli, M., Kinzler, K.W., Lengauer, C. and Vogelstein, B. Tumour suppression: Disruption of HAUSP gene stabilizes p53. *Nature* **428** 2004, 486–7. <https://doi.org/10.1038/nature02501>
- [131] Cummins, J.M. and Vogelstein, B. HAUSP is required for p53 destabilization. *Cell Cycle (Georgetown, Tex)* **3** 2004, 689–92. <https://doi.org/10.4161/cc.3.6.924>
- [132] Cheng, J., Yang, H., Fang, J., Ma, L., Gong, R., Wang, P., Li, Z. and Xu, Y. Molecular mechanism for USP7-mediated DNMT1 stabilization by acetylation. *Nature Communications* **6** 2015, 7023. <https://doi.org/10.1038/ncomms8023>
- [133] Zhang, Z.-M., Rothbart, S.B., Allison, D.F., Cai, Q., Harrison, J.S., Li, L., Wang, Y., Strahl, B.D., Wang, G.G. and Song, J. An Allosteric Interaction Links USP7 to Deubiquitination and Chromatin Targeting of UHRF1. *Cell Reports* **12** 2015, 1400–6. <https://doi.org/10.1016/j.celrep.2015.07.046>
- [134] Zlatanou, A., Sabbioneda, S., Miller, E.S., Greenwalt, A., Aggathangelou, A., Maurice, M.M., Lehmann, A.R., Stankovic, T., Reverdy, C., Colland, F., Vaziri, C. and Stewart, G.S. USP7 is essential for maintaining Rad18 stability and DNA damage tolerance. *Oncogene* **35** 2016, 965–76. <https://doi.org/10.1038/onc.2015.149>
- [135] Qian, J., Pentz, K., Zhu, Q., Wang, Q., He, J., Srivastava, A.K. and Wani, A.A. USP7 modulates UV-induced PCNA monoubiquitination by regulating DNA polymerase eta stability. *Oncogene* **34** 2015, 4791–6. <https://doi.org/10.1038/onc.2014.394>

- [136] Lecona, E., Rodriguez-Acebes, S., Specks, J., Lopez-Contreras, A.J., Ruppen, I., Murga, M., Muñoz, J., Mendez, J. and Fernandez-Capetillo, O. USP7 is a SUMO deubiquitinase essential for DNA replication. *Nature Structural & Molecular Biology* **23** 2016, 270–7. <https://doi.org/10.1038/nsmb.3185>
- [137] Lecona, E., Narendra, V. and Reinberg, D. USP7 Cooperates with SCML2 To Regulate the Activity of PRC1. *Molecular and Cellular Biology* **35** 2015, 1157–68. <https://doi.org/10.1128/MCB.01197-14>
- [138] Li, M., Brooks, C.L., Kon, N. and Gu, W. A dynamic role of HAUSP in the p53-Mdm2 pathway. *Molecular Cell* **13** 2004, 879–86.
- [139] Kessler, B.M., Fortunati, E., Melis, M., Pals, C.E.G.M., Clevers, H. and Maurice, M.M. Proteome Changes Induced by Knock-Down of the Deubiquitylating Enzyme HAUSP/USP7. *Journal of Proteome Research* **6** 2007, 4163–72. <https://doi.org/10.1021/pr0702161>
- [140] Hu, M., Gu, L., Li, M., Jeffrey, P.D., Gu, W. and Shi, Y. Structural basis of competitive recognition of p53 and MDM2 by HAUSP/USP7: implications for the regulation of the p53-MDM2 pathway. *PLoS Biology* **4** 2006, e27. <https://doi.org/10.1371/journal.pbio.0040027>
- [141] Kim, R.Q. and Sixma, T.K. Regulation of USP7: A High Incidence of E3 Complexes. *Journal of Molecular Biology* **429** 2017, 3395–408. <https://doi.org/10.1016/j.jmb.2017.05.028>
- [142] Canning, M., Boutell, C., Parkinson, J. and Everett, R.D. A RING finger ubiquitin ligase is protected from autocatalyzed ubiquitination and degradation by binding to ubiquitin-specific protease USP7. *The Journal of Biological Chemistry* **279** 2004, 38160–8. <https://doi.org/10.1074/jbc.M402885200>
- [143] Boutell, C., Canning, M., Orr, A. and Everett, R.D. Reciprocal activities between herpes simplex virus type 1 regulatory protein ICP0, a ubiquitin E3 ligase, and ubiquitin-specific protease USP7. *Journal of Virology* **79** 2005, 12342–54. <https://doi.org/10.1128/JVI.79.19.12342-12354.2005>
- [144] Mouchantaf, R., Azakir, B.A., McPherson, P.S., Millard, S.M., Wood, S.A. and Angers, A. The ubiquitin ligase itch is auto-ubiquitylated in vivo and in vitro but is protected from degradation by interacting with the deubiquitylating enzyme FAM/USP9X. *The Journal of Biological Chemistry* **281** 2006, 38738–47. <https://doi.org/10.1074/jbc.M605959200>
- [145] Tavana, O. and Gu, W. Modulation of the p53/MDM2 interplay by HAUSP inhibitors. *Journal of Molecular Cell Biology* Oxford University Press. **9** 2017, 45–52. <https://doi.org/10.1093/jmcb/mjw049>
- [146] Sahtoe, D.D. and Sixma, T.K. Layers of DUB regulation. *Trends in Biochemical Sciences* **40** 2015, 456–67. <https://doi.org/10.1016/j.tibs.2015.05.002>
- [147] Hu, M., Li, P., Song, L., Jeffrey, P.D., Chenova, T. a., Wilkinson, K.D., Cohen, R.E. and Shi, Y. Structure and mechanisms of the proteasome-associated deubiquitinating enzyme USP14. *The EMBO Journal* **24** 2005, 3747–56. <https://doi.org/10.1038/sj.emboj.7600832>
- [148] Misaghi, S., Galardy, P.J., Meester, W.J.N., Ovaa, H., Ploegh, H.L. and Gaudet, R. Structure of the ubiquitin hydrolase UCH-L3 complexed with a suicide substrate. *The Journal of Biological Chemistry* **280** 2005, 1512–20. <https://doi.org/10.1074/jbc.M410770200>
- [149] Du, X., Li, Y., Xia, Y.-L., Ai, S.-M., Liang, J., Sang, P., Ji, X.-L. and Liu, S.-Q. Insights into Protein–Ligand Interactions: Mechanisms, Models, and Methods. *International Journal of Molecular Sciences* **17** 2016, 144. <https://doi.org/10.3390/ijms17020144>
- [150] Pang, X. and Zhou, H.-X. Rate Constants and Mechanisms of Protein–Ligand Binding. *Annual Review of Biophysics* **46** 2017, 105–30. <https://doi.org/10.1146/annurev-biophys-070816-033639>
- [151] Meulmeester, E., Kunze, M., Hsiao, H.H., Urlaub, H. and Melchior, F. Mechanism and Consequences for Paralog-Specific Sumoylation of Ubiquitin-Specific Protease 25. *Molecular Cell* **30** 2008, 610–9. <https://doi.org/10.1016/j.molcel.2008.03.021>
- [152] Komander, D., Reyes-Turcu, F., Licchesi, J.D.F., Odenwaelder, P., Wilkinson, K.D. and Barford, D. Molecular discrimination of structurally equivalent Lys 63-linked and linear polyubiquitin chains. *EMBO Reports* **10** 2009, 466–73. <https://doi.org/10.1038/embor.2009.55>
- [153] Hayes, S.D., Liu, H., MacDonald, E., Sanderson, C.M., Coulson, J.M., Clague, M.J. and Urbé, S. Direct and indirect control of mitogen-activated protein kinase pathway-associated components, BRAP/IMP E3 ubiquitin ligase and CRAF/RAF1 kinase, by the deubiquitylating enzyme USP15. *The Journal of Biological Chemistry* **287** 2012, 43007–18. <https://doi.org/10.1074/jbc.M112.386938>
- [154] Holowaty, M.N., Sheng, Y., Nguyen, T., Arrowsmith, C. and Frappier, L. Protein interaction domains of the ubiquitin-specific protease, USP7/HAUSP. *The Journal of Biological Chemistry* **278** 2003, 47753–61. <https://doi.org/10.1074/jbc.M307200200>

Chapter 0. General Introduction

- [155] Lee, H.-R., Choi, W.-C., Lee, S., Hwang, J., Hwang, E., Guchhait, K., Haas, J., Toth, Z., Jeon, Y.H., Oh, T.-K., Kim, M.H. and Jung, J.U. Bilateral inhibition of HAUSP deubiquitinase by a viral interferon regulatory factor protein. *Nature Structural & Molecular Biology* Nature Publishing Group, a division of Macmillan Publishers Limited. All Rights Reserved. **18** 2011, 1336–44. <https://doi.org/10.1038/nsmb.2142>
- [156] Dang, L.C., Melandri, F.D. and Stein, R.L. Kinetic and Mechanistic Studies on the Hydrolysis of Ubiquitin C-Terminal 7-Amido-4-Methylcoumarin by Deubiquitinating Enzymes. *Biochemistry* **37** 1998, 1868–79. <https://doi.org/10.1021/bi9723360>
- [157] Faesen, A.C., Luna-Vargas, M.P.A. and Sixma, T.K. The role of UBL domains in ubiquitin-specific proteases. *Biochemical Society Transactions* **40** 2012, 539–45. <https://doi.org/10.1042/BST20120004>
- [158] Kelley, L.A., Mezulis, S., Yates, C.M., Wass, M.N. and Sternberg, M.J.E. The Phyre2 web portal for protein modeling, prediction and analysis. *Nature Protocols* **10** 2015, 845–58. <https://doi.org/10.1038/nprot.2015.053>
- [159] Piao, J., Tashiro, A., Nishikawa, M., Aoki, Y., Moriyoshi, E., Hattori, A. and Kakeya, H. Expression, purification and enzymatic characterization of a recombinant human ubiquitin-specific protease 47. *Journal of Biochemistry* 2015,. <https://doi.org/10.1093/jb/mvv063>
- [160] Weinstock, J., Wu, J., Cao, P., Kingsbury, W.D., McDermott, J.L., Kodrasov, M.P., McKelvey, D.M., Suresh Kumar, K.G., Goldenberg, S.J., Mattern, M.R. and Nicholson, B. Selective Dual Inhibitors of the Cancer-Related Deubiquitylating Proteases USP7 and USP47. *ACS Medicinal Chemistry Letters* **3** 2012, 789–92. <https://doi.org/10.1021/ml200276j>
- [161] Li, S., Wang, D., Zhao, J., Weathington, N.M., Shang, D. and Zhao, Y. The deubiquitinating enzyme USP48 stabilizes TRAF2 and reduces E-cadherin-mediated adherens junctions. *The FASEB Journal* **32** 2018, 230–42. <https://doi.org/10.1096/fj.201700415RR>
- [162] Lockhart, P.J., Hulihan, M., Lincoln, S., Hussey, J., Skipper, L., Bisceglia, G., Wilkes, K. and Farrer, M.J. Identification of the human ubiquitin specific protease 31 (USP31) gene: structure, sequence and expression analysis. *DNA Sequence : The Journal of DNA Sequencing and Mapping* **15** 2004, 9–14.
- [163] Uckelmann, M., Densham, R.M., Baas, R., Winterwerp, H.H.K., Fish, A., Sixma, T.K. and Morris, J.R. USP48 restrains resection by site-specific cleavage of the BRCA1 ubiquitin mark from H2A. *Nature Communications* Nature Publishing Group. **9** 2018, 229. <https://doi.org/10.1038/s41467-017-02653-3>
- [164] Takagi, H., Nishibori, Y., Katayama, K., Katada, T., Takahashi, S., Kiuchi, Z., Takahashi, S.-I., Kamei, H., Kawakami, H., Akimoto, Y., Kudo, A., Asanuma, K., Takematsu, H. and Yan, K. USP40 gene knockdown disrupts glomerular permeability in zebrafish. *American Journal of Physiology - Renal Physiology* **312** 2017, F702–15. <https://doi.org/10.1152/ajprenal.00197.2016>
- [165] Li, Y., Schrodi, S., Rowland, C., Tacey, K., Catanese, J. and Grupe, A. Genetic evidence for ubiquitin-specific proteases USP24 and USP40 as candidate genes for late-onset Parkinson disease. *Human Mutation* **27** 2006, 1017–23. <https://doi.org/10.1002/humu.20382>
- [166] Christianson, D.W. and Scrutton, N.S. Editorial overview: Catalysis and regulation: enzyme structure, mechanism, and biosynthetic pathways. *Current Opinion in Structural Biology* Elsevier Ltd. **41** 2016, viii–x. <https://doi.org/10.1016/j.sbi.2016.09.005>
- [167] Helliwell, J.R. New developments in crystallography: exploring its technology, methods and scope in the molecular biosciences. *Bioscience Reports* Portland Press Limited. **37** 2017, BSR20170204. <https://doi.org/10.1042/BSR20170204>
- [168] Turnbull, A.P., Ioannidis, S., Krajewski, W.W., Pinto-Fernandez, A., Heride, C., Martin, A.C.L., Tonkin, L.M., Townsend, E.C., Buker, S.M., Lancia, D.R., Caravella, J.A., Toms, A. V, Charlton, T.M., Lahdenranta, J., Wilker, E., Follows, B.C., Evans, N.J., Stead, L., Alli, C. et al. Molecular basis of USP7 inhibition by selective small-molecule inhibitors. *Nature* **550** 2017, 481–6. <https://doi.org/10.1038/nature24451>
- [169] Pozhidaeva, A., Valles, G., Wang, F., Wu, J., Sterner, D.E., Nguyen, P., Weinstock, J., Kumar, K.G.S., Kanyo, J., Wright, D. and Bezsonova, I. USP7-Specific Inhibitors Target and Modify the Enzyme's Active Site via Distinct Chemical Mechanisms. *Cell Chemical Biology* Cell Press. **24** 2017, 1501–1512.e5. <https://doi.org/10.1016/J.CHEMBIOL.2017.09.004>
- [170] Lamberto, I., Liu, X., Seo, H.-S., Schauer, N.J., Iacob, R.E., Hu, W., Das, D., Mikhailova, T., Weisberg, E.L., Engen, J.R., Anderson, K.C., Chauhan, D., Dhe-Paganon, S. and Buhrlage, S.J. Structure-Guided Development of a Potent and Selective Non-covalent Active-Site Inhibitor of USP7. *Cell Chemical Biology* Cell Press. **24** 2017, 1490–1500.e11. <https://doi.org/10.1016/J.CHEMBIOL.2017.09.003>

- [171] Sato, Y., Yoshikawa, A., Yamagata, A., Mimura, H., Yamashita, M., Ookata, K., Nureki, O., Iwai, K., Komada, M. and Fukai, S. Structural basis for specific cleavage of Lys 63-linked polyubiquitin chains. *Nature* **455** 2008, 358–62. <https://doi.org/10.1038/nature07254>
- [172] Dharadhar, S., Clerici, M., van Dijk, W.J., Fish, A. and Sixma, T.K. A conserved two-step binding for the UAF1 regulator to the USP12 deubiquitinating enzyme. *Journal of Structural Biology* **196** 2016, 437–47. <https://doi.org/10.1016/j.jsb.2016.09.011>
- [173] Kim, R.Q., van Dijk, W.J. and Sixma, T.K. Structure of USP7 catalytic domain and three Ubl-domains reveals a connector α -helix with regulatory role. *Journal of Structural Biology* **195** 2016, 11–8. <https://doi.org/10.1016/j.jsb.2016.05.005>
- [174] Bateman, A., Martin, M.J., O'Donovan, C., Magrane, M., Alpi, E., Antunes, R., Bely, B., Bingley, M., Bonilla, C., Britto, R., Bursteinas, B., Bye-A-Jee, H., Cowley, A., Silva, A. Da, Giorgi, M. De, Dogan, T., Fazzini, F., Castro, L.G., Figueira, L. et al. UniProt: the universal protein knowledgebase. *Nucleic Acids Research Oxford University Press*. **45** 2017, D158–69. <https://doi.org/10.1093/nar/gkw1099>

Chapter 1.

Regulation of USP7

1

Robbert Q. Kim¹, Titia K. Sixma¹

¹Division of Biochemistry and Cancer Genomics Center, Netherlands Cancer Institute, Plesmanlaan 121, 1066 CX Amsterdam, the Netherlands

Adapted from:

Kim, R.Q. and Sixma, T.K.
Regulation of USP7: A High Incidence of E3 Complexes.
Journal of Molecular Biology 429 2017, 3395–408.
<https://doi.org/10.1016/j.jmb.2017.05.028>

Chapter 1. Regulation of USP7

Abstract

Ubiquitin conjugation is a critical signalling process in eukaryotic cells. The precise regulation of deubiquitination is an important component of this signalling cascade. Here we discuss how USP7 (or HAUSP), one of the most abundant deubiquitinating enzymes (DUBs) is regulated by complex formation with regulatory proteins and targets.

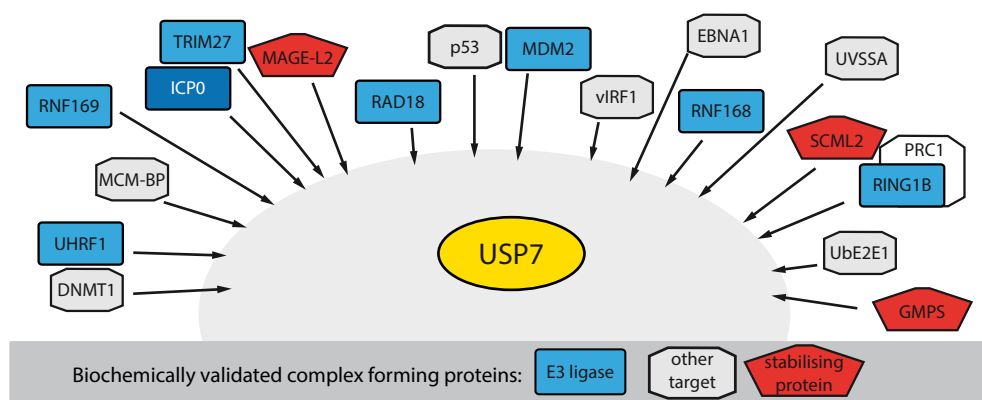
Full activity of USP7 requires that its C-terminal ubiquitin-like domains fold back onto the catalytic domain, to allow remodelling of the active site to a catalytically competent state by the very C-terminal peptide. This regulatory mode can be modulated by complex formation with other proteins.

USP7 is found in a large number of relatively stable complexes with different possible functions. Complex formation can provide recruitment of a target, bring in an E3 ubiquitin ligase or modulate the activation of the DUB activity. These complexes make up potential cellular 'switches', using their (de)ubiquitination ability to switch pathways on or off upon cellular signals. Here we summarize what is known for USP7 complexes, focussing on the prevalence of E3 ubiquitin ligases and how complex formation can affect ubiquitin switches.

Introduction

Ubiquitin (Ub) conjugation is important in virtually every eukaryotic cellular pathway^{1,2}. By conjugation of a ubiquitin molecule to amino-groups in lysines or the N-terminus of a target, a signal for downstream ubiquitin binding proteins is provided. Since ubiquitin itself contains seven lysines that can be ubiquitinated and an amino-terminus, allowing for different types of ubiquitin chains and leading to a particularly rich variety in outcomes³. In the ubiquitin signalling cascade, control and trimming of ubiquitin marks by deubiquitination play important roles⁴. Ongoing analysis is starting to show that these deubiquitinating enzymes (DUBs) are themselves very carefully regulated^{5,6}.

A particularly interesting example of complex regulation is found in USP7, a member of the Ubiquitin Specific Protease (USP) subgroup of DUBs⁷. USP7 is highly expressed and was found to have many interactors⁸. Among these interactors are a large number of target proteins, which are regulated through the USP7 deubiquitinating activity. Not all of the interacting proteins are targets however, and several of these proteins form stable protein complexes.



Some of them could serve as scaffolds, localising USP7 to the correct place, but a subset of these could be activity modulators, altering USP7 conformation and thereby regulating USP7 activity.

USP7 functions in various pathways⁹; from apoptosis¹⁰ and transcription regulation¹¹ to DNA replication¹² and neuronal development¹³. USP7 knockout has been shown to be lethal in mice, even in the absence of p53^{14,15}. To function selectively, USP7 requires careful regulation of activity. A first layer of regulation is intrinsic in USP7's multi-domain architecture; USP7 requires its C-terminal region for full activity, as the catalytic domain (CD) is 120-fold less active than the full-length protein^{16,17}. Furthermore, post-translational modification (PTM) of USP7 may change its enzymatic activity, or its ability to form complexes¹⁸. A second layer of regulation is the ability of USP7 to form multiple complexes that modulate its function. Such a complex could make USP7 switch from being target-associated to interact with another protein like an E3 ubiquitin ligase. In this review we discuss the current knowledge of USP7 interactors, focussing on crystallographic and biochemical data that describe how USP7 is regulated by itself and its interactors.

USP7 is self-activated by its C-terminal region

USP7 is a multi-domain protein of 1102 amino acids and although no full-length structure is available, a lot of information could be derived from individual domains and partial structures (Fig. 1a-b). The catalytic domain (CD; res. 208-560) contains the ubiquitin hydrolase activity. Structure analysis showed how it exists in an inactive empty state, where the active site cysteine, C223, is located 10 Å away from the deprotonating histidine H464 and aspartate D481 (PDB: 1NB8; Fig. 1b)¹⁹. In the crystal structure of the ubiquitin-bound state (PDB: 1NBF), conformational changes result in an active conformation of the catalytic triad (Fig. 1b)¹⁹ and rearrangement of a loop around W285, dubbed the 'switching loop'¹⁶.

Intriguingly, the USP7^{CD} is much less active than full-length USP7. The C-terminal half, which has five ubiquitin-like (Ubl) domains (PDB: 2YLM)^{16,20}, is necessary for full activity of USP7¹⁷. In particular the very C-terminal tail is sufficient for activation, but requires Ubl45¹⁶ or an artificial linker²¹ for recruitment to the CD. A recent structure showed how this C-terminal tail, with essential residues I1098 and I1100, binds onto a groove of CD (PDB: 5JTV; Fig. 1c)²¹. Ubl45 binds CD close to where the C-terminus of Ub is bound by the catalytic domain (PDB: 5JTV²¹), bringing the C-terminal tail close enough to reach the 'switching loop' (Fig. 3a)¹⁶. The binding of the tail remodels the CD and stabilizes the 'switching loop' in a catalytically competent configuration^{16,21}.

The crystal structure (PDB: 5JTV) shows dimer formation and thereby hints at *in trans* activation of the CD by the C-terminal tail²¹. Although this peptide is essential for activation, it binds with only 1 mM affinity *in trans*, a concentration far higher than present in the cell or used in *in vitro* experiments that show full activity^{16,21,22}. The ambiguity is further illustrated when trying to merge the existing structures into a full-length model (Fig. 1b): the gap between Ubl3 and the CD can be bridged by Ubl45 and the flexible tail, but this would require large movements, compared to the Ubl45-bound structure (PDB: 5JTV, Fig. 1c)²¹. Whether USP7 functions as a dimer or monomer is still one of the open questions in the field.

Chapter 1. Regulation of USP7

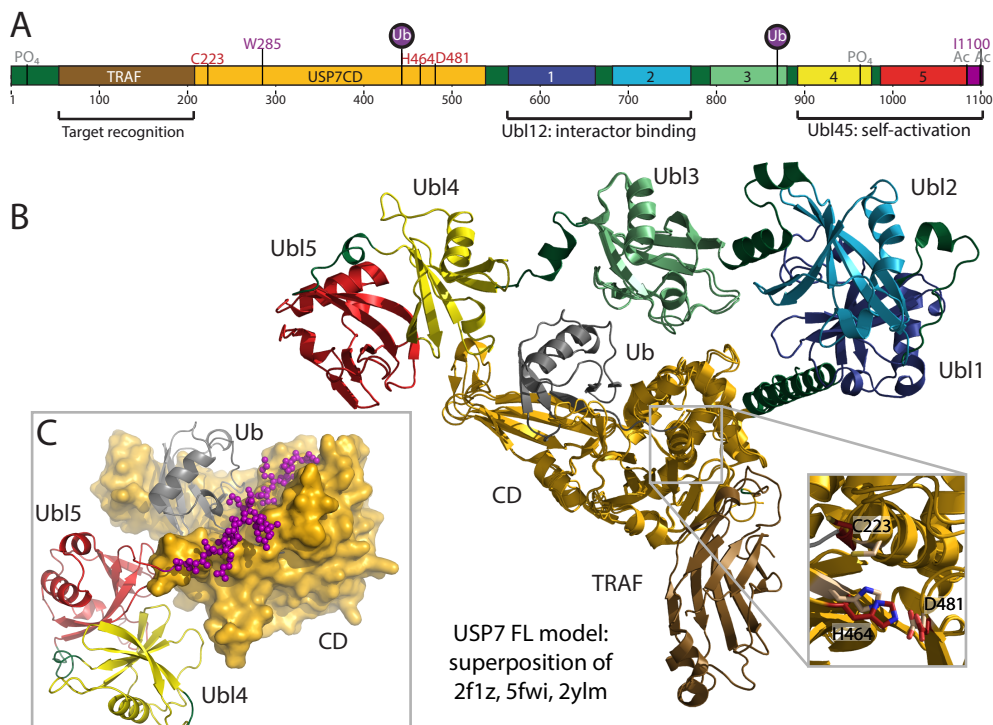


Figure 1. Structure model of USP7. **A.** Schematic figure of USP7 domain architecture, with important residues and established PTM sites highlighted. Colours are as used throughout figure 1. **B.** A model of the full-length USP7 structure, generated by superposition of overlapping regions in partial crystal structures (2F1Z, 1NBF, 5FWI, 2YLM). Colours as in A., ubiquitin in grey. A zoom depicts the active site residues of inactive USP7 (dark red) and active USP7 (beige). **C.** The crystal structure of USP7 in activated state (5JTV) illustrating how Ubl45 and the activating peptide bind onto CD.

USP7 domain architecture

The N-terminus of USP7, contains an unstructured 50 amino-acid region with poly-Q stretch, followed by a TNF receptor associated factor domain (TRAF; res. 50-208) that is required for the nuclear localisation (Fig. 1c)¹⁷. The TRAF domain is important for recognition of target proteins²³, but does not affect deubiquitinating activity on a minimal Ub-substrate¹⁶. Co-crystal structures of the TRAF domain with peptides from target proteins (p53, MDM2, EBNA, MCM-BP) show that TRAF binds its targets in the groove on one side of the β -sheet, extending the sheet with a fifth β -strand (PDB: 1YY6, 2F1Y, 2FOO, 4KG9; Fig. 2a)^{23–25}, in contrast to the perpendicular binding commonly observed in other proteins with a TRAF domain. Consequently, the interacting residues of the TRAF domain are different from ‘canonical’ TRAF binding²⁶ and TRAF recognizes its targets through a P/A-x-x-S motif (Fig. 2b)^{27,28}. This broad motif allows for many different interactors and could explain the promiscuity of USP7 in screens⁸. Although TRAF has been shown to interact with other TRAF domains²⁹, there have been no reports of self-association of USP7 through this domain or functional interactions between USP7 and other TRAF proteins. The absence of TRAF domains in other USPs indicates

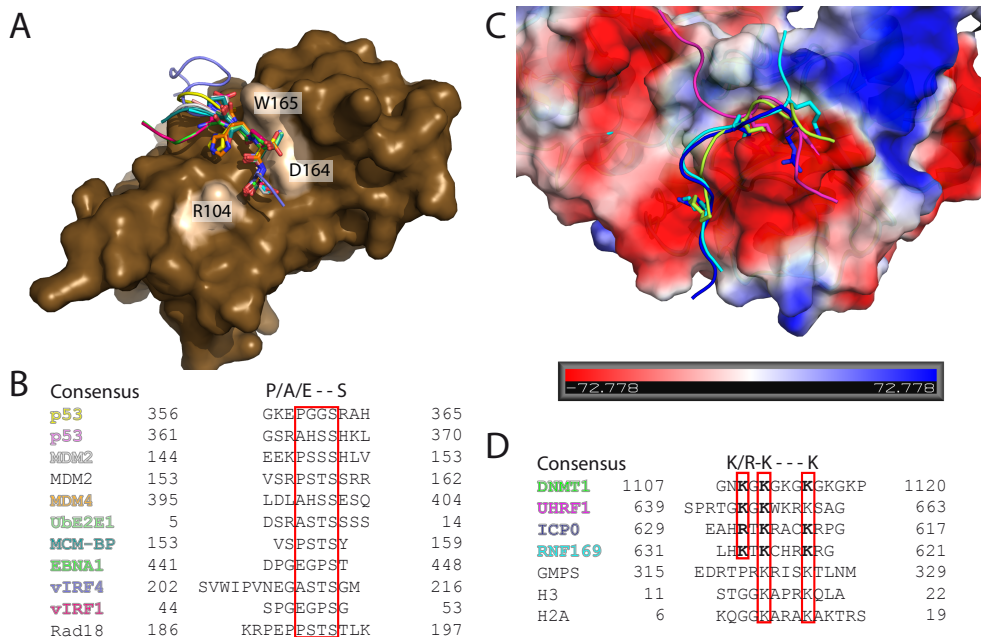


Figure 2: Co-crystal structures indicate conserved binding motifs. **A.** Interaction between TRAF and interacting peptides from EBNA1 (1YY6), p53 (2FOO), MDM2 (2F1Y), MDM4 (3MQR), Ube2E1 (4JJQ), MCM-BP (4KG9), vIRF-1 (4YSI) and vIRF-4 (2XXN). Structures were superposed by SSM, showing the surface of the TRAF domain in brown with the main interacting residues in a lighter shade. The co-crystallized peptides are displayed as ribbons, with binding residues shown as sticks, colours as in **B.**; the conserved serine makes hydrogen bonds to R104 and D164 on the TRAF; the upstream residues have their backbone stabilized by W165. **B.** A TRAF recognition motif, although not very strict, is found upon alignment of interacting peptides found in crystal structures (in colours corresponding to **A.**) or affinity assays. **C.** Interaction between Ubl12 and interacting peptides from DNMT1, ICP0, RNF169 and UHRF1 show how the interaction is anchored by insertion of positively charged amino acid onto a negative patch of Ubl12 (PDB codes: 4Z96, 4WPI, 5GG4, 5CD6). Electrostatic surface was generated using APBS Plugin for PyMol. **D.** Sequence alignment, aided by crystal structures (colours correspond to **C.**), of tested interacting peptides reveal Ubl12 recognition motif. Shown peptides were confirmed with ITC for interaction with Ubl12 with K_D -values of maximally $10 \mu\text{M}$ ^{16,34,37,81}. Residues in bold are confirmed anchors in the crystal structures, note that ICP0 and RNF169 seem to be reversed sequence-wise.

this mode of target recognition is unique to USP7⁵.

The C-terminal half of USP7 contains five ubiquitin-like domains, connected to the CD by an α -helix of 26 residues (PDB: 5FWI; Fig. 1b)^{16,22}. This helical element is proposed to have some influence on the positioning of the following Ubl domains, thereby altering the enzyme's activity²². The Ubl domains have the typical ubiquitin β -grasp fold, where five strands straddle the α -helix^{30,31}. Despite their very low sequence similarity, either to Ub or to each other (max 20%), the Ubls resemble each other with r.m.s.d.'s of maximal 2.9 \AA ¹⁶, similar to more conserved Ubl domains³². Their frequent occurrence in USPs²⁰ suggests regulatory roles, although the specific function may vary between different USPs³³.

Chapter 1. Regulation of USP7

The five Ubl domains of USP7 have a 2+1+2 structure, where Ubl12 (res. 562-771) and Ubl45 (res. 894-1102) combine to stable structural regions (Fig. 1a). Whereas the latter has a tail important for self-activation, Ubl12 serves as a binding spot for interactors^{16,34}. Crystallographic studies have identified DNMT1, UHRF1 and ICP0 to bind in an acidic pocket of Ubl2 (PDB: 4YOC, 4Z96, 5C6D, 4WPH; Fig. 2c)³⁴⁻³⁷. Using sequence alignment and affinity studies with derived peptides consensus binding motifs for Ubl12 (R/K-x-K or K-x-x-x-K) could be identified (Fig. 2d)^{34,35}. The site of binding, although far from the activating C-terminal tail, could modulate USP7 activity through allostery (Fig. 3a). The linker between Ubl12 and Ubl13 adopts variable conformations in crystal structures^{22,34}. Furthermore, flexibility between Ubl13 and Ubl45 is deduced from SAXS analysis¹⁶ and is required for successful folding back of the Ubl45 domain onto CD (Fig. 1b)^{21,22}. Binding of proteins within the Ubl region could stabilise these linkers, promoting either an active or inactive conformation of USP7.

Alterations like post-translational modifications (PTM) in the Ubl region could modulate USP7 activity. Several PTMs have been described for USP7; phosphorylation of S18 and S963, ubiquitination of K443 and K869 and acetylation of K1084 and K1099 among others (Fig. 1a)^{17,38-40}. Their effect on activity has not been described, except for the ubiquitination on K443,

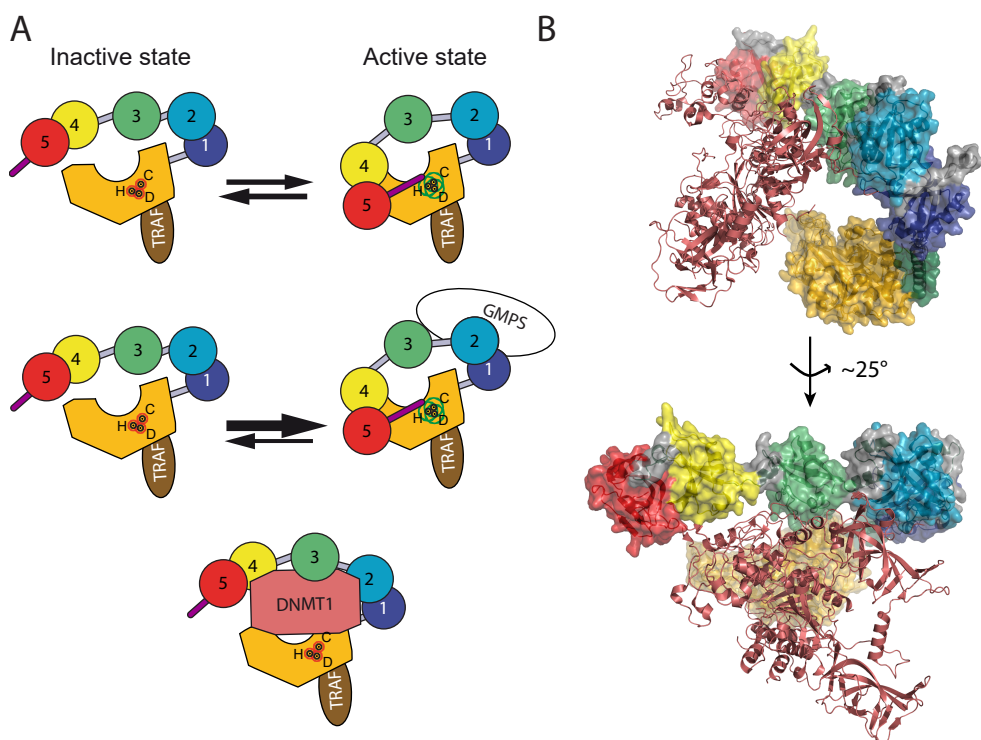


Figure 3: Ways of USP7 regulation. A. The allosteric activation by GMPS and the potential allosteric inhibition by DNMT1 of USP7 are both mediated through the Ubl domains. The active site residues (C, H, D) are highlighted in red (inactive conformation) or green (active). **B.** Model, based on the structure of DNMT1, solved in complex with Ubl12345 (4YOC) superposed on the CD123 structure (5FWI), suggests a relative position of DNMT1 (soft pink) and CD. In this conformation, DNMT1 may affect the ability of Ubl45 to interact with the CD (modelled here as in figure 1b), which would cause inhibition of activity.

within CD. This creates a binding scaffold for CBP, that can recruit HIF1- α for deubiquitination by USP7³⁸.

Modifications in the Ubl region, like K869Ub in Ubl3 or S963 phosphorylation in Ubl4, could potentially interfere with the folding back ability of Ubl45 to bind the CD, while acetylation in the C-terminal peptide⁴⁰ could prevent binding to the CD, modulating USP7 self-activation. The phosphorylation sites at S18 and S963 are located near protein-protein interaction regions and could affect interaction¹⁷. Further analysis of these PTMs is required to assess the extent of change of USP7 activity.

Aside from PTMs that could potentially modulate USP7 activity, a plethora of interacting proteins is described that could assert some USP7 modulation^{8,9}. Among the various regions of USP7: there are two interaction hotspots predominantly used by protein-USP7 interactions. The TRAF domain is predominantly used for target recognition (Fig. 2a), whereas the site on Ubl12 seems to be used for recruitment of interaction partners (Fig. 2c).

Among these interaction partners a surprisingly large number of E3 ubiquitin ligases is found, enzymes with the opposite activity to USP7¹. Such a DUB-E3 interaction may result in a complex that is protected from auto-ubiquitination, with predominant E3 ligase activity. Upon an external signal, the DUB may 'switch', shifting its activity from the E3 to its target, allowing the E3 to be degraded and protection of the target from degradation. This creates a rapid response to a signal, such as e.g. cellular stress. Throughout the text we will refer to this type of response as a 'switch': USP7 switches from being target-associated to forming a complex with the E3 ubiquitin ligase, or *vice versa*.. Here we discuss the E3-USP7 interactions on a biochemical level as well as the potential of these complexes to form a molecular switch.

The MDM2/p53 switch

The E3 ubiquitin ligase MDM2 targets the tumour suppressor p53 for degradation by the proteasome⁴¹. Levels of p53 are critical for transcriptional regulation of cellular fate after stress⁴². Both p53 and its E3 ubiquitin ligase MDM2 are thought to be targets of USP7^{43,44}. Under normal circumstances, USP7 associates with MDM2, possibly with help of adaptor protein DAXX⁴⁵ and/or acetylation of MDM2⁴⁶, to protect the E3 ubiquitin ligase from auto-ubiquitination. This allows MDM2 to ubiquitinate p53 for proteasomal degradation⁴⁷. Upon stress signals like DNA damage however, USP7 preferentially binds p53, stabilizing it through deubiquitination and allowing induction of the apoptosis pathway (Fig. 4a)^{45,48}.

Both MDM2 and p53 bind USP7 on the TRAF domain and co-crystal structures with peptides of both targets are available (PDB: 2FOJ, 2F1Y; Fig. 2a-b)^{23,24}. A secondary interaction site has been reported in USP7's Ubl region for both p53 and MDM2⁴⁹, but this interaction is hard to capture²¹. The shared binding site and cell biological data⁴³ indicate that USP7 regulates both MDM2 and p53 in a 'switch-like' manner (Fig. 4a)⁵⁰.

Other regulatory proteins can make USP7 switch from one complex to the other⁵¹. TSPYL5, known as a breast cancer risk protein, has been shown to disrupt the p53-USP7 complex⁵² and *in vivo* results suggest that ABRO1 (FAM175B), a member of the DUB complex BRISC, promotes the p53-USP7 complex, stabilising p53⁵³. On the other side of this molecular switch are proteins that affect the MDM2-USP7 interaction. *Ras* association domain-containing protein RASSF1A is a potential tumour suppressor that disrupts the association of USP7 to MDM2, allowing the latter to self-ubiquitinate and stabilising p53⁵⁴. The deacetylase SIRT1 has been shown to affect the interaction similarly; by deacetylating MDM2, the DUB USP7 can dissociate

Chapter 1. Regulation of USP7

and deubiquitinate p53⁴⁶. A positive regulator of the MDM2-USP7 complex, and thus p53 degradation, is the aforementioned DAXX⁴⁵, a protein that also has been found to sequester USP7 away from the target PTEN, resulting in higher levels of ubiquitinated PTEN⁵⁵. This set of proteins balances the p53/MDM2 axis through USP7⁵¹ and it would be interesting to see how these interactions change by modifications through, for instance, DNA damage signals.

USP7 forms an E3/target switch with DNMT1 and UHRF1

Another E3 ubiquitin ligase that interacts with USP7 is UHRF1, involved in DNA methylation maintenance³⁶. A recent crystal structure of USP7 with a peptide of UHRF1 (PDB: 5C6D) shows how UHRF1 binds onto a negative patch of Ubl12 (Fig. 2c)³⁶. Interestingly, a ubiquitination target of UHRF1, the methyltransferase DNMT1, also interacts with USP7³⁵. The crystal structure of the C-terminal part of DNMT1 in complex with Ubl12345 (PDB: 4YOC) shows that DNMT1 binds on the same patch of Ubl12, but also binds the third Ubl and has van der Waals contacts with Ubl45³⁵. The stability of DNMT1 depends on the E3 ubiquitin ligase UHRF1, that binds and ubiquitinates DNMT1^{56,57}. USP7 in turn, protects both UHRF1 and DNMT1 from ubiquitination, which stabilizes these proteins and promotes chromatin binding^{35,58}. The shared binding site on USP7 however indicates that DNMT1 and UHRF1 bind mutually exclusive to USP7 and suggests competition for this binding site on USP7⁵⁹.

Combining proteins with seemingly reciprocal activity together in a complex could indicate a cellular switch (Fig. 4b). USP7 controls both UHRF1 and DNMT1 via protection from proteasomal degradation, through the seemingly mutually exclusive binding site. Breaking up these USP7 complexes could therefore allow for degradation of the DNA methylation maintenance complex. This feature comes into play when cell cycle events require, for instance in late S-phase⁶⁰. This switch could be similar to that proposed for MDM2 and p53, with USP7 shifting from protection of the E3 ubiquitin ligase to protection of the target protein DNMT1 (Fig. 4b).

One potentially complicating factor comes to light when superposing the crystal structure of the USP7/DNMT1 complex (PDB: 4YOC) to that of Ubl45 bound to CD (PDB: 5JTV): Ubl4 clashes with DNMT1 in this position. This could potentially indicate that the DNMT1 is incompatible with USP7 activation, although the activation groove on CD is not blocked by DNMT1 (Fig. 3b). Therefore flexibility between Ubl domains and the tail could allow activation in the presence of DNMT1²¹. Analysis of the effect of DNMT1 interaction on USP7 activity will be interesting to study. Furthermore, whether UHRF1 has multiple interaction sites as well, and if this has any effect on USP7 activity remains unknown.

It has been shown that UHRF1/DNMT1/USP7 complexes are regulated through cell cycle-dependent phosphorylation⁶¹, acetylation by the histone acetyltransferase Tip60 (KAT5)⁵⁶ or association of DNA glycosylase, the methyl-CpG-binding domain protein MBD4⁶². These modifications could disrupt the complex and thereby allow modulation of USP7 function, making it a cell-cycle dependent USP7/E3/target complex. Nevertheless, many questions remain: a) how USP7 chooses between UHRF1 or DNMT1, b) whether they exist as a feedback complex and c) how the decision is made to promote degradation or protection of DNMT1.



1

1

1

1

Chapter 1. Regulation of USP7

This E3/DUB cooperativity allows for great control to keep optimal WASH activity.

Thus far no secondary interactors that influence this regulatory complex are known. The TRIM27/USP7 complex however has also been implicated in apoptosis, where TRIM27's ubiquitin ligase activity was shown to target USP7 at K869, with poly-ubiquitin chains of various linkage types. This probably creates a binding platform as it stabilizes the interaction with the cytoplasmic RIP1, allowing its subsequent deubiquitination³⁹. This ties the TRIM27/USP7 complex to TNF- α induced apoptosis⁶⁷.

It is not clear whether the functions of the TRIM27/USP7 complex are separated between control of WASH and stabilization of RIP1 or whether these two pathways influence each other. It would be interesting to see whether secondary interactors influence these tight balances, and the viral factor ICP0 seems a major candidate, as it was shown to interact with both TRIM27⁶⁸ and USP7⁶⁹.

USP7 complexes with a viral E3 ubiquitin ligase

Viruses, known for their hijacking of human proteins, also can create such E3/USP7 complexes. ICP0, is an E3 ubiquitin ligase from *herpes simplex*. Its interaction with USP7 gave it its original name, Herpes-Associated Ubiquitin-Specific Protease or HAUSP⁷⁰. ICP0 residues 617-629 interact with Ubl12^{34,69}, at the potential allosteric binding site also used by DNMT1 and UHRF1 (Fig. 2c-d).

The N-terminal region of ICP0 contains a RING-type E3 ubiquitin ligase domain⁷¹. USP7 prevents ICP0 auto-ubiquitination⁷² and suppresses viral infection responses⁷³. As ICP0 binds Ubl12 with a C-terminal part, it leaves both the E3 ubiquitin ligase domain of ICP0 and the USP domain of USP7 available for enzymatic action; indeed ICP0 does not modulate USP7-activity⁷⁴. Interestingly, the E3 ubiquitin ligase activity of ICP0 is directed towards TRIM27⁶⁸, possibly interfering with the aforementioned TRIM27/USP7 complex (Fig. 4c). The hijacking of USP7 by ICP0 evidently suppresses viral infection response, but doesn't seem to have major effects on other USP7 complexes⁷⁵. This modulation is apparently subtle enough to not disturb the other functions of USP7, leaving a functioning host cell.

USP7/E3 complexes in DNA damage signalling and repair

USP7 has been implicated in DNA repair through its interaction with E3 ubiquitin ligase Rad18 and PCNA^{76,77}. USP7 can deubiquitinate both PCNA⁷⁸ and RAD18⁷⁶, the E3 ubiquitin ligase responsible for this ubiquitination⁷⁹. The exact interaction with PCNA hasn't been characterized, but for RAD18 it seems that the TRAF domain recognizes a PSTS motif (Fig. 2b) at residues 191-194⁷⁶. This way USP7 protects the E3 ubiquitin ligase from auto-ubiquitination, allowing ubiquitination of PCNA⁷⁷. As the DUB targets both the E3 ubiquitin ligase and its target, it makes this triad look like a cellular switch similar to p53/MDM2/USP7 (Fig. 4d). The details are however less defined, as we don't know whether RAD18 or PCNA can alter the deubiquitinating activity or what triggers the switching. Additional modulators might be in place to tip this balance upon DNA damage.

Furthermore, USP7 interacts with the E3 ubiquitin ligase RNF168, responsible for ubiquitination on H2A in DNA damage response⁸⁰. Although the binding site on RNF168 is still unknown, this interaction is mediated through the Ubl12 domain of USP7 and is shown to stabilize RNF168, protecting it from auto-ubiquitination (Fig. 4e)⁸⁰. During submission of this review a paper was

published describing the interaction of USP7 with RNF169, a paralogue of RNF168, resulting in protection from auto-ubiquitination of this E3 ubiquitin ligase⁸¹. This crystal structure (PDB: 5GG4) showed that RNF169 uses the conserved binding motif for interaction with Ubl12 (Fig. 2c-d), which could help to pinpoint the interaction site for RNF168 as well.

It would be interesting to see if the USP7/E3 complex functions as a type of ‘switch’, for instance after a DNA damage signal. For such a switch both components require the same target, but thus far there is no evidence showing that H2A K13 and K15, the target of RNF168, can be deubiquitinated by USP7. Furthermore, it is unknown whether RNF168 affects USP7 activity and what signals are required to engage these two proteins.

USP7 and polycomb group proteins

USP7 stabilizes E3 ubiquitin ligases in the polycomb repressive complex 1 (PRC1)^{82,83}. The PRC1 complex can be made up with various components⁸⁴, but USP7 seemingly interacts directly with the common PRC1 component RING1B (RNF2)⁸². The interacting domain of USP7 is still unknown, but the complex seems to require the intact RING domain of the PRC1 protein RING1B⁸³. However, if RING1B is complexed to BMI1 or MEL18 (PCGF2), this direct interaction seems very unlikely⁸⁵. For these PRC1 complexes the interaction with USP7 is bridged by SCML2⁸⁶. SCML2 binds the TRAF domain through its N-terminal MBT-DUF domain⁸⁵ and bridges between USP7 and PRC1 complex components BMI1 and MEL18 via PHC1⁸⁷. SCML2 is reported to co-purify with all components of PRC1 and seems required for the co-localisation of USP7 to the polycomb complex⁸⁵. However, it doesn’t recruit USP7 to RING1B-only PRC complexes, so perhaps another bridging protein may be involved here⁸⁵, or the RING1B-USP7 interaction is direct⁸³.

The association of USP7 to PRC1 does not have the exact same characteristics of the MDM2/USP7 switch: the target of PRC1, H2A K119, does not seem to be deubiquitinated by USP7^{88,89}. Rather, USP7 promotes the placement of this mark as it protects the RING domains from self-ubiquitination (Fig. 4e)⁸³ and depletion of USP7 lowers the levels of H2A ubiquitination⁸⁵. That said, disruption of the PRC1-USP7 interaction could function as a switch⁹⁰. Further research will most probably find factors that disturb this complexation, inhibiting PRC1-mediated gene repression.

BRISC and/or BRCA1-A complex

USP7 can also interact with another DUB, the metalloprotease BRCC36 (BRCC3), part of the larger, BRISC complex⁹¹. Consequently, USP7 has been found to interact with proteins from this cytoplasmic complex (BABAM1, BRE, BRCC36 and ABRO1) in a mass spectroscopy screen⁸, but through which domains remains unclear. Only for ABRO1 interactions with USP7 have been shown *in vitro*, resulting in an effect on p53-deubiquitination by USP7⁵³. Where in the cell the USP7 interaction with the cytoplasmic ABRO1 takes place and how it affects the nuclear p53 protein requires further research. The nuclear counterpart of BRISC, the BRCA1-A complex, with ABRO1 substituted with the nuclear Abraxas (FAM175A)⁹², could be involved. This complex would entail two DUB moieties (USP7 and BRCC36) as well as ubiquitin ligase activity in the subunit BRCA1⁹³. Further investigation is required to find out whether USP7 is required at a BRCA1-associated DNA break⁹⁴. These interactions may indicate yet another way in which USP7 is involved the DNA damage response.

Chapter 1. Regulation of USP7

Activity modulation by GMPS

One USP7 interactor that directly influences USP7 activity is the metabolic enzyme Guanine MonoPhosphate Synthetase (GMPS)^{16,95}. GMPS interacts with Ubl12 (Fig. 2d) with two conserved lysines (K321, K326)³⁴ and thereby allosterically activates the enzyme. By binding onto Ubl12 it is thought to positively influence the folding back of Ubl45 onto the CD^{16,34}. This favours the active conformation where Ubl45 can activate the catalytic domain, resulting in an increase in catalytic efficiency. As GMPS doesn't affect K_M -values, a model has been proposed where it shifts the active/inactive equilibrium of USP7 towards the catalytically competent state (Fig. 3a)¹⁶.

This 'hyperactivation' (an extra activation over the self-activation) by GMPS could have a regulatory role in cells. Indeed, for proper deubiquitination of nuclear targets, such as H2B or p53, GMPS is required^{88,96}. Studies have shown that not the enzymatic activity of GMPS is essential for this hyperactivation, but rather its cellular location⁹⁶. The cellular location of GMPS is controlled through its ubiquitination by the E3 ubiquitin ligase TRIM21, but there is no evidence this E3 ubiquitin ligase also complexes with USP7. It merely retains GMPS in the cytoplasm under normal conditions through ubiquitination, with genomic stress however, GMPS can accumulate in the nucleus and influence USP7 activity in the MDM2/p53 complex. This cytoplasmic-nuclear partitioning of GMPS can be considered a switch for activity of nuclear USP7⁹⁶, where GMPS hyperactivates through the interaction with Ubl12.

Furthermore USP7 interacts with the UV-stimulated scaffold protein A (UVSSA) in transcription-coupled nucleotide excision repair (TC-NER)^{97,98}, via its TRAF domain. This protects UVSSA from proteasomal degradation⁹⁹, but interestingly the association of the two factors has an effect on the deubiquitinating activity of USP7 *in vitro*⁹⁹. Although the affinity for a minimal substrate remains the same, the catalytic turnover drops: a hint that USP7 activity needs modulation in TC-NER.

A long, yet undefined list of USP7 interactors

Besides the complexes and interactors mentioned above, there is a long list of proteins that have been implicated to interact with USP7⁸. These proteins could of course be targets of USP7, but could also make up new, yet unknown, complexes.

Many of these are E3 ubiquitin ligases, including MARCH7 that uses USP7 to prevent auto-ubiquitination¹⁰⁰, and RNF220 that complexes with the TRAF domain, promoting deubiquitination of β -catenin in the Wnt pathway¹⁰¹. HECTH9/HUWE1 ubiquitinates USP7 itself under hypoxia, and thereby allows for CBP binding and subsequent HIF1- α deubiquitination^{8,38}. Similar to E3 ubiquitin ligase complexes that have been studied in more detail, these ubiquitin ligase interactions could use USP7 for protection against self-ubiquitination or to recruit them into a switch-like complex, having both ubiquitination and deubiquitination at the ready in stressful circumstances.

In addition to the E3 ubiquitin ligase complexes there are also other USP7 interactors with functions in the ubiquitin pathway, such as UbE2E1¹⁰² and USP11⁸². USP7 binds UbE2E1 N-terminal part with its TRAF domain (PDB: 4JJQ), suggesting it is a target for deubiquitination²⁸. Indeed, USP7 attenuates UbE2E1 by counteracting its poly-ubiquitin chains²⁸. Interestingly, this E2 is also implied in PRC1 complexes¹⁰². Within the same PRC pathway, USP11 was also picked up as an USP7 interactor⁸². This interaction has been picked up in a screen⁸, but whether it's direct and what function it has is still under investigation.

USP7 is also interacting with viral proteins without ubiquitin ligase activity. EBNA-1 (from Epstein-Barr virus; PDB: 1YY6) as well as vIRF-1 (PDB 4YSI), vIRF-4 (PDB:2XXN) and LANA (all from Kaposi's Sarcoma-associated Herpes Virus) bind USP7 at the TRAF domain (Fig. 2a-b)^{103–105}, and could therefore influence deubiquitination of targets like p53 and MDM2. Although the affinity of the TRAF is much higher for these viral interactors than for p53 or MDM2¹⁰⁴, there seems to be no effect on p53 upon infection¹⁰⁵. This could suggest that the viruses employ another cellular function of USP7. Interestingly, LANA and vIRF-4 seem to have a secondary interaction site on USP7, presumably on the CD¹⁰⁴. This could mean that, apart from sequestering USP7, these viral proteins modulate USP7 activity.

The USP7 interactor list furthermore contains various targets of its DUB activity as well as not fully characterized interactors. These targets imply USP7 in various pathways, such as DNA replication through the association with MCM-BP (PDB: 4KG9; Fig. 2a-b)²⁵, or in the development of regulatory T cells by the deubiquitination of FOXP3¹⁰⁶. Thus far, only information is available on such target-DUB interaction, but not whether such a complex regulates USP7 and these targets are therefore outside of the scope of this review. Obviously, as research progresses, these interactors could have an impact on (allosteric) regulation of USP7 activity.

USP7 inhibitors

Due to its importance in various pathways USP7 is an interesting target for drug development⁵¹. As USP7 is an important player in many pathways, disturbing one may lead to (undesirable) effects in the other¹⁰⁷. Nevertheless, now that first-generation USP7 inhibitors have been developed¹⁰⁸, they can also aid in understanding USP7 function¹⁰⁹. These small molecule inhibitors are mostly discovered through DUB activity profiling¹¹⁰ and further developed to be specific for USP7^{111,112}. Others approached the inhibitor search from the substrate point of view: by developing ubiquitin variants with increased affinity for the DUB, these could function as USP inhibitors¹¹³ with good specificity for USP7¹¹⁴.

The resulting inhibitors are promising but seem to have effects outside the targeted MDM2/p53 pathway^{115,116}. This shows that the different complexes of USP7 are targeted, resulting in potentially unwanted outcomes. Substrate-derived inhibitors could be a potential answer, but whether these can discern different USP7 complexes is yet unknown. Better understanding of the various complexes can aid in development of selective drugs directed to a subset of USP7 complexes. If one can selectively inhibit USP7 in one particular complex, it may result in better defined targeting. Using the described wealth of information on allosteric regulation of USP7 could allow inhibition of USP7 right where it is most needed.

Chapter 1. Regulation of USP7

Conclusion and Outlook

In this review we described how USP7, one of the most studied DUBs, has a self-activating mechanism, one that can be allosterically modulated, either by inhibition or by stabilization of the active state. Apart from this type of regulation, USP7 also seems to be regulated by complex formation. These complexes can recruit USP7 to their preferred location, regulating USP7 through localisation. Many of these complexes contain E3 ubiquitin ligase activity, seemingly counteracting USP7's DUB activity. Such a USP7/E3 'switch' allows for rapid feedback upon cellular signals like DNA damage. Accessory proteins that associate with the complex, allow fine-tuning of the E3 and USP7 activity. These ternary complexes could be a way to selectively study or inhibit the various roles of USP7.

Acknowledgements

The authors would like to acknowledge KWF (grant number 2012-5398) for funding and thank Andrea Murachelli, Roy Baas and Shreya Dharadhar for critical reading of the manuscript.

References

- [1] Pickart, C.M. and Eddins, M.J. Ubiquitin: structures, functions, mechanisms. *Biochimica et Biophysica Acta* **1695** 2004, 55–72. <https://doi.org/10.1016/j.bbamcr.2004.09.019>
- [2] Komander, D. and Rape, M. The ubiquitin code. *Annual Review of Biochemistry* **81** 2012, 203–29. <https://doi.org/10.1146/annurev-biochem-060310-170328>
- [3] Pickart, C.M. Ubiquitin in chains. *Trends in Biochemical Sciences* **25** 2000, 544–8.
- [4] Clague, M.J., Barsukov, I., Coulson, J.M., Liu, H., Rigden, D.J. and Urbe, S. Deubiquitylases From Genes to Organism. *Physiological Reviews* **93** 2013, 1289–315. <https://doi.org/10.1152/physrev.00002.2013>
- [5] Komander, D., Clague, M.J. and Urbé, S. Breaking the chains: structure and function of the deubiquitinases. *Nature Reviews Molecular Cell Biology* Nature Publishing Group. **10** 2009, 550–63. <https://doi.org/10.1038/nrm2731>
- [6] Sahtoe, D.D. and Sixma, T.K. Layers of DUB regulation. *Trends in Biochemical Sciences* **40** 2015, 456–67. <https://doi.org/10.1016/j.tibs.2015.05.002>
- [7] Nijman, S.M.B., Luna-Vargas, M.P. a, Velds, A., Brummelkamp, T.R., Dirac, A.M.G., Sixma, T.K. and Bernards, R. A genomic and functional inventory of deubiquitinating enzymes. *Cell* **123** 2005, 773–86. <https://doi.org/10.1016/j.cell.2005.11.007>
- [8] Sowa, M.E., Bennett, E.J., Gygi, S.P. and Harper, J.W. Defining the human deubiquitinating enzyme interaction landscape. *Cell Elsevier Ltd.* **138** 2009, 389–403. <https://doi.org/10.1016/j.cell.2009.04.042>
- [9] Kessler, B.M., Fortunati, E., Melis, M., Pals, C.E.G.M., Clevers, H. and Maurice, M.M. Proteome Changes Induced by Knock-Down of the Deubiquitylating Enzyme HAUSP/USP7. *Journal of Proteome Research* **6** 2007, 4163–72. <https://doi.org/10.1021/pr0702161>
- [10] Cummins, J.M. and Vogelstein, B. HAUSP is required for p53 destabilization. *Cell Cycle (Georgetown, Tex)* **3** 2004, 689–92. <https://doi.org/10.4161/cc.3.6.924>
- [11] McClurg, U.L. and Robson, C.N. Deubiquitinating enzymes as oncotargets. *Oncotarget* **6** 2015, 9657–68. <https://doi.org/10.18632/oncotarget.3922>
- [12] Lecona, E., Rodriguez-Acebes, S., Specks, J., Lopez-Contreras, A.J., Ruppen, I., Murga, M., Muñoz, J., Mendez, J. and Fernandez-Capetillo, O. USP7 is a SUMO deubiquitinase essential for DNA replication. *Nature Structural & Molecular Biology* **23** 2016, 270–7. <https://doi.org/10.1038/nsmb.3185>
- [13] Hao, Y.-H., Fountain, M.D., Fon Tacer, K., Xia, F., Bi, W., Kang, S.-H.L., Patel, A., Rosenfeld, J.A., Le Caignec, C., Isidor, B., Krantz, I.D., Noon, S.E., Pfotenhauer, J.P., Morgan, T.M., Moran, R., Pedersen, R.C., Saenz, M.S., Schaaf, C.P. and Potts, P.R. USP7 Acts as a Molecular Rheostat to Promote WASH-Dependent Endosomal Protein Recycling and Is Mutated in a Human Neurodevelopmental Disorder. *Molecular Cell* **59** 2015, 956–69. <https://doi.org/10.1016/j.molcel.2015.07.033>
- [14] Kon, N., Kobayashi, Y., Li, M., Brooks, C.L., Ludwig, T. and Gu, W. Inactivation of HAUSP in vivo modulates p53 function. *Oncogene* **29** 2010, 1270–9. <https://doi.org/10.1038/onc.2009.427>

- [15] Kon, N., Zhong, J., Kobayashi, Y., Li, M., Szabolcs, M., Ludwig, T., Canoll, P.D. and Gu, W. Roles of HAUSP-mediated p53 regulation in central nervous system development. *Cell Death and Differentiation* **18** 2011, 1366–75. <https://doi.org/10.1038/cdd.2011.12>
- [16] Faesen, A.C., Dirac, A.M.G., Shanmugham, A., Ovaa, H., Perrakis, A. and Sixma, T.K. Mechanism of USP7/HAUSP activation by its C-terminal ubiquitin-like domain and allosteric regulation by GMP-synthetase. *Molecular Cell Elsevier Inc.* **44** 2011, 147–59. <https://doi.org/10.1016/j.molcel.2011.06.034>
- [17] Fernández-Montalván, A., Bouwmeester, T., Joberty, G., Mader, R., Mahnke, M., Pierrat, B., Schlaeppli, J.-M., Worpenberg, S. and Gerhartz, B. Biochemical characterization of USP7 reveals post-translational modification sites and structural requirements for substrate processing and subcellular localization. *The FEBS Journal* **274** 2007, 4256–70. <https://doi.org/10.1111/j.1742-4658.2007.05952.x>
- [18] Pang, C.N.I., Hayen, A. and Wilkins, M.R. Surface Accessibility of Protein Post-Translational Modifications. *Journal of Proteome Research* **6** 2007, 1833–45. <https://doi.org/10.1021/pr060674u>
- [19] Hu, M., Li, P., Li, M., Li, W., Yao, T., Wu, J.-W., Gu, W., Cohen, R.E. and Shi, Y. Crystal Structure of a UBP-Family Deubiquitinating Enzyme in Isolation and in Complex with Ubiquitin Aldehyde. *Cell* **111** 2002, 1041–54. [https://doi.org/10.1016/S0092-8674\(02\)01199-6](https://doi.org/10.1016/S0092-8674(02)01199-6)
- [20] Zhu, X., Ménard, R. and Sulea, T. High incidence of ubiquitin-like domains in human ubiquitin-specific proteases. *Proteins: Structure, Function, and Bioinformatics* **69** 2007, 1–7. <https://doi.org/10.1002/prot.21546>
- [21] Rougé, L., Bainbridge, T.W., Kwok, M., Tong, R., Di Lello, P., Wertz, I.E., Maurer, T., Ernst, J.A. and Murray, J. Molecular Understanding of USP7 Substrate Recognition and C-Terminal Activation. *Structure* **24** 2016, 1335–45. <https://doi.org/10.1016/j.str.2016.05.020>
- [22] Kim, R.Q., van Dijk, W.J. and Sixma, T.K. Structure of USP7 catalytic domain and three Ubl-domains reveals a connector α -helix with regulatory role. *Journal of Structural Biology* **195** 2016, 11–8. <https://doi.org/10.1016/j.jsb.2016.05.005>
- [23] Sheng, Y., Saridakis, V., Sarkari, F., Duan, S., Wu, T., Arrowsmith, C.H. and Frappier, L. Molecular recognition of p53 and MDM2 by USP7/HAUSP. *Nature Structural & Molecular Biology* **13** 2006, 285–91. <https://doi.org/10.1038/nsmb1067>
- [24] Hu, M., Gu, L., Li, M., Jeffrey, P.D., Gu, W. and Shi, Y. Structural basis of competitive recognition of p53 and MDM2 by HAUSP/USP7: implications for the regulation of the p53-MDM2 pathway. *PLoS Biology* **4** 2006, e27. <https://doi.org/10.1371/journal.pbio.0040027>
- [25] Jagannathan, M., Nguyen, T., Gallo, D., Luthra, N., Brown, G.W., Saridakis, V. and Frappier, L. A Role for USP7 in DNA Replication. *Molecular and Cellular Biology* **34** 2014, 132–45. <https://doi.org/10.1128/MCB.00639-13>
- [26] Ye, H., Park, Y.C., Kreishman, M., Kieff, E. and Wu, H. The structural basis for the recognition of diverse receptor sequences by TRAF2. *Molecular Cell* **4** 1999, 321–30.
- [27] Saridakis, V., Sheng, Y., Sarkari, F., Holowaty, M.N., Shire, K., Nguyen, T., Zhang, R.G., Liao, J., Lee, W., Edwards, A.M., Arrowsmith, C.H. and Frappier, L. Structure of the p53 binding domain of HAUSP/USP7 bound to Epstein-Barr nuclear antigen 1 implications for EBV-mediated immortalization. *Molecular Cell* **18** 2005, 25–36. <https://doi.org/10.1016/j.molcel.2005.02.029>
- [28] Sarkari, F., Wheaton, K., La Delfa, A., Mohamed, M., Shaikh, F., Khatun, R., Arrowsmith, C.H., Frappier, L., Saridakis, V. and Sheng, Y. Ubiquitin-specific Protease 7 Is a Regulator of Ubiquitin-conjugating Enzyme Ube2E1. *Journal of Biological Chemistry* **288** 2013, 16975–85. <https://doi.org/10.1074/jbc.M113.469262>
- [29] Zapata, J.M., Pawlowski, K., Haas, E., Ware, C.F., Godzik, A. and Reed, J.C. A Diverse Family of Proteins Containing Tumor Necrosis Factor Receptor-associated Factor Domains. *Journal of Biological Chemistry* **276** 2001, 24242–52. <https://doi.org/10.1074/jbc.M100354200>
- [30] Vijay-Kumar, S., Bugg, C.E. and Cook, W.J. Structure of ubiquitin refined at 1.8 Å resolution. *Journal of Molecular Biology* **194** 1987, 531–44.
- [31] Kiel, C. and Serrano, L. The ubiquitin domain superfold: structure-based sequence alignments and characterization of binding epitopes. *Journal of Molecular Biology* **355** 2006, 821–44. <https://doi.org/10.1016/j.jmb.2005.10.010>
- [32] Faesen, A.C., Luna-Vargas, M.P.A. and Sixma, T.K. The role of UBL domains in ubiquitin-specific proteases. *Biochemical Society Transactions* **40** 2012, 539–45. <https://doi.org/10.1042/BST20120004>

Chapter 1. Regulation of USP7

- [33] Clerici, M., Luna-Vargas, M.P.A., Faesen, A.C. and Sixma, T.K. The DUSP-Ubl domain of USP4 enhances its catalytic efficiency by promoting ubiquitin exchange. *Nature Communications* **5** 2014, 5399. <https://doi.org/10.1038/ncomms6399>
- [34] Pfoh, R., Lacdao, I.K., Georges, A.A., Capar, A., Zheng, H., Frappier, L. and Saridakis, V. Crystal Structure of USP7 Ubiquitin-like Domains with an ICPO Peptide Reveals a Novel Mechanism Used by Viral and Cellular Proteins to Target USP7. *PLoS Pathogens* **11** 2015, e1004950. <https://doi.org/10.1371/journal.ppat.1004950>
- [35] Cheng, J., Yang, H., Fang, J., Ma, L., Gong, R., Wang, P., Li, Z. and Xu, Y. Molecular mechanism for USP7-mediated DNMT1 stabilization by acetylation. *Nature Communications* **6** 2015, 7023. <https://doi.org/10.1038/ncomms8023>
- [36] Zhang, Z.-M., Rothbart, S.B., Allison, D.F., Cai, Q., Harrison, J.S., Li, L., Wang, Y., Strahl, B.D., Wang, G.G. and Song, J. An Allosteric Interaction Links USP7 to Deubiquitination and Chromatin Targeting of UHRF1. *Cell Reports* **12** 2015, 1400–6. <https://doi.org/10.1016/j.celrep.2015.07.046>
- [37] Cheng, J., Li, Z., Gong, R., Fang, J., Yang, Y., Sun, C., Yang, H. and Xu, Y. Molecular mechanism for the substrate recognition of USP7. *Protein & Cell* Springer. **6** 2015, 849–52. <https://doi.org/10.1007/s13238-015-0192-y>
- [38] Wu, H.-T., Kuo, Y.-C., Hung, J.-J., Huang, C.-H., Chen, W.-Y., Chou, T.-Y., Chen, Y.-J.Y.-J., Chen, Y.-J.Y.-J., Chen, Y.-J.Y.-J., Cheng, W.-C., Teng, S.-C. and Wu, K.-J. K63-polyubiquitinated HAUSP deubiquitinates HIF-1 α and dictates H3K56 acetylation promoting hypoxia-induced tumour progression. *Nature Communications* **7** 2016, 13644. <https://doi.org/10.1038/ncomms13644>
- [39] Zaman, M.M.-U., Nomura, T., Takagi, T., Okamura, T., Jin, W., Shinagawa, T., Tanaka, Y. and Ishii, S. Ubiquitination-Deubiquitination by the TRIM27-USP7 Complex Regulates Tumor Necrosis Factor Alpha-Induced Apoptosis. *Molecular and Cellular Biology* **33** 2013, 4971–84. <https://doi.org/10.1128/MCB.00465-13>
- [40] Choudhary, C., Kumar, C., Gnad, F., Nielsen, M.L., Rehman, M., Walther, T.C., Olsen, J. V. and Mann, M. Lysine acetylation targets protein complexes and co-regulates major cellular functions. *Science (New York, NY)* **325** 2009, 834–40. <https://doi.org/10.1126/science.1175371>
- [41] Prives, C. Signaling to p53: breaking the MDM2-p53 circuit. *Cell* **95** 1998, 5–8.
- [42] Joerger, A.C. and Fersht, A.R. Structural biology of the tumor suppressor p53. *Annual Review of Biochemistry* **77** 2008, 557–82. <https://doi.org/10.1146/annurev.biochem.77.060806.091238>
- [43] Li, M., Brooks, C.L., Kon, N. and Gu, W. A dynamic role of HAUSP in the p53-Mdm2 pathway. *Molecular Cell* **13** 2004, 879–86.
- [44] Cummins, J.M., Rago, C., Kohli, M., Kinzler, K.W., Lengauer, C. and Vogelstein, B. Tumour suppression: Disruption of HAUSP gene stabilizes p53. *Nature* **428** 2004, 486–7. <https://doi.org/10.1038/nature02501>
- [45] Tang, J., Qu, L.-K., Zhang, J., Wang, W., Michaelson, J.S., Degenhardt, Y.Y., El-Deiry, W.S. and Yang, X. Critical role for Daxx in regulating Mdm2. *Nature Cell Biology* **8** 2006, 855–62. <https://doi.org/10.1038/ncb1442>
- [46] Nihira, N.T., Ogura, K., Shimizu, K., North, B.J., Zhang, J., Gao, D., Inuzuka, H. and Wei, W. Acetylation-dependent regulation of MDM2 E3 ligase activity dictates its oncogenic function. *Science Signaling* **10** 2017, eaai8026. <https://doi.org/10.1126/scisignal.aai8026>
- [47] Brooks, C.L. and Gu, W. p53 Ubiquitination: Mdm2 and Beyond. *Molecular Cell* **21** 2006, 307–15. <https://doi.org/10.1016/j.molcel.2006.01.020>
- [48] Meulmeester, E., Maurice, M.M., Boutell, C., Teunisse, A.F.A.S.A.S., Ovaa, H., Abraham, T.E., Dirks, R.W. and Jochemsen, A.G. Loss of HAUSP-mediated deubiquitination contributes to DNA damage-induced destabilization of Hdmx and Hdm2. *Molecular Cell* **18** 2005, 565–76. <https://doi.org/10.1016/j.molcel.2005.04.024>
- [49] Ma, J., Martin, J.D., Xue, Y., Lor, L.A., Kennedy-Wilson, K.M., Sinnamon, R.H., Ho, T.F., Zhang, G., Schwartz, B., Tummino, P.J. and Lai, Z. C-terminal region of USP7/HAUSP is critical for deubiquitination activity and contains a second mdm2/p53 binding site. *Archives of Biochemistry and Biophysics* **503** 2010, 207–12. <https://doi.org/10.1016/j.abb.2010.08.020>
- [50] Brazhnik, P. and Kohn, K.W. HAUSP-regulated switch from auto- to p53 ubiquitination by Mdm2 (in silico discovery). *Mathematical Biosciences* **210** 2007, 60–77. <https://doi.org/10.1016/j.mbs.2007.05.005>
- [51] Tavana, O. and Gu, W. Modulation of the p53/MDM2 interplay by HAUSP inhibitors. *Journal of Molecular Cell Biology* Oxford University Press. **9** 2017, 45–52. <https://doi.org/10.1093/jmcb/mjw049>

- [52] Epping, M.T., Meijer, L.A.T., Krijgsman, O., Bos, J.L., Pandolfi, P.P. and Bernards, R. TSPYL5 suppresses p53 levels and function by physical interaction with USP7. *Nature Cell Biology* **13** 2011, 102–8. <https://doi.org/10.1038/ncb2142>
- [53] Zhang, J., Cao, M., Dong, J., Li, C., Xu, W., Zhan, Y., Wang, X., Yu, M., Ge, C., Ge, Z. and Yang, X. ABRQ1 suppresses tumorigenesis and regulates the DNA damage response by stabilizing p53. *Nature Communications* **5** 2014, 5059. <https://doi.org/10.1038/ncomms6059>
- [54] Song, M.S., Song, S.J., Kim, S.Y., Oh, H.J. and Lim, D.-S. The tumour suppressor RASSF1A promotes MDM2 self-ubiquitination by disrupting the MDM2–DAXX–HAUSP complex. *The EMBO Journal* European Molecular Biology Organization. **27** 2008, 1863–74. <https://doi.org/10.1038/emboj.2008.115>
- [55] Song, M.S., Salmena, L., Carracedo, A., Egia, A., Lo-Coco, F., Teruya-Feldstein, J. and Pandolfi, P.P. The deubiquitinylation and localization of PTEN are regulated by a HAUSP–PML network. *Nature* **455** 2008, 813–7. <https://doi.org/10.1038/nature07290>
- [56] Du, Z., Song, J., Wang, Y., Zhao, Y., Guda, K., Yang, S., Kao, H.-Y.H.-Y., Xu, Y., Willis, J., Markowitz, S.D., Sedwick, D., Ewing, R.M. and Wang, Z. DNMT1 stability is regulated by proteins coordinating deubiquitination and acetylation-driven ubiquitination. *Science Signaling* **3** 2010, ra80. <https://doi.org/10.1126/scisignal.2001462>
- [57] Qin, W., Leonhardt, H. and Spada, F. Usp7 and Uhrf1 control ubiquitination and stability of the maintenance DNA methyltransferase Dnmt1. *Journal of Cellular Biochemistry* **112** 2011, 439–44. <https://doi.org/10.1002/jcb.22998>
- [58] Felle, M., Joppien, S., Németh, A., Diermeier, S., Thalhammer, V., Dobner, T., Kremmer, E., Kappler, R., Längst, G., Nemeth, A., Diermeier, S., Thalhammer, V., Dobner, T., Kremmer, E., Kappler, R. and Langst, G. The USP7/Dnmt1 complex stimulates the DNA methylation activity of Dnmt1 and regulates the stability of UHRF1. *Nucleic Acids Research* **39** 2011, 8355–65. <https://doi.org/10.1093/nar/gkr528>
- [59] Rothbart, S.B., Dickson, B.M., Ong, M.S., Krajewski, K., Houliston, S., Kireev, D.B., Arrowsmith, C.H. and Strahl, B.D. Multivalent histone engagement by the linked tandem Tudor and PHD domains of UHRF1 is required for the epigenetic inheritance of DNA methylation. *Genes & Development* **27** 2013, 1288–98. <https://doi.org/10.1101/gad.220467.113>
- [60] Bronner, C. Control of DNMT1 Abundance in Epigenetic Inheritance by Acetylation, Ubiquitylation, and the Histone Code. *Science Signaling* **4** 2011, pe3–pe3. <https://doi.org/10.1126/scisignal.2001764>
- [61] Ma, H., Chen, H., Guo, X., Wang, Z., Sowa, M.E., Zheng, L., Hu, S., Zeng, P., Guo, R., Diao, J., Lan, F., Harper, J.W., Shi, Y.G., Xu, Y. and Shi, Y. M phase phosphorylation of the epigenetic regulator UHRF1 regulates its physical association with the deubiquitylase USP7 and stability. *Proceedings of the National Academy of Sciences* **109** 2012, 4828–33. <https://doi.org/10.1073/pnas.1116349109>
- [62] Meng, H., Harrison, D.J. and Meehan, R.R. MBD4 Interacts With and Recruits USP7 to Heterochromatic Foci. *Journal of Cellular Biochemistry* **116** 2015, 476–85. <https://doi.org/10.1002/jcb.25001>
- [63] Hao, Y.-H., Doyle, J.M., Ramanathan, S., Gomez, T.S., Jia, D., Xu, M., Chen, Z.J., Billadeau, D.D., Rosen, M.K. and Potts, P.R. Regulation of WASH-dependent actin polymerization and protein trafficking by ubiquitination. *Cell* NIH Public Access. **152** 2013, 1051–64. <https://doi.org/10.1016/j.cell.2013.01.051>
- [64] Doyle, J.M., Gao, J., Wang, J., Yang, M. and Potts, P.R. MAGE-RING protein complexes comprise a family of E3 ubiquitin ligases. *Molecular Cell* **39** 2010, 963–74. <https://doi.org/10.1016/j.molcel.2010.08.029>
- [65] Schaaf, C.P., Gonzalez-Garay, M.L., Xia, F., Potocki, L., Gripp, K.W., Zhang, B., Peters, B.A., McElwain, M.A., Drmanac, R., Beaudet, A.L., Caskey, C.T. and Yang, Y. Truncating mutations of MAGEL2 cause Prader-Willi phenotypes and autism. *Nature Genetics* **45** 2013, 1405–8. <https://doi.org/10.1038/ng.2776>
- [66] Mercer, R.E., Kwolek, E.M., Bischof, J.M., van Eede, M., Henkelman, R.M. and Wevrick, R. Regionally reduced brain volume, altered serotonin neurochemistry, and abnormal behavior in mice null for the circadian rhythm output gene Magel2. *American Journal of Medical Genetics Part B, Neuropsychiatric Genetics : The Official Publication of the International Society of Psychiatric Genetics* **150B** 2009, 1085–99. <https://doi.org/10.1002/ajmg.b.30934>
- [67] Bertrand, M.J.M., Milutinovic, S., Dickson, K.M., Ho, W.C., Boudreault, A., Durkin, J., Gillard, J.W., Jaquith, J.B., Morris, S.J. and Barker, P.A. cIAP1 and cIAP2 facilitate cancer cell survival by functioning as E3 ligases that promote RIP1 ubiquitination. *Molecular Cell* **30** 2008, 689–700. <https://doi.org/10.1016/j.molcel.2008.05.014>
- [68] Conwell, S.E., White, A.E., Harper, J.W. and Knipe, D.M. Identification of TRIM27 as a Novel Degradation Target of Herpes Simplex Virus 1 ICPO. Sandri-Goldin RM, editor. *Journal of Virology* **89** 2015, 220–9. <https://doi.org/10.1128/JVI.02635-14>

Chapter 1. Regulation of USP7

- [69] Pozhidaeva, A.K., Mohni, K.N., Dhe-Paganon, S., Arrowsmith, C.H., Weller, S.K., Korzhnev, D.M. and Bezsonova, I. Structural Characterization of Interaction between Human Ubiquitin-specific Protease 7 and Immediate-Early Protein ICP0 of Herpes Simplex Virus-1. *Journal of Biological Chemistry* **290** 2015, 22907–18. <https://doi.org/10.1074/jbc.M115.664805>
- [70] Everett, R.D., Meredith, M., Orr, A., Cross, A., Kathoria, M. and Parkinson, J. A novel ubiquitin-specific protease is dynamically associated with the PML nuclear domain and binds to a herpesvirus regulatory protein. *The EMBO Journal* **16** 1997, 1519–30. <https://doi.org/10.1093/emboj/16.7.1519>
- [71] Lanfranca, M.P., Mostafa, H.H. and Davido, D.J. HSV-1 ICP0: An E3 Ubiquitin Ligase That Counteracts Host Intrinsic and Innate Immunity. *Cells* **3** 2014, 438–54. <https://doi.org/10.3390/cells3020438>
- [72] Boutell, C., Canning, M., Orr, A. and Everett, R.D. Reciprocal activities between herpes simplex virus type 1 regulatory protein ICP0, a ubiquitin E3 ligase, and ubiquitin-specific protease USP7. *Journal of Virology* **79** 2005, 12342–54. <https://doi.org/10.1128/JVI.79.19.12342-12354.2005>
- [73] Daubeuf, S., Singh, D., Tan, Y., Liu, H., Federoff, H.J., Bowers, W.J. and Tolba, K. HSV ICP0 recruits USP7 to modulate TLR-mediated innate response. *Blood* **113** 2009, 3264–75. <https://doi.org/10.1182/blood-2008-07-168203>
- [74] Canning, M., Boutell, C., Parkinson, J. and Everett, R.D. A RING finger ubiquitin ligase is protected from autocatalyzed ubiquitination and degradation by binding to ubiquitin-specific protease USP7. *The Journal of Biological Chemistry* **279** 2004, 38160–8. <https://doi.org/10.1074/jbc.M402885200>
- [75] Boutell, C. and Everett, R.D. Herpes simplex virus type 1 infection induces the stabilization of p53 in a USP7- and ATM-independent manner. *Journal of Virology* **78** 2004, 8068–77. <https://doi.org/10.1128/JVI.78.15.8068-8077.2004>
- [76] Zlatanou, A., Sabbioneda, S., Miller, E.S., Greenwalt, A., Aggathangelou, A., Maurice, M.M., Lehmann, A.R., Stankovic, T., Reverdy, C., Colland, F., Vaziri, C. and Stewart, G.S. USP7 is essential for maintaining Rad18 stability and DNA damage tolerance. *Oncogene* **35** 2016, 965–76. <https://doi.org/10.1038/onc.2015.149>
- [77] Qian, J., Pentz, K., Zhu, Q., Wang, Q., He, J., Srivastava, A.K. and Wani, A.A. USP7 modulates UV-induced PCNA monoubiquitination by regulating DNA polymerase eta stability. *Oncogene* **34** 2015, 4791–6. <https://doi.org/10.1038/onc.2014.394>
- [78] Kashiwaba, S., Kanao, R., Masuda, Y., Kusumoto-Matsuo, R., Hanaoka, F. and Masutani, C. USP7 Is a Suppressor of PCNA Ubiquitination and Oxidative-Stress-Induced Mutagenesis in Human Cells. *Cell Reports* **13** 2015, 2072–80. <https://doi.org/10.1016/j.celrep.2015.11.014>
- [79] Hoege, C., Pfander, B., Moldovan, G.-L., Pyrowolakis, G. and Jentsch, S. RAD6-dependent DNA repair is linked to modification of PCNA by ubiquitin and SUMO. *Nature* **419** 2002, 135–41. <https://doi.org/10.1038/nature00991>
- [80] Zhu, Q., Sharma, N., He, J., Wani, G. and Wani, A.A. USP7 deubiquitinase promotes ubiquitin-dependent DNA damage signaling by stabilizing RNF168*. *Cell Cycle Taylor & Francis*. **14** 2015, 1413–25. <https://doi.org/10.1080/15384101.2015.1007785>
- [81] An, L., Jiang, Y., Ng, H.H.W., Man, E.P.S., Chen, J., Khoo, U.-S., Gong, Q. and Huen, M.S.Y. Dual-utility NLS drives RNF169-dependent DNA damage responses. *Proceedings of the National Academy of Sciences of the United States of America* 2017, 201616602. <https://doi.org/10.1073/pnas.1616602114>
- [82] Maertens, G.N., El Messaoudi-Aubert, S., Elderkin, S., Hiom, K. and Peters, G. Ubiquitin-specific proteases 7 and 11 modulate Polycomb regulation of the INK4a tumour suppressor. *The EMBO Journal Nature Publishing Group*. **29** 2010, 2553–65. <https://doi.org/10.1038/emboj.2010.129>
- [83] de Bie, P., Zaaroor-Regev, D. and Ciechanover, A. Regulation of the Polycomb protein RING1B ubiquitination by USP7. *Biochemical and Biophysical Research Communications* **400** 2010, 389–95. <https://doi.org/10.1016/j.bbrc.2010.08.082>
- [84] Gao, Z., Zhang, J., Bonasio, R., Strino, F., Sawai, A., Parisi, F., Kluger, Y. and Reinberg, D. PCGF homologs, CBX proteins, and RYBP define functionally distinct PRC1 family complexes. *Molecular Cell* **45** 2012, 344–56. <https://doi.org/10.1016/j.molcel.2012.01.002>
- [85] Lecona, E., Narendra, V. and Reinberg, D. USP7 Cooperates with SCML2 To Regulate the Activity of PRC1. *Molecular and Cellular Biology* **35** 2015, 1157–68. <https://doi.org/10.1128/MCB.01197-14>
- [86] Luo, M., Zhou, J., Leu, N.A., Abreu, C.M., Wang, J., Anguera, M.C., de Rooij, D.G., Jasini, M. and Wang, P.J. Polycomb Protein SCML2 Associates with USP7 and Counteracts Histone H2A Ubiquitination in the XY Chromatin during Male Meiosis. *PLoS Genetics* **11** 2015, e1004954. <https://doi.org/10.1371/journal.pgen.1004954>

- [87] Bonasio, R., Lecona, E., Narendra, V., Voigt, P., Parisi, F., Kluger, Y. and Reinberg, D. Interactions with RNA direct the Polycomb group protein SCML2 to chromatin where it represses target genes. *ELife* **3** 2014, e02637.
- [88] van der Knaap, J.A., Kumar, B.R.P., Moshkin, Y.M., Langenberg, K., Krijgsveld, J., Heck, A.J.R., Karch, F. and Verrijzer, C.P. GMP synthetase stimulates histone H2B deubiquitylation by the epigenetic silencer USP7. *Molecular Cell* **17** 2005, 695–707. <https://doi.org/10.1016/j.molcel.2005.02.013>
- [89] Sarkari, F., Sanchez-Alcaraz, T., Wang, S., Holowaty, M.N., Sheng, Y. and Frappier, L. EBNA1-mediated recruitment of a histone H2B deubiquitylating complex to the Epstein-Barr virus latent origin of DNA replication. *PLoS Pathogens* **5** 2009, e1000624. <https://doi.org/10.1371/journal.ppat.1000624>
- [90] Nguyen, L.K., Muñoz-García, J., Maccario, H., Ciechanover, A., Kolch, W. and Kholodenko, B.N. Switches, Excitable Responses and Oscillations in the Ring1B/Bmi1 Ubiquitination System. Rao C V., editor. *PLoS Computational Biology* Public Library of Science. **7** 2011, e1002317. <https://doi.org/10.1371/journal.pcbi.1002317>
- [91] Hu, X., Kim, J.A., Castillo, A., Huang, M., Liu, J. and Wang, B. NBA1/MERIT40 and BRE interaction is required for the integrity of two distinct deubiquitinating enzyme BRCC36-containing complexes. *The Journal of Biological Chemistry* **286** 2011, 11734–45. <https://doi.org/10.1074/jbc.M110.200857>
- [92] Feng, L., Wang, J. and Chen, J. The Lys63-specific deubiquitinating enzyme BRCC36 is regulated by two scaffold proteins localizing in different subcellular compartments. *The Journal of Biological Chemistry* **285** 2010, 30982–8. <https://doi.org/10.1074/jbc.M110.135392>
- [93] Wang, B., Matsuoka, S., Ballif, B.A., Zhang, D., Smogorzewska, A., Gygi, S.P. and Elledge, S.J. Abraxas and RAP80 form a BRCA1 protein complex required for the DNA damage response. *Science (New York, NY)* **316** 2007, 1194–8. <https://doi.org/10.1126/science.1139476>
- [94] Coleman, K.A. and Greenberg, R.A. The BRCA1-RAP80 complex regulates DNA repair mechanism utilization by restricting end resection. *The Journal of Biological Chemistry* **286** 2011, 13669–80. <https://doi.org/10.1074/jbc.M110.213728>
- [95] van der Knaap, J.A., Kozhevnikova, E., Langenberg, K., Moshkin, Y.M. and Verrijzer, C.P. Biosynthetic enzyme GMP synthetase cooperates with ubiquitin-specific protease 7 in transcriptional regulation of ecdysteroid target genes. *Molecular and Cellular Biology* **30** 2010, 736–44. <https://doi.org/10.1128/MCB.01121-09>
- [96] Reddy, B.A., van der Knaap, J.A., Bot, A.G.M., Mohd-Sarip, A., Dekkers, D.H.W., Timmermans, M.A., Martens, J.W.M., Demmers, J.A.A. and Verrijzer, C.P. Nucleotide biosynthetic enzyme GMP synthase is a TRIM21-controlled relay of p53 stabilization. *Molecular Cell* **53** 2014, 458–70. <https://doi.org/10.1016/j.molcel.2013.12.017>
- [97] Schwertman, P., Vermeulen, W. and Marteijn, J.A. UVSSA and USP7, a new couple in transcription-coupled DNA repair. *Chromosoma* **122** 2013, 275–84. <https://doi.org/10.1007/s00412-013-0420-2>
- [98] Schwertman, P., Lagarou, A., Dekkers, D.H.W., Raams, A., van der Hoek, A.C., Laffebler, C., Hoeijmakers, J.H.J., Demmers, J.A.A., Foustieri, M., Vermeulen, W. and Marteijn, J.A. UV-sensitive syndrome protein UVSSA recruits USP7 to regulate transcription-coupled repair. *Nature Genetics* **44** 2012, 598–602. <https://doi.org/10.1038/ng.2230>
- [99] Higa, M., Zhang, X., Tanaka, K. and Saijo, M. Stabilization of Ultraviolet (UV)-stimulated Scaffold Protein A by Interaction with Ubiquitin-specific Peptidase 7 Is Essential for Transcription-coupled Nucleotide Excision Repair. *Journal of Biological Chemistry* **291** 2016, 13771–9. <https://doi.org/10.1074/jbc.M116.724658>
- [100] Nathan, J.A., Sengupta, S., Wood, S.A., Admon, A., Markson, G., Sanderson, C. and Lehner, P.J. The Ubiquitin E3 Ligase MARCH7 is Differentially Regulated by the Deubiquitylating Enzymes USP7 and USP9X. *Traffic* **9** 2008, 1130–45. <https://doi.org/10.1111/j.1600-0854.2008.00747.x>
- [101] Ma, P., Yang, X., Kong, Q., Li, C., Yang, S., Li, Y. and Mao, B. The ubiquitin ligase RNF220 enhances canonical Wnt signaling through USP7-mediated deubiquitination of β -catenin. *Molecular and Cellular Biology* **34** 2014, 4355–66. <https://doi.org/10.1128/MCB.00731-14>
- [102] Wheaton, K., Sarkari, F., Stanly Johns, B., Davarinejad, H., Egorova, O., Kaustov, L., Raught, B., Saridakis, V. and Sheng, Y. UbE2E1/UBCH6 is a Critical in Vivo E2 for the PRC1-catalyzed Ubiquitination of H2A at Lys-119. *Journal of Biological Chemistry* **292** 2017, 2893–902. <https://doi.org/10.1074/jbc.M116.749564>
- [103] Holowaty, M.N., Sheng, Y., Nguyen, T., Arrowsmith, C. and Frappier, L. Protein interaction domains of the ubiquitin-specific protease, USP7/HAUSP. *The Journal of Biological Chemistry* **278** 2003, 47753–61. <https://doi.org/10.1074/jbc.M307200200>

Chapter 1. Regulation of USP7

- [104] Lee, H.-R., Choi, W.-C., Lee, S., Hwang, J., Hwang, E., Guchhait, K., Haas, J., Toth, Z., Jeon, Y.H., Oh, T.-K., Kim, M.H. and Jung, J.U. Bilateral inhibition of HAUSP deubiquitinase by a viral interferon regulatory factor protein. *Nature Structural & Molecular Biology* Nature Publishing Group, a division of Macmillan Publishers Limited. All Rights Reserved. **18** 2011, 1336–44. <https://doi.org/10.1038/nsmb.2142>
- [105] Jäger, W., Santag, S., Weidner-Glunde, M., Gellermann, E., Kati, S., Pietrek, M., Viejo-Borbolla, A. and Schulz, T.F. The ubiquitin-specific protease USP7 modulates the replication of Kaposi's sarcoma-associated herpesvirus latent episomal DNA. *Journal of Virology* **86** 2012, 6745–57. <https://doi.org/10.1128/JVI.06840-11>
- [106] van Loosdregt, J., Fleskens, V., Fu, J., Brenkman, A.B., Bekker, C.P.J., Pals, C.E.G.M., Meering, J., Berkers, C.R., Barbi, J., Gröne, A., Sijts, A.J.A.M., Maurice, M.M., Kalkhoven, E., Prakken, B.J., Ovaa, H., Pan, F., Zaiss, D.M.W. and Coffey, P.J. Stabilization of the Transcription Factor Foxp3 by the Deubiquitinase USP7 Increases Treg-Cell-Suppressive Capacity. *Immunity* **39** 2013, 259–71. <https://doi.org/10.1016/j.immuni.2013.05.018>
- [107] Reverdy, C., Conrath, S., Lopez, R., Planquette, C., Atmanene, C., Collura, V., Harpon, J., Battaglia, V., Vivat, V., Sippl, W. and Colland, F. Discovery of specific inhibitors of human USP7/HAUSP deubiquitinating enzyme. *Chemistry & Biology* **19** 2012, 467–77. <https://doi.org/10.1016/j.chembiol.2012.02.007>
- [108] Colland, F., Formstecher, E., Jacq, X., Reverdy, C., Planquette, C., Conrath, S., Trouplin, V., Bianchi, J., Aushev, V.N., Camonis, J., Calabrese, A., Borg-Capra, C., Sippl, W., Collura, V., Boissy, G., Rain, J.-C., Guedat, P., Delansorne, R. and Daviet, L. Small-molecule inhibitor of USP7/HAUSP ubiquitin protease stabilizes and activates p53 in cells. *Molecular Cancer Therapeutics* **8** 2009, 2286–95. <https://doi.org/10.1158/1535-7163.MCT-09-0097>
- [109] Dar, A., Shibata, E. and Dutta, A. Deubiquitination of Tip60 by USP7 Determines the Activity of the p53-Dependent Apoptotic Pathway. *Molecular and Cellular Biology* **33** 2013, 3309–20. <https://doi.org/10.1128/MCB.00358-13>
- [110] Altun, M., Kramer, H.B., Willems, L.I., McDermott, J.L., Leach, C.A., Goldenberg, S.J., Kumar, K.G.S.G.S., Konietzny, R., Fischer, R., Kogan, E., Mackeen, M.M., McGouran, J., Khoronenkova, S. V., Parsons, J.L., Dianov, G.L., Nicholson, B. and Kessler, B.M. Activity-based chemical proteomics accelerates inhibitor development for deubiquitylating enzymes. *Chemistry & Biology* **18** 2011, 1401–12. <https://doi.org/10.1016/j.chembiol.2011.08.018>
- [111] Weinstock, J., Wu, J., Cao, P., Kingsbury, W.D., McDermott, J.L., Kodrasov, M.P., McKelvey, D.M., Suresh Kumar, K.G., Goldenberg, S.J., Mattern, M.R. and Nicholson, B. Selective Dual Inhibitors of the Cancer-Related Deubiquitylating Proteases USP7 and USP47. *ACS Medicinal Chemistry Letters* **3** 2012, 789–92. <https://doi.org/10.1021/ml200276j>
- [112] Chen, C., Song, J., Wang, J., Xu, C., Chen, C., Gu, W., Sun, H. and Wen, X. Synthesis and biological evaluation of thiazole derivatives as novel USP7 inhibitors. *Bioorganic & Medicinal Chemistry Letters* **27** 2017, 845–9. <https://doi.org/10.1016/j.bmcl.2017.01.018>
- [113] Zhang, Y., Zhou, L., Rouge, L., Phillips, A.H., Lam, C., Liu, P., Sandoval, W., Helgason, E., Murray, J.M., Wertz, I.E. and Corn, J.E. Conformational stabilization of ubiquitin yields potent and selective inhibitors of USP7. *Nature Chemical Biology* Nature Publishing Group. **9** 2013, 51–8. <https://doi.org/10.1038/nchembio.1134>
- [114] Ernst, A., Avvakumov, G., Tong, J., Fan, Y., Zhao, Y., Alberts, P., Persaud, A., Walker, J.R., Neculai, A.-M., Neculai, D., Vorobyov, A., Garg, P., Beatty, L., Chan, P.-K., Juang, Y.-C., Landry, M.-C., Yeh, C., Zeqiraj, E., Karamboulas, K. et al. A Strategy for Modulation of Enzymes in the Ubiquitin System. *Science (New York, NY)* **339** 2013, 590–5. <https://doi.org/10.1126/science.1230161>
- [115] Fan, Y.-H., Cheng, J., Vasudevan, S.A., Dou, J., Zhang, H., Patel, R.H., Ma, I.T., Rojas, Y., Zhao, Y., Yu, Y., Zhang, H., Shohet, J.M., Nuchtern, J.G., Kim, E.S. and Yang, J. USP7 inhibitor P22077 inhibits neuroblastoma growth via inducing p53-mediated apoptosis. *Cell Death & Disease* **4** 2013, e867. <https://doi.org/10.1038/cddis.2013.400>
- [116] Lee, G., Oh, T.-I., Um, K.B., Yoon, H., Son, J., Kim, B.M., Kim, H.-I., Kim, H., Kim, Y.J., Lee, C.-S. and Lim, J.-H. Small-molecule inhibitors of USP7 induce apoptosis through oxidative and endoplasmic reticulum stress in cancer cells. *Biochemical and Biophysical Research Communications* **470** 2016, 181–6. <https://doi.org/10.1016/j.bbrc.2016.01.021>

Chapter 2.

Structure of USP7 CD123

2

Robbert Q. Kim, Willem J. van Dijk, Titia K. Sixma

*Division of Biochemistry and Cancer Genomics Center, Netherlands Cancer Institute,
Plesmanlaan 121, 1066 CX Amsterdam, the Netherlands*

Adapted from:

Kim, R.Q., van Dijk, W.J. and Sixma, T.K.
Structure of USP7 catalytic domain and three Ubl-domains reveals a connector α -helix with regulatory role.
Journal of Structural Biology 195 2016, 11–8.
<https://doi.org/10.1016/j.jsb.2016.05.005>

Chapter 2. Structure of USP7 CD123

Abstract

Ubiquitin conjugation is an important signal in cellular pathways, changing the fate of a target protein, by degradation, relocalisation or complex formation. These signals are balanced by deubiquitinating enzymes (DUBs), which antagonize ubiquitination of specific protein substrates.

Because ubiquitination pathways are critically important, DUB activity is often carefully controlled. USP7 is a highly abundant DUB with numerous targets that plays complex roles in diverse pathways, including DNA regulation, p53 stress response and endosomal protein recycling. Full-length USP7 switches between an inactive and an active state, tuned by the positioning of 5 Ubl folds in the C-terminal HUBL domain. The active state requires interaction between the last two UbIs (USP7-Ubl45) and the catalytic domain (USP7CD), and this can be promoted by allosteric interaction from the first 3 Ubl domains of USP7 (USP7-Ubl123) interacting with GMPS.

Here we study the transition between USP7 states. We provide a crystal structure of USP7-CD123 and show that CD and Ubl123 are connected via an extended charged alpha helix. Mutational analysis is used to determine whether the charge and rigidity of this 'connector helix' are important for full USP7 activity.

Introduction

The covalent attachment of ubiquitin (Ub) to lysines of target proteins is an important post-translational modification^{1,2} that is carried out by a cascade of E1 activating enzymes, E2 conjugating enzymes and E3 ligases^{3–5}. Apart from mono-ubiquitination, ubiquitin can form chains, by further ubiquitination on any of its seven lysines or the N-terminus⁶. Different ubiquitination states, either mono-ubiquitination or different types of poly-ubiquitination, will have different signalling outcomes for the target protein; ranging from cellular location to proteasomal degradation^{7,8}.

To reverse the ubiquitination, deubiquitinating enzymes (DUBs) can hydrolyse the bond between ubiquitin and the target lysine^{9,10}. Besides functions in ubiquitin processing and at the proteasome, DUBs can antagonise the ubiquitination step and affect the cellular fate of the target protein¹¹. Dysfunction of DUBs can cause an imbalance in cells and therefore DUBs play important roles in infectious diseases, cancer and neurological diseases^{12–14}.

DUBs are specialized isopeptidases that hydrolyse the ubiquitin bond. In the human genome about 80 different DUBs have been identified providing specificity for different targets^{11,15}. These are divided into five classes, based on their catalytic domain (CD) architecture. Next to this class defining catalytic domain, DUBs may have a series of regulatory domains¹⁶. These extra domains can confer substrate specificity, by recruiting the target, but may also influence the overall activity of the DUB¹⁷.

USP7, or HAUSP¹⁸, is one of the first DUBs identified and remains one of the best studied ones^{19,20}. USP7 is involved in many pathways as it deubiquitinates a wide range of targets. It functions in apoptosis and senescence through its deubiquitinating activity in the p53 pathway, primarily affecting MDM2^{21,22}, but also p53²³ and TSPYL5²⁴. It acts on a large number of targets in chromatin and DNA regulation, such as H2B²⁵, Chk1²⁶, Claspin²⁷, UVSSA²⁸, SCML2²⁹, DNMT1³⁰, BRCA1-A³¹ and RNF168³², but also interacts with FOXO4³³, PTEN³⁴, MAGE-L2³⁵, GMPS²⁵ and viral proteins like ICPO and EBNA-1³⁶, making it an interesting but complex protein to study. USP7 belongs to the family of ubiquitin specific proteases (USP), which have a papain-like catalytic domain (USP7-CD). USP7 is one of the larger USP family members with an N-terminal TRAF domain (Fig. 1a), which is critical for recruitment of its targets like p53 or MDM2^{37,38}, and on the C-terminal side five ubiquitin-like (Ubl) domains. These five Ubl domains together are dubbed HUBL (for HAUSP-Ubl) domain and denoted here as Ubl12345. Interestingly, proteins like GMPS, DNMT1³⁹ and ICPO^{19,40} interact primarily with Ubl12, while others like MDM2 and p53⁴¹ seem to have a secondary binding site here, showing that different types of interaction and regulation may occur.

Structural analysis has revealed that the *apo* structure of USP7-CD has a catalytic triad that is not functional, as the distance between active site residues is too large⁴². In the presence of a covalently bound ubiquitin aldehyde, the catalytic triad is rearranged to generate a catalytically competent state of CD⁴². Interestingly, for full activity the C-terminal domains are required, as the CD on its own showed a hundred-fold decrease in activity compared to full-length or USP7-CD12345⁴³.

Faesen et. al. showed that USP7 exists in an equilibrium between the active and inactive state and that the active state requires the presence of the Ubl45 domain. Ubl45 can bind to the CD, which then promotes the interaction between a C-terminal peptide on Ubl45 that causes a rearrangement of the switching loop on CD and induces the rearrangement of the catalytic triad into an active state⁴⁴. The equilibrium between the active and inactive state

Chapter 2. Structure of USP7 CD123

can be modulated further by the binding of the allosteric activator GMPS²⁵. This protein binds to Ubl123 but promotes the interaction between CD and Ubl45, thus shifting USP7 towards the active side of the equilibrium.

Structural studies have shown that the Ubl domains are arranged in a 2-1-2 fashion⁴⁴. The crystal structure of the full HUBL domain showed that the 5 Ubl domains can exist in an extended state, but geometrical restraints indicate that this domain needs to rearrange to enable interaction with the CD. This conclusion was supported by SAXS and binding data. Since the first two (Ubl12) and last two (Ubl45) Ubl domains are connected to Ubl3 by small linkers, some flexibility between the domains was proposed. However, how this 'folding back' is achieved is not clear and structures are required that show the arrangement of these domains relative to the CD.

Here we present a crystal structure of USP7-CD123 containing the CD and the Ubl domains 1, 2 and 3. It shows that the catalytic domain is connected to the HUBL domain through a 26 amino-acid α -helical linker. This apparently rigid linker shows how the first three Ubl domains are positioned relative to the catalytic domain. We studied the role of this connecting element in positioning of the C-terminal domains and were able to show that the rigidity, length and charges on this linker may affect the activity of USP7.

Materials and Methods

Constructs and mutations

USP7 constructs CD123 (residues 208-882) and CD12345 (res. 208-1102) were cloned into expression vector pGEX-6P-1 (GE Healthcare) using BamHI and NotI restriction sites based on the codon-optimized USP7 from Faesen et al, 2011. Mutations were introduced in CD12345 using site-directed mutagenesis with overhanging primers.

Protein expression and purification

USP7 constructs were expressed in *Escherichia coli* BL21(DE3) T¹⁸ cells using auto-induction medium overnight at 18°C⁴⁵. Cells were pelleted and resuspended in lysis buffer (50 mM HEPES pH7.5; 250 mM NaCl; 1 mM EDTA; 1 mM DTT). DNaseI and 0.1 mM PMSF were added prior to lysis using Emulsiflex. The lysate was cleared by centrifuging at 20k G and supernatant was applied to Glutathione Sepharose 4B beads (GE Healthcare). After washing the beads, the protein was eluted using 15 mM reduced glutathione and subjected to cleavage using 3C protease and dialysis versus 10 mM HEPES pH7.5, 50 mM NaCl, 1 mM EDTA, 1 mM DTT. Anion exchange on a PorosQ column (GE Healthcare) was performed using a salt gradient (50 to 500 mM NaCl; 10 mM HEPES pH7.5; 1 mM DTT). Protein fractions were pooled and concentrated, followed by size exclusion chromatography on a Superdex 200 column (GE Healthcare) equilibrated against 10 mM HEPES pH7.5; 100 mM NaCl; 1 mM DTT. If necessary, a GST FF column (GE Healthcare) was attached to the end of the gel filtration column to remove residual GST. The peak fractions were analysed by SDS-PAGE and pooled accordingly. Proteins were concentrated to 10 mg mL⁻¹ for assays and up to 25 mg mL⁻¹ for crystallization purposes. Generally, 1 litre of culture yields 2 mg of purified protein.

Crystallization and Data collection

USP7-CD123 was used at a concentration of 25 mg mL⁻¹ in a sitting drop vapour diffusion experiment using 96-well plates at 4°C. Crystallization plates were set up using Mosquito (TTP Labtech) with 0.1 µL of mother liquor (15% PEG-3350; 0.2 M Sodium citrate pH ~8.5) and 0.1 µL of protein solution. Crystals appeared within one week and were flash-frozen in liquid nitrogen after being cryo-protected in mother liquor supplemented with 20% ethylene glycol. X-ray diffraction data could be obtained from a single crystal to 3.4 Å on beamline ID 14-1 at the ESRF, Grenoble, France. The crystal belongs to space group F222 and the data were processed using XDS⁴⁶, yielding statistics shown in Table 1.

Structure Determination

The structure of CD123 was solved by molecular replacement using *PHASER*⁴⁷ with search models for the catalytic domain (PDB code 1NB8⁴²) and the Ubl-domains (2YLM⁴⁴), split into separate searches for Ubl12 and Ubl3. The separate solutions were merged to one monomer in the asymmetric unit. In the resulting electron density map, the connector helix could be built manually using *COOT*⁴⁸. The resulting structure was refined, using *PROSMART* geometric restraints from the higher resolution reference structures⁴⁹, in iterative cycles of maximum-likelihood restrained refinement in *REFMAC* from the *CCP4* suite^{50,51}. The model was further validated and optimised using *MolProbity*⁵² and *PDB_REDO*⁵³. The final model had R_{work} and R_{free} values of 22.2% and 26.7% respectively.

Enzyme activity assays

The DUB activity of the USP7 variants was monitored by measuring the increase in fluorescence upon release of the Rhodamine fluorophore from quenched substrate Ub-Rho (UbiQ) using Pherastar plate reader (BMG LABTECH GmbH, Germany), with excitation wavelength 485 nm (±10 nm) and emission at 520 nm (±10 nm). For Michaelis-Menten analysis, 1 nM enzyme was used to react with concentrations of substrate as indicated. The initial rates were plotted against substrate concentration and fitted with a Michaelis-Menten model using non-linear regression in Prism 6 (GraphPad). These experiments were performed in triplicate on two different batches of protein.

Molecular weight determination using MALLS

Purified proteins were run on analytical gel filtration coupled to Multi-angle Laser Light Scattering (MALLS) detector MiniDawn Tri-star (Wyatt Technologies, USA). Molecular weights of corresponding peaks were determined with refractive index using manufacturer's software (ASTRA).

Melting temperature assessment

Stability of wild type protein and mutants was tested using the Optim 1000 (Avacta, now Unchained Labs, USA). Using an excitation wavelength of 266 nm, scattering at 266 nm and fluorescence intensity over the spectrum between 300 nm and 400 nm were measured and analysed as function of the temperature using the manufacturer's software. Barycentric fluorescence curves were plotted using Prism 6 (GraphPad) and used to obtain melting temperatures.

Chapter 2. Structure of USP7 CD123

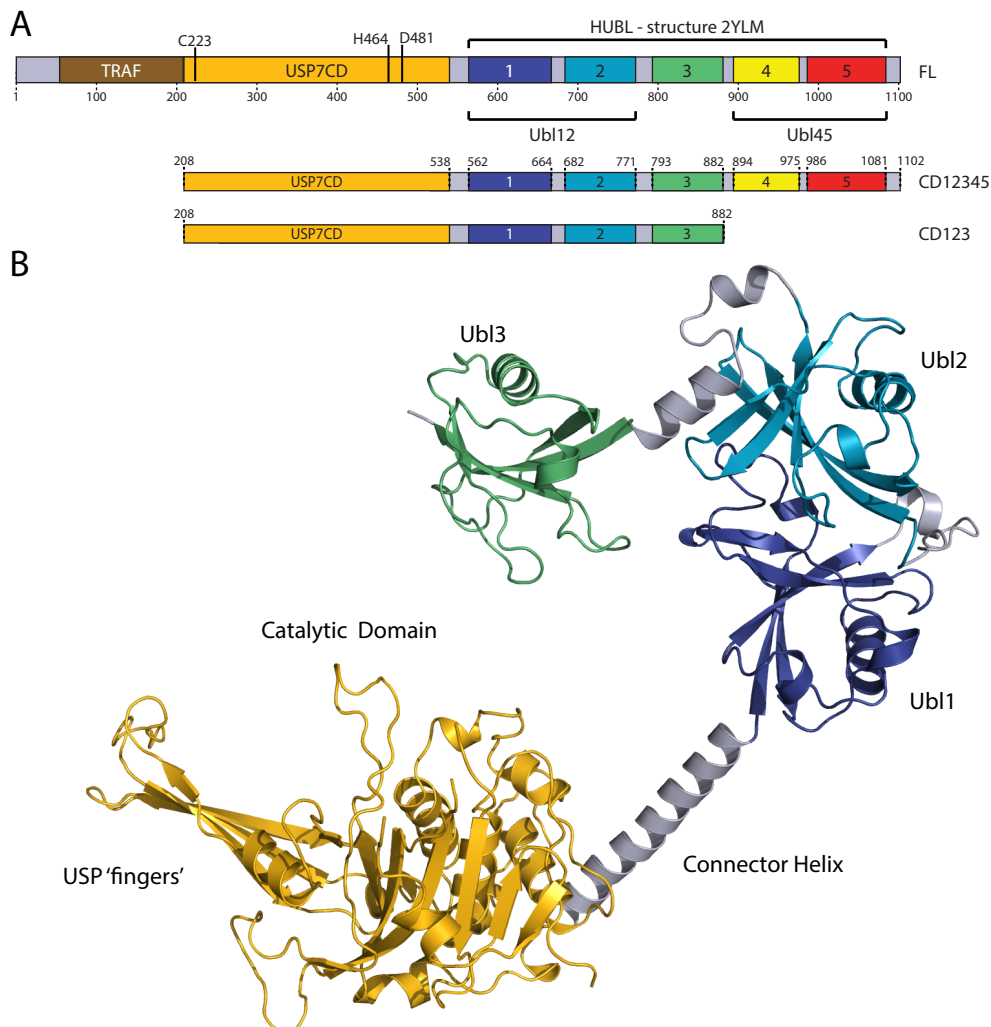


Figure 1. The crystal structure of USP7-CD123. **A.** Schematic overview of USP7 domains and constructs used. Also indicated are the catalytic residues and domain boundaries. The 'connector' helix, spanning from residue 538 to 562, is here defined as the full α -helix, stemming from the CD. The other domain boundaries are based on previously solved structures. Domain colours are used for all structural representation of CD123. **B.** The crystal structure of CD123 reveals a curved architecture of domains and a 'connector' α -helix that links the CD to Ubl1.

Results

USP7-CD123 crystal structure

We were able to express and purify a USP7 construct comprising residues 208-882. This construct contains the catalytic domain (CD) and the first three Ubl domains, from here on referred to as CD123 (Fig. 1a). We obtained single crystals in a vapour diffusion setup at 4°C with mother liquor of pH > 7, containing multivalent acids. During optimization sodium

citrate was found to yield the best diffracting crystals, resulting in a dataset diffracting to 3.4 Å (Table 1). The crystal belonged to space group F222 with unit cell parameters $a = 115.2$, $b = 195$ and $c = 219.8$ Å, with a rather high solvent content (68%) for a single monomer of 79 kDa (Table 1). The structure was solved by molecular replacement using *apo* USP7-CD (1NB8⁴²) followed by separate searches for Ubl12 and Ubl3 (2YLM⁴⁴). After manual building of the connector helix, the model could be refined to R-values of $R_{\text{work}} = 0.22$ and $R_{\text{free}} = 0.27$ with good geometry (Table 1). The R-values are relatively good for a structure at this resolution, probably thanks to the external restraints generated by ProSmart from the higher resolution search models⁴⁹.

The failure of molecular replacement using Ubl123 from the previous structure as a whole, already indicates a conformational change in CD123 with respect to the crystal structure of the extended HUBL (2YLM⁴⁴). Indeed, the structural model for CD123 shows the four domains in a curved, crescent-shaped conformation, where Ubl3 ‘bends’ inwards, back to the catalytic domain (Fig. 1b). This backward bending contrasts with the extended conformation of the HUBL domain, and results in a globular overall shape for CD123.

Structural analysis of USP7-CD123

As shown previously CD123 has the low activity that was observed for the catalytic domain alone (Fig. 2b⁴⁴). Accordingly, we observe that the catalytic triad is misaligned, with the active-site cysteine and histidine separated by more than 10 Å (Fig. 2a). The catalytic domain aligns much better with the *apo* structure of CD (1NB8⁴²) separately (RMSD 0.53 Å on 322 Ca’s) than with the activated ubiquitin-bound CD (1NBF⁴²) (RMSD 1.34 Å on 314 Ca’s). The main differences with the *apo* structure are in a series of loops, that could not be modelled confidently in this low resolution structure, and the relatively poor density in the β -strands of the fingers region, which is mobile in other USP structures⁵⁴.

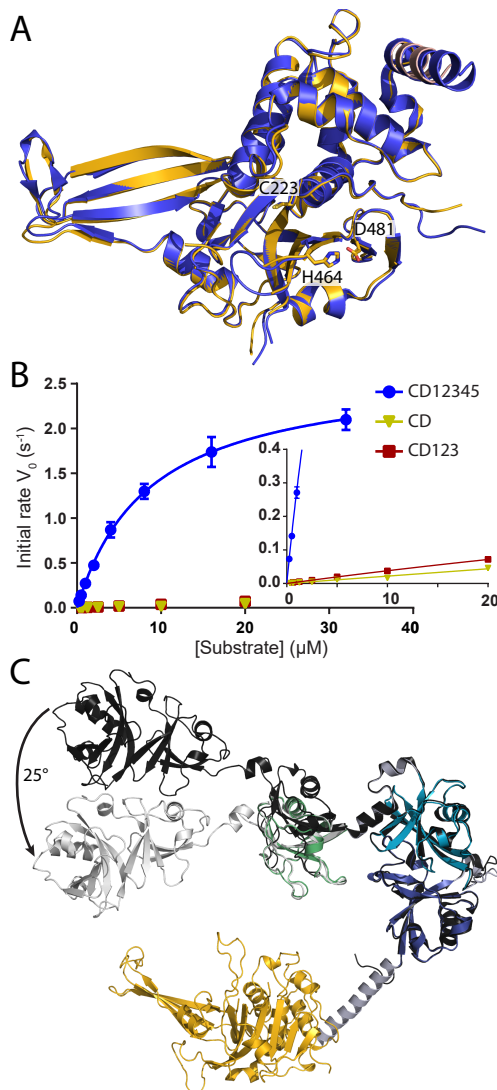
The overall arrangement of the Ubl123 is different from that observed in the extended state structure of the five Ubl domains (Figure 2c, 2YLM⁴⁴). When aligning the first two Ubls, the third Ubl shows a 25° rotation with respect to the extended structure (Fig. 2c). Such an angle was

Table 1. Data processing and refinement statistics for the crystal structure of USP7CD123. Values within parentheses are for the outer resolution shell

USP7-CD123	
PDB accession code	5FWI
Space group	F222
Cell dimensions	
a (Å)	115.18
b (Å)	195.04
c (Å)	219.78
α (°)	90
β (°)	90
γ (°)	90
Monomers in ASU	1
Resolution (Å)	48.76-3.40
Outer shell (Å)	3.67-3.40
Beamline	ESRF ID14-1
Wavelength (Å)	0.97935
Observed reflections	77295 (15487)
Unique reflections	17198 (3504)
R_{merge}	0.061 (0.733)
Multiplicity	4.5 (4.5)
Completeness	99.9 (100)
Mean $I/\sigma(I)$	13.4 (1.9)
N° of protein atoms	5352
R_{work} (%)	22.2
R_{free} (%)	26.7
RMSD from ideality	
Bond lengths (Å)	0.008
Bond angles (°)	1.278
Chiral volume (Å ³)	0.071
Ramachandran plot	
Favoured (%)	634 (96%)
Disallowed (%)	3 (0%)
Average B-values (Å ²)	104.0

Chapter 2. Structure of USP7 CD123

also observed in the co-crystal structures of Ubl123 with an ICP0-peptide⁴⁰ and the structure of HUBL with DNMT1³⁹. Both these structures could exhibit this rotation as consequence of binding of the protein partner, but the CD123 structure shows that the protein alone can have this flexibility.



The bending of Ubl3 fits with the model proposed⁴⁴, as this curving lessens the gap between the CD and the very C-terminus, reducing the distance between K882, the last residue of the construct crystallized, and C223, the active site, to 47Å. In this gap, the remaining Ubl45 domain of 45Å would fit perfectly (Fig. 2c), keeping in mind the extending, activating C-terminal peptide. As proposed earlier⁴⁰, this distance could be further bridged by a hinge motion at the region between Ubl3 and Ubl4, an area notoriously flexible, as seen in the full-length degradation pattern (results not shown and ⁴⁴).

USP7-CD is connected to the Ubl domains by an α -helix

A new finding in the CD123 crystal structure is the long α -helix connecting the catalytic domain to the Ubl domains (Fig. 1b). Previous structures have shown parts of the helix^{40,42}, and the structure of CD123 confirms these helical fragments. This 39 Å helix (26 residues) connects the CD to the HUBL domains, and will be referred to as 'connector helix' from here onwards. The density for this part of the protein is relatively well-defined, most probably thanks to crystal packing and the rigidity in the element. Having two domains

Figure 2. Comparison of USP7-CD123 to USP7 variants. **A.** Structural alignment of the apo structure of USP7-CD (purple) and USP7-CD of USP7-CD123 (gold) yields an RMSD of 0.53 Å. Both have the misaligned catalytic triad, confirming their inactive state. **B.** Michaelis-Menten analysis of enzyme activities on minimal substrate Ub-Rho, comparing CD12345 with CD and CD123 shows that Ubl45 is necessary for full activity of USP7. Insert is a magnification of the larger figure. **C.** Superposition of the HUBL structure (2YLM) on either Ubl12 (dark grey) or Ubl3 (light grey) of the CD123 structure. The structural alignment shows an angle of 25°, emanating between Ubl2 and Ubl3.

connecting over such a length with a rigid α -helical element could imply that the helix has an important function in the protein. Therefore we analysed whether this connector helix was important for activity.

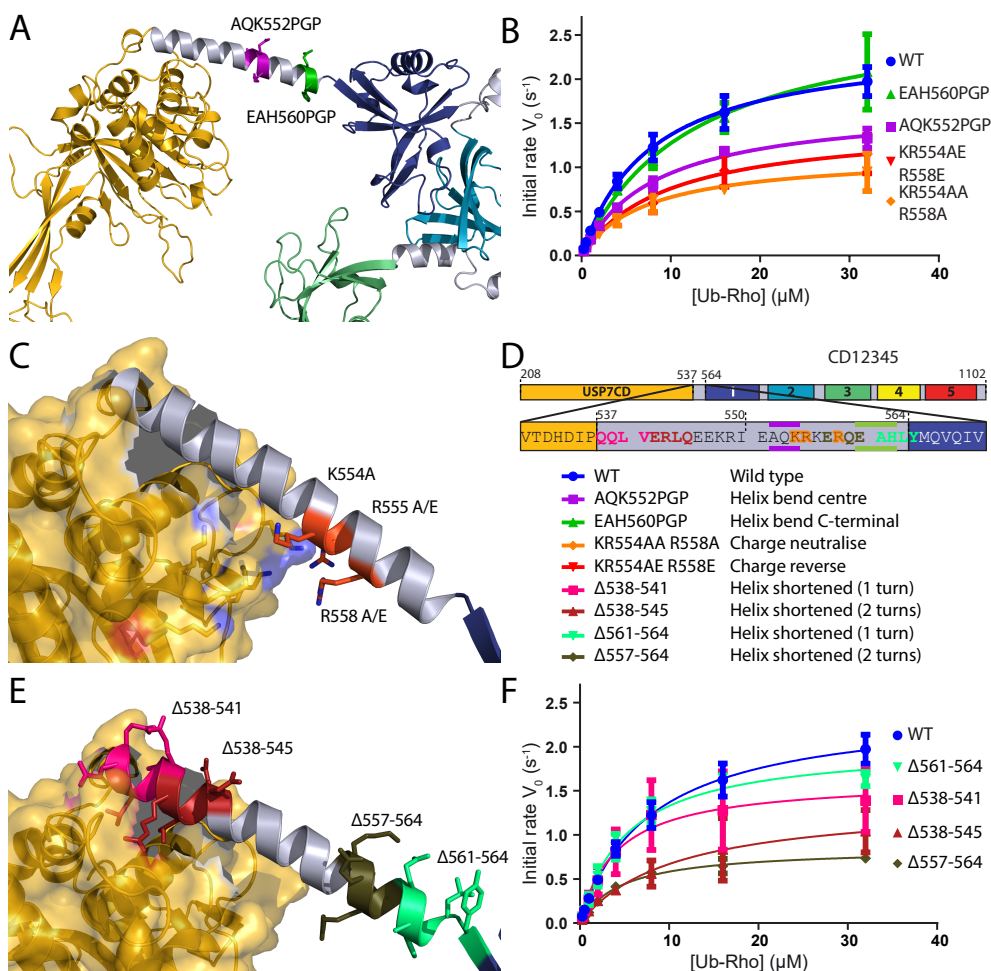


Figure 3. The connector helix is important for full activity of USP7. **A.** Mutations in the connector helix that affect its rigidity were introduced in two location AOK552PGP (purple) and EAH560PGP (green). **B.** Michaelis menten analysis of mutants that affect the charge or bending of the helix show similar K_M -values as wild type CD12345, but yield differences in k_{cat} . Curve colours are matched throughout the panels as indicated in panel D. **C.** Mutations in the connector helix that affect a charged patch were introduced. Zoom in on the connector helix and surroundings shows a charged patch on both the connector helix and the CD. **D.** Overview of the mutants made, serving as a legend to all panels in figure 3. **E.** Zoom in on the connector helix, showing the deleted helix turns on its N-terminal end (red and pink) and the C-terminal end (shades of green). **F.** Michaelis-Menten analysis for deletion mutants show little changes in K_M -values, but indicate a decrease in k_{cat} upon removal of 2 helical turns of the connector helix.

Chapter 2. Structure of USP7 CD123

Table 2. Michaelis-Menten analysis of USP7-CD12345 constructs

	k_{cat} (s ⁻¹)	K_M (μM)	k_{cat} / K_M (μM ⁻¹ s ⁻¹)
WT	2.80 ±0.04	8.80 ±0.32	0.32
AQK552PGP	1.69 ±0.02	8.48 ±0.28	0.20
EAH560PGP	2.45 ±0.03	9.47 ±0.31	0.26
KR554AA R558A	1.10 ±0.03	7.17 ±0.54	0.15
KR554AE R558E	1.46 ±0.05	9.75 ±0.78	0.15
Δ538-541	2.47 ±0.08	9.11 ±0.86	0.27
Δ538-545	1.54 ±0.09	11.86 ±1.61	0.13
Δ561-564	2.87 ±0.07	7.13 ±0.39	0.40
Δ557-564	1.03 ±0.02	6.04 ±0.34	0.17

The connector helix is necessary for full USP7 activity

First we studied whether the rigid extended nature of the connector is important for activity. The connector helix' rigidity can influence the correct positioning, because such an extended element will create distance between the CD and Ubl1. This distance could be necessary to position the activating C-terminal tail correctly for folding back onto the catalytic domain and promoting its activation. In order to investigate the role of the helix, we introduced two 'bending motifs' by mutating stretches AQK552 and EAH560 (Fig. 3a) to proline-glycine-proline in the CD12345 construct, which contains the full HUBL domain.

These CD12345 mutants could be expressed and purified according to the wild type protocol, although both mutants eluted later from the gel filtration column (Supplementary Fig. 1a). The wild type construct dimerises at concentrations above 1 mg/mL, and with the introduced mutations the dimerization equilibrium seems to have shifted to higher concentrations (Supplementary Fig. 1b). Furthermore, melting temperature analysis (Supplementary Fig. 1c) was performed, resulting in similar values, indicating the mutants are as stable as wild type protein.

Both AQK552PGP and EAH560PGP were analysed in a deubiquitination assay and compared to wildtype CD12345 (Fig. 3b). The K_M values were similar, but the k_{cat} rates showed interesting differences (Table 2). The mutant with the bend at the end of the connector helix (EAH560PGP) exhibited similar activity as wildtype. This would indicate that the HUBL domain has enough intrinsic flexibility to overcome such a bending disruption at the end of the extending connector helix. In contrast, the mutant with a bend in the middle of the helix (AQK552PGP) has lower activity, due to a lower k_{cat} (Table 2, Fig. 3b). The increased flexibility within the helix may have changed the spatial location of the Ubl domains with respect to the CD and this could explain why the activation by Ubl45 is affected.

A charged patch in the connector helix has influence on USP7 activity

We identified a cluster of charged residues in the connector helix (K554, R555 and R558) all pointing inwards, towards the catalytic domain. On the complementary surface of the catalytic domain a similar positive cluster of five lysines was identified (Fig. 3c). These positive surfaces (with distances between 4Å and 10Å) could repel the connector helix away from the catalytic domain. We wondered if this would be relevant for the activity of USP7.

We made mutations in the active CD12345 construct that neutralised (KR554AA R558A) or reverted (KR554AE R558E) the charge on the linker. These could be expressed and purified in a similar fashion as wild type CD12345 (Supplementary Fig. 1a), indicating no drastic changes in fold. When comparing the mutants with wild type protein in a deubiquitination assay (Fig. 3b), they showed reduced activity, indicating that the charge has a role in the activity of USP7. The K_M -values are similar for the mutants and wild type, indicating that these mutants do not affect the binding of ubiquitin (Table 2). The values for k_{cat} are two-fold lower, which suggests that the charged patch influences the efficiency of the Ubl45 domain activation of the CD.

The connector helix has a minimum length to allow for full activity

Next to the helix' rigidity and charged patch, the length could influence the positioning of Ubl45, and thereby the activation. Therefore, we investigated the length of the connector and its effect on the activity of the CD12345 construct. To this end we removed one or two α -helical turns (4 residues per turn) on the C-terminal (Δ 561-564 and Δ 557-564) as well as the N-terminal part (Δ 538-542 and Δ 538-546) of the helix (Fig. 3e).

These mutants could be expressed and purified using the CD12345 protocol and the gel filtration profiles indicated a monomeric species (Supplementary Fig. 1a). The activity assays yielded similar K_M -values, however the activity of the mutants differed in k_{cat} (Fig. 3f and Table 2), indicating that the effect is not on the final positioning, but on the efficiency of reaching this stage. In agreement with the findings for the mutant EAH560PGP, where the last helical turn is affected, deletion of one turn does not affect catalysis. Deletion of a second turn, whether at the start or the end of the helix, affects the activity as shown by the two-fold lower values k_{cat} .

Discussion and conclusions

The large number of important targets reported for USP7 indicates that it has a number of separately regulated functions in the human cell, but its exact molecular functioning remains elusive. Here we present a partial structure of USP7, which shows how previously solved crystal structures are connected and allows near full-length modelling. The crystal structure reveals a long extended α -helix that connects the CD to the HUBL domain. We studied the importance of this connector helix and found that it may play in a role in regulation of activity by positioning the C-terminal element.

In the mutational analysis, both the charged patch, the rigidity and the length of the connector helix play a role in activation. Mutations in the helical element lead to a modest decrease in k_{cat} , but do not affect K_M . The observed effect is analogous to the changes seen in the presence of the allosteric activator GMPS, but in the opposite direction^{25,44}. In both cases the actual activation has not changed, but the equilibrium between the active and inactive state has shifted, in this case towards the inactive state. When this is disrupted, the equilibrium between active and inactive USP7 will shift as the efficiency of 'folding back' onto the CD of Ubl45 is somewhat disrupted (Fig. 4).

The HUBL domain has some flexibility on its own, as USP7 activity remains similar for the mutant EAH560PGP and upon removal of an α -helical turn on either side of the connector helix. Only upon tampering with the charge or removing multiple turns the activity drops to roughly half the k_{cat} . This suggests that the Ubl45 domain is still able to activate the catalytic domain, albeit less efficiently. The exact positioning of Ubl45 is still unknown, but our

Chapter 2. Structure of USP7 CD123

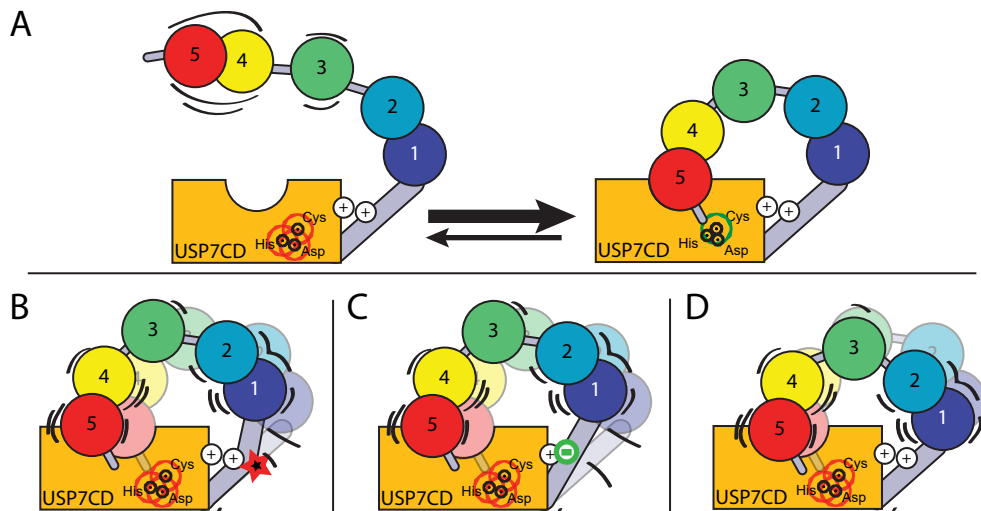


Figure 4. Model of USP7 activation. **A.** The model of USP7 self-activation shows an equilibrium between the inactive and active state, the transition requiring a rearrangement of the HUBL domain. **B.** A bend within the connector helix of USP7 could change the efficiency of the positioning of Ubl45, affecting the overall activity of USP7. **C.** Mutating the charged patch could have a similar effect, affecting the efficiency of the positioning of Ubl45 and thereby the USP7 self-activation. **D.** Shortening of the connector helix with two helical turns affects the self-activation, possibly due to the efficiency of positioning of Ubl45.

mutational analysis shows that changes in the connector helix play a modest role in USP7 activity, probably by less efficient positioning of Ubl45.

We know that the linker regions of HUBL are rather flexible, as they are susceptible to proteolysis in protein purification. The first linker, between Ubl12 and Ubl13, can allow Ubl13 to make an angular motion of up to 35°⁴⁰, but most of the kinking should take place in the second linker, between Ubl13 and Ubl45. This second pivot point should allow for another 50° to get Ubl45 towards the CD. Distance-wise our structure shows that it can fit, but the exact interaction spot on the catalytic domain is not known.

Our structure begins to show the flexibility of the linker between Ubl12 and Ubl13, in line with recent co-crystal structures of (parts of) the HUBL domain with DNMT1 and ICP0^{39,40}. The relative bending of Ubl13 in these structures could have been induced by binding of the protein partner. In the CD123 structure however, we don't have a binding partner, suggesting that USP7 does not need a specific modulator for this 'folding back' motion.

The HUBL domain is an important regulatory region in USP7. It contains the second binding site (Ubl12) of targets p53 and MDM, but where this interaction exactly takes place and whether this influences the activity on these targets is yet unknown. Ubl12 is known to bind GMPS, an allosteric activator, as well as DNMT1³⁹, URHF1 and ICP0⁴⁰. The co-crystal structure of the UbIs with the ICP0 interactor peptide (4WPH⁴⁰) shows a similar bend of Ubl13 as we found in the structure of CD123 and this is also seen in the structure of the full HUBL domain with DNMT1 (4YOC³⁹). However, the Ubl45 in this structure has an extended conformation, and how 'closing' of the gap towards the catalytic domain occurs, an important step in USP7 self-activation, remains unclear.

The changes in k_{cat} observed upon mutation of the connector helix, and upon GMPS binding to Ubl123⁴⁴ indicate that these regions can be allosterically modulated. One could imagine that binding of small molecules at these sites could have a function in regulation of USP7 activity. As the charged patch of the connector helix is required for full activity, this could be a good starting point for structure-guided inhibitor design in a USP7 specific manner, especially as USP7 is emerging as an important drug target^{55–59}. Good understanding of the conformational changes and allosteric regulation of this critical DUB will be important to understand the effects of bound inhibitors. Our new structure will contribute to these efforts.

Acknowledgements

The authors would like to acknowledge the ESRF for their support, in particular beamline scientists at beamline 14-1. We thank the NKI protein facility for contributions to protein quality control experiments, Jonas Dörr and Hedwich Vlieg for assistance in the circular dichroism experiments, Robbie Joosten for help in refinement and Alexander Fish for critical discussion. KWF (NKI 2012-5398) and NWO Gravity project CGC.nl have contributed funding for this project.

References

- [1] Hershko, A. and Ciechanover, A. The ubiquitin system. *Annual Review of Biochemistry* 67 1998, 425–79. <https://doi.org/10.1146/annurev.biochem.67.1.425>
- [2] Varshavsky, A. The ubiquitin system, an immense realm. *Annual Review of Biochemistry* 81 2012, 167–76. <https://doi.org/10.1146/annurev-biochem-051910-094049>
- [3] Streich, F.C. and Lima, C.D. Structural and functional insights to ubiquitin-like protein conjugation. *Annual Review of Biophysics* 43 2014, 357–79. <https://doi.org/10.1146/annurev-biophys-051013-022958>
- [4] Passmore, L.A. and Barford, D. Getting into position: the catalytic mechanisms of protein ubiquitylation. *The Biochemical Journal* 379 2004, 513–25. <https://doi.org/10.1042/BJ20040198>
- [5] Pickart, C.M. Mechanisms underlying ubiquitination. *Annual Review of Biochemistry* 70 2001, 503–33. <https://doi.org/10.1146/annurev.biochem.70.1.503>
- [6] Komander, D. and Rape, M. The ubiquitin code. *Annual Review of Biochemistry* 81 2012, 203–29. <https://doi.org/10.1146/annurev-biochem-060310-170328>
- [7] Shabek, N. and Ciechanover, A. Degradation of ubiquitin: The fate of the cellular reaper. *Cell Cycle* 9 2010, 523–30. <https://doi.org/10.4161/cc.9.3.11152>
- [8] Hicke, L. and Dunn, R. Regulation of membrane protein transport by ubiquitin and ubiquitin-binding proteins. *Annual Review of Cell and Developmental Biology* 19 2003, 141–72. <https://doi.org/10.1146/annurev.cellbio.19.110701.154617>
- [9] Clague, M.J., Barsukov, I., Coulson, J.M., Liu, H., Rigden, D.J. and Urbé, S. Deubiquitylases From Genes to Organism. *Physiological Reviews* 93 2013, 1289–315. <https://doi.org/10.1152/physrev.00002.2013>
- [10] Komander, D., Clague, M.J. and Urbé, S. Breaking the chains: structure and function of the deubiquitinases. *Nature Reviews Molecular Cell Biology* Nature Publishing Group. 10 2009, 550–63. <https://doi.org/10.1038/nrm2731>
- [11] Clague, M.J., Coulson, J.M. and Urbé, S. Cellular functions of the DUBs. *Journal of Cell Science* 125 2012, 277–86. <https://doi.org/10.1242/jcs.090985>
- [12] Hussain, S., Zhang, Y. and Galardy, P. DUBs and cancer. *Cell Cycle* 8 2009, 1688–97.
- [13] Nanduri, B., Suvarnapunya, A.E., Venkatesan, M. and Edelman, M.J. Deubiquitinating enzymes as promising drug targets for infectious diseases. *Current Pharmaceutical Design* 19 2013, 3234–47.
- [14] Todi, S. V and Paulson, H.L. Balancing act: deubiquitinating enzymes in the nervous system. *Trends in Neurosciences* 34 2011, 370–82. <https://doi.org/10.1016/j.tins.2011.05.004>

Chapter 2. Structure of USP7 CD123

- [15] Nijman, S.M.B., Luna-Vargas, M.P. a, Velds, A., Brummelkamp, T.R., Dirac, A.M.G., Sixma, T.K. and Bernards, R. A genomic and functional inventory of deubiquitinating enzymes. *Cell* 123 2005, 773–86. <https://doi.org/10.1016/j.cell.2005.11.007>
- [16] Reyes-Turcu, F.E., Ventii, K.H. and Wilkinson, K.D. Regulation and cellular roles of ubiquitin-specific deubiquitinating enzymes. *Annual Review of Biochemistry* 78 2009, 363–97. <https://doi.org/10.1146/annurev.biochem.78.082307.091526>
- [17] Sahtoe, D.D. and Sixma, T.K. Layers of DUB regulation. *Trends in Biochemical Sciences* 40 2015, 456–67. <https://doi.org/10.1016/j.tibs.2015.05.002>
- [18] Everett, R.D., Meredith, M., Orr, A., Cross, A., Kathoria, M. and Parkinson, J. A novel ubiquitin-specific protease is dynamically associated with the PML nuclear domain and binds to a herpesvirus regulatory protein. *The EMBO Journal* 16 1997, 1519–30. <https://doi.org/10.1093/emboj/16.7.1519>
- [19] Holowaty, M.N., Sheng, Y., Nguyen, T., Arrowsmith, C. and Frappier, L. Protein interaction domains of the ubiquitin-specific protease, USP7/HAUSP. *The Journal of Biological Chemistry* 278 2003, 47753–61. <https://doi.org/10.1074/jbc.M307200200>
- [20] Wrigley, J.D., Eckersley, K., Hardern, I.M., Millard, L., Walters, M., Peters, S.W., Mott, R., Nowak, T., Ward, R.A., Simpson, P.B. and Hudson, K. Enzymatic characterisation of USP7 deubiquitinating activity and inhibition. *Cell Biochemistry and Biophysics* 60 2011, 99–111. <https://doi.org/10.1007/s12013-011-9186-4>
- [21] Cummins, J.M., Rago, C., Kohli, M., Kinzler, K.W., Lengauer, C. and Vogelstein, B. Tumour suppression: Disruption of HAUSP gene stabilizes p53. *Nature* 428 2004, 486–7. <https://doi.org/10.1038/nature02501>
- [22] Brooks, C.L. and Gu, W. p53 Ubiquitination: Mdm2 and Beyond. *Molecular Cell* 21 2006, 307–15. <https://doi.org/10.1016/j.molcel.2006.01.020>
- [23] Li, M., Chen, D., Shiloh, A., Luo, J., Nikolaev, A.Y., Qin, J. and Gu, W. Deubiquitination of p53 by HAUSP is an important pathway for p53 stabilization. *Nature* 416 2002, 648–53. <https://doi.org/10.1038/nature737>
- [24] Epping, M.T., Meijer, L.A.T., Krijgsman, O., Bos, J.L., Pandolfi, P.P. and Bernards, R. TSPYL5 suppresses p53 levels and function by physical interaction with USP7. *Nature Cell Biology* 13 2011, 102–8. <https://doi.org/10.1038/ncb2142>
- [25] van der Knaap, J.A., Kumar, B.R.P., Moshkin, Y.M., Langenberg, K., Krijgsveld, J., Heck, A.J.R., Karch, F. and Verrijzer, C.P. GMP synthetase stimulates histone H2B deubiquitylation by the epigenetic silencer USP7. *Molecular Cell* 17 2005, 695–707. <https://doi.org/10.1016/j.molcel.2005.02.013>
- [26] Alonso-de Vega, I., Martín, Y. and Smits, V.A.J. USP7 controls Chk1 protein stability by direct deubiquitination. *Cell Cycle (Georgetown, Tex)* 13 2014, 3921–6. <https://doi.org/10.4161/15384101.2014.973324>
- [27] Faustrup, H., Bekker-Jensen, S., Bartek, J., Lukas, J. and Mailand, N. USP7 counteracts SCFbetaTrCP- but not APCdh1-mediated proteolysis of Claspin. *The Journal of Cell Biology* 184 2009, 13–9. <https://doi.org/10.1083/jcb.200807137>
- [28] Schwertman, P., Vermeulen, W. and Marteijn, J.A. UVSSA and USP7, a new couple in transcription-coupled DNA repair. *Chromosoma* 122 2013, 275–84. <https://doi.org/10.1007/s00412-013-0420-2>
- [29] Lecona, E., Narendra, V. and Reinberg, D. USP7 Cooperates with SCML2 To Regulate the Activity of PRC1. *Molecular and Cellular Biology* 35 2015, 1157–68. <https://doi.org/10.1128/MCB.01197-14>
- [30] Du, Z., Song, J., Wang, Y., Zhao, Y., Guda, K., Yang, S., Kao, H.-Y.H.-Y., Xu, Y., Willis, J., Markowitz, S.D., Sedwick, D., Ewing, R.M. and Wang, Z. DNMT1 stability is regulated by proteins coordinating deubiquitination and acetylation-driven ubiquitination. *Science Signaling* 3 2010, ra80. <https://doi.org/10.1126/scisignal.2001462>
- [31] Sowa, M.E., Bennett, E.J., Gygi, S.P. and Harper, J.W. Defining the human deubiquitinating enzyme interaction landscape. *Cell Elsevier Ltd.* 138 2009, 389–403. <https://doi.org/10.1016/j.cell.2009.04.042>
- [32] Zhu, Q., Sharma, N., He, J., Wani, G. and Wani, A.A. USP7 deubiquitinase promotes ubiquitin-dependent DNA damage signaling by stabilizing RNF168*. *Cell Cycle Taylor & Francis.* 14 2015, 1413–25. <https://doi.org/10.1080/15384101.2015.1007785>
- [33] van der Horst, A., de Vries-Smits, A.M.M., Brenkman, A.B., van Triest, M.H., van den Broek, N., Colland, F., Maurice, M.M. and Burgering, B.M.T. FOXO4 transcriptional activity is regulated by monoubiquitination and USP7/HAUSP. *Nature Cell Biology* 8 2006, 1064–73. <https://doi.org/10.1038/ncb1469>

- [34] Song, M.S., Salmena, L., Carracedo, A., Egia, A., Lo-Coco, F., Teruya-Feldstein, J. and Pandolfi, P.P. The deubiquitinylation and localization of PTEN are regulated by a HAUSP-PML network. *Nature* 455 2008, 813–7. <https://doi.org/10.1038/nature07290>
- [35] Hao, Y.-H., Fountain, M.D., Fon Tacer, K., Xia, F., Bi, W., Kang, S.-H.L., Patel, A., Rosenfeld, J.A., Le Caignec, C., Isidor, B., Krantz, I.D., Noon, S.E., Pfotenhauer, J.P., Morgan, T.M., Moran, R., Pedersen, R.C., Saenz, M.S., Schaaf, C.P. and Potts, P.R. USP7 Acts as a Molecular Rheostat to Promote WASH-Dependent Endosomal Protein Recycling and Is Mutated in a Human Neurodevelopmental Disorder. *Molecular Cell* 59 2015, 956–69. <https://doi.org/10.1016/j.molcel.2015.07.033>
- [36] Holowaty, M.N. and Frappier, L. HAUSP/USP7 as an Epstein-Barr virus target. *Biochemical Society Transactions* 32 2004, 731–2. <https://doi.org/10.1042/BST0320731>
- [37] Saridakis, V., Sheng, Y., Sarkari, F., Holowaty, M.N., Shire, K., Nguyen, T., Zhang, R.G., Liao, J., Lee, W., Edwards, A.M., Arrowsmith, C.H. and Frappier, L. Structure of the p53 binding domain of HAUSP/USP7 bound to Epstein-Barr nuclear antigen 1 implications for EBV-mediated immortalization. *Molecular Cell* 18 2005, 25–36. <https://doi.org/10.1016/j.molcel.2005.02.029>
- [38] Sheng, Y., Saridakis, V., Sarkari, F., Duan, S., Wu, T., Arrowsmith, C.H. and Frappier, L. Molecular recognition of p53 and MDM2 by USP7/HAUSP. *Nature Structural & Molecular Biology* 13 2006, 285–91. <https://doi.org/10.1038/nsmb1067>
- [39] Cheng, J., Yang, H., Fang, J., Ma, L., Gong, R., Wang, P., Li, Z. and Xu, Y. Molecular mechanism for USP7-mediated DNMT1 stabilization by acetylation. *Nature Communications* 6 2015, 7023. <https://doi.org/10.1038/ncomms8023>
- [40] Pfoh, R., Lacdao, I.K., Georges, A.A., Capar, A., Zheng, H., Frappier, L. and Saridakis, V. Crystal Structure of USP7 Ubiquitin-like Domains with an ICPO Peptide Reveals a Novel Mechanism Used by Viral and Cellular Proteins to Target USP7. *PLoS Pathogens* 11 2015, e1004950. <https://doi.org/10.1371/journal.ppat.1004950>
- [41] Ma, J., Martin, J.D., Xue, Y., Lor, L.A., Kennedy-Wilson, K.M., Sinnamon, R.H., Ho, T.F., Zhang, G., Schwartz, B., Tummino, P.J. and Lai, Z. C-terminal region of USP7/HAUSP is critical for deubiquitination activity and contains a second mdm2/p53 binding site. *Archives of Biochemistry and Biophysics* 503 2010, 207–12. <https://doi.org/10.1016/j.abb.2010.08.020>
- [42] Hu, M., Li, P., Li, M., Li, W., Yao, T., Wu, J.-W., Gu, W., Cohen, R.E. and Shi, Y. Crystal Structure of a UBP-Family Deubiquitinating Enzyme in Isolation and in Complex with Ubiquitin Aldehyde. *Cell* 111 2002, 1041–54. [https://doi.org/10.1016/S0092-8674\(02\)01199-6](https://doi.org/10.1016/S0092-8674(02)01199-6)
- [43] Fernández-Montalván, A., Bouwmeester, T., Joberty, G., Mader, R., Mahnke, M., Pierrat, B., Schlaeppli, J.-M., Worpenberg, S. and Gerhartz, B. Biochemical characterization of USP7 reveals post-translational modification sites and structural requirements for substrate processing and subcellular localization. *The FEBS Journal* 274 2007, 4256–70. <https://doi.org/10.1111/j.1742-4658.2007.05952.x>
- [44] Faesen, A.C., Dirac, A.M.G., Shanmugham, A., Ovaa, H., Perrakis, A. and Sixma, T.K. Mechanism of USP7/HAUSP activation by its C-terminal ubiquitin-like domain and allosteric regulation by GMP-synthetase. *Molecular Cell Elsevier Inc.* 44 2011, 147–59. <https://doi.org/10.1016/j.molcel.2011.06.034>
- [45] Studier, F.W. Protein production by auto-induction in high-density shaking cultures. *Protein Expression and Purification* 41 2005, 207–34. <https://doi.org/10.1016/j.pep.2005.01.016>
- [46] Kabsch, W. XDS. *Acta Crystallographica Section D, Biological Crystallography* 66 2010, 125–32. <https://doi.org/10.1107/S0907444909047337>
- [47] McCoy, A.J., Grosse-Kunstleve, R.W., Adams, P.D., Winn, M.D., Storoni, L.C. and Read, R.J. Phaser crystallographic software. *Journal of Applied Crystallography International Union of Crystallography.* 40 2007, 658–74. <https://doi.org/10.1107/S0021889807021206>
- [48] Emsley, P., Lohkamp, B., Scott, W.G. and Cowtan, K. Features and development of Coot. *Acta Crystallographica Section D, Biological Crystallography* 66 2010, 486–501. <https://doi.org/10.1107/S0907444910007493>
- [49] Nicholls, R.A., Fischer, M., McNicholas, S. and Murshudov, G.N. Conformation-independent structural comparison of macromolecules with ProSMART. *Acta Crystallographica Section D, Biological Crystallography International Union of Crystallography.* 70 2014, 2487–99. <https://doi.org/10.1107/S1399004714016241>
- [50] Murshudov, G.N., Skubák, P., Lebedev, A.A., Pannu, N.S., Steiner, R.A., Nicholls, R.A., Winn, M.D., Long, F. and Vagin, A.A. REFMAC5 for the refinement of macromolecular crystal structures. *Acta Crystallographica Section D, Biological Crystallography* 67 2011, 355–67. <https://doi.org/10.1107/S0907444911001314>

Chapter 2. Structure of USP7 CD123

- [51] Winn, M.D., Ballard, C.C., Cowtan, K.D., Dodson, E.J., Emsley, P., Evans, P.R., Keegan, R.M., Krissinel, E.B., Leslie, A.G.W., McCoy, A., McNicholas, S.J., Murshudov, G.N., Pannu, N.S., Potterton, E.A., Powell, H.R., Read, R.J., Vagin, A. and Wilson, K.S. Overview of the CCP4 suite and current developments. *Acta Crystallographica Section D, Biological Crystallography* 67 2011, 235–42. <https://doi.org/10.1107/S0907444910045749>
- [52] Davis, I.W., Murray, L.W., Richardson, J.S. and Richardson, D.C. MOLPROBITY: structure validation and all-atom contact analysis for nucleic acids and their complexes. *Nucleic Acids Research* 32 2004, W615–9. <https://doi.org/10.1093/nar/gkh398>
- [53] Joosten, R.P., Long, F., Murshudov, G.N. and Perrakis, A. The PDB_REDO server for macromolecular structure model optimization. *IUCr* 1 2014, 213–20. <https://doi.org/10.1107/S2052252514009324>
- [54] Clerici, M., Luna-Vargas, M.P.A., Faesen, A.C. and Sixma, T.K. The DUSP–Ubl domain of USP4 enhances its catalytic efficiency by promoting ubiquitin exchange. *Nature Communications* 5 2014, 5399. <https://doi.org/10.1038/ncomms6399>
- [55] Nicholson, B. and Suresh Kumar, K.G. The multifaceted roles of USP7: new therapeutic opportunities. *Cell Biochemistry and Biophysics* 60 2011, 61–8. <https://doi.org/10.1007/s12013-011-9185-5>
- [56] Colland, F., Formstecher, E., Jacq, X., Reverdy, C., Planquette, C., Conrath, S., Trouplin, V., Bianchi, J., Aushev, V.N., Camonis, J., Calabrese, A., Borg-Capra, C., Sippl, W., Collura, V., Boissy, G., Rain, J.-C., Guedat, P., Delansorne, R. and Daviet, L. Small-molecule inhibitor of USP7/HAUSP ubiquitin protease stabilizes and activates p53 in cells. *Molecular Cancer Therapeutics* 8 2009, 2286–95. <https://doi.org/10.1158/1535-7163.MCT-09-0097>
- [57] Weinstock, J., Wu, J., Cao, P., Kingsbury, W.D., McDermott, J.L., Kodrasov, M.P., McKelvey, D.M., Suresh Kumar, K.G., Goldenberg, S.J., Mattern, M.R. and Nicholson, B. Selective Dual Inhibitors of the Cancer-Related Deubiquitylating Proteases USP7 and USP47. *ACS Medicinal Chemistry Letters* 3 2012, 789–92. <https://doi.org/10.1021/ml200276j>
- [58] Kessler, B.M. Selective and reversible inhibitors of ubiquitin-specific protease 7: a patent evaluation (WO2013030218). Informa UK, Ltd. London. 2014,.
- [59] Lee, G., Oh, T.-I., Um, K.B., Yoon, H., Son, J., Kim, B.M., Kim, H.-I., Kim, H., Kim, Y.J., Lee, C.-S. and Lim, J.-H. Small-molecule inhibitors of USP7 induce apoptosis through oxidative and endoplasmic reticulum stress in cancer cells. *Biochemical and Biophysical Research Communications* 470 2016, 181–6. <https://doi.org/10.1016/j.bbrc.2016.01.021>

Chapter 2.

Structure of USP7 CD123

Supplemental data

2

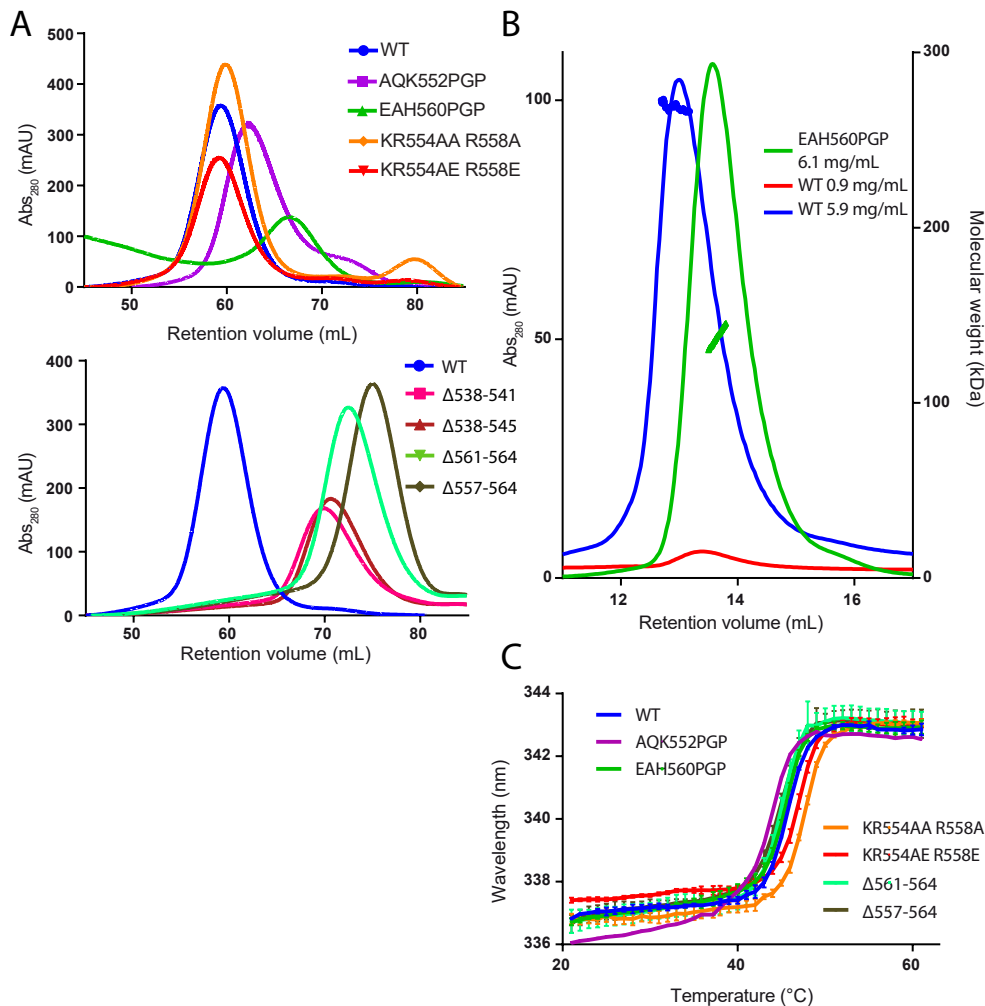
Robbert Q. Kim, Willem J. van Dijk, Titia K. Sixma

*Division of Biochemistry and Cancer Genomics Center, Netherlands Cancer Institute,
Plesmanlaan 121, 1066 CX Amsterdam, the Netherlands*

Adapted from:

Kim, R.Q., van Dijk, W.J. and Sixma, T.K.
Structure of USP7 catalytic domain and three Ubl-domains reveals a connector α -helix with regulatory role.
Journal of Structural Biology 195 2016, 11–8.
<https://doi.org/10.1016/j.jsb.2016.05.005>

Chapter 2. Structure of USP7 CD123



Supplemental figure 1. Quality control of USP7-CD12345 mutants. **A.** Gel filtration profiles for CD12345 constructs indicate dimer formation for wild type CD12345 and charge mutants, but less so for the other mutants. Analysis was done on Superdex 200 16/60 during purification. **B.** MALLS analysis of WT CD12345 versus EAH560PGP shows that WT behaves as dimer and EAH560PGP is a monomer at ~6 mg mL⁻¹. At lower concentrations WT is also monomeric as seen from the gel filtration profile, but no useful MALLS signal can be obtained at this concentration. All runs were performed on an analytical Superdex 200 10/300 gel filtration column, the resulting molecular weight (by MALLS analysis) in the peaks are plotted on the right-hand axis. **C.** Analysis of the barycentric fluorescence curves show that the mutants have a similar melting temperature as wild type protein, indicating the mutations do not affect stability.

Chapter 3.

USP7 activity mechanism

Robbert Q. Kim¹, Paul P. Geurink^{2,3}, Monique P.C. Mulder^{2,3}, Alexander Fish¹, Reggy Ekkebus^{2,3}, Farid El Oualid⁴, Willem J. van Dijk¹, Duco van Dalen^{2,6}, Huib Ovaa^{2,3}, Hugo van Ingen^{5,7}, Titia K. Sixma¹

¹*Division of Biochemistry and Oncode Institute, Netherlands Cancer Institute, Plesmanlaan 121, 1066 CX Amsterdam, the Netherlands*

²*Division of Cell Biology II, Netherlands Cancer Institute, Plesmanlaan 121, 1066 CX Amsterdam, the Netherlands*

³*Current address: Oncode Institute and Department of Cell and Chemical Biology, Leiden University Medical Center, Leiden, the Netherlands*

⁴*UbiQ Bio BV, Science Park 408, 1098 XH Amsterdam, the Netherlands*

⁵*Macromolecular Biochemistry, Leiden Institute of Chemistry, Leiden University, the Netherlands*

⁶*Current address: Tumor Immunology department, Radboud Institute for Molecular Sciences, Nijmegen, the Netherlands*

⁷*Current address: Bijvoet center, Utrecht University, the Netherlands*

In press as:

Kim, R.Q., Geurink, P.P., Mulder, M.P.C., Fish, A., Ekkebus R., El Oualid, F., van Dijk, W.J., van Dalen, D., Ovaa, H., van Ingen H. and Sixma, T.K.

Kinetic analysis of multistep USP7 mechanism shows critical role for target protein in activity

Nature Communications

<https://doi.org/10.1038/s41467-018-08231-5>

Chapter 3. USP7 activity mechanism

Abstract

USP7 is a highly abundant deubiquitinating enzyme (DUB), involved in cellular processes including DNA damage response and apoptosis. It has an unusual catalytic mechanism, where the low intrinsic activity of the catalytic domain (CD) increases when the C-terminal Ubl domains (Ubl45) fold onto the CD, allowing binding of the activating C-terminal tail near the catalytic site. Here we delineate how the target protein promotes the activation. Using NMR analysis and biochemistry we describe the order of activation steps, showing that ubiquitin binding is an instrumental step in USP7 activation. With chemically synthesised p53-peptides we identify how the correct ubiquitinated substrate promotes catalytic activity dramatically. This allows transient reaction kinetic modelling to define how the USP7 multistep mechanism is driven by target recognition. Our data show how this pleiotropic DUB can gain specificity for its cellular targets.

Introduction

Ubiquitination is recognised as an important post-translational modification (PTM), influencing protein fate in every cellular process^{1,2}. This modification of a target protein conjugates the C-terminus of ubiquitin (Ub) to a lysine residue on a target protein via an E1-E2-E3 cascade³. As Ub has 7 lysines and an available amino terminus it can be ubiquitinated itself, resulting in poly-ubiquitination through 8 different possible linkages⁴. These different ubiquitin marks generate distinct signals that determine the fate of the target protein, ranging from proteasomal degradation to cellular relocation or recruitment of complex partners^{2,5,6}.

Similar to other PTMs, ubiquitination can be reversed, modulating and fine-tuning the ubiquitin signal⁷. This deubiquitination is carried out by deubiquitinating enzymes (DUBs) that can hydrolyse the isopeptide bond between Ub and the target protein⁸. DUBs play a balancing role in ubiquitination: dysfunction can lead to serious diseases such as cancer^{9,10}, and their activity is tightly controlled¹¹.

One of the most abundant DUBs is Ubiquitin Specific Protease 7 (USP7, also known as HAUSP¹²). It has been assigned multiple critical functions ranging from DNA repair and apoptosis to suppression of regulatory T-cell function^{13,14}. USP7 is shown to correlate with paediatric cancer^{15,16} and is actively targeted for cancer therapy^{17–19}, primarily for its nuclear functions, while USP7 haploinsufficiency leads to a neurodevelopmental disorder²⁰ through a cytosolic role.

USP7 is found in a variety of protein complexes, many of which contain an E3 ligase and its target²¹. In these complexes both the E3 ligase and its substrate are targets of USP7, like the substrate pair of E3 ligase MDM2 and target p53²², the master regulator of the response to cellular stress²³. This creates a situation where USP7 can either deubiquitinate and stabilise MDM2, promoting p53 ubiquitination and its proteasomal degradation^{24,25}, or target p53 by which the apoptotic pathway is activated²⁶. The balance between these two targets is influenced by various other proteins shifting USP7 activity towards MDM2²⁷ or p53²⁸.

For the interaction with both MDM2 and p53, USP7 relies on its N-terminal TRAF (Fig. 1a) domain on USP7. This domain interacts with a TRAF recognition motif on the target proteins with a moderate affinity of $\sim 10 \mu\text{M}$ ^{29,30}, but does not affect the actual hydrolysis of the ubiquitin isopeptide bond on a minimal substrate³¹.

The TRAF domain is connected to the adjacent catalytic domain (CD) through a flexible linker³⁰, allowing the CD to find and cleave off the ubiquitin from the target (Fig. 1a). This catalytic domain alone has low intrinsic deubiquitinating activity while full-length USP7 is a much more active DUB³². Crystal structures of this CD show that the *apo* state of the enzyme has an inactive conformation, with a misaligned catalytic triad³³. When ubiquitin is bound, the catalytic triad (C223, H464 and D481) realigns into an active conformation, involving significant changes in a loop above the active site. This 'switching loop' is essential for full activity of full-length USP7³¹.

Located C-terminally of the CD are five ubiquitin-like (Ubl) domains which are essential for the increased activity of full length USP7^{31,32}. The three Ubl domains just downstream of the CD (Fig. 1a) do not influence the activity directly, but rather serve as a binding platform for interactors such as GMPS or DNMT1^{31,34,35}. The last two Ubl domains with the activating tail (Ubl45), however, are indispensable for full activity of USP7: Ubl45 readily activates the CD as does the very C-terminal tail by itself, at high concentrations³⁶.

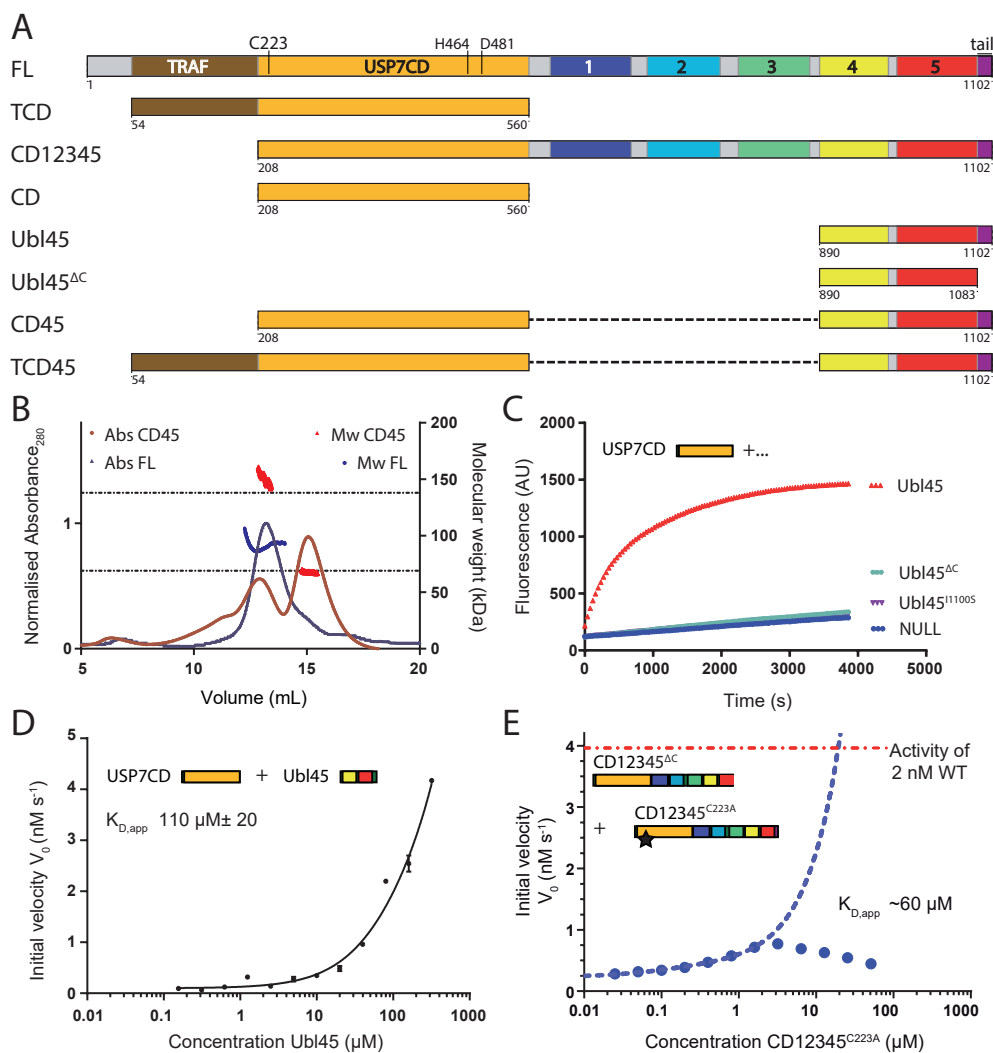
Chapter 3. USP7 activity mechanism

The Ubl domain region can adopt an extended conformation, as seen in the crystal structure of Ubl12345 (PDB: 2YLM), but has considerable flexibility, as shown by small-angle X-ray scattering (SAXS)³¹. Detailed biochemistry combined with SAXS analysis led to a proposed mechanism where the Ubl domains curve and the Ubl45 domain ‘folds back’ onto the CD. The C-terminal tail then interacts with the ‘switching loop’, stabilising a catalytically competent conformation of USP7. Various mutations in either the tail or the loop substantiated this model³¹. The role of the C-terminal tail was further defined in a crystal structure of ubiquitin-bound CD linked to Ubl45. This showed how the C-terminal tail binds the CD, stabilising the ‘switching loop’³⁶ in the active conformation. Intriguingly in this analysis the C-terminal peptide alone, when directly linked can reconstitute much of the activation, but from the structure, it was unclear whether it was bound *in cis* or *trans*. This ambiguity prompted us to further investigate the role of the Ubl45 domain in this interaction and its effect on USP7 activity.

Most molecular studies on DUB activity utilise minimal substrates, focussing on the role of the ubiquitin moiety, essentially the product of the reaction. In the last years the focus has therefore shifted towards Ub-chains⁴, uncovering chain-specificity of DUBs, which allowed relating them to distinct biological processes³⁷. For USP7 the active conformation of the catalytic domain has only been observed when it was conjugated to ubiquitin³³. Ubiquitin alone is not sufficient to induce the rearrangement and a fusion at its C-terminus, such as ubiquitin aldehyde or a ubiquitinated substrate, is required for proper active site rearrangement³⁸. The roles of other substrate proteins, however have received relatively little attention in biochemical DUB analyses. Quantifying contributions of a realistic substrate requires a homogeneous, well-defined target. For p53, the interaction with USP7 has been described in detail^{29,39}, allowing generation of synthetic mimics of the substrate. Using such ubiquitinated p53 mimics as model targets we can investigate the effect of a more realistic substrate on USP7 activity in an *in vitro* setting.

Here we made use of chemical synthesis to generate well-defined tools to address how a p53 model substrate interaction may modulate the activation process. Structural analysis suggests that a monomeric USP7 undergoes an activation process that can be further improved by binding to a valid substrate. Using the p53 model substrate and global modelling on the experimental data we could determine the order of events and quantify the steps involved in the USP7 ubiquitin hydrolysis cycle.

Figure 1. USP7 activation by the C-terminal tail happens in cis. A. Schematic domain representation of USP7 and constructs used in this study. Active site residues and domain names are indicated: TRAF; TRAF domain, CD; Catalytic domain, 1-5; Ubl domains 1 through 5, tail; The activating C-terminal peptide (res. 1083-1102), marked in purple. The graphical representation of the constructs is used in other figures. **B.** Analysis of USP7 constructs on SEC-MALLS shows monomer/dimer equilibrium. CD45 (100 μ L of 45 μ M) or FL (80 μ L of 20 μ M) were loaded on a Superdex200 gel filtration column. Absorbance at 280 nm (dark red: CD45; dark blue: FL) was monitored and eluted peaks were analysed for molecular weight (red: CD45; blue: FL) by in-line MALLS. For CD45 the molecular weights of the monomer (69 kDa) and dimer (138 kDa) are indicated with the dotted line. **C.** Activation of USP7CD by Ubl45 requires the very C-terminal



tail. 20 nM of CD was mixed with Ubl45 variants as indicated and tested for DUB activity using UbRho. **D.** 20 nM USP7CD was incubated with a titration range of Ubl45, and tested in a deubiquitination assay as in 1c. These initial velocities were plotted against the concentration to yield an apparent K_D , with the displayed standard deviation. **E.** 20 nM CD12345^{ΔC} has similar activity to CD and can be activated by the tail: when titrating in CD12345^{C223A}, which has no activity, the tail will activate the tailless construct upon dimerization. The activity readout shows that this dimerization-dependent activation of USP7 happens at micromolar concentrations in line with affinity of 1d. Binding of ubiquitin substrate to CD12345^{C223A} causes an inhibitory effect above 2 μ M, therefore only lower concentrations were used to extrapolate a $K_{D,app}$ (blue dashes). The red dotted lines indicate the activity of WT CD12345 for comparison.

Chapter 3. USP7 activity mechanism

Results

USP7 activation requires the C-terminal tail in cis

The activation of USP7 requires interaction between the CD and the C-terminal peptide (see Fig. 1a for domain definitions and nomenclature). The details of this interaction were described in a recent crystal structure (PDB: 5JTV) of Ubl45 and CD³⁶. This structure convincingly shows the binding of the activating C-terminal peptide, however the connection to Ubl45 was disordered making it difficult to decide whether the C-terminus of USP7 binds into the activation cleft *in cis* or *in trans*.

When we analysed the ability of USP7 to form dimers in size-exclusion chromatography with multi-angle laser light scattering detection (SEC-MALLS), we observed no dimerization for FL (injected at 20 μ M, peak elutes at \sim 4 μ M) and only partially for the construct used in the crystallization experiment (injected at 45 μ M, monomer peak elutes at \sim 7 μ M) (Fig. 1b). This indicates that at the much lower concentration in cells (\sim 0.3 μ M⁴⁰), USP7 is more likely to behave as a monomer.

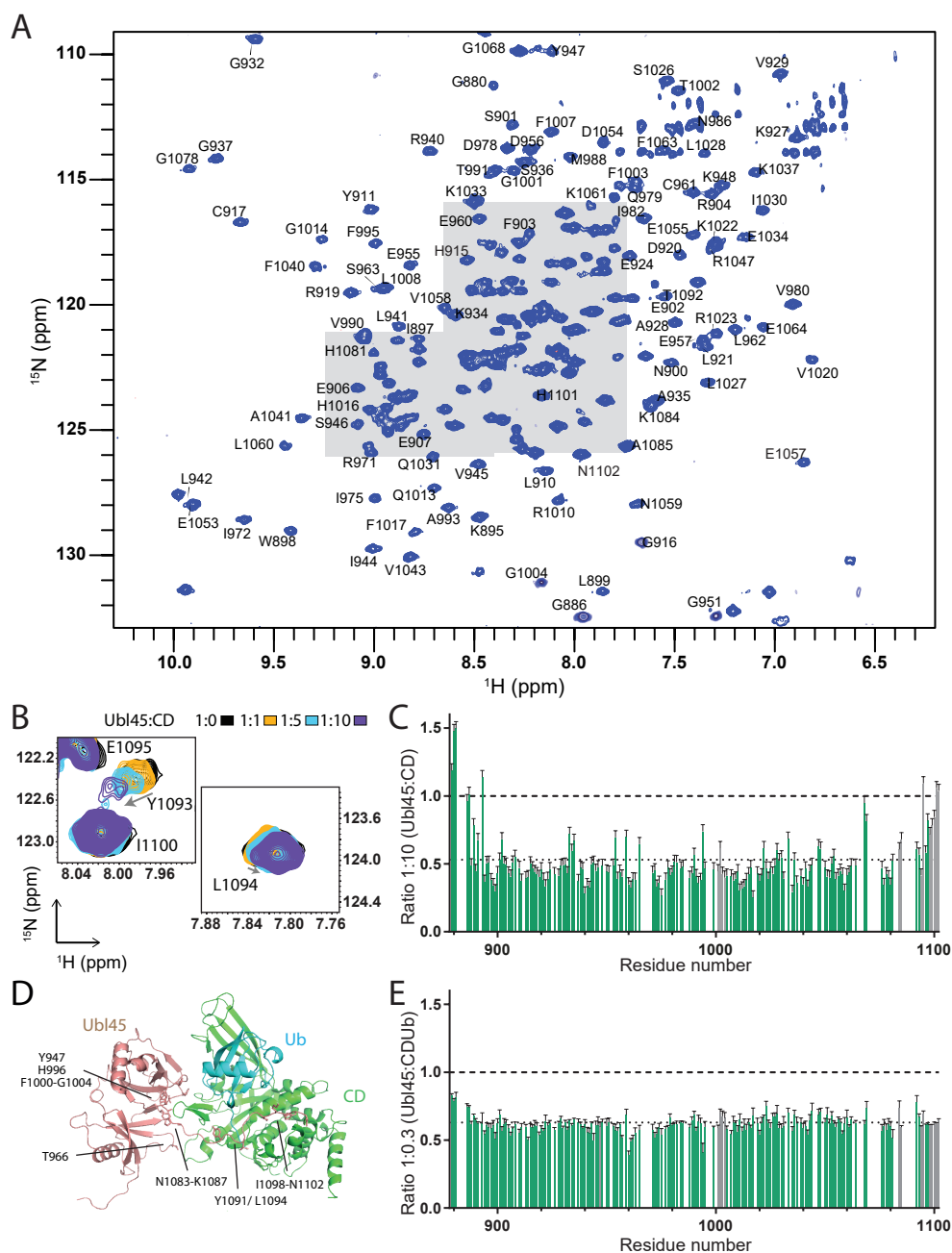
We then checked what concentrations of Ubl45 are needed for *in trans* activation of CD (Fig. 1c). We find this is possible, but only occurs at high concentrations, with an apparent K_D of 110 μ M (Fig. 1d). Consistently, a construct lacking the C-terminal tail (CD12345^{ΔC}) can be activated by a catalytically dead FL USP7, (CD12345^{C223A}) only at similarly high concentrations, with an apparent K_D of 60 μ M (Fig. 1e). Both these apparent *in trans* activation constants are orders of magnitude higher than the concentrations (1 to 20 nM) that are sufficient for USP7 activity assays of full-length or CD-Ubl45 constructs³¹. We therefore conclude that although *trans* activation of USP7 is possible at high concentrations, it is not the predominant mechanism of its self-activation.

Definition of the interaction interface between CD and Ubl45

These results suggest that the interaction of CD and Ubl45 likely takes place *in cis*. The interaction of the C-terminal peptide with CD, as determined by Rougé et. al. in the crystal structure³⁶, is indisputable, but the positioning of the Ubl45 core did not seem as well-defined. We therefore wanted to investigate this interaction further, using solution methods. In an attempt to explore the role of the tail in the interaction and identify the interaction site on

Figure 2. Interaction between Ubl45 and CD identified in solution using NMR. A. The peak dispersion and resolution in the ^1H - ^{15}N correlation spectrum of Ubl45 (45 μ M; 25 kDa; coloured blue) indicates a well-folded protein. Assignments are indicated, those for the crowded regions, indicated in grey, are shown in Supp. Fig. 1a. **B.** The addition of 450 μ M CD prompted very little chemical shift perturbations (CSPs). The biggest observed CSP of 0.019 ppm for Y1093 is illustrated in this zoom. **C.** Upon titration of CD the peaks in the Ubl45 spectrum show significant decrease in intensity. Here the intensity ratios between the apo spectrum (1:0) and the highest titration (1:10) are plotted against the residue numbers. The average is indicated by a dotted line, while residues that were found in the crystal structure to interact (see D) are highlighted in the bar graph. **D.** Structure and intermolecular interface in the Ubl45-CDUb structure (PDB: 5JTV³⁶), showing contacts between both the tail and the core of Ubl45 to CD. Ubl45 residues that are within 4 Å of CD are shown as sticks and indicated. **E.** The same intensity plot as in C, but now done for the titration with CDUb indicates that the tail now does get immobilised.

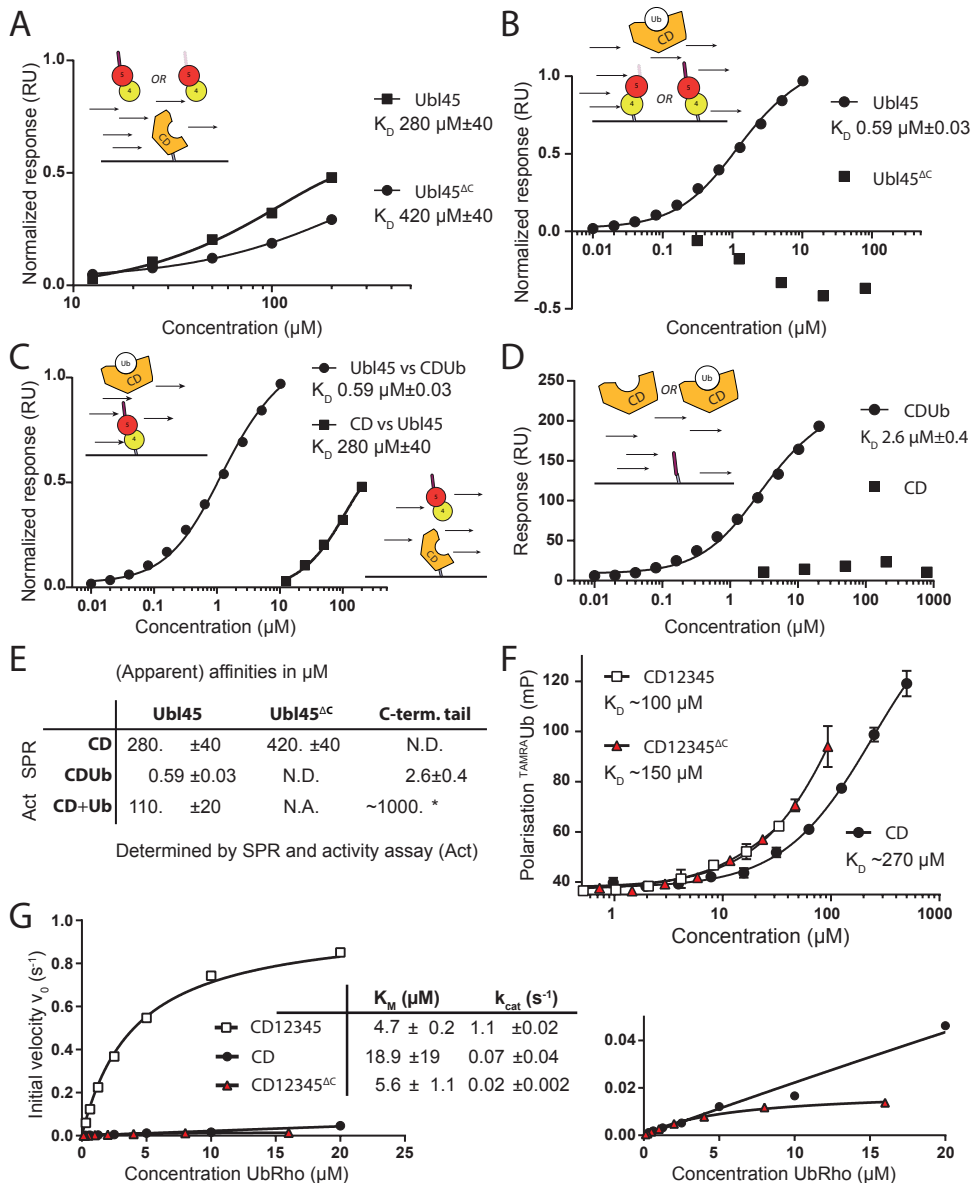
the Ubl45 core in solution, we used NMR spectroscopy to map the binding interface (Fig. 2, Supp. methods), starting by assignment of the backbone resonances of Ubl45 (Supp. Fig. 1a). The resulting predicted secondary structure in solution matches that of the crystal structure (PDB: 5JTV; Supp. Fig. 1b), indicating that NMR conditions allow functional interaction analysis.



Chapter 3. USP7 activity mechanism

We titrated the unlabelled CD (42 kDa) into labelled Ubl45 (25 kDa) up to a ratio of 1:10 and followed changes in peak position or intensity (Fig. 2a-b). Upon addition of CD, we observe only very minor chemical shift perturbations (CSPs) (Fig. 2b), but a marked decrease in intensity for residues in the core of the Ubl45 domains (Fig. 2c). The amount of peak intensity decrease agrees well with the formation of a 67 kDa complex with affinity as determined by SPR (see below and Supp. Fig. 2a). Under these conditions, residues with large changes in their chemical environment upon binding are expected to show an even more dramatic intensity loss (Supp. Fig. 2c). From the absence of such effect for residues that are predicted to be in the interface based on the crystal structure (Fig. 2d) or for any other site on the core surface, we conclude that the Ubl45 core is not involved in a single, specific interaction with CD. Only a few, very minimal CSPs are observed, localized to C-terminal tail residues, with the strongest shift seen for Y1093 (Fig. 2b). The tail residues however remain sharp and intense peaks throughout the titration, indicating that the tail is not immobilized on the CD surface. As the tail is immobilised in the crystal structure, which was solved in the presence of ubiquitin we decided to assess the influence that ubiquitin would have on this interaction. Because ubiquitin monomers bind poorly to USP7 CD³⁸, we first generated a covalent complex between CD and Ub, using a suicide probe, ubiquitin-propargyl (Ub-PA⁴¹) to generate CDUb. Upon titration of CDUb onto Ubl45, the effect of binding is only apparent through peak intensity decrease. Upon addition of CDUb, the Ubl45 peak intensity decrease is now nearly directly proportional to the equivalents of CDUb added. At 30% of CDUb added, peak intensity for all Ubl45 residues, including the C-terminal residue has been reduced by ~30% (Fig. 2e). This indicates that Ubl45 forms a tight complex with CDUb in which the tail, particularly the C-terminal residues are immobilized. The absence of CSPs indicates that the free protein is in slow exchange with the complex (75 kDa) (see also Supp. Fig. 2c). Together, these results suggest that while the Ubl45 binds to CD, it does so in multiple, weak binding modes predominantly involving the Ubl45 core to form a dynamic complex. Our data further suggest that the presence of ubiquitin or a ubiquitinated target may induce the specific binding mode of the C-terminal tail as observed in the crystal structure.

Figure 3. Affinity of CD for Ubl45 increases with Ub present and is dependent on C-terminal tail. A. SPR binding results indicate a weak affinity of USP7CD for either Ubl45 or Ubl45^{ΔC}. CD was immobilized through GST on the chip and tested for binding with Ubl45 or Ubl45^{ΔC}. Equilibrium binding values were plotted against concentration and fitted to get an estimated K_D . Responses were normalised using the B_{max} and the standard deviation for resulting values is given. **B.** The increased binding between Ubl45 and CDUb depends on the C-terminal tail. Ubl45 or Ubl45^{ΔC} was immobilized on the chip and the covalent CDUb complex was flown over. A fit was made using the equilibrium binding values yielding a K_D of 590 nM for Ubl45, whereas no binding could be observed for Ubl45^{ΔC}. Normalisation was carried out using B_{max} . **C.** Comparison of the affinity of Ubl45 for CD or CDUb shows a remarkable increase. Specified curves from Fig. 3a and 3b are replotted to exemplify the change in K_D . **D.** The C-terminal tail was immobilized using biotin and CD or CDUb was flown over to confirm that the tail interacts with the transition state (CDUb) only and not the apo CD. **E.** Overview of affinities between Ubl45 and CD show that Ub enhances the binding of the tail. The values for the upper two rows are determined using SPR, see A-D. The values



in the last row have been derived from activity assays, see Fig. 1d and ³⁶ for the estimated affinity of the C-terminal tail (*). N.A.: not applicable; N.D.: No binding detected. **F.** The presence of the Ubl45 domain is essential for increased affinity of CD for ubiquitin, but not the C-terminal tail. The affinity for ubiquitin was measured in an FP assay where TAMRA-labelled ubiquitin was incubated with various USP7 constructs. **G.** Steady state kinetics analysis of USP7 constructs indicates that the C-terminal tail mainly affects the catalytic rate, while the presence of Ubl45 without the tail enhances the affinity for the ubiquitin substrate. The Michaelis-Menten constant (K_M) and k_{cat} were obtained by fitting the initial velocity data for various concentrations of UbRho.

Chapter 3. USP7 activity mechanism

Interaction between Ubl45 and CD does not require the tail

For full activity the C-terminal tail is essential, but its affinity for the catalytic domain could only be measured indirectly in activity assays. In surface plasmon resonance (SPR) experiments, interaction was not detectable³¹, but in an activation assay, the apparent K_D -value was estimated at $\sim 1000 \mu\text{M}$ ³⁶. This is one order of magnitude weaker than the apparent K_D determined for Ubl45 ($110 \mu\text{M}$, Fig. 1d), in line with our NMR result that suggested that the Ubl domains contribute to the binding and activation of the catalytic domain. To investigate the interaction between Ubl45^{ΔC} and the catalytic domain we immobilised GST-USP7CD on the SPR chip, flowing over the tailless construct Ubl45^{ΔC}. We were able to detect binding at high concentrations. Extrapolation of the curve, suggests a K_D of $420 \mu\text{M}$ (Fig. 3a), similar to that observed for the C-terminal peptide interaction in the activity assay. This suggests that both Ubl45^{ΔC} and the tail bind weakly to the CD.

We then tested the affinity of CD for Ubl45 including the tail, and get an approximate K_D of $280 \mu\text{M}$ (Fig. 3a), comparable to the tailless construct. This suggests that the C-terminal tail is not the main driving force for the interaction between the CD and Ubl45 as the affinity is similar with or without the tail. This result is in agreement with the lack of binding between the C-terminal peptide and CD observed in the NMR experiment (Fig. 2c) and earlier data³¹, but seems at odds with the activating role of the tail in the activity assay. The NMR experiment seemed to suggest that ubiquitin needs to be present for immobilization of the tail on CD.

Interaction between C-terminal tail and CD requires Ub

To quantify this effect of ubiquitin on the binding of the activating, C-terminal tail, we used the covalently coupled ubiquitin to the catalytic cysteine in the CD (CDUb). As CD on its own has low activity, the reaction between Ub-PA and CD had to be driven to completion using the *trans* activation of Ubl45. After incubation however, Ubl45 could not be separated from CDUb on gel filtration (Supp. Fig. 3a) requiring additional ion exchange chromatography, indicating that complex formation between CDUb and Ubl45 was tighter than expected, as a complex with a K_D of $280 \mu\text{M}$ (Fig. 3a) generally dissociates on such gel filtration experiments. We quantified the interaction by SPR flowing CDUb over GST-immobilised Ubl45 (Fig. 3b). Data analysis in Evifit⁴² identified a K_D of $0.59 \mu\text{M} \pm 0.03$ with a k_{off} of 0.8 s^{-1} (Supp. Fig. 3b) for the interaction between CDUb and Ubl45. The presence of ubiquitin in CD therefore increased the affinity four hundred-fold compared to CD only (Fig. 3c). As the C-terminal tail is necessary for activation, we hypothesised that it would directly facilitate the interaction with the intermediate, ubiquitin-bound, state. To test this, we immobilised the tailless construct (Ubl45^{ΔC}) in our SPR experiment setup and flowed over CDUb with concentrations up to $80 \mu\text{M}$ (Fig. 3b). We could not detect any binding of Ubl45^{ΔC} in this experiment, suggesting that the Ubl domains can no longer bind ubiquitin-bound catalytic domain, contrary to *apo* CD (Fig. 3a). This would mean that, after ubiquitin binding, the increased activity depends exclusively on the C-terminal tail.

In agreement to this, the immobilised tail peptide (residues 1083-1102) interacted with CDUb, with a K_D of $2.6 \mu\text{M}$, but showed no binding to the CD alone (Fig. 3d). This is analogous to what we found for Ubl45 (Fig. 3b) and in line with our NMR experiments where the tail did not show clear binding to CD alone (Fig. 2b).

Our results are in line with previously published NMR data that showed that a linked Ub is necessary to induce rearrangement of the catalytic site³⁸. The binding of ubiquitin to CD

apparently facilitates binding of the C-terminal tail (Fig. 3d). Together, these data explain how CD can still be activated by the C-terminal tail on its own, albeit with a lower resulting activity than the FL construct³⁶. We conclude that once the ubiquitin-bound intermediate state is achieved, the C-terminal tail is sufficient for self-activation.

Ubl45^{ΔC} promotes ubiquitin binding

Knowing that the C-terminal tail has high affinity for CD only after ubiquitin binding (Fig. 3e), we wondered if Ubl45^{ΔC} might affect the Ub binding. Such an outcome is consistent with our previous results indicating that in full-length USP7 self-activation increases the catalytic rate (k_{cat}) but also the K_M (which is, on a minimal substrate, dominated by the affinity to ubiquitin), from $>>35 \mu M$ to roughly $4 \mu M$ ³¹. It may also explain why direct linkage of the C-terminal peptide to the CD almost, but not completely recapitulates the full length activity³⁶.

We therefore tested ubiquitin binding qualitatively in a fluorescence polarization (FP) assay, following polarisation of TAMRA-labelled Ub upon incubation with various USP7 constructs (Fig. 3f). In this assay we see the increased affinity for ubiquitin in the presence of the Ubl45 domain (when comparing CD12345 with CD only) even when the tail is absent (comparing CD12345^{ΔC} to CD). The data indicate that the presence of the C-terminal tail does not affect the CD affinity for Ub, in line with its lack of affinity for CD observed in the NMR (Fig. 2b) and SPR experiments (Fig. 3d).

We could confirm the Ubl45-induced increase in affinity of CD for Ub by analysis of the steady state kinetics of these constructs in activity assays (Fig. 3g). When we fit Michaelis-Menten curves for CD, CD12345 and CD12345^{ΔC} we could see that presence of the C-terminal tail dramatically increases k_{cat} ³¹, whereas the Ubl45^{ΔC} is responsible for the increase in K_M (compare CD and CD12345^{ΔC} in Fig. 3g).

A multi-step mechanism for USP7 activity

These data suggest that USP7 is likely to follow a multi-step mechanism during its catalytic cycle. In the first step, binding of ubiquitin is facilitated by the core of Ubl45, which does not involve the C-terminal tail. After binding of ubiquitin, conformational changes align the catalytic triad³³. In this state, the affinity of the CD for Ubl45 is decreased (Fig. 3e), but the affinity for the tail is dramatically increased, allowing optimal orientation of the activating C-terminal tail to form the activated state. This mechanism is reminiscent of the classical induced fit in enzymology, where binding of the substrate can activate the enzyme: here, ubiquitin-induced binding of the C-terminal peptide stabilizes the active CD conformation and promotes fast hydrolysis of substrate, which is observed as an increase in k_{cat} .

Next, we wanted to address the role of the target protein in the USP7 mechanism. To study whether interactions with a ubiquitinated target protein would affect USP7 activation we make use of a chemical biology approach.

Role of the target p53

We chose p53 as our model target protein (Fig. 4a), which has six lysines near the C-terminus that can be ubiquitinated³⁹ as well as motifs that can be recognized by the USP7 TRAF domain^{29,43}. We made a synthetic toolbox of ubiquitinated C-terminal p53 peptides⁴⁴ and initial tests on these conjugates indicated that all six lysines could be cleaved by USP7.

Chapter 3. USP7 activity mechanism

We generated two versions of the ubiquitinated p53 peptides with K382 as the ubiquitination site, either with the TRAF recognition motif (p53Ub, res. 357-389) or without this region (p53_{short}Ub, res. 368-389, Fig. 4a). The ubiquitin attachment was varied to allow different assays: a suicide version with a vinylamide (VA) linkage (I)⁴⁵ that can bind covalently, like the better-known vinyl methyl ester^{46,47}, a non-hydrolysable triazole linkage (II)⁴⁸ and a cleavable native isopeptide linkage (III)^{44,49}, for both the short and long versions of the peptide (Fig. 4b).

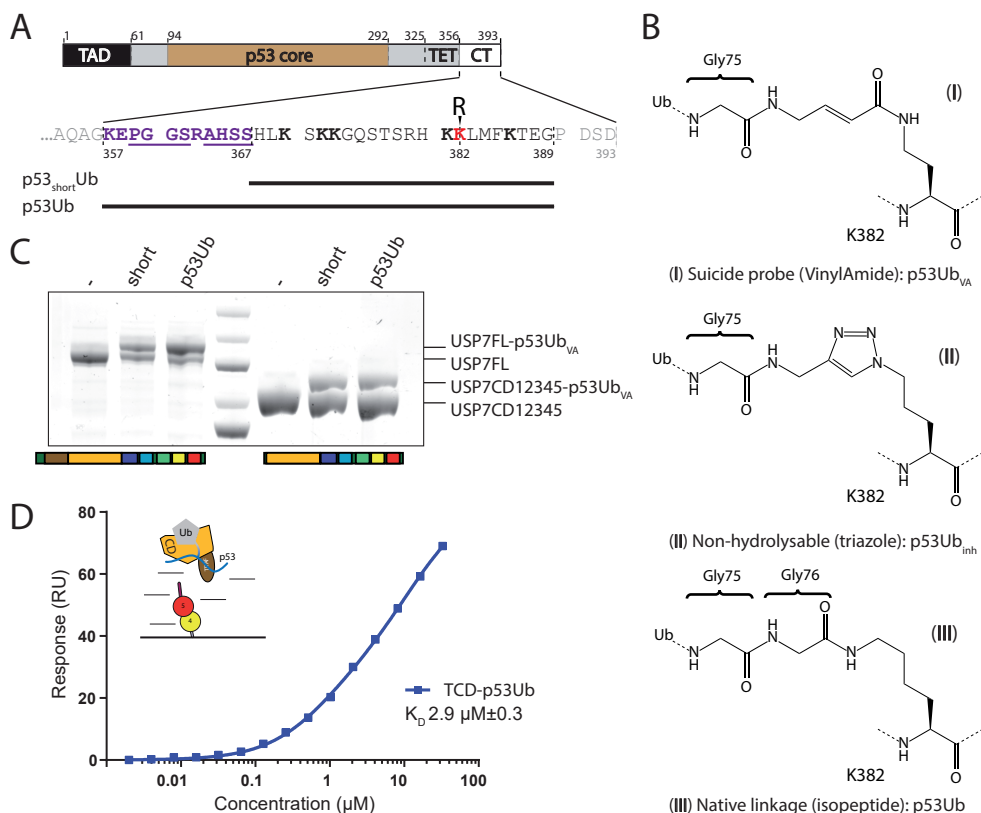


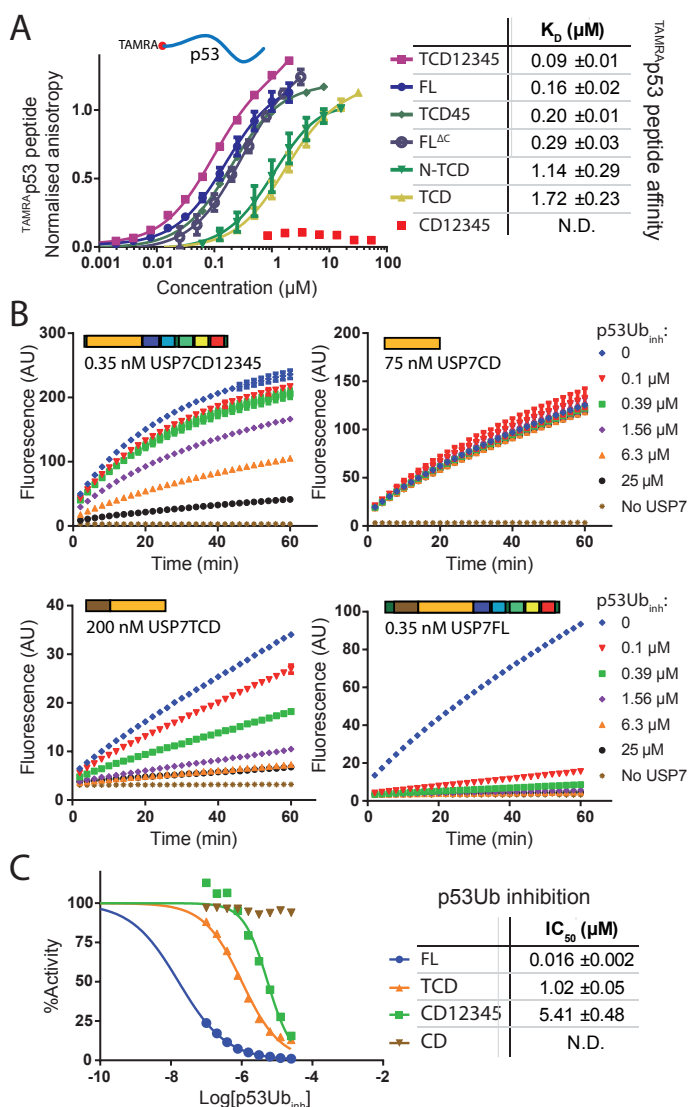
Figure 4. Development of synthetic p53-derived substrates for USP7. **A.** Schematic domain structure of p53 with transactivation domain (TAD), core region, tetramerization domain (TET) and C-terminal region indicated (CT). Close-up of CT highlights lysines (bold) known to be ubiquitinated³⁹ and the TRAF recognition motif (underlined)^{29,43}. K382 (red) is used as target lysine in the synthetic p53Ub reagents, underneath the sequence coverage of the peptides is indicated. **B.** Three synthetic p53Ub-peptides are generated with different linkage types: covalently-binding (vinylamide linkage, (I)), uncleavable (triazole linkage, (II)) and cleavable (native linkage, (III)). **C.** The affinity of USP7 for the covalent-binding p53Ub_{VA} increases if the TRAF domain is present. USP7 constructs with and without TRAF domain have been incubated with the probe for 15 minutes at RT and analysed on a Coomassie gel. **D.** The affinity of Ubl45 for the substrate-bound TCD is similar to CDUb (2.9 μM compared to 0.59 μM, Fig 3c). Around 50 units of Ubl45 were immobilized on the chip before a titration range of p53Ub-bound TCD was flown over. Their equilibrium binding values were plotted and fitted to get the K_D -value.

Using the p53Ub_{VA} suicide probes we were able to assess the role of the TRAF interaction in substrate binding. Although both short and long versions of the probe reacted readily with CD12345 (Fig. 4c), the full-length USP7, which contains the TRAF domain, showed increased complex formation, specifically for the p53Ub peptide that has the TRAF recognition sequence. This indicates that the TRAF recognition sequence promotes the USP7 interaction with the model substrate. In the remainder of this report we will focus on the long peptide.

Next, we used the p53Ub_{VA} probe to generate a non-hydrolysable complex with TCD, a construct that lacks all Ubl domains (Fig. 1a) to address whether the p53 interaction affects the interaction of CD with Ubl45. Using SPR, the complex was flowed over immobilised Ubl45 and we could determine the affinity between Ubl45 and TCD-p53Ub (Fig. 4d, Supp. Fig. 3d). With a K_D of 2.9 μ M it is similar to the affinity found for the C-terminal tail interacting with CDUb (2.6 μ M, Fig. 3d). Apparently the presence of the TRAF-p53 interaction does not further change the interaction with Ubl45. This is in line with the fact that the presence of the TRAF domain does not affect activity on a minimal substrate³¹ or the association of the activating Ubl45 domain.

A second p53 interaction

To further investigate the role of the p53 peptide interaction with the TRAF domain in the activation process, we decided to look at the affinity between USP7 and the model target. As previous reports have alluded to an additional binding site (other than TRAF) for the USP7 targets p53 and MDM2 in the C-terminal domains of USP7⁵⁰, we first assessed the binding of the peptide to USP7 constructs in a FP assay (Fig. 5a). These direct binding assays with TAMRA-p53



Chapter 3. USP7 activity mechanism

peptide confirmed the presence of an additional p53 binding site and map it to the Ubl45 domains, without requiring the C-terminal tail (compare FL^{ΔC} and TCD45 to TCD). Interestingly, this additional site depends on the TRAF domain since CD12345 alone does not bind the peptide at these concentrations (Fig. 5a). These results suggest an extended binding interface between the TRAF domain and the p53 peptide that is aided by Ubl45, but the hypothesis of a second, very weak, binding site within Ubl45 cannot be excluded.

To then assess a potential increase in affinity for the ubiquitinated substrate, we used the non-hydrolysable compound (Fig. 4b; p53Ub_{inh}) as inhibitor in an activity assay, on minimal substrate UbRho (Fig. 5b). We found that both TRAF domain (compare TCD and CD) as well as Ubl12345 improve the IC₅₀ independently (Fig. 5c). However, the full-length construct displays a further avidity effect, resulting in an IC₅₀ of 16 nM, ~60-fold better than either TCD or CD12345. This underlines that the TRAF domain, CD and Ubl12345 all contribute to the effective substrate (p53Ub) recognition and that the sum of these interactions yields a tight, effective interaction.

Visualisation of the multi-step enzymatic mechanism

As both the ubiquitin acceptance (aided by Ubl45) and the target recognition positively influence deubiquitination, we wanted to explore how these collaborate during the deubiquitination process and whether there is a defined order of events. To this end, we utilised the synthetic ubiquitinated p53 target with a native linkage (Fig. 4b; p53Ub) and a fluorophore at the N-terminus of the p53 peptide to allow tracking of substrate and product⁴⁴. We monitored the substrate during its hydrolysis in an FP assay where 100 nM of TAMRA-labelled reagent is incubated with various USP7 constructs (Fig. 6b for FL, Supp. Fig. 5-7b for TCD, CD12345 and CD). Both FL and CD12345 could readily hydrolyse the substrate, resulting in a drop of the FP signal. The other two constructs, CD and TCD, required higher concentrations in order to see a decrease in FP signal, while the TCD construct actually started out with an increased signal (Supp. Fig. 5b). This increased signal would be a result of binding, as the TRAF domain increases the affinity for the p53-substrate but the rate of catalysis is still low for TCD. Although these experiments efficiently monitored substrate hydrolysis, we were interested in the early events that could not be caught in our plate reader setup.

To get insight into the very early phase of the reaction, we decided to use a stopped-flow setup (Fig. 6c,d). We followed the reaction by fluorescence polarization, which is sensitive to the size of the complex (as this affects the tumbling rate and thus polarisation), and by fluorescence

Figure 5. The p53-derived tools stress the importance of both the TRAF and Ubl45 domain. A. Binding of the TAMRA-labelled p53 peptide is determined by incubating 25 nM of TAMRA-p53 with a dilution series of various USP7 constructs in FP assays. The obtained K_D values for each USP7 construct are stated and indicate that in presence of the TRAF domain, the Ubl12345 domain affects recognition. **B.** The non-hydrolysable p53Ub construct acts as an inhibitor for USP7 in deubiquitination assays. USP7 constructs, corrected for their activity (CD12345: 0.35 nM, TCD: 200 nM, CD: 75 nM, USP7FL: 0.35 nM) were incubated with increasing amounts of p53Ub_{inh} and analysed for activity in a deubiquitination assay using a single concentration of UbRho. The raw data indicate that both the TRAF domain and the C-terminal Ubl domains increase the affinity towards the p53 construct. For clarity's sake a limited number of concentrations is shown. **C.** The observed activity for USP7 constructs after incubation with p53Ub_{inh} (see B), is plotted against the concentration of inhibitor used. Fitting yielded IC50 values and standard deviation as shown.

intensity, which responds to changes in local conformation affecting the fluorophore. As these experiments were performed under near-equimolar amounts of enzyme and substrate, we also measured binding to the product ^{TAMRA}p53 peptide in this stopped-flow setup (Fig. 6e,f). In the stopped-flow anisotropy data we could detect an increase in signal when we titrated FL into ^{TAMRA}p53Ub (Fig. 6c). After this binding phase (0.02-0.2 s) we observe a decrease in anisotropy, indicating a second phase (0.2-2 s) indicative of hydrolysis. The signal however does not drop below baseline for the highest concentration, indicating retention of the product, in line with our p53 peptide binding data (Fig. 6e).

For the constructs CD and CD12345 we can hardly detect the ^{TAMRA}p53Ub binding phase (Supp. Fig. 6c, 7c) or the decrease in anisotropy, indicating that these require the presence of the TRAF domain. When it is present, in TCD, the binding and the decrease are visible (Supp. Fig. 5c), but the decrease only occurs after a lag phase (>5 s), indicating the presence of intermediate states between binding and hydrolysis.

This step is more explicitly visualised in the intensity data from these stopped-flow experiments. For TCD, with the long delay between binding and hydrolysis (Supp. Fig. 5c), we see a significant decrease in intensity in this delay (Supp. Fig. 5d), which we interpret as a conformational change in the protein (see Supp. methods). For full-length USP7 a minor intensity increase (Fig. 6d) occurs, with a slight delay (0.05-0.5 s) relative to the binding phase. This suggests that a further conformational change affects the intensity signal, which we interpret as binding of the C-terminal tail read out by rearrangement of the TAMRA label. The non-synchronicity of the events in the anisotropy and intensity experiments suggests that multiple steps are involved in the hydrolysis mechanism.

Kinetic analysis of USP7 activity on p53 model substrate

To model these multiple steps we proceeded to describe every phase, with as few reaction steps as possible. We imported the raw stopped-flow, FP and activity data into KinTek⁵¹ and let the program scale the data based on the negative controls (Supp. methods). This rendered the data interpretable by KinTek modelling which we performed by using a minimal set of reaction equations. To be able to model the non-synchronous changes in the FP and intensity signals we decided to introduce intermediate steps in the reaction (Fig. 6h). These include binding events (*Steps 1, 6 and 7*), conformational changes (*Steps 2, 3 and 5*) and the enzymatic hydrolysis (*Step 4*). The introduction of these steps allowed KinTek to fit the data, obtaining rate constants (k_i and k_j) for every step of the mechanism (Fig. 6h).

For the shorter constructs, introduction of one intermediate step between the binding (*Step 1*) and the hydrolysis step (*Step 4*, Supp. Fig. 5, 6, 7) was sufficient to fit the experimental traces. For the full-length construct however we required a second intermediate step to match the model to the experimental data. The order of release of the reaction products p53 and Ub could not be determined based on activity data alone. Therefore we used their respective affinities (Fig. 3f and Fig. 5a) to set the order of release. This order, with later release of the p53 peptide, also allowed adding the secondary binding site to the model, as induced by Ubl45 (Fig. 5a), which fitted well in the stopped-flow data (Fig. 6e,f).

The modelling of the experimental curves allowed us to tease apart the various steps that USP7 performs in catalysis and reveals how the different domains affect the target processing. For instance, the intensity decrease observed upon p53Ub binding by the TCD construct (Supp. Fig. 5d) is not seen for FL (Fig. 6d). We can interpret this absence as an effect of the ‘folding

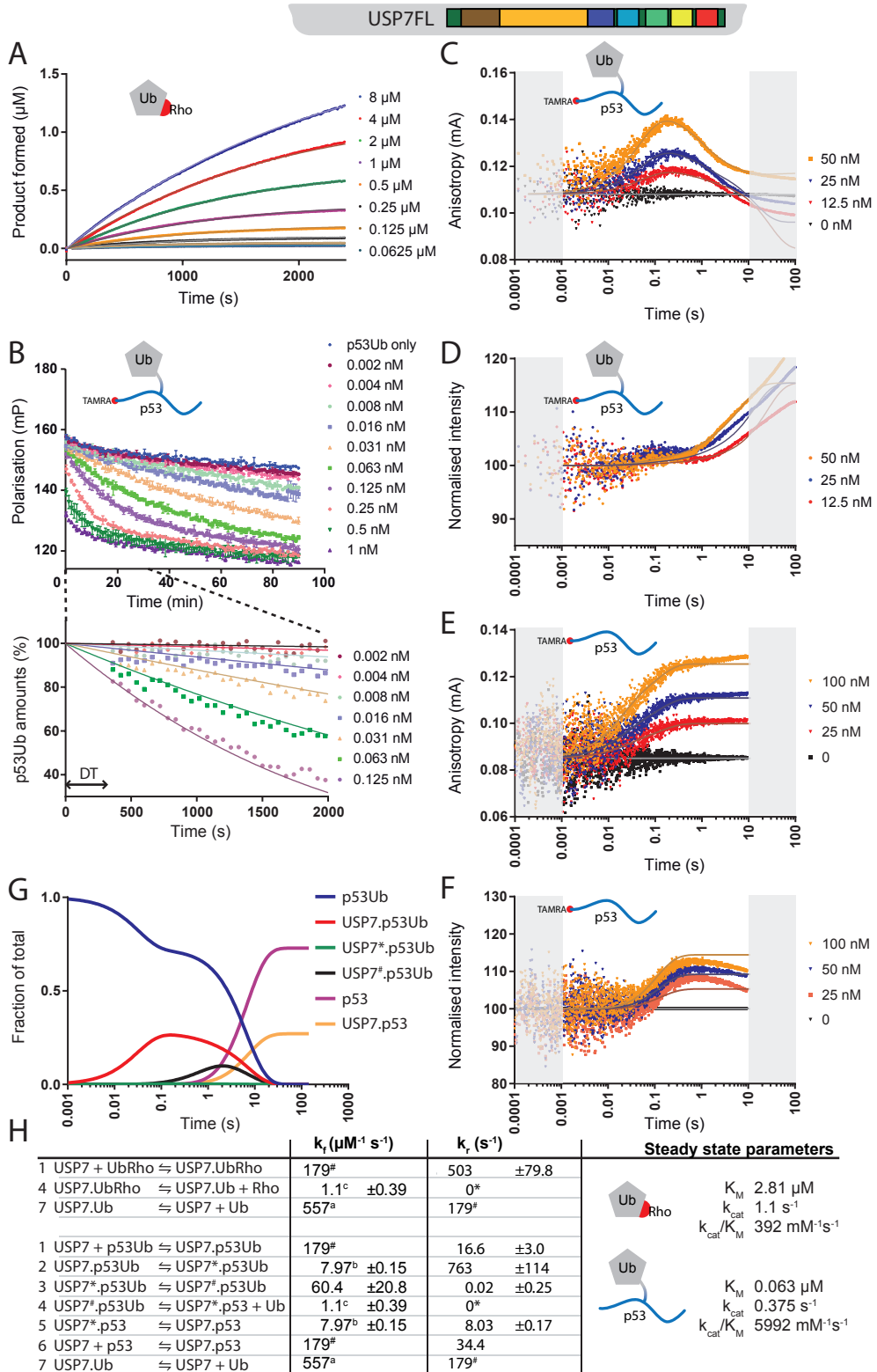
Chapter 3. USP7 activity mechanism

back' of the Ubl domains towards the CD ³¹ and changing the p53 interaction⁵⁰. Likewise, the long delay time seen for TCD is much shorter for constructs that still contain the Ubl domains. As these domains activate CD, it seems reasonable to assume the delay time in TCD is required to remodel the catalytic site into an active conformation³³ without help of the Ubl domains. The KinTek analysis results in a model where we can quantify each component (Fig. 6g) and reaction kinetics (Fig. 6h). In the first step, anisotropy changes are interpreted as binding of substrate p53Ub (*Step 1*; Fig. 6h), followed by multiple changes in intensity, interpreted as conformational changes (*Step 2* and *3*). This is then followed by the phase where the intensity shoots up and the anisotropy decreases (*Step 4*), interpreted as hydrolysis and release of the ubiquitin product. Further intensity changes (*Step 5*) take place before p53 peptide release returns USP7 to the ground state (*Step 6*).

Validation and evaluation of the kinetic model

Our kinetic model fully agrees with the order of events observed in NMR and SPR analysis in Fig. 2-3. We decided to test if this could be used quantitatively as an independent control. We applied the model to fit the experiments done on the minimal substrate UbRho (Fig. 6a, Supp. Fig. 5a, 6a, 7a). Besides validating the kinetic model, this would also allow better definition of the rate constants by co-refining the values within KinTek. The intermediate states were used in the fitting, making a direct comparison between the ubiquitinated target protein and the minimal substrate possible. For the FL construct the efficiency of the reaction precluded fitting the intermediate steps in the minimal substrate analysis, so we only used steps 1, 4 and 7 (Fig. 6h).

Figure 6. Global fitting of activity and affinity data of USP7 allows determination of a quantitative kinetic model for USP7 enzymatic activity. Icons in each panel indicate the substrate used. The lines describe the fit of the data in the various experiments performed. **A.** Minimal substrate activity assay of USP7FL (1 nM), using a dilution range of UbRho. **B.** FP enzyme activity assay on ^{TAMRA}p53Ub (100 nM). The amounts of USP7 are indicated. After conversion to p53Ub amounts (lower panel) a delay time (DT) was introduced. **C.** Stopped-flow FP enzyme activity assay on ^{TAMRA}p53Ub (50 nM), the anisotropy signal allows observation of the early binding and hydrolysis phases. Areas marked in grey were not included in the fit as they represent the mixing time (<0.001 s) or a timescale where bleaching effects start to dominate (>10 s). **D.** Intensity readings of the experiment in C indicates a change in chemical environment upon binding of substrate. **E.** Like C for using peptide only (25 nM p53) shows equivalent binding phases as the full substrate. **F.** Intensity readings of the experiment in E. **G.** Behaviour of p53-substrate states during overall model in an equimolar (1 to 1; 50 nM) ratio of enzyme and substrate. Intermediate states as in **H.** Model used for KinTek fitting with kinetic constants obtained. USP7FL indicated as USP7, intermediates with # or *. For binding steps (*Step 1, 6 and 7*) on-rates are in $\mu\text{M}^{-1}\text{s}^{-1}$ and off-rates in s^{-1} . Rates for conformational changes (*Step 2, 3 and 5*) are in s^{-1} . The forward reaction for enzymatic hydrolysis (*Step 4*) is in s^{-1} , but the reverse step (labelled with ϑ) was assumed irreversible (fixed at $0 \mu\text{M}^{-1}\text{s}^{-1}$). Equation constants with matching Greek characters (α , β , γ and δ) were linked in the refinement. The on-rate for binding steps (labelled with ϵ) is diffusion-controlled, determined separately and fixed during modelling. These on- and off-rates reflect the optimal ratio that models the individual steps, since the experiment does not have sufficient resolution to fully resolve rates. For both UbRho and p53Ub the resulting steady state parameters were calculated to allow for a direct comparison (last column).



Chapter 3. USP7 activity mechanism

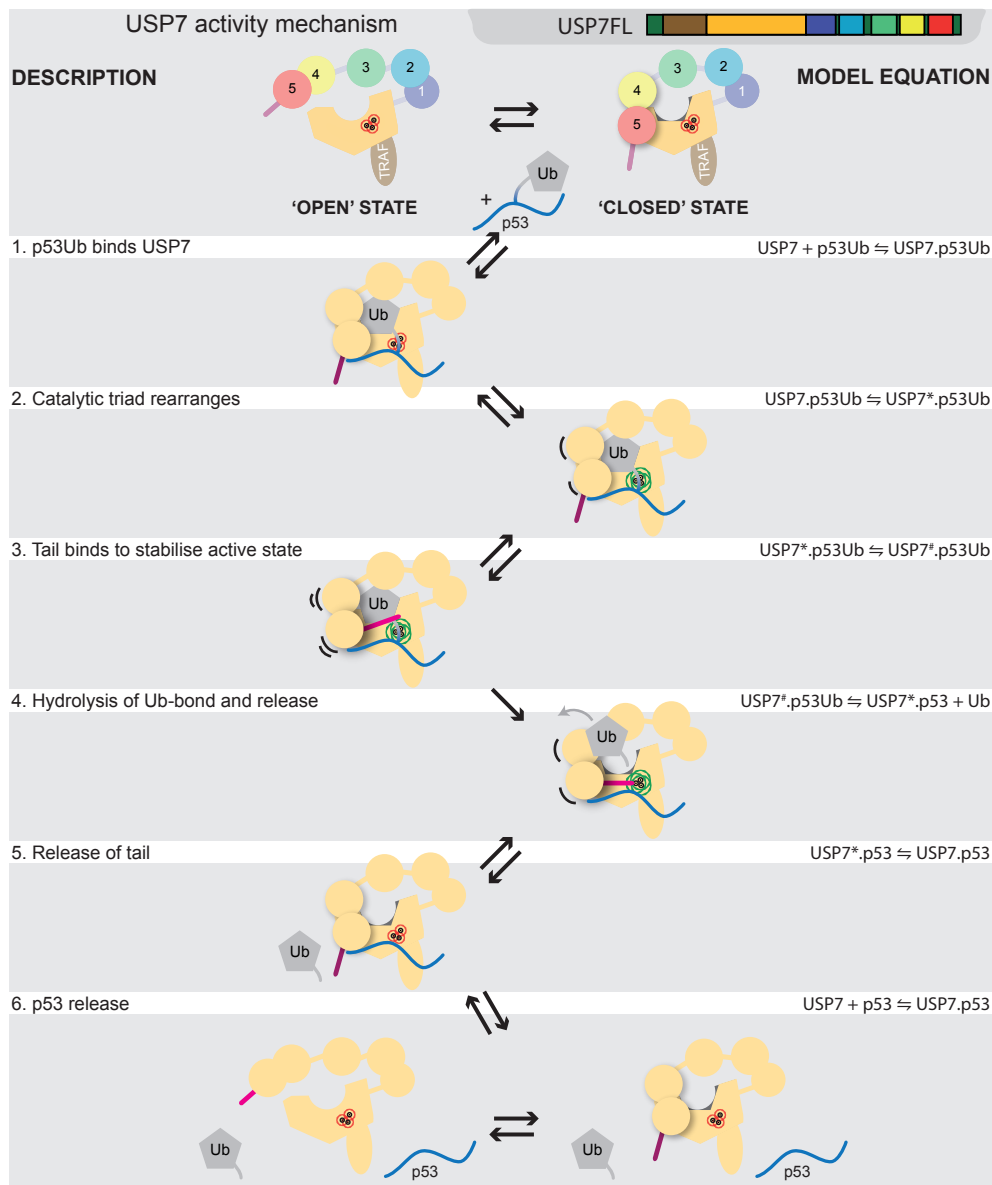


Figure 7. Kinetic model for USP7 mechanism on p53Ub. The kinetic model (right hand equations) and their interpretation are depicted schematically. The weak affinity between Ubl45 and CD suggests that free USP7 is in equilibrium between an 'open' and 'closed' state³¹. The p53Ub substrate is bound by TRAF and CD, as well as an additional binding site that depends on the Ubl domains (1). Ubiquitin binding induces a rearrangement of the catalytic triad³³ (2), which dramatically increases the affinity the activating C-terminal tail, but diminishes the contact between CD and Ubl45. Binding of the tail peptide (3) stabilises the active state. This promotes the hydrolysis of the isopeptide bond, allowing Ub release (4). This in turn diminishes affinity for the C-terminal tail, causing its release (5) and the subsequent release of the p53 peptide (6) to return USP7 to the ground state.

The validity of the fitted constants was then analysed using the FitSpace module of KinTek⁵². Here we found that only TCD and FL data had sufficient amplitudes to allow for a full statistical analysis (Supp. Fig. 8a,c). To avoid overfitting within this analysis we linked rate constants (Supp. Fig. 8a,c; left panel), testing the statistical relevance for their ratios rather than their absolute values. The overall result indicated a well-constrained model where Step 2, the catalytic rearrangement, is the rate-limiting step. Finally, we converted the rate constants into steady-state kinetics parameters using the appropriate formula for one (Supp. Fig. 8d) or two (Supp. Fig. 8b) intermediates⁵³ (Supp. Fig. 5g, 6f, Fig. 6h). This yielded K_M and k_{cat} values similar to those determined previously³¹, and validated the descriptions used in our modelling.

USP7 activity is driven by target recognition

The conversion to steady-state parameters allows for easy comparison of USP7 activity on minimal substrate and the p53 model substrate. Interestingly, on the p53Ub substrate k_{cat} is slightly diminished as soon as a TRAF domain is present, but this is offset by the improved target recognition (here expressed as K_M) leading to substantially increased processivity. These findings indicate that, although studies on a minimal substrate are essential in studying the enzymatic mechanism, using a realistic substrate can give better understanding of the working of a DUB and its possible regulation.

Discussion

Updated model for the USP7 mechanism of action

Here we studied USP7 self-activation by its C-terminal peptide and its target protein. We show that although *trans* activation by self-association is possible at high concentrations, the normal USP7 self-activation happens *in cis*. We show that interaction of Ubl45 with the CD promotes ubiquitin binding and only this promotes the correct positioning of the C-terminal peptide next to the catalytic site. Thus self-activation takes place in multiple distinct steps. Next we showed how the substrate protein strengthens activation and provided a kinetic model for the cooperative activation process.

The combination of our findings allows us to generate an updated model for the USP7 mode of action (Fig. 7). Ubiquitinated targets associate initially with the TRAF domain (*Step 1*, Fig. 7) and this binding is improved by the additional p53 binding site, induced by presence of the Ubl domains (Fig. 5c). The target association brings the attached ubiquitin in close proximity to the catalytic domain, overcoming its poor affinity for ubiquitin, enhanced by the Ubl45 domain (Fig. 3f). The binding of ubiquitin into the active site (*Step 2*) not only induces rearrangements of the catalytic triad³³, but also reduces intramolecular interaction with Ubl45 (Fig. 3e) and promotes binding of the activating C-terminal tail, through a dramatic increase in affinity (Fig. 3) where it stabilises the active conformation (*Step 3*). In this activated state the hydrolysis of the isopeptide bond (*Step 4*) occurs much faster than for CD only³¹.

After hydrolysis, release of products takes place, which we modelled according to their respective affinities. In full-length USP7 the leaving ubiquitin has a poor affinity compared to the p53 peptide (Fig. 5c), so we expect Ub to leave first (*Step 4*), leaving p53 bound to USP7, enabling a change due to the additional binding site (*Step 5*). The p53 release (*Step 6*) is modelled here as the last step in order to let USP7 return to the ground state, but given the tight interaction (160 nM) and the protein concentrations found in cells the p53-USP7

Chapter 3. USP7 activity mechanism

complex may last longer *in vivo*. Another ubiquitinated substrate or additional regulatory step could be required to perturb this complex and release p53.

Model implications

With this model we assumed a sequential order of reactions (Supp. methods) and we could not model all steps explicitly (Supp. Fig. 7). Nevertheless, the modelled intermediate steps agree very well with our SPR experiments that were not used for the model (Fig. 3). Based on the model we can separate intermediates in both time and place, allowing to connect species tested by SPR to states found in the kinetic model. Thus we see that Ubl45^{ΔC} is responsible for the increased K_M whereas the C-terminal tail for the faster k_{cat} ³¹.

It is clear from our data that USP7 activation follows a multistep activation scheme that generates high specificity for the target. As USP7 interacts with many different targets²¹, such a mechanism could make sure activity is targeted to the right substrate at the right time. Our results indicate that the substrate recognition collaborates with the intrinsic self-activation. The complexity of the self-activation provides regulatory opportunities through external factors. One example is hyperactivation by GMPS³¹, but other binding partners, such as ICP0 and DNMT1^{35,54} and/or post-translational modifications may further affect activity.

Interestingly, the p53 peptide collaborates with the C-terminal domains through the additional binding site that we quantified. An earlier report suggested binding in the Ubl domains to both p53⁵⁰ and MDM2³⁶, but whether such a bipartite binding of substrates by USP7 is a common theme in other substrates remains to be investigated. Further definition of the different interactions would be needed to explain why USP7 usually prefers MDM2 over p53^{25,55}.

Our data provide opportunities for specific targeting in drug discovery programmes: both the secondary substrate binding site and the self-activation by Ubl45 are allosteric sites of interest. Working out the specifics of the interaction, using our NMR backbone assignment for Ubl45 and the recent assignment of CD⁵⁶, can be helpful in this process. Better molecular understanding of this interaction would help to design inhibitors specifically targeted at USP7 self-activation.

In this study we employed both a model substrate and the minimal substrate to assess the USP7 mechanism of action. The usefulness of the ubiquitinated model substrate is not only illustrated by our findings on the activity effect of the TRAF domain, it also allowed us to monitor intermediate steps of the reaction and the order in which they occur. Combining these chemical ubiquitin tools with a domain-by-domain approach we could pinpoint what part of USP7 is important in which part of the hydrolysis cycle. The results highlight the importance of the target protein and hopefully these insights will allow for the development of more specific USP7 inhibitors, targeting USP7 activity on specific substrates.

Materials and methods

Constructs and mutations

USP7 constructs (Fig. 1a) are from³¹, cloned from the codon-optimized sequence, (Addgene, #63573). USP7-TCD was cloned into pGEXNKI-GST-3C using ligase independent cloning⁵⁷. Constructs lacking the C-terminal tail were made by introducing a stop codon at residue 1083 using site-directed mutagenesis. Mutation constructs were introduced using partially overlapping primers and Phusion Flash polymerase (Thermo Fisher). All clones were sequence-verified.

Protein expression

USP7 constructs that included the TRAF region were expressed in *Escherichia coli* BL21 Rosetta2 (DE3) using Terrific Broth medium and overnight induction using 0.2 mM IPTG at 18°C. Other USP7 constructs were expressed in *E. coli* BL21 cells using overnight auto-induction⁵⁸ at 18°C. Isotope-labelled USP7-Ubl45 intended for interaction analysis by NMR was expressed in *E. coli* BL21 cells using M9 minimal medium supplemented with ¹⁵NH₄Cl (CortecNet), glucose, vitamin mix and micronutrient mix⁵⁹. For three-dimensional NMR experiments ¹³C-glucose (CortecNet) was used. To acquire deuterated sample, D₂O (CortecNet) was used to make the medium. Cells were grown in 5 mL LB from a single colony and transferred to a 50 mL minimal medium preculture after washing to grow overnight at 37°C. The preculture was dispensed in 4 L minimal medium and cells were grown until OD₆₀₀ reached 0.6. Protein expression was then induced overnight at 18°C by addition of 0.2 mM IPTG.

Protein purification

Proteins were purified as described previously³⁴. In short, proteins were isolated from the lysate using Glutathione Sepharose 4B beads (GE Healthcare). After elution the GST tag was removed under dialysis using 3C protease and the sample was subsequently applied to PorosXQ anion exchange (Thermo Fisher). After analysis appropriate fractions were pooled, concentrated and further purified on a Superdex gel filtration column (GE Healthcare). The peak fractions were pooled, concentrated up to 10 mg mL⁻¹ and flash frozen.

MALLS experiments

Purified protein was run on a Superdex 200 gel filtration column (GE Healthcare) using GF buffer (20 mM HEPES 7.5, 100 mM NaCl, 1 mM DTT) in line with a MiniDawn Tristar (Wyatt Technologies) Multi-Angle Laser Light Scattering (MALLS) detector, connected to a Shodex RI 101 (SHOWA DENKO K.K.) refractive index detector. Wyatt Technologies software (ASTRA) was used to determine the corresponding peaks' molecular weight based on the refractive index.

Deubiquitination assays on a minimal substrate

Enzyme activity of USP7 was measured using the fluorescence of rhodamine upon cleavage of the quenched minimal substrate UbRho (Ubiquitin-Rhodamine110Gly, Ub-Rh110Gly; UbiQ, the Netherlands). Experiments were performed in running buffer (20 mM HEPES 7.5, 100 mM NaCl, 1 mM DTT, 1 mM EDTA and 0.05% v/v Tween-20). Protein samples were prepared at 2X concentration and added to 8 μM UbRho just before measuring, reaching an end volume of 20 μL in the plate.

Chapter 3. USP7 activity mechanism

The release of rhodamine was measured at the emission wavelength of 520 nm (± 10 nm) after excitation at 485 nm (± 10 nm) in a Pherastar plate reader (BMG LABTECH GmbH, Germany). Either the raw data were plotted directly in Prism 7 (GraphPad), or the slopes were converted to initial velocity values for plotting against the titration range. Assays were performed three times with two different protein batches.

For steady-state kinetics analysis a single concentration of USP7 constructs (CD, CD12345 and CD12345^{ΔC}) was incubated with a dilution range of UbRho and assessed for activity using the same experimental setup as described above. The initial velocities were determined using the linear slope of the reaction and plotted against the concentration UbRho used. Using Prism 7 the data were fitted using the Michaelis-Menten equation, yielding the reported steady state kinetics parameters.

For kinetics analysis in KinTek, a concentration series of UbRho was used with USP7 constructs FL, (1 nM), TCD and CD (both 20 nM). To get resolution at the earliest time points the assay was performed using the injector, injecting the enzyme into the UbRho solution followed by direct detection (as described above). The resulting values were converted to rhodamine concentrations before being loaded into KinTek.

NMR experiments

All NMR experiments were carried out on Bruker Avance III HD spectrometer operating at 850 MHz ^1H Larmor frequency and equipped with a cryoprobe. All NMR spectra were processed using Bruker TopSpin or NMRPipe⁶⁰. NMR samples for assignment contained 180 μM USP7-Ubl45 with either uniform ^1H , ^{15}N , ^{13}C or fractional ^2H , uniform ^{15}N , ^{13}C labelling in 50 mM HEPES pH 7.5, 100 mM NaCl, 7% D_2O and 1 mM DTT (NMR buffer). Backbone resonances of Ubl45 were assigned to 84% completeness, using 3D TROSY HNCO, HN(CA)CO, HNCA, HNCOCA, HNCB, HNCOCB, HNCACB, and CBCA(CO)NH spectra. Assignment was done using CCPN⁶¹. The program TALOS⁶² was used to analyse the secondary structure based on the assigned backbone chemical shifts.

Titration of $^1\text{H}^{15}\text{N}$ -labelled Ubl45 (45 μM) with either USP7CD (using Ubl45:CD molar ratios of 1:0, 1:1, 1:5 and 1:10) or USP7CDUb (using ratios of 1:0.1 and 1:0.3) were performed after extensive dialysis of the proteins to NMR buffer. We monitored residue-specific intensity change and chemical shift perturbations (CSP) of Ubl45 amide backbone resonances in 2D $^1\text{H}^{15}\text{N}$ TROSY spectra. The CSPs were calculated from the perturbations in the ^1H ($\Delta\delta_{\text{H}}$) and ^{15}N ($\Delta\delta_{\text{N}}$) dimensions as the weighted average (composite) CSP in ppm according to⁶³. The intensity changes were plotted against residue number for the end point of both titrations.

Generation of covalent Ubiquitin-USP7 complexes

120 μM CD was incubated overnight with an excess of Ub-PA⁶⁴ and Ubl45 (both 150 μM) under dialysis (against 20 mM HEPES pH7.5, 50 mM NaCl, 2 mM DTT), yielding 80% of the CD reacted with the ubiquitin probe. The sample was subjected to anion exchange (PorosXQ) and gel filtration (Superdex 75) to remove unreacted ubiquitin and Ubl45. Fractions were concentrated for use in affinity assays. For USP7-TCD a similar approach was used, only substituting p53Ub_{VA} for Ub-PA, resulting in 100% reaction.

Surface Plasmon Resonance assays

All Surface Plasmon Resonance (SPR) experiments were carried out on a Biacore T200 machine (GE Healthcare) at 25°C. A polyclonal GST antibody from the GST capture Kit (GE Healthcare) was covalently bound on a CM5 sensor chip via amino coupling. 200 units of GST-tagged USP7 constructs were immobilised on the test flow cell, whilst the blank flow cell had an equal amount of GST only immobilised. The C-terminal peptide (residue 1083-1102) was synthesized with a biotin at the N-terminus and immobilized up to ~30 RU on a SA chip. A concentration series of USP7 constructs with or without covalently bound ubiquitin probe was tested for binding using running buffer (20 mM HEPES 7.5, 100 mM NaCl, 1 mM DTT, 1 mM EDTA and 0.05% v/v Tween-20) supplemented with 1 mg mL⁻¹ BSA and 1 mg mL⁻¹ dextran. Interaction values (K_D) were determined by plotting steady-state equilibrium values against the concentration and fitting these with 1:1 stoichiometry using Prism 7 (Graphpad). For easy comparison purpose, responses were normalised using B_{max} . For binding curves with detectable dissociation and a K_D below 10 μ M we used EvilFit⁴² to determine kinetic rate constants. All experiments were performed at least *in duplo* and representative curves are shown.

Synthesis of p53-conjugated ubiquitin reagents

Both ubiquitin and the C-terminus of p53 were produced synthetically by solid phase peptide synthesis, for the native reagent the p53 peptide was N-terminally labelled with 5-carboxytetramethylrhodamine (TAMRA). The peptide was linked to ubiquitin using click chemistry or native chemical ligation⁴⁹ to yield the non-hydrolysable⁴⁸, natively linked⁴⁴ and covalently binding⁴⁵ p53Ub and p53_{short}Ub probes. Details are available in the Supplemental methods section.

Fluorescence Polarization binding assays

To measure the affinity for ubiquitin, N-terminally tetramethylrhodamine (TAMRA) labelled ubiquitin was incubated with a titration range of each USP7 construct. All assays were performed in running buffer (20 mM HEPES 7.5, 100 mM NaCl, 1 mM DTT, 1 mM EDTA and 0.05% v/v Tween-20) on a Pherastar plate reader (BMG LABTECH GmbH, Germany), using excitation wavelength 540 nm (± 20 nm) and detection of polarization at 590 nm (± 20 nm). The anisotropy of TAMRA^{Ub} was calibrated at 35 mA, any change in anisotropy upon USP7 interaction was calculated using MARS data analysis software (BMG LABTECH GmbH, Germany) and plotted using Prism 7 (GraphPad).

The affinity between the USP7 constructs and a TAMRA-labelled p53 peptide (TAMRA^{p53}) was measured on a ClarioStar plate reader (BMG LABTECH GmbH, Germany). Assays were performed *in triplo* using the same running buffer and wavelength filters (Ex. 540 ± 20 nm, Em. 590 ± 20 nm). TAMRA^{p53} anisotropy was calibrated to be 35 mA and changes in anisotropy were plotted and fitted in Prism 7 to obtain affinities.

The p53 FP binding assay was repeated for USP7FL using a stopped-flow setup. 25 nM of TAMRA^{p53} was incubated with a concentration range of USP7 in running buffer. The binding was monitored using an excitation wavelength of 548 nm on a TgK Scientific instrument (model SF-61DX2) equipped with photomultiplier tube R10699 (Hamamatsu) and Kinetic Studio was used to merge ten separate, sequential injections for each protein concentration.

Chapter 3. USP7 activity mechanism

USP7 inhibition assays

USP7 constructs were incubated for 30 minutes in assay buffer (50 mM Tris-HCl pH 7.6, 100 mM NaCl, 2 mM cysteine, 1 mg mL⁻¹ CHAPS) with various concentrations of the non-hydrolysable p53Ub_{inh} construct, prior to assessment in a deubiquitination assay. To account for difference in activity, protein concentrations were adapted for FL (0.35 nM), CD12345 (0.35 nM), TCD (200 nM) and CD (75 nM), whilst the substrate (UbRho) concentration was kept constant at 0.4 μM. Protein samples and substrate were prepared at 4x the final concentration. The initial raw velocities were derived and plotted against the titration range of inhibitor reagent. Using Prism 7 the data were fitted to yield IC₅₀-values.

Fluorescence Polarization activity assays

Various USP7 constructs at indicated concentrations were incubated with 100 nM of TAMRA-labelled, natively linked p53Ub (TAMRA-p53Ub) to trace the binding and hydrolysis of the reagent. Assays were performed in assay buffer (20 mM Tris-HCl pH 7.6, 100 mM NaCl, 1 mM DTT and 1 mg mL⁻¹ CHAPS) on a Pherastar plate reader measuring at 590 nm after excitation at 540 nm. The FP signal for TAMRA-p53Ub only was used as a starting baseline, whilst the TAMRA-labelled p53-peptide represents the fully cleaved reagent.

The fluorescence polarization activity assays were repeated in a stopped-flow setup. USP7 constructs at three concentrations (50 nM, 25 nM and 12.5 nM) were incubated with 50 nM of TAMRA-p53Ub to trace the binding and hydrolysis of the reagent. TAMRA-p53Ub was monitored in running buffer (20 mM HEPES pH 7.5, 150 mM NaCl, 1 mM DTT and 0.05% v/v Tween-20) using an excitation wavelength of 548 nm on a TgK Scientific instrument (model SF-61DX2) equipped with photomultiplier tube R10699 (Hamamatsu), the manufacturer's software (Kinetic Studio) was used to merge the ten measurements performed for each concentration.

KinTek modelling

All data used were imported into KinTek with concentrations in μM and time in seconds: for minimal substrate activity curves, converted to released rhodamine, could be loaded into KinTek directly. The curves resulting from USP7 inhibition assays were read with a delay time of 120 seconds. The FP activity assay data from the stopped-flow instrument could also be read-in directly. With the data for every construct imported, the model (Fig. 6h) was fitted per construct in separately for each experiment. When the fits proved stable, reaction constants were linked and a global fit was performed. The resulting values were then statistically tested using the FitSpace module of the Kintek software. For detailed information see Supp. Methods.

Data availability

NMR assignments for Ubl45 (residues 890-1102) have been deposited in the Biomolecular Magnetic Resonance Bank (BMRB; www.bmrwisc.edu) under accession number 27627. Other datasets generated during and/or analysed during the current study are available from the corresponding author on reasonable request.

Acknowledgements

We thank an anonymous reviewer for helpful advice on the NMR analysis. The authors thank Shreya Dharadhar, Robbie Joosten, Anastassis Perrakis and Michael Uckelmann for critical reading of the manuscript. Research was supported by KWF (2012-5398), NWO TOP grant (TOP 714.016.002) and the Oncode institute to T.K.S, NWO VIDI grant (723.013.010) to H.v.I. and NWO VICI grant (724.013.002) to H.O.

Author contributions

R.Q.K. designed, performed and analysed experiments and wrote the manuscript, W.J.v.D and R.Q.K. expressed and purified proteins. P.P.G., R.E., and M.P.C.M. designed and synthesised a p53Ub toolbox, performed inhibition experiments and initial validation of the synthesised ubiquitin reagents. F.E.O. and D.v.D. performed ubiquitin and peptide synthesis. F.E.O. contributed to peptide and chemical design and provision of reagents. A.F. and R.Q.K. performed SPR and stopped-flow, their analysis and global modelling. H.v.I. and R.Q.K. performed NMR experiments and analysis. H.O. supervised synthetic ubiquitin research. T.K.S. supervised and designed research and wrote the manuscript. All authors read the manuscript critically.

Competing interests statement

Competing interests: F.E.O. is a current employee, co-founder, and shareholder of UbiQ Bio BV. Huib Ovaa is co-founder, and shareholder of UbiQ Bio BV. T.K.S. is member of the scientific advisory board of Mission Therapeutics.

References

- [1] Varshavsky, A. The ubiquitin system, an immense realm. *Annual Review of Biochemistry* 81 2012, 167–76. <https://doi.org/10.1146/annurev-biochem-051910-094049>
- [2] Rape, M. Ubiquitylation at the crossroads of development and disease. *Nature Reviews Molecular Cell Biology* 19 2017, 59–70. <https://doi.org/10.1038/nrm.2017.83>
- [3] Komander, D. and Rape, M. The ubiquitin code. *Annual Review of Biochemistry* 81 2012, 203–29. <https://doi.org/10.1146/annurev-biochem-060310-170328>
- [4] Yau, R. and Rape, M. The increasing complexity of the ubiquitin code. *Nature Cell Biology* 18 2016, 579–86. <https://doi.org/10.1038/ncb3358>
- [5] Shabek, N. and Ciechanover, A. Degradation of ubiquitin: The fate of the cellular reaper. *Cell Cycle* 9 2010, 523–30. <https://doi.org/10.4161/cc.9.3.11152>
- [6] Husnjak, K. and Dikic, I. Ubiquitin-binding proteins: decoders of ubiquitin-mediated cellular functions. *Annual Review of Biochemistry* 81 2012, 291–322. <https://doi.org/10.1146/annurev-biochem-051810-094654>
- [7] Clague, M.J., Barsukov, I., Coulson, J.M., Liu, H., Rigden, D.J. and Urbe, S. Deubiquitylases From Genes to Organism. *Physiological Reviews* 93 2013, 1289–315. <https://doi.org/10.1152/physrev.00002.2013>
- [8] Mevissen, T.E.T. and Komander, D. Mechanisms of Deubiquitinase Specificity and Regulation. *Annual Review of Biochemistry* 86 2017, 159–92. <https://doi.org/10.1146/annurev-biochem-061516-044916>
- [9] Clague, M.J., Coulson, J.M. and Urbé, S. Cellular functions of the DUBs. *Journal of Cell Science* 125 2012, 277–86. <https://doi.org/10.1242/jcs.090985>
- [10] Xiao, Z., Zhang, P. and Ma, L. The role of deubiquitinases in breast cancer. *Cancer and Metastasis Reviews* 35 2016, 589–600. <https://doi.org/10.1007/s10555-016-9640-2>
- [11] Sahtoe, D.D. and Sixma, T.K. Layers of DUB regulation. *Trends in Biochemical Sciences* 40 2015, 456–67. <https://doi.org/10.1016/j.tibs.2015.05.002>

Chapter 3. USP7 activity mechanism

- [12] Everett, R.D., Meredith, M., Orr, A., Cross, A., Kathoria, M. and Parkinson, J. A novel ubiquitin-specific protease is dynamically associated with the PML nuclear domain and binds to a herpesvirus regulatory protein. *The EMBO Journal* 16 1997, 1519–30. <https://doi.org/10.1093/emboj/16.7.1519>
- [13] van Loosdregt, J., Fleskens, V., Fu, J., Brenkman, A.B., Bekker, C.P.J., Pals, C.E.G.M., Meerdling, J., Berkers, C.R., Barbi, J., Gröne, A., Sijts, A.J.A.M., Maurice, M.M., Kalkhoven, E., Prakken, B.J., Ovaa, H., Pan, F., Zaiss, D.M.W. and Coffey, P.J. Stabilization of the Transcription Factor Foxp3 by the Deubiquitinase USP7 Increases Treg-Cell-Suppressive Capacity. *Immunity* 39 2013, 259–71. <https://doi.org/10.1016/j.immuni.2013.05.018>
- [14] Wang, L., Kumar, S., Dahiya, S., Wang, F., Wu, J., Newick, K., Han, R., Samanta, A., Beier, U.H., Akimova, T., Bhatti, T.R., Nicholson, B., Kodrasov, M.P., Agarwal, S., Sterner, D.E., Gu, W., Weinstock, J., Butt, T.R., Albelda, S.M. et al. Ubiquitin-specific Protease-7 Inhibition Impairs Tip60-dependent Foxp3+ T-regulatory Cell Function and Promotes Antitumor Immunity. *EBioMedicine* 13 2016, 99–112. <https://doi.org/10.1016/j.ebiom.2016.10.018>
- [15] Ma, X., Liu, Y., Liu, Y., Alexandrov, L.B., Edmonson, M.N., Gawad, C., Zhou, X., Li, Y., Rusch, M.C., Easton, J., Huether, R., Gonzalez-Pena, V., Wilkinson, M.R., Hermida, L.C., Davis, S., Sioson, E., Pounds, S., Cao, X., Ries, R.E. et al. Pan-cancer genome and transcriptome analyses of 1,699 paediatric leukaemias and solid tumours. *Nature* 555 2018, 371–6. <https://doi.org/10.1038/nature25795>
- [16] Huether, R., Dong, L., Chen, X., Wu, G., Parker, M., Wei, L., Ma, J., Edmonson, M.N., Hedlund, E.K., Rusch, M.C., Shurtleff, S.A., Mulder, H.L., Boggs, K., Vadordaria, B., Cheng, J., Yergeau, D., Song, G., Becksfort, J., Lemmon, G. et al. The landscape of somatic mutations in epigenetic regulators across 1,000 paediatric cancer genomes. *Nature Communications Nature Publishing Group*. 5 2014, 1–7. <https://doi.org/10.1038/ncomms4630>
- [17] Lamberto, I., Liu, X., Seo, H.-S., Schauer, N.J., Jacob, R.E., Hu, W., Das, D., Mikhailova, T., Weisberg, E.L., Engen, J.R., Anderson, K.C., Chauhan, D., Dhe-Paganon, S. and Buhrlage, S.J. Structure-Guided Development of a Potent and Selective Non-covalent Active-Site Inhibitor of USP7. *Cell Chemical Biology Cell Press*. 24 2017, 1490–1500.e11. <https://doi.org/10.1016/j.CHEMBIOL.2017.09.003>
- [18] Turnbull, A.P., Ioannidis, S., Krajewski, W.W., Pinto-Fernandez, A., Heride, C., Martin, A.C.L., Tonkin, L.M., Townsend, E.C., Buker, S.M., Lancia, D.R., Caravella, J.A., Toms, A. V, Charlton, T.M., Lahdenranta, J., Wilker, E., Follows, B.C., Evans, N.J., Stead, L., Alli, C. et al. Molecular basis of USP7 inhibition by selective small-molecule inhibitors. *Nature* 550 2017, 481–6. <https://doi.org/10.1038/nature24451>
- [19] Kategaya, L., Di Lello, P., Rougé, L., Pastor, R., Clark, K.R., Drummond, J., Kleinheinz, T., Lin, E., Upton, J.-P., Prakash, S., Heideker, J., McClelland, M., Ritorto, M.S., Alessi, D.R., Trost, M., Bainbridge, T.W., Kwok, M.C.M., Ma, T.P., Stiffler, Z. et al. USP7 small-molecule inhibitors interfere with ubiquitin binding. *Nature Nature Publishing Group*. 550 2017, 534–8. <https://doi.org/10.1038/nature24006>
- [20] Hao, Y.-H., Fountain, M.D., Fon Tacer, K., Xia, F., Bi, W., Kang, S.-H.L., Patel, A., Rosenfeld, J.A., Le Caignec, C., Isidor, B., Krantz, I.D., Noon, S.E., Pfotenhauer, J.P., Morgan, T.M., Moran, R., Pedersen, R.C., Saenz, M.S., Schaaf, C.P. and Potts, P.R. USP7 Acts as a Molecular Rheostat to Promote WASH-Dependent Endosomal Protein Recycling and Is Mutated in a Human Neurodevelopmental Disorder. *Molecular Cell* 59 2015, 956–69. <https://doi.org/10.1016/j.molcel.2015.07.033>
- [21] Kim, R.Q. and Sixma, T.K. Regulation of USP7: A High Incidence of E3 Complexes. *Journal of Molecular Biology* 429 2017, 3395–408. <https://doi.org/10.1016/j.jmb.2017.05.028>
- [22] Tavana, O. and Gu, W. Modulation of the p53/MDM2 interplay by HAUSP inhibitors. *Journal of Molecular Cell Biology Oxford University Press*. 9 2017, 45–52. <https://doi.org/10.1093/jmcb/mjw049>
- [23] Kruiswijk, F., Labuschagne, C.F. and Vousden, K.H. p53 in survival, death and metabolic health: a lifeguard with a licence to kill. *Nature Reviews Molecular Cell Biology* 16 2015, 393–405. <https://doi.org/10.1038/nrm4007>
- [24] Brooks, C.L. and Gu, W. p53 Ubiquitination: Mdm2 and Beyond. *Molecular Cell* 21 2006, 307–15. <https://doi.org/10.1016/j.molcel.2006.01.020>
- [25] Cummins, J.M. and Vogelstein, B. HAUSP is required for p53 destabilization. *Cell Cycle (Georgetown, Tex)* 3 2004, 689–92. <https://doi.org/10.4161/cc.3.6.924>
- [26] Li, M., Chen, D., Shiloh, A., Luo, J., Nikolaev, A.Y., Qin, J. and Gu, W. Deubiquitination of p53 by HAUSP is an important pathway for p53 stabilization. *Nature* 416 2002, 648–53. <https://doi.org/10.1038/nature737>

- [27] Epping, M.T., Meijer, L.A.T., Krijgsman, O., Bos, J.L., Pandolfi, P.P. and Bernards, R. TSPYL5 suppresses p53 levels and function by physical interaction with USP7. *Nature Cell Biology* 13 2011, 102–8. <https://doi.org/10.1038/ncb2142>
- [28] Song, M.S., Song, S.J., Kim, S.Y., Oh, H.J. and Lim, D.-S. The tumour suppressor RASSF1A promotes MDM2 self-ubiquitination by disrupting the MDM2–DAXX–HAUSP complex. *The EMBO Journal European Molecular Biology Organization*. 27 2008, 1863–74. <https://doi.org/10.1038/emboj.2008.115>
- [29] Sheng, Y., Saridakis, V., Sarkari, F., Duan, S., Wu, T., Arrowsmith, C.H. and Frappier, L. Molecular recognition of p53 and MDM2 by USP7/HAUSP. *Nature Structural & Molecular Biology* 13 2006, 285–91. <https://doi.org/10.1038/nsmb1067>
- [30] Hu, M., Gu, L., Li, M., Jeffrey, P.D., Gu, W. and Shi, Y. Structural basis of competitive recognition of p53 and MDM2 by HAUSP/USP7: implications for the regulation of the p53-MDM2 pathway. *PLoS Biology* 4 2006, e27. <https://doi.org/10.1371/journal.pbio.0040027>
- [31] Faesen, A.C., Dirac, A.M.G., Shanmugham, A., Ovaa, H., Perrakis, A. and Sixma, T.K. Mechanism of USP7/HAUSP activation by its C-terminal ubiquitin-like domain and allosteric regulation by GMP-synthetase. *Molecular Cell Elsevier Inc.* 44 2011, 147–59. <https://doi.org/10.1016/j.molcel.2011.06.034>
- [32] Fernández-Montalván, A., Bouwmeester, T., Joberty, G., Mader, R., Mahnke, M., Pierrat, B., Schlaeppli, J.-M., Worpenberg, S. and Gerhartz, B. Biochemical characterization of USP7 reveals post-translational modification sites and structural requirements for substrate processing and subcellular localization. *The FEBS Journal* 274 2007, 4256–70. <https://doi.org/10.1111/j.1742-4658.2007.05952.x>
- [33] Hu, M., Li, P., Li, M., Li, W., Yao, T., Wu, J.-W., Gu, W., Cohen, R.E. and Shi, Y. Crystal Structure of a UBP-Family Deubiquitinating Enzyme in Isolation and in Complex with Ubiquitin Aldehyde. *Cell* 111 2002, 1041–54. [https://doi.org/10.1016/S0092-8674\(02\)01199-6](https://doi.org/10.1016/S0092-8674(02)01199-6)
- [34] Kim, R.Q., van Dijk, W.J. and Sixma, T.K. Structure of USP7 catalytic domain and three Ubl-domains reveals a connector α -helix with regulatory role. *Journal of Structural Biology* 195 2016, 11–8. <https://doi.org/10.1016/j.jsb.2016.05.005>
- [35] Cheng, J., Yang, H., Fang, J., Ma, L., Gong, R., Wang, P., Li, Z. and Xu, Y. Molecular mechanism for USP7-mediated DNMT1 stabilization by acetylation. *Nature Communications* 6 2015, 7023. <https://doi.org/10.1038/ncomms8023>
- [36] Rougé, L., Bainbridge, T.W., Kwok, M., Tong, R., Di Lello, P., Wertz, I.E., Maurer, T., Ernst, J.A. and Murray, J. Molecular Understanding of USP7 Substrate Recognition and C-Terminal Activation. *Structure* 24 2016, 1335–45. <https://doi.org/10.1016/j.str.2016.05.020>
- [37] Heideker, J. and Wertz, I.E. DUBs, the regulation of cell identity and disease. *Biochemical Journal* 465 2015, 1–26. <https://doi.org/10.1042/BJ20140496>
- [38] Pozhidaeva, A., Valles, G., Wang, F., Wu, J., Sterner, D.E., Nguyen, P., Weinstock, J., Kumar, K.G.S., Kanyo, J., Wright, D. and Bezsonova, I. USP7-Specific Inhibitors Target and Modify the Enzyme's Active Site via Distinct Chemical Mechanisms. *Cell Chemical Biology Cell Press*. 24 2017, 1501–1512.e5. <https://doi.org/10.1016/J.CHEMBIOL.2017.09.004>
- [39] Rodríguez, M.S., Desterro, J.M.P., Lain, S., Lane, D.P. and Hay, R.T. Multiple C-Terminal Lysine Residues Target p53 for Ubiquitin-Proteasome-Mediated Degradation. *Molecular and Cellular Biology American Society for Microbiology*. 20 2000, 8458–67. <https://doi.org/10.1128/MCB.20.22.8458-8467.2000>
- [40] Hein, M.Y., Hubner, N.C., Poser, I., Cox, J., Nagaraj, N., Toyoda, Y., Gak, I.A., Weisswange, I., Mansfeld, J., Buchholz, F., Hyman, A.A. and Mann, M. A Human Interactome in Three Quantitative Dimensions Organized by Stoichiometries and Abundances. *Cell* 163 2015, 712–23. <https://doi.org/10.1016/j.cell.2015.09.053>
- [41] Ekkebus, R., van Kasteren, S.I., Kulathu, Y., Scholten, A., Berlin, I., Geurink, P.P., de Jong, A., Goerdal, S., Neeffjes, J., Heck, A.J.R., Komander, D. and Ovaa, H. On terminal alkynes that can react with active-site cysteine nucleophiles in proteases. *Journal of the American Chemical Society* 135 2013, 2867–70. <https://doi.org/10.1021/ja309802n>
- [42] Schuck, P. and Zhao, H. The role of mass transport limitation and surface heterogeneity in the biophysical characterization of macromolecular binding processes by SPR biosensing. *Methods in Molecular Biology (Clifton, NJ)* 627 2010, 15–54. https://doi.org/10.1007/978-1-60761-670-2_2
- [43] Saridakis, V., Sheng, Y., Sarkari, F., Holowaty, M.N., Shire, K., Nguyen, T., Zhang, R.G., Liao, J., Lee, W., Edwards, A.M., Arrowsmith, C.H. and Frappier, L. Structure of the p53 binding domain of HAUSP/USP7 bound to Epstein-Barr nuclear antigen 1 implications for EBV-mediated immortalization. *Molecular Cell* 18 2005, 25–36. <https://doi.org/10.1016/j.molcel.2005.02.029>

Chapter 3. USP7 activity mechanism

- [44] Geurink, P.P., El Oualid, F., Jonker, A., Hameed, D.S. and Ovaa, H. A General Chemical Ligation Approach Towards Isopeptide-Linked Ubiquitin and Ubiquitin-Like Assay Reagents. *ChemBioChem* 13 2012, 293–7. <https://doi.org/10.1002/cbic.201100706>
- [45] Mulder, M.P.C., El Oualid, F., ter Beek, J. and Ovaa, H. A Native Chemical Ligation Handle that Enables the Synthesis of Advanced Activity-Based Probes: Diubiquitin as a Case Study. *ChemBioChem* 15 2014, 946–9. <https://doi.org/10.1002/cbic.201402012>
- [46] de Jong, A., Merx, R., Berlin, I., Rodenko, B., Wijdeven, R.H.M., El Atmioui, D., Yalçin, Z., Robson, C.N., Neefjes, J.J. and Ovaa, H. Ubiquitin-Based Probes Prepared by Total Synthesis To Profile the Activity of Deubiquitinating Enzymes. *ChemBioChem Wiley-Blackwell*. 13 2012, 2251–8. <https://doi.org/10.1002/cbic.201200497>
- [47] Borodovsky, A., Ovaa, H., Kolli, N., Gan-Erdene, T., Wilkinson, K.D., Ploegh, H.L. and Kessler, B.M. Chemistry-Based Functional Proteomics Reveals Novel Members of the Deubiquitinating Enzyme Family. *Chemistry & Biology* 9 2002, 1149–59. [https://doi.org/10.1016/S1074-5521\(02\)00248-X](https://doi.org/10.1016/S1074-5521(02)00248-X)
- [48] Flierman, D., Van Der Heden Van Noort, G.J., Ekkebus, R., Geurink, P.P., Mevissen, T.E.T., Hospenthal, M.K., Komander, D. and Ovaa, H. Non-hydrolyzable Diubiquitin Probes Reveal Linkage-Specific Reactivity of Deubiquitylating Enzymes Mediated by S2 Pockets. *Cell Chemical Biology The Authors*. 23 2016, 472–82. <https://doi.org/10.1016/j.chembiol.2016.03.009>
- [49] El Oualid, F., Merx, R., Ekkebus, R., Hameed, D.S., Smit, J.J., de Jong, A., Hilkmann, H., Sixma, T.K. and Ovaa, H. Chemical synthesis of ubiquitin, ubiquitin-based probes, and diubiquitin. *Angewandte Chemie (International Ed in English)* 49 2010, 10149–53. <https://doi.org/10.1002/anie.201005995>
- [50] Ma, J., Martin, J.D., Xue, Y., Lor, L.A., Kennedy-Wilson, K.M., Sinnamon, R.H., Ho, T.F., Zhang, G., Schwartz, B., Tummino, P.J. and Lai, Z. C-terminal region of USP7/HAUSP is critical for deubiquitination activity and contains a second mdm2/p53 binding site. *Archives of Biochemistry and Biophysics* 503 2010, 207–12. <https://doi.org/10.1016/j.abb.2010.08.020>
- [51] Li, A., Ziehr, J.L. and Johnson, K.A. A new general method for simultaneous fitting of temperature and concentration dependence of reaction rates yields kinetic and thermodynamic parameters for HIV reverse transcriptase specificity. *The Journal of Biological Chemistry American Society for Biochemistry and Molecular Biology*. 292 2017, 6695–702. <https://doi.org/10.1074/jbc.M116.760827>
- [52] Johnson, K.A., Simpson, Z.B. and Blom, T. FitSpace explorer: an algorithm to evaluate multidimensional parameter space in fitting kinetic data. *Analytical Biochemistry* 387 2009, 30–41. <https://doi.org/10.1016/j.ab.2008.12.025>
- [53] Johnson, K.A. 1 Transient-State Kinetic Analysis of Enzyme Reaction Pathways. *The Enzymes* 20 1992, 1–61. [https://doi.org/10.1016/S1874-6047\(08\)60019-0](https://doi.org/10.1016/S1874-6047(08)60019-0)
- [54] Pföh, R., Lacdao, I.K., Georges, A.A., Capar, A., Zheng, H., Frappier, L. and Saridakis, V. Crystal Structure of USP7 Ubiquitin-like Domains with an ICPO Peptide Reveals a Novel Mechanism Used by Viral and Cellular Proteins to Target USP7. *PLoS Pathogens* 11 2015, e1004950. <https://doi.org/10.1371/journal.ppat.1004950>
- [55] Cummins, J.M., Rago, C., Kohli, M., Kinzler, K.W., Lengauer, C. and Vogelstein, B. Tumour suppression: Disruption of HAUSP gene stabilizes p53. *Nature* 428 2004, 486–7. <https://doi.org/10.1038/nature02501>
- [56] Di Lello, P., Rougé, L., Pan, B. and Maurer, T. 1H, 13C and 15N backbone resonance assignment for the 40.5 kDa catalytic domain of Ubiquitin Specific Protease 7 (USP7). *Biomolecular NMR Assignments* 7 2016, 5–9. <https://doi.org/10.1007/s12104-016-9698-3>
- [57] Luna-Vargas, M.P.A., Christodoulou, E., Alfieri, A., van Dijk, W.J., Stadnik, M., Hibbert, R.G., Sahtoe, D.D., Clerici, M., Marco, V. De, Littler, D., Celie, P.H.N., Sixma, T.K. and Perrakis, A. Enabling high-throughput ligation-independent cloning and protein expression for the family of ubiquitin specific proteases. *Journal of Structural Biology* 175 2011, 113–9. <https://doi.org/10.1016/j.jsb.2011.03.017>
- [58] Studier, F.W. Protein production by auto-induction in high-density shaking cultures. *Protein Expression and Purification* 41 2005, 207–34. <https://doi.org/10.1016/j.pep.2005.01.016>
- [59] Sivashanmugam, A., Murray, V., Cui, C., Zhang, Y., Wang, J. and Li, Q. Practical protocols for production of very high yields of recombinant proteins using *Escherichia coli*. *Protein Science : A Publication of the Protein Society* 18 2009, 936–48. <https://doi.org/10.1002/pro.102>
- [60] Delaglio, F., Grzesiek, S., Vuister, G.W., Zhu, G., Pfeifer, J. and Bax, A. NMRPipe: a multidimensional spectral processing system based on UNIX pipes. *Journal of Biomolecular NMR* 6 1995, 277–93. <https://doi.org/10.1007/BF00197809>

- [61] Vranken, W.F., Boucher, W., Stevens, T.J., Fogh, R.H., Pajon, A., Llinas, M., Ulrich, E.L., Markley, J.L., Ionides, J. and Laue, E.D. The CCPN data model for NMR spectroscopy: Development of a software pipeline. *Proteins: Structure, Function, and Bioinformatics* 59 2005, 687–96. <https://doi.org/10.1002/prot.20449>
- [62] Shen, Y. and Bax, A. Protein backbone and sidechain torsion angles predicted from NMR chemical shifts using artificial neural networks. *Journal of Biomolecular NMR Springer Netherlands*. 56 2013, 227–41. <https://doi.org/10.1007/s10858-013-9741-y>
- [63] Mulder, F.A., Schipper, D., Bott, R. and Boelens, R. Altered flexibility in the substrate-binding site of related native and engineered high-alkaline *Bacillus subtilis*ins 1 1 Edited by P. E. Wright. *Journal of Molecular Biology* 292 1999, 111–23. <https://doi.org/10.1006/jmbi.1999.3034>
- [64] Ekkebus, R., Flierman, D., Geurink, P.P. and Ovaa, H. Catching a DUB in the act: novel ubiquitin-based active site directed probes. *Current Opinion in Chemical Biology* 23 2014, 63–70. <https://doi.org/10.1016/j.cbpa.2014.10.005>
- [65] Kabsch, W. and Sander, C. Dictionary of protein secondary structure: Pattern recognition of hydrogen-bonded and geometrical features. *Biopolymers* 22 1983, 2577–637. <https://doi.org/10.1002/bip.360221211>
- [66] Helgstrand, M., Härd, T. and Allard, P. Simulations of NMR pulse sequences during equilibrium and non-equilibrium chemical exchange. *Journal of Biomolecular NMR* 18 2000, 49–63.
- [67] Allard, P., Helgstrand, M. and Härd, T. The Complete Homogeneous Master Equation for a Heteronuclear Two-Spin System in the Basis of Cartesian Product Operators. *Journal of Magnetic Resonance* 134 1998, 7–16. <https://doi.org/10.1006/jmre.1998.1509>
- [68] Toseland, C.P. *Fluorescence to Study the ATPase Mechanism of Motor Proteins*. Springer, Basel. p. 67–86. https://doi.org/10.1007/978-3-0348-0856-9_4
- [69] Johnson, K.A. Chapter 23 Fitting Enzyme Kinetic Data with KinTek Global Kinetic Explorer. *Methods in Enzymology* p. 601–26. [https://doi.org/10.1016/S0076-6879\(09\)67023-3](https://doi.org/10.1016/S0076-6879(09)67023-3).

Chapter 3. USP7 activity mechanism

Chapter 3.

USP7 activity mechanism

Supplemental data

Robbert Q. Kim¹, Paul P. Geurink^{2,3}, Monique P.C. Mulder^{2,3}, Alexander Fish¹, Reggy Ekkebus^{2,3}, Farid El Oualid⁴, Willem J. van Dijk¹, Duco van Dalen^{2,6}, Huib Ovaa^{2,3}, Hugo van Ingen^{5,7}, Titia K. Sixma¹

¹*Division of Biochemistry and Oncode Institute, Netherlands Cancer Institute, Plesmanlaan 121, 1066 CX Amsterdam, the Netherlands*

²*Division of Cell Biology II, Netherlands Cancer Institute, Plesmanlaan 121, 1066 CX Amsterdam, the Netherlands*

³*Current address: Oncode Institute and Department of Cell and Chemical Biology, Leiden University Medical Center, Leiden, the Netherlands*

⁴*UbiQ Bio BV, Science Park 408, 1098 XH Amsterdam, the Netherlands*

⁵*Macromolecular Biochemistry, Leiden Institute of Chemistry, Leiden University, the Netherlands*

⁶*Current address: Tumor Immunology department, Radboud Institute for Molecular Sciences, Nijmegen, the Netherlands*

⁷*Current address: Bijvoet center, Utrecht University, the Netherlands*

In press as:

Kim, R.Q., Geurink, P.P., Mulder, M.P.C., Fish, A., Ekkebus R., El Oualid, F., van Dijk, W.J., van Dalen, D., Ovaa, H., van Ingen H. and Sixma, T.K.

Kinetic analysis of multistep USP7 mechanism shows critical role for target protein in activity

Nature Communications

<https://doi.org/10.1038/s41467-018-08231-5>

Chapter 3. USP7 activity mechanism

Supplemental Methods: NMR assignment

To characterize the weak interaction between USP7-Ubl45 and USP7CD in trans we used solution NMR spectroscopy to map the binding interface at the residue-level. We isotope-labelled the smallest of the two domains, Ubl45, including the C-terminal peptide, and first assessed the quality of its NMR spectrum. The ^1H - ^{15}N correlation spectrum of the 25 kDa Ubl45 domain, spanning from residue 889 until 1102, shows the dispersion and number of peaks that is expected for a well-folded domain of this size (Fig. 2a). We could confidently assign resonances for 84% of the residues present in the construct (Supplemental Fig. 1a). The assigned backbone chemical shifts were used to predict the secondary structure using the TALOS-N webserver⁶²: the identified secondary structure matched the crystal structure of Ubl45 (PDB: 5JTV) very well (Supplemental Fig. 1b).

Next, we titrated in the unlabelled interaction partner CD and followed the chemical shift perturbations (CSPs) for the assigned Ubl45 residues. The titration was performed using Ubl45:CD ratios of 1:1, 1:5 and 1:10 where the Ubl45 concentration is kept constant at 45 μM and the highest concentration of CD is 450 μM . Binding is apparent from the overall loss in peak intensities for residues in the folded core of the protein (Fig. 2c). Due to the large size of the complex (60 kDa) resonances of the bound state are severely broadened. This is not the case for the tails of Ubl45, indicating that they remain flexible.

The tails did show the same uniform broadening however when titrating in covalently linked CDUb (Fig. 2e). Again we kept the concentration of Ubl45 constant at 45 μM , titrating in CDUb in an 0.1 and 0.3 ratio, as the determined affinity is in the low micromolar range (Fig. 3). The resulting intensity plot for the Ubl45 residues show a decrease correlated to the fraction of CDUb titrated in. Furthermore, we can now see that, unlike the CD only titration, the intensities belonging to both termini decrease, uniformly with the core domain. This could be due to the overall tighter binding, restraining the flexible termini, or to the interaction of the termini with the CDUb.

Supplemental Methods: chemical synthesis

Fmoc solid phase peptide synthesis

Peptides were synthesized on a Syro II MultiSyntech Automated Peptide synthesizer by standard 9-fluorenylmethoxycarbonyl (Fmoc) based solid phase peptide chemistry on a 25 or 50 μmol scale. Starting with the pre-loaded Fmoc amino acid resin (Applied Biosystems), each successive amino acid (Novabiochem) was coupled in 4 molar excess for 45 min with PyBOP and DiPEA. Deprotection of the Fmoc group was achieved with 20% piperidine in NMP (2 \times 2 and 1 \times 5 min). Peptides were cleaved with TFA/ H_2O /phenol/ $i\text{Pr}_3\text{SiH}$ (90.5/5/2.5/2 v/v/v/v) for 3 hrs., precipitated in cold *n*-hexane/diethyl ether and washed 3 \times with diethylether. The pellet was dissolved in H_2O / CH_3CN /formic acid (65/35/10; v/v/v) and lyophilized. The purity of the peptides was determined by LC-MS analysis and peptides were purified by RP-HPLC where appropriate.

p53Ub and p53_{short}Ub

p53 peptides (residues 357-389 and 368-389) containing an thioLys at position 382 and a 5-carboxy-TAMRA at the N-terminus were synthesized according to the procedure described above. Ub was coupled to the peptides by native chemical ligation: To 0.1 M sodium phosphate

pH 8.0 were added: 5 mM MgCl_2 (from 0.2 M aq. stock), 150 mM NaCl (from 5 M stock), 50 mM MESNa (from 2 M stock), 5 mM ATP (from 0.5 M aq. stock), Ub (50 μM) and TAMRA-thiolysine modified p53 peptide (250 μM). After adjusting the pH to 7.5 – 8.0 using 1M NaOH, E1 enzyme (150 nM, UBE1, Boston Biochem) was added and the ligation mixture was incubated at 37°C for 6 hrs. Next, 20 mM VA-044 (from freshly prepared 0.1 M stock in buffer), 40 mM GSH and 0.25 M TCEP (0.5 M stock, pH 7.0) were added to the crude ligation mixture. The pH was corrected to 7.0 using 1N NaOH and the reaction mixture was incubated at 37°C for 6 hrs. The constructs were purified by RP-HPLC on a Shimadzu LC-20AD/T using a C8 Vydac column (Grace Davison Discovery Sciences™). Column mobile phases: A= 0.05% aq. TFA and B= 0.05% TFA in CH_3CN . T= 40°C. Flow rate= 5 mL min⁻¹. Gradient: 30→75%B over 18 min.

p53Ub_{inh} and p53_{short}Ub_{inh}

p53 peptides (residues 357-389 and 368-389) containing an azido-ornithine at position 382 were synthesized according to the procedure described above. Ub was coupled to the peptides by the copper-catalyzed alkyne-azide cycloaddition (CuAAC or 'click') reaction: Ub-PA and the azido-modified p53 peptide were dissolved in warm DMSO at a concentration of 50 mg mL⁻¹. 1 eq. of the p53 peptide was mixed with 0.9 eq. of Ub-PA (typically 90 μL) in 1 mL 8M urea, 100 mM phosphate buffer pH 7. To the resulting solution 10 μL of catalyst solution containing 20 mg mL⁻¹ Cu(I)Br in MeCN and 50 mg mL⁻¹ TBTA-analogue in MeCN (2:3, v/v) was added followed by a short vortex, repeated in 5 minute intervals 5 times in total. After reactions were finished, as judged by LC-MS (~ 1 hr.), the reaction was quenched by the addition of 100 μL of 0.5 M EDTA, pH 7.0. The product was purified using RP-HPLC on a Waters Atlantis T3 C18 30x250 5 μm . Column Mobile phases: A= 0.05% aq. TFA and B= 0.05% TFA in CH_3CN . Flow rate= 18 mL min⁻¹. Gradient: 20→32%B over 20 min.

p53Ub_{VA} and p53_{short}Ub_{VA}

p53 peptides (residues 357-389 and 368-389) containing a Dab(Alloc) at position 382 were synthesized according to the procedure described above. The resin was treated with $\text{Pd}(\text{PPh}_3)_4$ (0.35 eq) and Ph_3SiH (20 eq) in DCM (2x 20 min) and shaken overnight at room temperature with 4-((*tert*-butoxycarbonyl)amino)-3-((*tert*-butyldisulfanyl)butanoic acid (3 eq), PyBOP (3 eq) and DiPEA (6 eq). After extensive washings (3x NMP, DCM and Et_2O) the resin was treated with TFA/ H_2O /phenol/ $i\text{Pr}_3\text{SiH}$ (90/5/2.5/2.5 v/v/v/v) for 3 hrs. followed by precipitation in cold Et_2O /pentane 3:1 v/v. The crude peptide was lyophilized and purified by HPLC. Ub₇₅SEt was coupled to the peptides by native chemical ligation: To a solution of the p53 Dab mutant in 0.15 M sodium phosphate buffer (pH 7) containing 6M Gdn·HCl and MPAA (250 mM), a solution of Ub₇₅SEt in 0.2 M sodium phosphate buffer (pH 7) containing 6M Gdn·HCl and MPAA (250 mM) was added and the mixture (conc.: 50 mg mL⁻¹) was incubated at 37°C overnight. Next, TCEP was added to reduce the MPAA disulfide. The product was purified using RP-HPLC on a Waters Atlantis T3 C18 30x250 5 μm . Column Mobile phases: A= 0.05% aq. TFA and B= 0.05% TFA in CH_3CN . Flow rate= 18 mL min⁻¹. Gradient: 20→40%B over 25 min.

TAMRA-p53 peptide

p53 peptide (residues 357-389) with a 5-carboxy-TAMRA at the N-terminus was synthesized according to the procedure described above. LC-MS analysis was performed on a system

Chapter 3. USP7 activity mechanism

equipped with a Waters 2795 separation Module (Alliance HT), Waters 2996 Photodiode Array Detector (190–700 nm) and a Micromass LCT-TOF Premier mass spectrometer. Samples were run over an XBridge BEH300 C18 column (5 μ m, 4.6×100mm, T= 40°C). Samples were run at 0.8 mL min⁻¹ using a gradient of two mobile phases: A= 1% acetonitrile and 0.1% formic acid in water; B= 1% water and 0.1% formic acid in acetonitrile. Gradient 30–60%B over 6.5 min.

Supplemental Methods: Global modelling of enzymatic activity

All the acquired data for USP7 activity on the model substrate p53Ub were loaded into KinTek⁵¹ per construct. Here we describe the corrections applied to the data before introduction and how we defined our observables. We also state our assumptions and what steps were taken to condense the model in order to be dependent on the least amount of variables.

KinTek observables definition and data treatment

The minimal substrate data (panel A in Fig. 6, S4, S5, S6) were obtained using an injector in our plate reader set up, so no time delay had to be introduced. The raw data could be converted to amounts (μ M) using a calibration curve and then directly read into KinTek.

The FP data on the model substrate from the plate reader (panel b, upper) required a delay before introduction into KinTek. This delay was estimated for each experiment by co-fitting the curves using Prism 7 to determine point “0”. The curves were corrected for a drift using the null experiment and subsequently normalised (panel b, lower). Fittable data (with good amplitudes) were then read into KinTek, omitting concentrations within two orders of magnitude to the substrate concentration due to their lack of signal at the early time points. We defined the observed curves as amount of uncleaved substrate (p53Ub) and the bound fraction of product (USP7.p53), although this is a minor influence, all scaled by a defined factor **c** of 1000 that converted the used 0.1 μ M substrate to 100%.

In the stopped-flow FP activity anisotropy data (panel c) the raw data were read-in as is. For data quality purposes we excluded the early time points (<0.001 s) due to the low signal to noise ratio as well as the late time points (>10s), as we observed bleaching of the fluorophore. Here we scaled the observables using factor **a** determined from the null experiment as this curve represents the appropriate signal for the amounts in the reaction. We noticed how the curves, especially for full-length, represented four different phases (Fig. 6c; description c) below), so we accounted for these with four different USP7 states each with their own scaling factor (FP1-4) that converged in the initial fitting of the experiment.

For the intensity signal accompanying the anisotropy data (Fig. 6d), the overall signal differences were less than 10 percent (before the 10 s mark), allowing use of the obtained anisotropy signal without correction⁶⁸. To use the intensity signal, we subtracted the baseline (null experiment) and normalised using the early time points (<0.005 s), setting these to an arbitrary 100. We then applied the same observables as for panel c, now scaling them with a defined factor **b** of 2000 (100 / 0.05 μ M). We found that the intensity of the free substrate and product did not differ from their initial bound state (USP7.p53Ub and USP7.p53), but that there are two different USP7 states in the hydrolysis. These observations have been described with their own scaling factors (I1-I3).

For the constructs TCD and FL affinity for the p53 peptide product was high enough to be relevant (Figure 5c). For TCD, this value (2 μ M) is far weaker than the 50 nM used in the

stopped-flow experiments, so introduction of the fitted FP data from Figure 5c was sufficient input. For the full-length construct however, the K_D (160 nM) was much closer to the used concentration, so we performed a separate stopped-flow experiment for the p53 product, to fit the data within the KinTek model. We pre-treated the anisotropy data similarly as in panel c, but now only for the product states, and a defined scaling factor **q** of 3.4 that related the used amount (25 nM) to the obtained signal in the null curve.

In panel f we used the intensity data belonging to the p53 product stopped-flow. The data are corrected just as in panel d, and the observables now only pertain to the product and its complexes. As the used concentration is two-fold lower (0.025 μ M) the scaling factor **r** is now 4000.

- a) Rho
- b) $c * (p53Ub + (USP7.p53 + USP7*.p53))$
- c) $a * (p53Ub + FP1*(USP7.p53Ub) + FP2*(USP7*.p53Ub + USP7\#.p53Ub) + FP3*p53 + FP4*(USP7.p53 + USP7*.p53))$
- d) $b * ((p53Ub + USP7.p53Ub) + I1*(USP7*.p53Ub) + I2*(USP7\#.p53Ub) + I3*(p53 + USP7.p53 + USP7*.p53))$
- e) $q * (p53 + P1*(USP7.p53 + USP7*.p53))$
- f) $r * (p53 + USP7.p53 + (P2*USP7*.p53))$

Reaction assumptions and rate determination

We fitted every experiment separately, to obtain good estimations for the scaling factors. We then determined the on-rate, which is diffusion-limited and should be shared over all experiments. To this end we used all stopped-flow anisotropy data, as these experiments have a direct indication of the association. We were able to pinpoint this rate at 179 μ M s^{-1} , well within the range considered reasonable for diffusion⁶⁹. Furthermore, we assumed an irreversible reaction, so only hydrolysis of the substrate (k_4), locking the reverse reaction (k_{-4}) at 0. For the model, we started out with as few steps as possible (binding, catalysis and release; Fig. 6h), only adding intermediates when the data required them.

Remarks on USP7 CD

For CD we found that the amplitudes for the stopped-flow data were too small, making them unusable for KinTek fitting. Therefore, we used only the minimal substrate (Supp. Fig. 6a) and plate reader FP enzyme activity data (Supp. Fig. 6b) for fitting and included data from TCD for step 3 (Supp. Fig. 6e), assuming that the observed conformational changes are the same.

Remarks on USP7 TCD

The stopped-flow data for TCD indicated a delay phase (0.1-5 s), which we modelled as a conformational change step (*Step 2*), based on the intensity data (Supp. Fig. 4d). The data could be fitted with one state, which did not change shape, thus the observables description for c) could be condensed, merging the FP1 and FP2 terms. Furthermore, the FP4 term seemed to have a minor effect only after 10 s, prompting us to omit the term in the fit. Similarly, we condensed the terms for the accompanying intensity experiment. With the data we modelled both the minimal and the model substrate with the same set of reactions, linking

Chapter 3. USP7 activity mechanism

the conformational change step (*Step 2*) as well as the catalytic step (*Step 4*). Assuming a similar reaction for both substrates resulted in a good fit and values stated in Supp. Fig. 4g.

Remarks on USP7 CD12345

The data for CD12345 had low amplitudes, indicative of the low affinity for the substrate. This resulted in high sigma values in the modelling. Just as in the TCD case, we had to model one intermediate step for reasonable fits. Therefore we condensed the observable terms in a similar fashion as for TCD. Furthermore, as there is no detectable binding of p53 to the construct (Supp. Fig. 5c) we did not require the p53 product retaining line in the model.

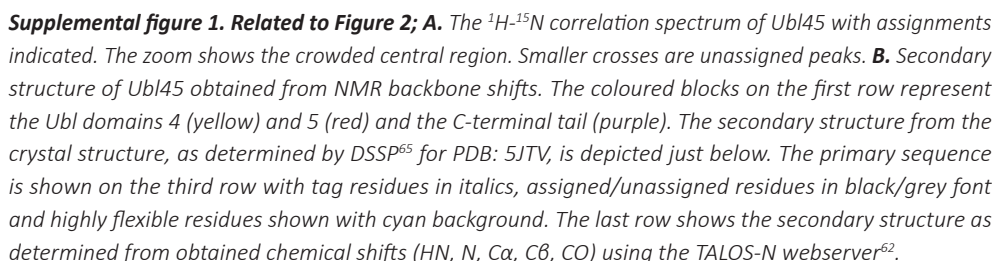
When attempting to link the found values for the p53 substrate with the minimal substrate we found the catalytic rates non-comparable, possibly due to interaction with the p53 peptide. We therefore could not assume a similar catalytic rate and constraining the fits was not possible through this linking. Combined with the low amplitudes, the less constrained values were not converged enough to be assessed by the statistical analysis.

Remarks on USP7 FL and statistical analysis

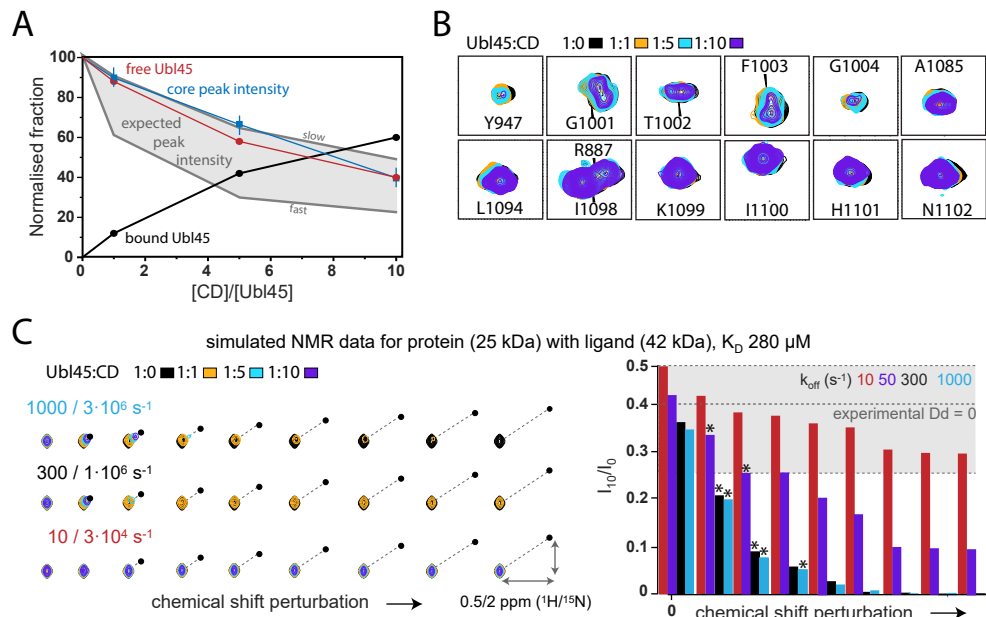
In the fitting of the FL construct two intermediate steps, instead of one, were required. As both TCD and CD12345 needed one intermediate, the requirement for two in the FL construct added up. We modelled these steps as two separate distinct steps, assumed to be sequential. Furthermore, at the product release steps we had to add a conformational change step upon binding of the p53 product (*Step 5*) to satisfy the p53 peptide stopped-flow data (Fig. 6f).

After fitting all the experimental data using the model description (Fig. 6h), we performed the statistical analysis using the FitSpace module of KinTek⁵² on the fitted data for TCD and FL (Supp. Fig. 7). The analysis showed us that some variables are heavily dependent on one another, but we could constrain their values by linking their ratios. Our data unfortunately do not have the resolution to pinpoint on- and off-rates for each step. The resulting values should therefore rather be interpreted as the optimal ratio to model the reaction or intermediate steps.

3



Chapter 3. USP7 activity mechanism

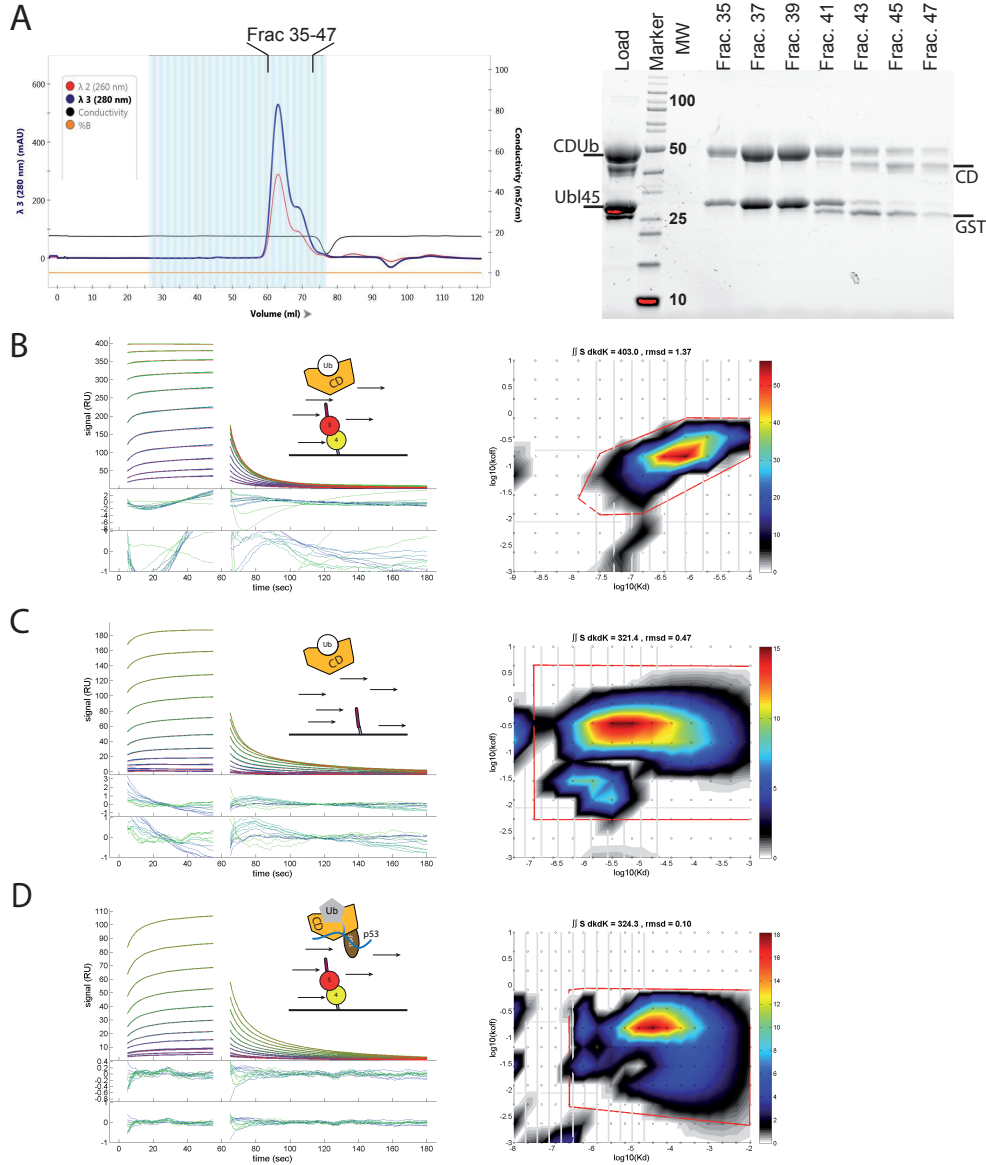


Supplemental figure 2. Quantitative analysis of USP7 Ubl45–CD NMR titration data.

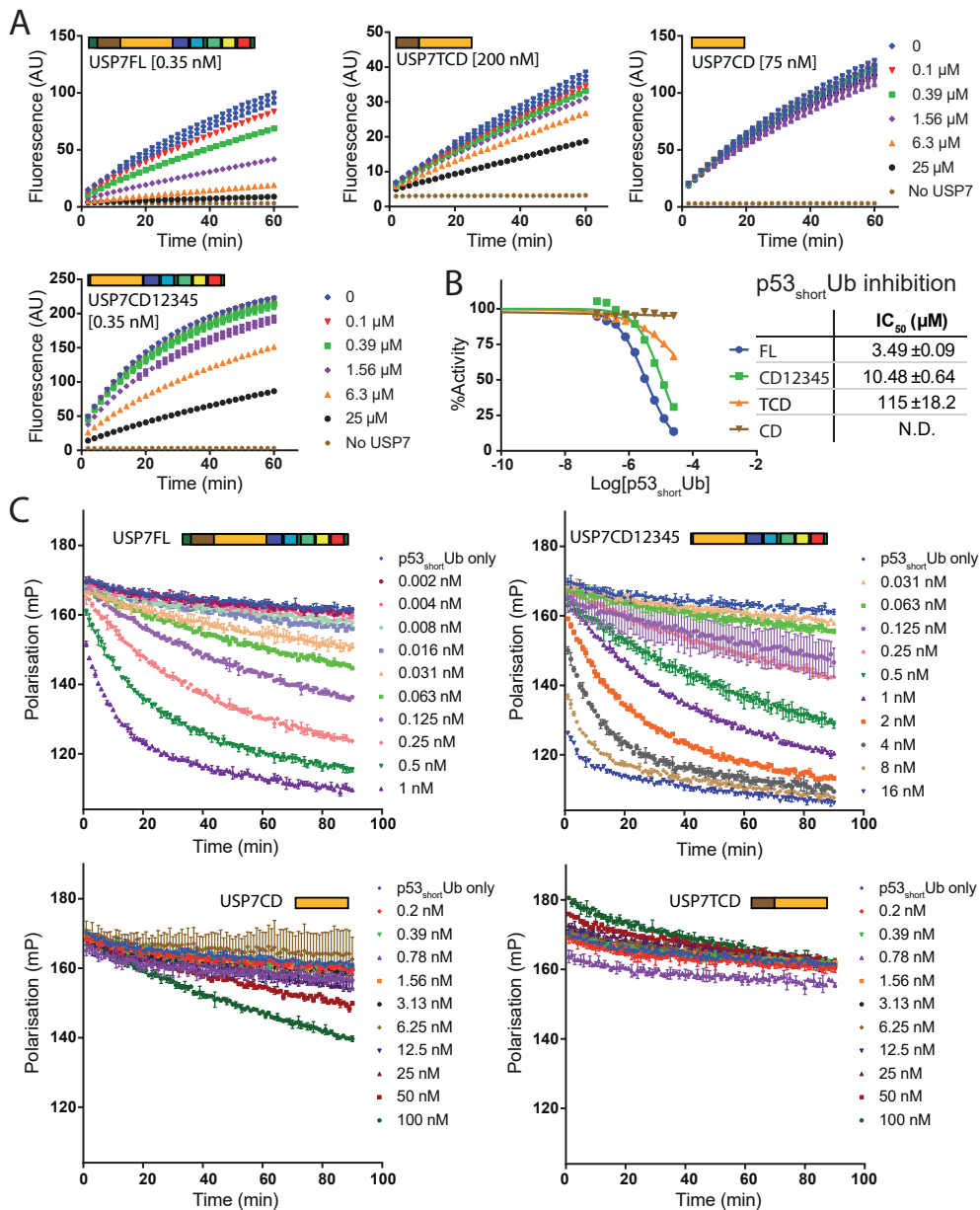
Supplemental figure 2. Related to Figure 2; Quantitative analysis of USP7 Ubl45-CD NMR titration data;

A. The overall peak intensity for Ubl45 residues in the folded core without chemical shift perturbations (blue) matches the expected values (grey) based on the affinity determined by SPR (Fig. 3A, main text). The core peak intensity was derived from the average intensity over 93 residues (all with no or minimal chemical shift changes), excluding the 50% most intense peaks. For residues without chemical shift perturbations (CSPs), peak intensity is determined by both the population of free (red) and bound (black) states. Notably, because of the significantly larger size of the complex (67 kDa) compared to the free protein (25 kDa), signals from the bound state will have a ~ 2.5 times larger line width in each dimension^{66,67} and will thus contribute less to the peak intensity. In addition, the dynamic exchange between free and bound state critically determines the observed peak shape and peak intensity, even for residues without chemical shift perturbation. In the limit of slow exchange, the signals of free and bound states add independently and a peak intensity of 50% of the initial value is expected. In the limit of fast exchange, both free and bound states have the same population-weighted relaxation rates and thus the same linewidths, which is significantly larger than the pure free state line width. Thus in this limit a final peak intensity of 25% is expected. **B.** Given the fact that the observed peak intensity decrease match well with the expectations for the formation of a 67 kDa complex, this indicates that the Ubl45-CD complex behaves as a globular assembly rather than two separate domains flexibly linked by the C-terminal tail. **C.** Simulated NMR peak trajectories (left) and peak intensity ratios (right) as function of chemical shift perturbation and off-rate (k_{off}). The simulated system is based on the Ubl45-CD interaction, using the appropriate molecular weights for the free protein and complex, the experimentally used titration scheme, and the affinity as determined by SPR. The CSP between free and bound state (indicated with a black circle) was systematically varied between 0 and maximally 0.5 ppm for ^1H and 2 ppm for ^{15}N . The titration was simulated for three combinations of on- and off-rates as indicated. Extrapolating from the experimentally observed off-rate for the Ubl45-CDUb interaction (K_D 1 μM , k_{off} 1 s^{-1} , Fig. 3c and S3b), the most likely scenario corresponds to k_{off} 300 s^{-1} and k_{on} $1 \cdot 10^6$ s^{-1} , which matches well with diffusion-controlled on-rate for biomolecular systems. At this off-rate, only small CSPs can be observed and residues with large chemical shift changes will show a strong reduction in peak intensity, beyond what is expected based on the amount of free protein. Higher off-rates will allow to observe larger CSPs. For very slow off-rates (< 10 s^{-1}) the free state and bound state become essentially isolated species and the observed peak will no longer encode properties of the bound state. The bound state will have peak intensity corresponding at most to $\sim 10\%$ (60% population of peak broadened 2.5 times in each dimension) of the apo state peak in the limit of no exchange and thus hardly observable in practice because of additional exchange broadening. The experimentally observed peak intensity ratio at position of the apo peak (42%) is best reproduced using a k_{off} of 50 s^{-1} (k_{on} $2 \cdot 10^5$ s^{-1}). Still, also for this slow exchange a large decrease in peak intensities (down to 10%) is expected for residues with large CSPs. The grey area indicates the expected peak intensities for residues without CSP from the slow to fast exchange limit. Peak intensities at the free state chemical shift position in the apo and 10 equivalent added spectrum are indicated as I_0 and I_{10} , respectively. In cases a CSP can be observed the actual intensity ratio will be higher, at most equal to the zero ppm CSP case; these are marked with a *.

Chapter 3. USP7 activity mechanism

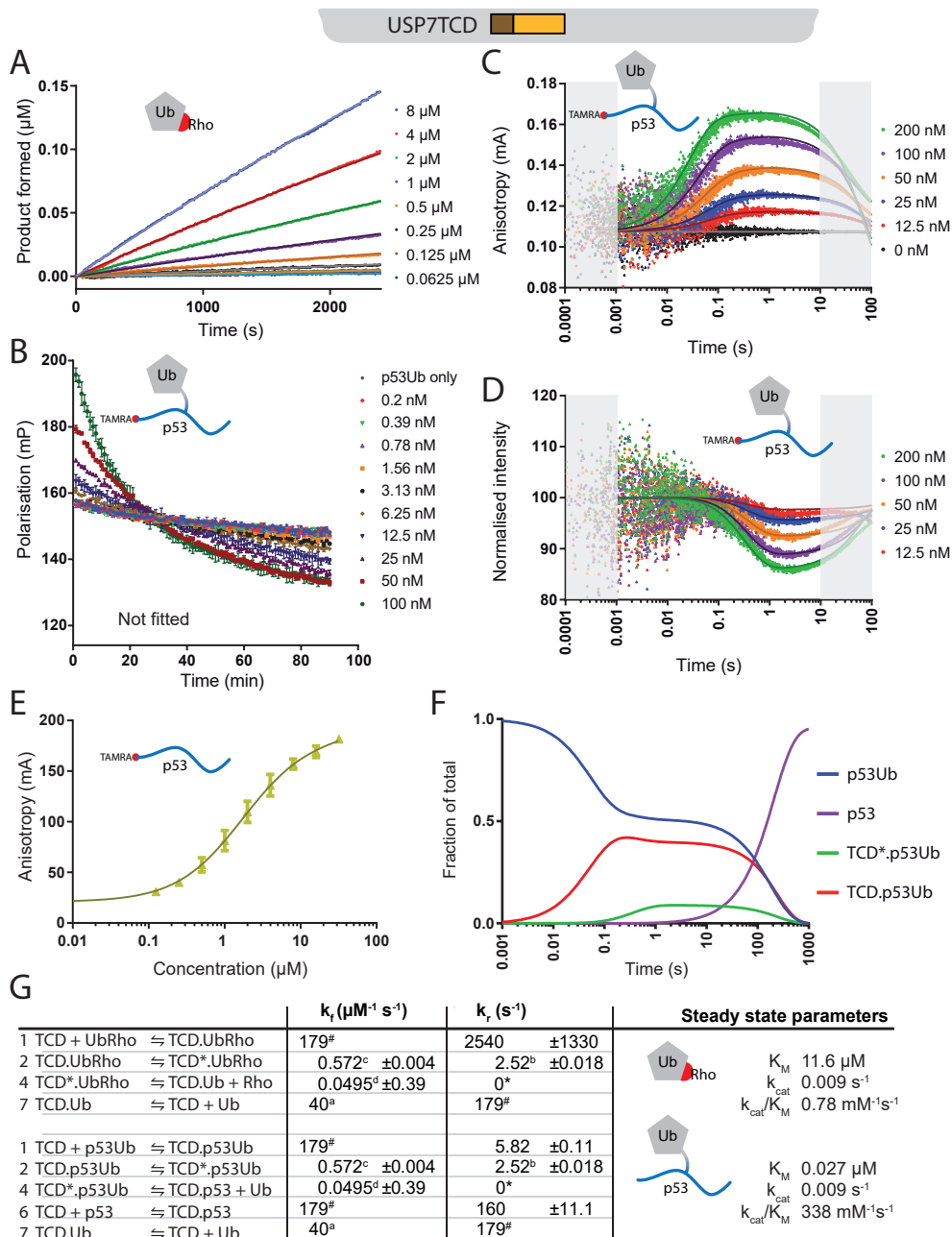


Supplemental figure 3. Related to Figure 3 and Figure 4d; A. Co-elution of CDUb and Ubl45 on Superdex75 gel filtration indicates a strong affinity. After incubation of CD and Ub-PA with Ubl45 to generate covalently bound CDUb, the product co-elutes with Ubl45 on gel filtration. The fractions indicated in the filtration profile are run on SDS-PAGE and imaged using the StainFree approach on the imager. **B.** The SPR curves from BiaCore were fitted using EvlFit to obtain both K_D and k_{off} values for the interaction between Ubl45 and CDUb. For every fitted interaction, the left panel shows the fit of the curves (rainbow-coloured) with the residuals displayed below. The right panel shows the heat map of the fitted values for K_D and k_{off} . **C.** The SPR curves from the interaction between the C-terminal peptide and CDUb fitted using EvlFit. **D.** The raw SPR data of the interaction between TCD-p53Ub and Ubl45 (Fig. 4d) fitted using EvlFit.



Supplemental figure 4. Related to Figure 5 and Figure 6b; A. The inhibition assay (see Fig. 5a) was repeated using the short non-hydrolysable p53Ub substrate, showing less inhibition when the TRAF motifs are left out. **B.** The initial velocities for the assay in A. are plotted against the used inhibitor concentration, yielding IC₅₀-values as stated in the adjacent table. **C.** The FP-assay as done in figure 6b is performed using TAMRA-p53Ub_{short} for the various protein constructs. The used protein concentrations are stated, they differ between constructs to cope with their difference in activity.

Chapter 3. USP7 activity mechanism

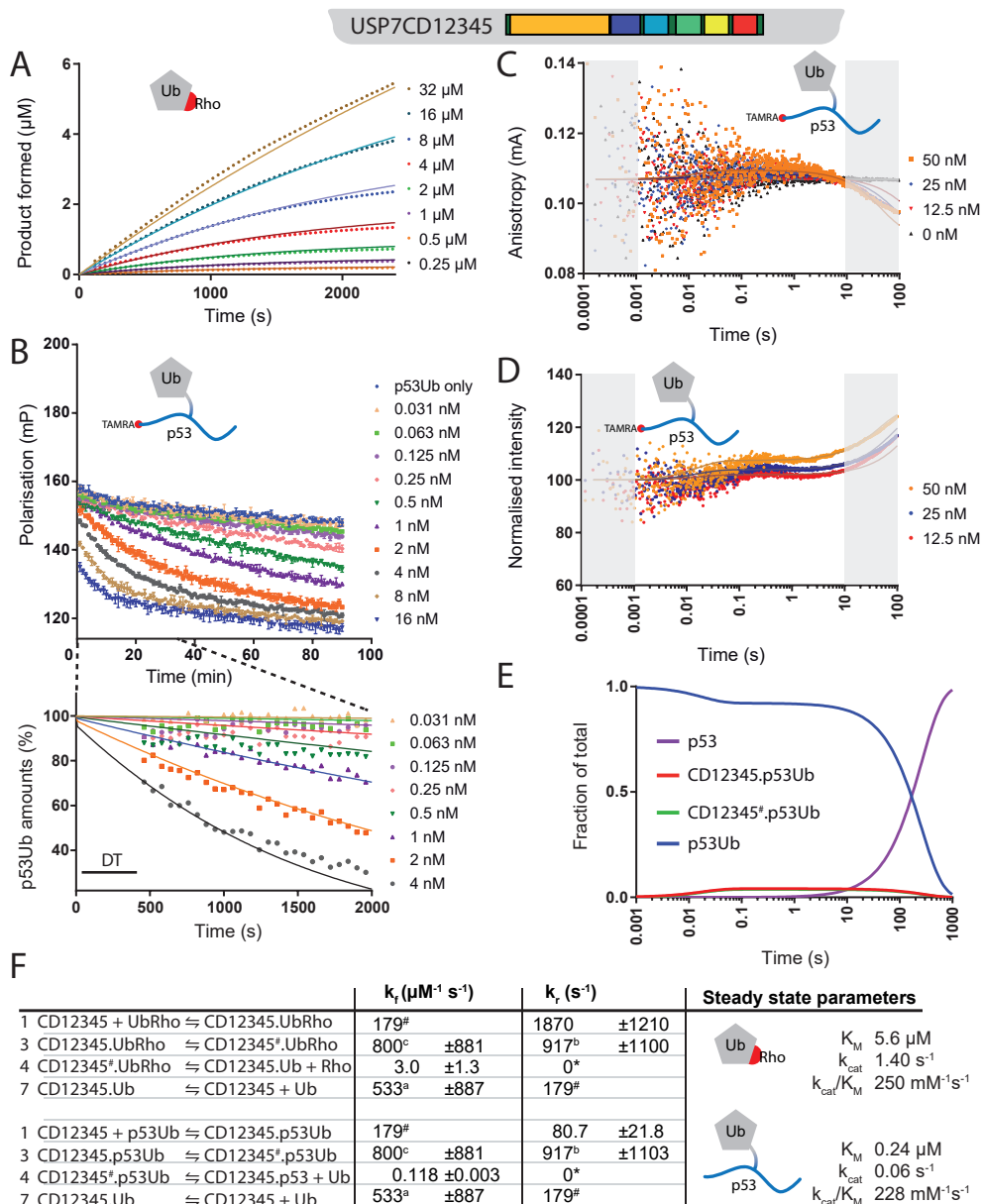


Supplemental figure 5. Global fitting of TCD data using KinTek.

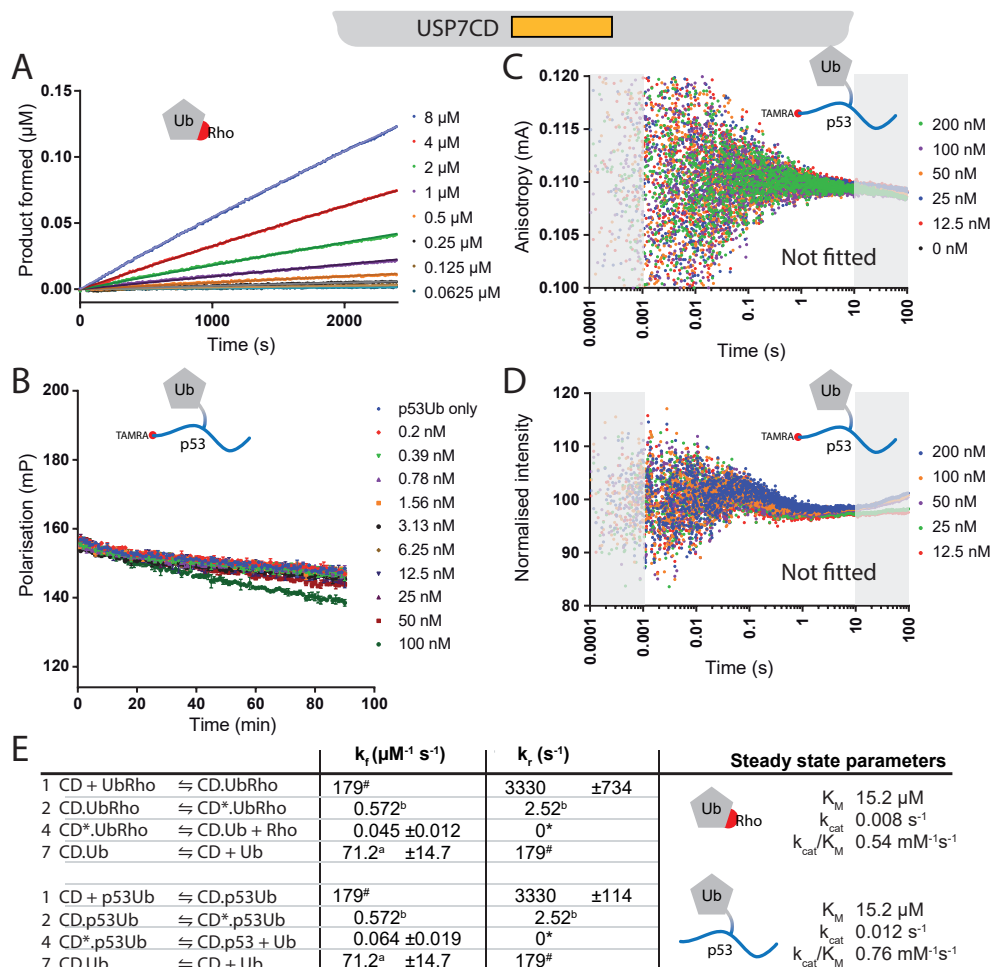
Supplemental figure 5. Related to Figure 6; Global fitting of TCD data using KinTek is displayed in a similar fashion as figure 6. Icons in each panel indicate the substrate used. Non-fitted are indicated in their panel. **A.** Minimal substrate activity assay of TCD (20 nM). **B.** FP enzyme activity assay on ^{TAMRA}p53Ub (100 nM) in plate reader setup. The used amounts of TCD are indicated in the legends. **C.** Stopped-flow FP enzyme activity assay on ^{TAMRA}p53Ub (50 nM), showing anisotropy signal allows observation of the binding and hydrolysis phases. **D.** The intensity signal for the experiment in C indicates a change in chemical environment upon binding of substrate. **E.** The end-point FP experiment measuring the affinity of TCD for the p53 product (Fig. 5c) was used to determine product binding of Step 6. **F.** Upon fitting of all experiments described here the fraction of each p53-substrate state could be modelled in an equimolar (1 to 1) setting. **G.** The model description used in KinTek to fit all the data. The intermediate state of TCD is indicated with an asterisk (TCD*). The forward and reverse rates reflect the optimal ratio that models the individual steps, since the experiment does not have sufficient resolution to fully resolve rates. The independently determined diffusion rate (ϵ) and the irreversible reaction (ϑ) have been fixed, whilst values with identical superscript identifiers ($\alpha, \beta, \gamma, \delta$) have been co-refined.

Supplemental figure 6. Related to Figure 6; Global fitting of CD12345 data using KinTek is displayed in a similar fashion as figure 6. Icons in each panel indicate the substrate used. **A.** Minimal substrate activity assay of CD12345 (1 nM). **B.** FP enzyme activity assay on ^{TAMRA}p53Ub (100 nM) in plate reader setup. The used amounts of CD12345 are indicated in the legends. **C.** Stopped-flow FP enzyme activity assay on ^{TAMRA}p53Ub (50 nM), showing anisotropy signal allows observation of the binding and hydrolysis phases. **D.** The intensity signal for the experiment in C indicates a change in chemical environment upon binding of substrate. **E.** Upon fitting of all experiments described here the fraction of each p53-substrate state could be modelled in an equimolar (1 to 1) setting. **F.** The model description used in KinTek to fit all the data. The intermediate state of CD12345 is indicated with a pound sign. The independently determined diffusion rate (ϵ) and the irreversible reaction (ϑ) were introduced as fixed values, whilst values with identical superscript identifiers ($\alpha, \beta, \gamma, \delta$) were co-refined.

Chapter 3. USP7 activity mechanism

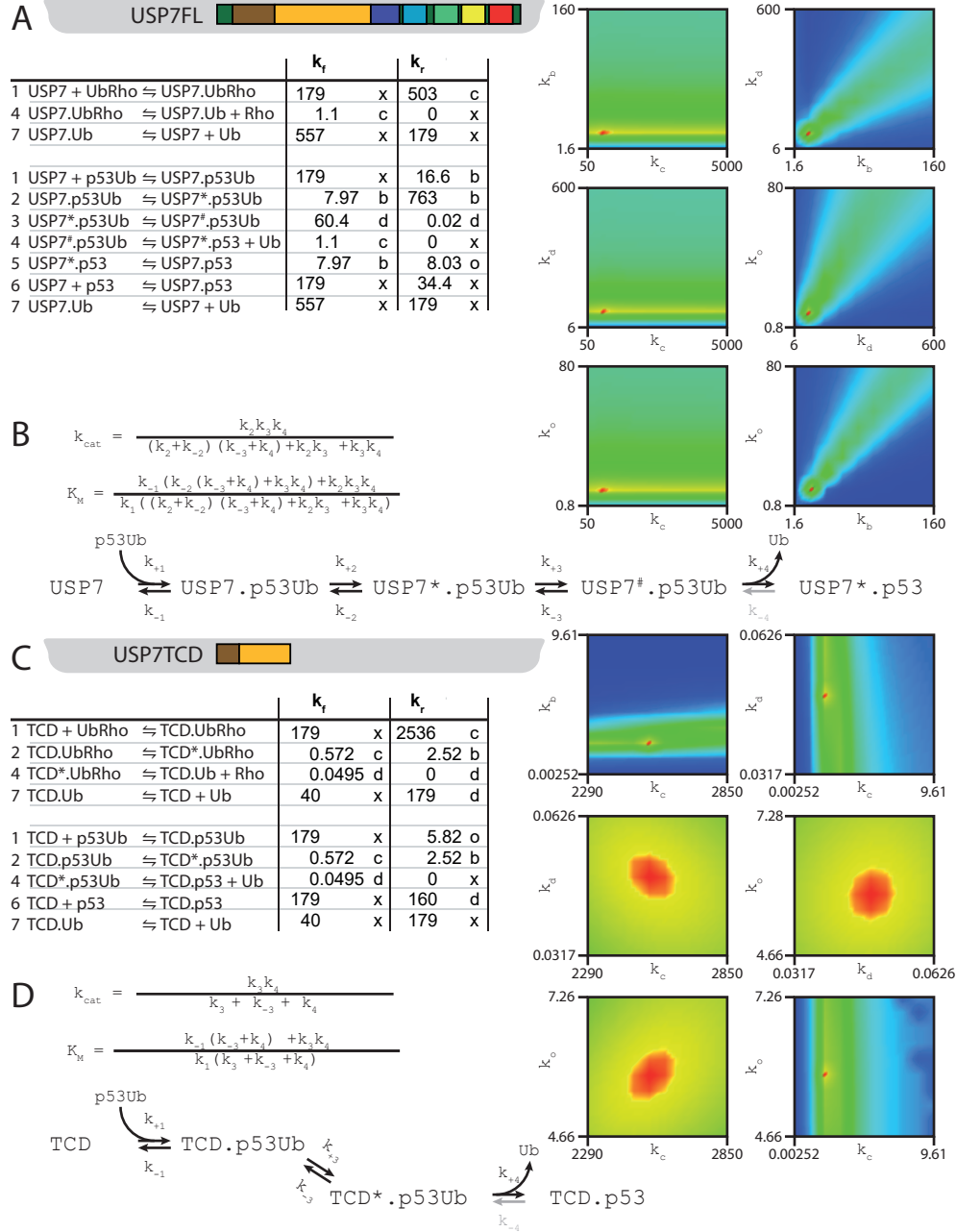


Supplemental figure 6. Global fitting of CD12345 data using KinTek.



Supplemental figure 7. Related to Figure 6; Global fitting of CD data using KinTek is displayed in a similar fashion as figure 6. Icons in each panel indicate the substrate used. Non-fitted are indicated in their panel. **A.** Minimal substrate activity assay of CD (20 nM). **B.** FP enzyme activity assay on ^{TAMRA}p53Ub (100 nM) in plate reader setup. The used amounts of CD are indicated in the legends. **C.** Stopped-flow FP enzyme activity assay on ^{TAMRA}p53Ub (50 nM), showing anisotropy signal allows observation of the binding and hydrolysis phases. **D.** The intensity signal for the experiment in C indicates a change in chemical environment upon binding of substrate. **E.** The model description used in KinTek to fit all the data. The intermediate state of CD indicated with an asterisk, is included based on the findings for TCD (Supplemental Fig. 4). These rates (β) were fixed in the refinement, just as the determined diffusion rate (ϵ) and the irreversible hydrolysis reaction (ϑ).

Chapter 3. USP7 activity mechanism



Supplemental figure 8. The statistical analyses

Supplemental figure 8. Related to Figure 6 and Figure S5; A. The statistical analyses as performed by the FitSpace module of KinTek. The equation constants (left panel) were linked were applicable and labelled (b,c,d or o). The statistical analyses of these constants are depicted in the heat plots (right panel). Constants that are marked with an x were locked during fitting and analysis of USP7 FL. **B.** To calculate steady state parameters from the KinTek fits the depicted formulas are used (top panel). The relationship of the used constants is drawn schematically in the simplified reaction scheme (lower panel). **C.** The same analyses as in A. performed for the TCD construct. **D.** The calculation of steady state parameters for reactions with one intermediate state (lower panel) requires the formulas depicted (top panel).

Chapter 3. USP7 activity mechanism

Chapter 5.
General Discussion

Chapter 5. General Discussion

Ubiquitination, and thereby deubiquitination, plays an important role in virtually every process of the cell. Its dysregulation can therefore have detrimental effects on cell survival. Knowledge on how these processes take place on a molecular level will therefore increase our understanding of the workings of the human cell. Furthermore, it can provide a starting point for drug development to intervene in certain diseases, such as Alzheimer's disease¹ or cancer^{2,3}.

In this thesis we describe the activation mechanisms of the deubiquitinating enzymes (DUB) USP7 and its homologue USP40. The findings pertain not only to these two DUBs, but could represent a general mode of activation for (a subclass of) USP enzymes. Moreover, this activation mechanism indicates a potential window for specific inhibition as the self-activation of these enzymes does not rely on the conserved USP-fold. Insights obtained from the research described in this thesis would help to develop such specific inhibitors and could help in studying other (deubiquitinating) enzymes.

USP7 activation mechanism

In **chapter 2** and **chapter 3** we have investigated the activity of USP7 in great detail. Using protein crystallography we could elucidate a partial structure of the catalytic domain (CD) and the first three Ubiquitin-like (Ubl) domains⁴. This structure on its own did not directly provide insight into the mechanism of action of USP7, but did supply an essential piece to merge the structures solved previously into one full-length model. The full-length model shows how the 7 different domains are arranged spatially.

As is often the case with multi-domain proteins, USP7 requires multiple domains for its full activity. For every separate domain a global function had been described previously, but in chapter three we have tried to identify, quantitatively where possible, the contribution of each domain to the deubiquitinating activity of USP7. For USP7 to reach its full activity, it requires the last two Ubl domains (Ubl45) with the very C-terminal tail⁵. When these are present, both the affinity and processivity for a minimal substrate increase⁶. The K_M improves five-fold, while k_{cat} goes up roughly twenty-fold. Using biochemistry, combined with biophysical techniques like nuclear magnetic resonance (NMR) and surface plasmon resonance (SPR), we were able to tease apart the effect of the Ubl domains and the very C-terminal tail. In a nutshell, the Ubl45 domains can bind the CD, thereby changing its conformation and increasing the affinity for ubiquitin. Once ubiquitin is bound in CD, it will adopt an active state⁷ and now the C-terminal tail can bind, which stabilises the active form, allowing for rapid hydrolysis. This state has been captured in a crystal structure by Rouge et. al.⁸.

For the enzyme to get from the open state to the closed, activated state however, the C-terminal domains will have to curve dramatically. Although such big movements are not unheard of for conformational changes in proteins⁹, it is the first DUB described to have this rearrangement. Interestingly, the second step where the tail binds is heavily dependent on the presence of ubiquitin. Such behaviour is reminiscent of the classic 'induced fit' theorem^{10,11}, where the substrate induces a rearrangement into the active state.

This particular activation mechanism could also have consequences for the design of a potential inhibitor of the enzyme. The ubiquitin/proteasome system (UPS) has been an interesting target for the development of drugs¹², as it is involved in many facets of cell biology. USP7 has received particular interest due to its multifaceted role in the cell (see **chapter 1**) and its name 'guardian of the genome'¹³ due to its interaction with p53 and its E3 ligase¹⁴. The

development of inhibitors for these deubiquitinating enzymes is usually done using activity profiling of various small compounds¹⁵. Promising leads are then combined to create better inhibiting compounds, which are then assessed for specificity against a panel of other DUBs^{16,17}. Quite often this results in compounds that compete with Ub for binding in the active site^{18–20}, as the activity profiling assays are done on a minimal substrate. As we show in **chapter 3**, the additive effect of the realistic target is rather large, so these types of inhibitors would require very tight binding affinities. This could potentially be achieved by adding a TRAF binding motif to the compounds (along the lines of the non-hydrolysable probe in **chapter 3**), but how this would work out for the pharmacokinetics remains to be seen.

The USP7 activation mechanism actually presents a potential to circumvent this problem. As the enzyme relies heavily on the self-activation by the tail, inhibiting this interaction would create a non-competitive inhibitor. Some studies have already yielded such allosteric inhibitors^{21,22} and they resulted in low nanomolar inhibitors. As USP7 plays a role (see **chapter 1**) in many cellular processes however, an USP7 inhibitor will target more pathways than initially anticipated and could result in off-target effects. Hopefully these inhibitors can be further developed to successfully modulate USP7 activity, where it is needed. The current progress of developing non-competitive, allosteric inhibitors is however promising. Targeting the catalytic domain only could yield dual-specific inhibitors, as is illustrated nicely with the cross-reactivity of USP7 and USP47 for various inhibitors¹⁷. Perhaps mimicking the biological target could not only increase the affinity of inhibitors, but also further specify the drugs towards one particular (state of) enzyme.

A new subclass of USPs

Cross-reactivity between close homologs is not unheard of¹⁷ and is not too surprising to find this between USPs. This class of DUBs contains 54 members in humans and all share the same catalytic domain. The catalytic domain on its own often has no specificity towards ubiquitin chains²³. The deubiquitinating specificity of USPs is largely dependent on the accessory domains, which for USPs are present in high numbers and varieties^{24,25}. To further understanding of their influence, each of these domains separately would need to be analysed in context of the CD. As this would present a huge amount of work, it is appealing to postulate some generalities and, based on these, divide the USPs in subclasses.

In this thesis two DUBs with C-terminal Ubl domains have been investigated. USP7, the main player in this thesis, has a quintet of Ubl domains of which the last two, including a twenty-residue tail, enhance its deubiquitinating activity dramatically. As we show in **chapter 4**, USP40 has a similar make-up, with now six Ubl domains in the C-terminal half. And, as with USP7, the latter two, again including a possibly flexible tail, greatly enhance the activity of the USP40 catalytic domain. Such a shared self-activation mechanism would put the two DUBs within the same subclass, from both a functional and structural point of view.

To identify other members of this class one could look at sequence conservation and structural similarities. Unfortunately, sequences of a Ubl domain can vary widely, despite their structural homology^{26,27}. BLAST searches using the final two domains therefore yield very little useable results while searches that use full-length sequences of USP7 or USP40 place emphasis on the catalytic domain. The latter search yielded a list of USPs, with some of them containing a (predicted) Ubl-domain. This limits the potential candidates for the new subclass, although this approach could miss others, due to difficulty in predicting Ubl domains²⁶. More in-depth

Chapter 5. General Discussion

analysis of these USP sequences readily shows three different positions in relation to the catalytic domain, perhaps indicating three different subclasses. Indeed USP4, USP11 and USP15 have previously been grouped together²⁸ as they all share the internal Ubl domain as well as an activation mechanism that involves the N-terminal DUSP-Ubl²⁸. Moving on to the group with C-terminal Ubl domains, we see that USP7 and USP40 are accompanied by USP47 and USP48, and we could propose that these four make up the new subclass of USPs that can get self-activated through their C-terminal Ubl domain.

For USP40 this activation has been shown in **chapter 4**, while for USP7 the self-activation has been described by us and others^{5,6,8}. The role of Ubl domains in USP47 and USP48 require experimental validation. Although USP47 has been produced and tested *in vitro* no in-depth activation experiments have been performed²⁹. For USP48 a thorough assessment of its activity on histone H2A was done³⁰. This study not only unearthed its target preference, it also indicated that for full activity it requires the putative Ubl domain located near its C-terminus. This reduction in activity upon omission of the Ubl domain is reminiscent of the requirement of Ubl45 in USP7 self-activation and could imply that USP48 follow a similar activation mechanism.

One other requirement for the activation mechanism as presented for USP7 however, is the presence of a 'switching loop' in the catalytic domain. This 'switching loop' acts through a rearrangement of aromatic residues⁶, but whether there are e.g. obligate tryptophan positions in this loop is not yet known. Alignment of all USP domains revealed that USP48 lacks a loop altogether in this place, but both USP40 and USP47 contain an aromatic motif like USP7³¹. This would suggest that, although only three members large, this subset of USPs activate itself in a similar way. Such a conserved mechanism would not only be interesting from an evolutionary point of view; if it is indeed conserved, the findings described in this thesis could help investigations on these DUBs as well.

External USP modulators

The conservation within this subclass is not limited to the C-terminal Ubl-domain and the proposed activation mechanism. All group members have a series of duplicated domains between the catalytic domain and the activating Ubl. For USP7, USP47 and USP40 these Ubl domains are sometimes grouped per two and can mediate protein-protein interactions: the interactions of Ubl123 of USP7 have been described in **chapter 1**. The presence of these domains between CD and the activation domain prompts to speculate about the effect on DUB activity upon binding an interactor.

Unfortunately binders in this region have only been described for USP7. And although many have been found, very few have been investigated for *in vitro* activity modulation. GMPS³² is the one exception and for this protein an activity-enhancing effect on USP7 has been observed⁶. The proposed mechanism for this hyper-activation revolves around the active conformation of USP7 and its stabilisation by GMPS through the intermediate Ubl domains. Thus far no co-crystal structure of this complex has been solved so how GMPS would keep USP7 in the active, bend form remains unknown thus far. Other binders of Ubl123 however have been solved and especially the viral protein ICP0 seems to create a bend within the Ubl domains³³. This could indicate an activating role for the protein, but no studies on this have been published. Another co-crystal structure, the one with DNMT1³⁴, shows an extended

form of the five Ubl domains, suggesting the opposite effect, but whether DNMT1 inhibits USP7 activity is yet to be uncovered.

The list of USP7 Ubl123 interactors is long, and for some hits a function could already be implied. Secondary proteins can use the interaction to recruit USP7 to a complex or site of interest. For example, UHRF1 can recruit USP7 to protect the DNA methylation maintenance complex from getting ubiquitinated and degraded^{35,36}. Such recruitment, or scaffolding, would not necessarily influence the activity, but does localise the DUB to a place in need. Finding such interactors for the other members of the subclass would therefore not only be interesting from a mechanistic point of view, but could shed some light on the biology of these, fairly unstudied, USPs. Thus far USP40 or USP47 have only been marginally implied in certain pathways and their biological target has yet to be discovered.

USP target specificity

As we have discussed in **chapter 3**, next to the internal (and external) domains, the actual target of the USP plays a big role in DUB activity. USP21 for instance readily cleaves most ubiquitin linkages³⁷ except K6-linked ubiquitin chains, as these chains sterically hinder the catalytic domain³⁸. For USP40 we see a similar behaviour, but now with K27 chains. The inability of the enzyme to cleave K27 diubiquitins could rise from a similar steric hindrance or from binding the ubiquitin with the free carboxyterminus. A structure of USP40CD alone or in complex with K27 diubiquitin would definitely help to gain insight. Not being able to process a certain ubiquitin chain could also have implications on a biological level. Thus far K27 chains have not been studied that extensively, but one can imagine K27 linkages serving as a protective cap, not allowing USP40 to digest the preceding chain.

In **chapter 3** we have looked at the contribution of a target on USP7 activity. We showed that, independent from the activating tail the recognised p53 sequence can enhance the activity roughly four hundred-fold, and roughly fifteen-fold in the full-length setting. These data give good insight to how deubiquitination specificity is obtained: under normal circumstances the DUB has moderate activity, but is able to increase it when the ubiquitinated target is present. This not only is an elegant way of target-regulated DUB activity, it opens up this specific DUB activity to regulation. By e.g. phosphorylation of either the TRAF recognition motif on p53 or the TRAF domain itself the activation effect can be diminished and USP7 remains a moderately active DUB. This type of DUB regulation might make the USP7-MDM2-p53 switch act when necessary.

Investigations into DUB mechanisms, or enzymes in general, might benefit greatly from using more realistic substrates in the assays. Finding the proper substrate and eventually generating derivatives that allow for biophysical examination from this substrate however can be a rather daunting task. For the case described in **chapter 3** both the binding and ubiquitination sites of p53 were previously determined, which allowed the chemists to generate the realistic substrate tools to study USP7. These studies can generate more biological insight as one mimics physiological circumstances. Studying USP mechanisms using more realistic substrates, alongside a minimal one, gives more information about the intrinsic regulation and can open new therapeutic avenues.

Chapter 5. General Discussion

References

- [1] Ristic, G., Tsou, W.-L. and Todi, S. V. An optimal ubiquitin-proteasome pathway in the nervous system: the role of deubiquitinating enzymes. *Frontiers in Molecular Neuroscience* **7** 2014, 72. <https://doi.org/10.3389/fnmol.2014.00072>
- [2] Ding, F., Xiao, H., Wang, M., Xie, X. and Hu, F. The role of the ubiquitin-proteasome pathway in cancer development and treatment. *Frontiers in Bioscience (Landmark Edition)* **19** 2014, 886–95.
- [3] Liu, J., Shaik, S., Dai, X., Wu, Q., Zhou, X., Wang, Z. and Wei, W. Targeting the ubiquitin pathway for cancer treatment. *Biochimica et Biophysica Acta (BBA) - Reviews on Cancer* **1855** 2015, 50–60. <https://doi.org/10.1016/j.bbcan.2014.11.005>
- [4] Kim, R.Q., van Dijk, W.J. and Sixma, T.K. Structure of USP7 catalytic domain and three Ubl-domains reveals a connector α -helix with regulatory role. *Journal of Structural Biology* **195** 2016, 11–8. <https://doi.org/10.1016/j.jsb.2016.05.005>
- [5] Fernández-Montalván, A., Bouwmeester, T., Joberty, G., Mader, R., Mahnke, M., Pierrat, B., Schlaeppi, J.-M., Worpenberg, S. and Gerhartz, B. Biochemical characterization of USP7 reveals post-translational modification sites and structural requirements for substrate processing and subcellular localization. *The FEBS Journal* **274** 2007, 4256–70. <https://doi.org/10.1111/j.1742-4658.2007.05952.x>
- [6] Faesen, A.C., Dirac, A.M.G., Shanmugham, A., Ovaa, H., Perrakis, A. and Sixma, T.K. Mechanism of USP7/HAUSP activation by its C-terminal ubiquitin-like domain and allosteric regulation by GMP-synthetase. *Molecular Cell* Elsevier Inc. **44** 2011, 147–59. <https://doi.org/10.1016/j.molcel.2011.06.034>
- [7] Hu, M., Li, P., Li, M., Li, W., Yao, T., Wu, J.-W., Gu, W., Cohen, R.E. and Shi, Y. Crystal Structure of a UBP-Family Deubiquitinating Enzyme in Isolation and in Complex with Ubiquitin Aldehyde. *Cell* **111** 2002, 1041–54. [https://doi.org/10.1016/S0092-8674\(02\)01199-6](https://doi.org/10.1016/S0092-8674(02)01199-6)
- [8] Rougé, L., Bainbridge, T.W., Kwok, M., Tong, R., Di Lello, P., Wertz, I.E., Maurer, T., Ernst, J.A. and Murray, J. Molecular Understanding of USP7 Substrate Recognition and C-Terminal Activation. *Structure* **24** 2016, 1335–45. <https://doi.org/10.1016/j.str.2016.05.020>
- [9] Rehmann, H., Arias-Palomo, E., Hadders, M.A., Schwede, F., Llorca, O. and Bos, J.L. Structure of Epac2 in complex with a cyclic AMP analogue and RAP1B. *Nature* **455** 2008, 124–7. <https://doi.org/10.1038/nature07187>
- [10] Koshland, D.E. Correlation of Structure and Function in Enzyme Action. *Science* **142** 1963, 1533–41. <https://doi.org/10.1126/science.142.3599.1533>
- [11] Koshland, D.E. The Key–Lock Theory and the Induced Fit Theory. *Angewandte Chemie International Edition in English* **33** 1995, 2375–8. <https://doi.org/10.1002/anie.199423751>
- [12] Bedford, L., Lowe, J., Dick, L.R., Mayer, R.J. and Brownell, J.E. Ubiquitin-like protein conjugation and the ubiquitin-proteasome system as drug targets. *Nature Reviews Drug Discovery* **10** 2011, 29–46. <https://doi.org/10.1038/nrd3321>
- [13] Zhang, W. and Sidhu, S.S. Drug development: Allosteric inhibitors hit USP7 hard. *Nature Chemical Biology* Nature Publishing Group. **14** 2018, 110–1. <https://doi.org/10.1038/nchembio.2557>
- [14] Tavana, O. and Gu, W. Modulation of the p53/MDM2 interplay by HAUSP inhibitors. *Journal of Molecular Cell Biology* Oxford University Press. **9** 2017, 45–52. <https://doi.org/10.1093/jmcb/mjw049>
- [15] Reverdy, C., Conrath, S., Lopez, R., Planquette, C., Atmanene, C., Collura, V., Harpon, J., Battaglia, V., Vivat, V., Sippl, W. and Colland, F. Discovery of specific inhibitors of human USP7/HAUSP deubiquitinating enzyme. *Chemistry & Biology* **19** 2012, 467–77. <https://doi.org/10.1016/j.chembiol.2012.02.007>
- [16] Altun, M., Kramer, H.B., Willems, L.I., McDermott, J.L., Leach, C.A., Goldenberg, S.J., Kumar, K.G.S.G.S., Konietzny, R., Fischer, R., Kogan, E., Mackeen, M.M., McGouran, J., Khoronenkova, S. V., Parsons, J.L., Dianov, G.L., Nicholson, B. and Kessler, B.M. Activity-based chemical proteomics accelerates inhibitor development for deubiquitylating enzymes. *Chemistry & Biology* **18** 2011, 1401–12. <https://doi.org/10.1016/j.chembiol.2011.08.018>
- [17] Weinstock, J., Wu, J., Cao, P., Kingsbury, W.D., McDermott, J.L., Kodrasov, M.P., McKelvey, D.M., Suresh Kumar, K.G., Goldenberg, S.J., Mattern, M.R. and Nicholson, B. Selective Dual Inhibitors of the Cancer-Related Deubiquitylating Proteases USP7 and USP47. *ACS Medicinal Chemistry Letters* **3** 2012, 789–92. <https://doi.org/10.1021/ml200276j>
- [18] Ernst, A., Avvakumov, G., Tong, J., Fan, Y., Zhao, Y., Alberts, P., Persaud, A., Walker, J.R., Neculai, A.-M., Neculai, D., Vorobyov, A., Garg, P., Beatty, L., Chan, P.-K., Juang, Y.-C., Landry, M.-C., Yeh, C., Zehiraj, E., Karamboulas, K. et al. A Strategy for Modulation of Enzymes in the Ubiquitin System. *Science (New York, NY)* **339** 2013, 590–5. <https://doi.org/10.1126/science.1230161>

- [19] Kategaya, L., Di Lello, P., Rougé, L., Pastor, R., Clark, K.R., Drummond, J., Kleinheinz, T., Lin, E., Upton, J.-P., Prakash, S., Heideker, J., McClelland, M., Ritorto, M.S., Alessi, D.R., Trost, M., Bainbridge, T.W., Kwok, M.C.M., Ma, T.P., Stiffler, Z. et al. USP7 small-molecule inhibitors interfere with ubiquitin binding. *Nature* Nature Publishing Group. **550** 2017, 534–8. <https://doi.org/10.1038/nature24006>
- [20] Pozhidaeva, A., Valles, G., Wang, F., Wu, J., Sterner, D.E., Nguyen, P., Weinstock, J., Kumar, K.G.S., Kanyo, J., Wright, D. and Bezsonova, I. USP7-Specific Inhibitors Target and Modify the Enzyme's Active Site via Distinct Chemical Mechanisms. *Cell Chemical Biology* Cell Press. **24** 2017, 1501–1512.e5. <https://doi.org/10.1016/j.CHEMBIOL.2017.09.004>
- [21] Gavory, G., O'Dowd, C.R., Helm, M.D., Flasz, J., Arkoudis, E., Dossang, A., Hughes, C., Cassidy, E., McClelland, K., Odrzywol, E., Page, N., Barker, O., Miel, H. and Harrison, T. Discovery and characterization of highly potent and selective allosteric USP7 inhibitors. *Nature Chemical Biology* Nature Publishing Group. **14** 2017, 118–25. <https://doi.org/10.1038/nchembio.2528>
- [22] Turnbull, A.P., Ioannidis, S., Krajewski, W.W., Pinto-Fernandez, A., Heride, C., Martin, A.C.L., Tonkin, L.M., Townsend, E.C., Buker, S.M., Lancia, D.R., Caravella, J.A., Toms, A. V, Charlton, T.M., Lahdenranta, J., Wilker, E., Follows, B.C., Evans, N.J., Stead, L., Alli, C. et al. Molecular basis of USP7 inhibition by selective small-molecule inhibitors. *Nature* **550** 2017, 481–6. <https://doi.org/10.1038/nature24451>
- [23] Luna-Vargas, M.P. a, Faesen, A.C., van Dijk, W.J., Rape, M., Fish, A. and Sixma, T.K. Ubiquitin-specific protease 4 is inhibited by its ubiquitin-like domain. *EMBO Reports* Nature Publishing Group. **12** 2011, 365–72. <https://doi.org/10.1038/embor.2011.33>
- [24] Komander, D. Mechanism, specificity and structure of the deubiquitinases. *Sub-Cellular Biochemistry* **54** 2010, 69–87. https://doi.org/10.1007/978-1-4419-6676-6_6
- [25] Mevissen, T.E.T. and Komander, D. Mechanisms of Deubiquitinase Specificity and Regulation. *Annual Review of Biochemistry* **86** 2017, 159–92. <https://doi.org/10.1146/annurev-biochem-061516-044916>
- [26] Zhu, X., Ménard, R. and Sulea, T. High incidence of ubiquitin-like domains in human ubiquitin-specific proteases. *Proteins: Structure, Function, and Bioinformatics* **69** 2007, 1–7. <https://doi.org/10.1002/prot.21546>
- [27] Harrison, J.S., Jacobs, T.M., Houlihan, K., Van Doorslaer, K. and Kuhlman, B. UbSRD: The Ubiquitin Structural Relational Database. *Journal of Molecular Biology* **428** 2016, 679–87. <https://doi.org/10.1016/j.jmb.2015.09.011>
- [28] Clerici, M., Luna-Vargas, M.P.A., Faesen, A.C. and Sixma, T.K. The DUSP–Ubl domain of USP4 enhances its catalytic efficiency by promoting ubiquitin exchange. *Nature Communications* **5** 2014, 5399. <https://doi.org/10.1038/ncomms6399>
- [29] Piao, J., Tashiro, A., Nishikawa, M., Aoki, Y., Moriyoshi, E., Hattori, A. and Kakeya, H. Expression, purification and enzymatic characterization of a recombinant human ubiquitin-specific protease 47. *Journal of Biochemistry* 2015,. <https://doi.org/10.1093/jb/mvv063>
- [30] Uckelmann, M., Densham, R.M., Baas, R., Winterwerp, H.H.K., Fish, A., Sixma, T.K. and Morris, J.R. USP48 restrains resection by site-specific cleavage of the BRCA1 ubiquitin mark from H2A. *Nature Communications* Nature Publishing Group. **9** 2018, 229. <https://doi.org/10.1038/s41467-017-02653-3>
- [31] Ye, Y., Scheel, H., Hofmann, K. and Komander, D. Dissection of USP catalytic domains reveals five common insertion points. *Molecular BioSystems* The Royal Society of Chemistry. **5** 2009, 1797–808. <https://doi.org/10.1039/b907669g>
- [32] van der Knaap, J.A., Kozhevnikova, E., Langenberg, K., Moshkin, Y.M. and Verrijzer, C.P. Biosynthetic enzyme GMP synthetase cooperates with ubiquitin-specific protease 7 in transcriptional regulation of ecdysteroid target genes. *Molecular and Cellular Biology* **30** 2010, 736–44. <https://doi.org/10.1128/MCB.01121-09>
- [33] Pföh, R., Lacdao, I.K., Georges, A.A., Capar, A., Zheng, H., Frappier, L. and Saridakis, V. Crystal Structure of USP7 Ubiquitin-like Domains with an ICP0 Peptide Reveals a Novel Mechanism Used by Viral and Cellular Proteins to Target USP7. *PLoS Pathogens* **11** 2015, e1004950. <https://doi.org/10.1371/journal.ppat.1004950>
- [34] Cheng, J., Yang, H., Fang, J., Ma, L., Gong, R., Wang, P., Li, Z. and Xu, Y. Molecular mechanism for USP7-mediated DNMT1 stabilization by acetylation. *Nature Communications* **6** 2015, 7023. <https://doi.org/10.1038/ncomms8023>

Chapter 5. General Discussion

- [35] Felle, M., Joppien, S., Németh, A., Diermeier, S., Thalhammer, V., Dobner, T., Kremmer, E., Kappler, R., Längst, G., Nemeth, A., Diermeier, S., Thalhammer, V., Dobner, T., Kremmer, E., Kappler, R. and Langst, G. The USP7/Dnmt1 complex stimulates the DNA methylation activity of Dnmt1 and regulates the stability of UHRF1. *Nucleic Acids Research* **39** 2011, 8355–65. <https://doi.org/10.1093/nar/gkr528>
- [36] Zhang, Z.-M., Rothbart, S.B., Allison, D.F., Cai, Q., Harrison, J.S., Li, L., Wang, Y., Strahl, B.D., Wang, G.G. and Song, J. An Allosteric Interaction Links USP7 to Deubiquitination and Chromatin Targeting of UHRF1. *Cell Reports* **12** 2015, 1400–6. <https://doi.org/10.1016/j.celrep.2015.07.046>
- [37] Ye, Y., Akutsu, M., Reyes-Turcu, F., Enchev, R.I., Wilkinson, K.D. and Komander, D. Polyubiquitin binding and cross-reactivity in the USP domain deubiquitinase USP21. *EMBO Reports* **12** 2011, 350–7. <https://doi.org/10.1038/embor.2011.17>
- [38] Hospenthal, M.K., Freund, S.M. V and Komander, D. Assembly, analysis and architecture of atypical ubiquitin chains. *Nature Structural & Molecular Biology* **20** 2013, 555–65. <https://doi.org/10.1038/nsmb.2547>

Addendum.

- A. *Summary***
- B. *Samenvatting***
- C. *Stellingen***
- D. *Curriculum Vitae***
- E. *PhD Portfolio***
- F. *List of Publications***
- G. *Acknowledgements***

Addendum. A. Summary

A. Summary

The human cell contains a lot of different proteins that need to collaborate to keep the cell healthy and in working order. In order to facilitate these collaborations and make changes to the way the proteins interact, the cell employs modifications such as ubiquitination. This attachment of a ubiquitin molecule can change the function of the protein after cellular events like damage on the DNA or send the signal that the protein is no longer required and needs to be degraded. As ubiquitination is involved in many cellular signals, its dysfunction can have adverse effects and lead to diseases.

To keep the system in balance, the ubiquitin modification can also be taken off, by so-called deubiquitinating enzymes (DUBs). As these enzymes exert control over the ubiquitination pathway through countering the ubiquitination state of targeted proteins, they can potentially be used for human intervention. By selectively inhibiting DUBs one could potentially battle diseases such as cancer. To acquire proper inhibitory drugs however, knowledge of the mechanistic workings of these enzymes is a key requirement.

In this thesis we investigated the molecular mechanism of a subset of USPs (Ubiquitin-Specific Proteases), a class of DUBs. Our findings describe how USP7, one of the subset members, can get activated by its biological target, sketching a role for its biological partner proteins. Furthermore, we describe on a molecular level how the domain structure of USP7, but also the paralogue USP40, aids in the intrinsic activity by activating the enzyme. We show that this self-activation is a conserved mechanism, yielding valuable information for the development of inhibitory molecules, but altogether also providing insight into the biological workings and role of these USP enzymes.

Review on USP7 regulation

USP7 interacts with a plethora of proteins, some of them targets of the enzyme, others interactors with a potential to modulate the enzyme activity. In chapter 1 we review the activation mechanism of USP7 (in-depth investigated in chapter 3) and describe a comprehensive list of validated USP7-interacting proteins. These interactions can link USP7 to various cellular pathways, but also represent a potential for regulating its activity, through e.g. recruiting USP7 to a specific site or affecting the intrinsic deubiquitination speed. We describe that, next to the activating GMPS protein, DNMT1 could have an effect on USP7 activity as both bind on the C-terminal part of USP7, possibly affecting the activating domain. Another striking find is the abundance of E3 ubiquitin ligases that have been reported to interact with USP7. As these proteins are responsible for the last step in the attachment of a ubiquitin onto a target protein, the co-occurrence with a DUB seems counterintuitive at first. However, the presence of one unit that can both add and remove ubiquitin would allow for quick switching between two states of the target protein. A good example is p53, a protein that can trigger cell apoptosis, which gets ubiquitinated by MDM2 and deubiquitinated by USP7. With MDM2, USP7 and p53 existing in a complex, the cell can quickly switch between the ubiquitinated or unubiquitinated state of p53 and thereby decide upon cell death or survival. If one understands this switch better and were able to modulate it explicitly in cancer cells, this would be a great step forward for cancer treatments.

Structure of USP7

Important information in the development of drugs often comes from acquired crystal structures. As such there have been many attempts to crystallise USP7, unfortunately only resulting in partial structures. We were able to crystallise a construct of USP7 that allowed to 'merge' the available structures of USP7 into a full-length model, painting a picture of what USP7 could look like.

Furthermore, this structure exposed a very long α -helical linker between the catalytic domain and the activating Ubl domains. We could show that this linker is important to obtain proper interaction in ubiquitin hydrolysis between the catalytic domain and the activating one.

Mechanism of USP7

This activation mechanism is one topic in chapter 3, where we looked into the self-activation of USP7 with molecular detail. USP7 has a domain architecture in which the catalytic domain, where the actual hydrolysis happens, is flanked by a TRAF domain at the N-terminus and five Ubiquitin-like (Ubl) domains at the C-terminus. The last two of these, including a flexible tail at the very C-terminal, are required in the self-activation of USP7.

Using biochemistry, NMR and biophysical methods we showed how the Ubl domain affect the catalytic activity in two distinct steps. The Ubl domains themselves, without the tail, interact with the catalytic domain and thereby increase its affinity for ubiquitin. When the catalytic domain, which normally has an unproductive conformation, binds ubiquitin, it rearranges and thereby changes the interaction with the activating Ubl45 domain. Instead of the Ubl domains, now the C-terminal tail plays the main role, it can bind the rearranged catalytic domain and stabilise this catalytically competent state. This stabilisation results in an increase in rate, overall resulting in faster hydrolysis of the ubiquitin bond. This self-activation mechanism makes the full-length protein a hundred-fold more active than the catalytic domain only.

Influence of a substrate

The domain at the N-terminus, the TRAF domain, can also play a role in the activity of the enzyme. This domain is required for the interaction with ubiquitinated proteins and in chapter 3 we can confirm this using the model substrate p53. We also show that this particular interaction also aids in the processing of the substrate, by making use of novel chemical tools and computational modelling of acquired biophysical data. Overall the activity on the p53 substrate is fifteen-fold higher, than the activity observed for the minimal substrate that is often used in these DUB studies. As these more realistic substrates represent biology much better, their usage could give more insight in the enzyme mechanisms.

A

Addendum. A. Summary

USP40 has a similar mechanism

For USP40, a close paralogue of USP7, however we mainly used the aforementioned minimal substrate, as for this DUB no targets are currently known. We used a bioinformatics approach, backed up with biochemistry and biophysical assays to confirm that USP40 shares the same activation mechanism as USP7. It uses its last two Ubl domains (Ubl56 in this case) and the flexible C-terminal tail to increase the affinity for ubiquitin and the rate of hydrolysis. Whilst it shares a lot with USP7, USP40 differs on certain aspects. The inability to efficiently cleave K27-linked diubiquitin might perhaps be the most interesting point. We show that this substrate competes with minimal ubiquitin substrate and can inhibit USP40. This inhibitory mechanism could be of interest to those studying K27 chains and our research lays the groundwork for a better understanding of the K27-DUB interaction.

B. Samenvatting

De menselijke cel is een complex systeem, duizenden verschillende eiwitten moeten nauw samenwerken om alles draaiende te houden. Eiwitten, en de processen waar ze bij betrokken zijn, zijn streng gereguleerd, alles moet op het juiste moment en de juiste plaats gebeuren om de cel gezond te houden. Om de werking, locatie of concentratie van specifieke eiwitten te beïnvloeden maakt de cel gebruik van labels, ook wel post translationele modificaties genoemd. Eén zo'n modificatie is ubiquitinatie, waarbij het kleine eiwit ubiquitine als label wordt vastgemaakt. Het ubiquitine label heeft een aantal verschillende functies, die afhangen van waar, hoe en hoeveel van het label is vastgemaakt. Ubiquitinatie kan worden gebruikt als signaal dat een eiwit moet worden afgebroken, het kan eiwitten activeren of juist deactiveren, eiwit-eiwit interacties versterken of juist verbreken of zorgen dat een gelabeld eiwit naar een bepaalde plaats in de cel wordt gestuurd, bijvoorbeeld naar het DNA als daar een beschadiging is opgetreden. Al deze regulatie is van cruciaal belang om de processen in de cel goed te laten verlopen, een probleem met ubiquitinatie kan desastreuze gevolgen hebben voor de cel en zelfs leiden tot het ontstaan van kanker.

Voor de juiste regulering van deze processen is het niet alleen belangrijk dat het ubiquitine label aan eiwitten kan worden vastgemaakt, maar ook dat het op specifieke momenten weer verwijderd kan worden. Het verwijderen van ubiquitine wordt uitgevoerd door deubiquitinerende enzymen (DUBs). Door het tegengaan van het ubiquitinesignaal oefenen deze enzymen controle uit over het lot van de eiwitten die ze deubiquitineren. Als deze gebalanceerde ubiquitinesignalering misgaat kan dat ziektes veroorzaken zoals kanker of Alzheimer. DUBs zijn daardoor een interessant doelwit voor medicijnen tegen deze ziektes. Gedetailleerde kennis van de structuur en het werkingsmechanisme van deze DUBs komt erg van pas bij de ontwikkeling van specifieke en effectieve enzymremmers.

In dit proefschrift hebben we gekeken naar het moleculaire mechanisme van twee deubiquitinerende enzymen uit de klasse van de Ubiquitine-Specifieke Proteases (USPs). Door middel van biochemische en structuurbiologische experimenten achterhalen we het mechanisme van USP7 en USP40. In deze thesis worden de stappen van het enzymatische mechanisme beschreven, identificeren we welke residuen essentieel zijn en vinden we een activerende rol voor het C-terminale gedeelte van het enzym. Hiermee wordt een moleculaire basis gelegd voor enzymremmers voor USPs.

De cellulaire rol van USP7

Het mechanisme achter de enzymatische activiteit van het deubiquitinerende enzym USP7 is het hoofdthema van dit proefschrift. USP7 speelt een rol in veel verschillende processen in de cel en is een onderdeel van uiteenlopende signaleringscascades. De bekendste rol van USP7 is de deubiquitinatie van p53, een tumor suppressie eiwit, dat door deubiquitinatie wordt gespaard van degradatie en daardoor celdood kan induceren. Het enzym is hierdoor onmisbaar voor de ontwikkeling van cellen en een slecht functionerend USP7 kan leiden tot neurologische defecten zoals autisme en ontwikkelingsstoornissen. Daarbovenop speelt USP7 ook een rol bij het herkennen en repareren van schade aan het DNA. Het enzym heeft dan ook interacties met een groot aantal andere eiwitten. Sommige van deze eiwitten zijn

A

Addendum. B. Samenvatting

een doeleiwit van USP7 en worden door USP7 gedeubiquitineerd. Anderen kunnen juist de activiteit van USP7 beïnvloeden of werken samen met USP7. In hoofdstuk 1 geven we een overzicht van de eiwitinteracties die USP7 maakt en gaan we in op de mogelijke effecten van deze interacties op de activiteit van USP7.

Kristalstructuur van USP7

Zoals hiervoor al besproken is het deubiquitinerende enzym USP7 een interessant doelwit voor het ontwikkelen voor medicijnen. Kennis van de moleculaire structuur van USP7 kan daarbij een grote rol spelen, er zijn daarom al veel pogingen gedaan om de structuur van USP7 op te lossen. Tot nu toe zijn er echter alleen gedeeltelijke structuren beschikbaar waarin slecht enkele domeinen te zien zijn.

USP7 bestaat uit zeven domeinen (zie Figuur 1 van Hoofdstuk 1): een TRAF-domein, waarmee (geubiquitineerde) doeleiwitten worden herkend, een katalytisch domein, waarin de hydrolyse van de ubiquitinebinding plaatsvindt, vijf ubiquitine-achtige (Ubl) domeinen en een flexibele staart aan de C-terminus. Vooral de laatste twee Ubl domeinen (Ubl45), inclusief de flexibele staart, zijn erg belangrijk voor de activatie van USP7.

In hoofdstuk 2 presenteren wij de structuur van het katalytisch domein en de eerste drie Ubl-domeinen van USP7. Hoewel dit weer een gedeeltelijke structuur betreft, is onze structuur zeer waardevol voor het begrijpen van de structuur van het hele eiwit. Onze structuur vormt namelijk een brug tussen de eerder gepubliceerde structuren, waardoor hij gebruikt kan worden om de losse structuren aan elkaar te koppelen en een model te maken van heel USP7 (Hoofdstuk 1 Figuur 1). Bovendien laat onze structuur een lange α -helix zien tussen het katalytische domein (CD) en de activerende, ubiquitine-achtige (Ubl) domeinen. Deze linker is van belang om het activerende domein op de juiste plek te brengen ten opzichte van het CD en beïnvloedt daarmee de activiteit van USP7.

Activatie van USP7

Naast het ophelderen van de structuur hebben we gekeken naar het katalytische mechanisme van USP7 en de functies van de verschillende domeinen. De essentiële stap van het katalytische mechanisme van USP7 is de activatie. USP7 is in staat tot zelfactivatie, een proces waarbij verschillende delen van het eiwit betrokken zijn. Met biochemische experimenten hebben wij aangetoond dat het katalytisch domein op zichzelf niet heel erg actief is; het verwijderen van ubiquitine van een modelsubstraat gaat zeer langzaam. Als de laatste twee Ubl domeinen en de flexibele staart (Ubl45) aanwezig zijn, wordt deze activiteit ruim honderd keer verhoogd. In hoofdstuk 3 laten wij met behulp van NMR en biofysische methoden zien dat Ubl45 het katalytisch domein in drie stappen activeert. Allereerst hebben de Ubl domeinen, maar niet de staart, een interactie met het katalytisch domein, waardoor de affiniteit voor ubiquitine wordt verhoogd. De volgende stap is de binding van ubiquitine, dit zorgt voor een conformatieverandering in het katalytisch domein. Deze conformatieverandering verhoogt de affiniteit van het katalytisch domein voor de flexibele staart van Ubl45. De derde stap is de binding van de flexibele staart. Deze binding stabiliseert de actieve conformatie van het katalytisch domein, waardoor het volledige eiwit zo'n honderd keer actiever is dan het katalytische domein alleen.

De invloed van het substraat op de enzymactiviteit

Naast de Ubl-domeinen, die een rol spelen in de zelfactivatie, en het katalytisch domein, heeft USP7 ook nog een TRAF-domein. Dit domein is verantwoordelijk voor de interactie met doeleiwitten en is daardoor belangrijk voor de activiteit bij natuurlijke substraten. In hoofdstuk 3 onderzoeken we hoe de interactie van het TRAF-domein met p53, een doeleiwit van USP7, de activiteit van USP7 beïnvloedt.

Om dit te bestuderen hebben we met innovatieve synthetische technieken een modelsubstraat van geubiquitineerd p53 gemaakt. Door een deel van dit natuurlijke doeleiwit chemisch na te maken verkregen we een homogeen substraat waar makkelijker studies aan gedaan kunnen worden. Met dit realistische modelsubstraat hebben we vervolgens de activiteit geanalyseerd van verschillende combinaties van USP7 domeinen. Door deze opgedane biofysische data te modelleren kregen we vervolgens informatie over de invloed van de verschillende domeinen en tonen we aan dat het TRAF-domein essentieel is voor de herkenning van doeleiwit p53. Bovendien ontdekten we dat de activiteit van USP7 grofweg vijftien keer hoger is door de betere herkenning en binding van het substraat is wanneer we de p53 herkenningssequentie gebruiken in het modelsubstraat.

USP40 en USP7 delen het activatiemechanisme

USP40 is een deubiquitinerend enzym uit dezelfde eiwitfamilie als USP7. Over USP40 is echter een stuk minder bekend in de literatuur. Zo is bijvoorbeeld niet bekend wat de natuurlijke doeleiwitten zijn voor USP40. Om toch onderzoek te kunnen doen naar de activiteit van USP40 en het werkingsmechanisme te kunnen bestuderen hebben we gebruik gemaakt van een modelsubstraat zonder een herkenningssequentie van een doeleiwit. Met dit substraat konden we verschillende USP40 domeinen en combinaties daarvan testen op deubiquitinatieactiviteit. De resultaten hiervan, tezamen met onze bioinformaticastudie leidden tot de conclusie dat USP40 een vergelijkbaar activatiemechanisme heeft als USP7. Ook bij USP40 vinden we dat de laatste twee Ubl-domeinen en de flexibele C-terminus essentieel zijn voor de volledige activiteit van het enzym. Ook konden we, aan de hand van de conservatie ten opzichte van USP7, de essentiële residuen identificeren.

Met deze kennis hebben we ook gekeken naar de specificiteit van USP40 ten opzichte van verschillende types ubiquitineketens. Hieruit blijkt dat USP40, in tegenstelling tot USP7, maar moeilijk K27 ketens knipt en dat deze ketens zelfs een inhiberend effect hebben. Onze resultaten laten zien dat USP7 en USP40 volgens hetzelfde mechanisme werken, maar dat ze toch verschillen in katalytische specificiteit.

Addendum. C. Stellingen

C. Stellingen

1. USP7 activiteit kan worden beïnvloed door al zijn domeinen. (dit proefschrift)
2. Het TRAF domein van USP7 is van belang voor de herkenning van het doeleiwit, maar beïnvloedt daarmee ook de enzymatische activiteit. (dit proefschrift)
3. De zelf-activatie van een USP domein door een peptide aan de C-terminus is een algemeen principe voor een subgroep van USP enzymen. (dit proefschrift)
4. Door het bestuderen van USP7 activiteit op verschillende, realistische, biologisch relevante substraten kan achterhaald worden hoe USP7 in de cel functioneert. (dit proefschrift)
5. Het modelleren van experimentele data helpt enorm om verschillende datasoorten kwantitatief te combineren en daarmee mechanismestappen te deconvolueren. (dit proefschrift)
6. “Volledige kennis van iets veronderstelt ook de kennis van zijn oorzaak.” (Baruch Spinoza)
7. De biochemie zou enorm geholpen zijn met het standardiseren van eiwitnamen en het uitbannen van alternatieve benamingen.
8. De huidige (bio)fysische en (bio)chemische technieken complementeren elkaar en enkel door meerdere methoden te gebruiken kan een werkingsmechanisme worden ontrafeld.
9. Het bestuderen van gerelateerde, maar biologisch minder interessante, eiwitten kan waardevolle informatie opleveren voor het relevantere doeleiwit, en de biologie in het algemeen.
10. Als domeinen in een eiwit wel samenwerken om een activatiemechanisme te vormen, waarom competeert men dan om dit te begrijpen?
11. “Als je ouder wordt, wordt je velletje dunner maar je huid dikker” (Pim van Dijk; 06-05-2013)

D. Curriculum Vitae

Robbert Kim was born October 10th, 1987, in Wageningen, The Netherlands. In 2005 he graduated from the Dorenweerd College, Doorwerth and started his chemistry studies at Utrecht University.

During his Bachelor's degree he performed internships at various groups, ranging the Physical and Colloid Chemistry group of prof. dr. Willem Kegel to the Crystal and Structural Chemistry group of Eric Huizinga. He finished his bachelor's degree in 2010 with a research thesis at the Membrane Biochemistry and Biophysics group of Eefjan Breukink. He continued his studies in Utrecht with a MSc in Molecular and Cellular Life Sciences. As part of this degree he performed a seven-month research internship on structural enzymology of futasosine hydrolase under the supervision of prof. dr. Gideon Davis in the York Structural Biology Laboratory at the University of York. Robbert received his master's degree in 2012.

In the same year, Robbert started his PhD research at the Netherlands Cancer Institute (NKI), in the group of prof. dr. Titia Sixma, on the structure and mechanism of deubiquitinating enzymes USP7 and USP40. The primary results of this research are described in this thesis. After his PhD, Robbert continued as a post-doc in the group of prof. Huib Ovaa, setting up a centre for protein expression, purification and characterisation.

Addendum. E. PhD Portfolio

E. PhD Portfolio

Name of the PhD student:	Robbert Kim
Erasmus MC Department:	Genetics
Graduate School:	Onderzoeksschool Oncologie Amsterdam
PhD period:	2012-2018
Promotor:	Prof. dr. Titia K. Sixma

1. PhD Training Courses

11-15 Apr 2016	INSTRUCT Practical course: Advanced methods for the integration of diverse structural data with NMR data, Utrecht, the Netherlands
Nov 2014	Writing and presenting in biomedicine, OOA, Amsterdam
7-11 Apr 2014	Basic Microscopy Course 'In the footsteps of Antoni van Leeuwenhoek', OOA, Amsterdam
6-10 Jan 2014	Replication stress and chromosomal instability, OOA, Amsterdam
Oct 2012	Experimental Oncology Course, NKI, Amsterdam

Seminars and workshops

2012-2018	NKI research club meeting (oral presentations)
2012-2018	Weekly division work discussion (oral presentations)
2012-2018	International NKI seminar (lunch with speakers)
9-11 Jan 2017	CCP4 Study Weekend 'From Crystal to Structure'; East Midlands Conference Centre; Nottingham, UK
1-2 June 2015	SYNchrotron and NEutron Workshop (Synew); Utrecht, NL
7-9 Jan 2015	CCP4 Study Weekend 'Advances in Experimental Phasing'; East Midlands Conference Centre; Nottingham, UK
3-5 Jan 2014	CCP4 Study Weekend 'Complementary Methods'; East Midlands Conference Centre; Nottingham, UK
24 Apr 2013	CCP4 MG tutorial; Amsterdam, NL
4-5 Jan 2013	CCP4 Study Weekend 'Molecular Replacements'; East Midlands Conference Centre; Nottingham, UK

(Inter)national conferences

- 5-6 Dec 2017 Chains 2017: NWO Chemical Sciences Conference; Veldhoven, NL
Oral presentation: USP7 activity mechanism
- 24-26 May 2017 3rd Instruct Biennial Structural Biology Meeting; Brno, CZ
- 22-24 May 2017 2nd Annual Users Meeting of iNEXT; Brno, CZ
Oral presentation: Probing USP7 mechanism of deubiquitination through p53
- 7-8 Dec 2016 Chains 2016: NWO Chemical Sciences Conference; Veldhoven, NL
- 31 Nov – 1 Oct 2015 Chains 2015: NWO Chemical Sciences Conference; Veldhoven, NL
Poster: "Partial structure of USP7 reveals regulatory element"
- 17-18 Nov 2014 Chains 2014: NWO Chemical Sciences Conference; Veldhoven, NL
Poster: Understanding USP7 activation
- 22-24 Oct 2014 Annual Graduate Student retreat; Renesse, NL
Oral presentation: USP7's activation mechanism through crystallography
- 23-25 Oct 2013 Annual Graduate Student retreat; Renesse, the Netherlands
Oral presentation: Activity mechanism of USP7 through FRET and crystallography
- 1-5 Oct 2013 EMBO Conference 'Ubiquitin and Ubiquitin-like Proteins: from structure to function', Astoria Park Hotel; Riva del Garda, IT
- 10-11 Dec 2012 NWO-CW Study Group Meeting 'Chemistry in Relation to Biology and Medical Sciences', NH Koningshof; Veldhoven, NL
Poster: Change is good? How conformational changes enhance USP7 function
- 17-19 Oct 2012 Annual Graduate Student retreat 'Inspiration in Ermelo'; Ermelo, NL
Poster: Change is good? How conformational changes enhance USP7 function
- 3-4 Sep 2012 Wim Hol Symposium, Trippenhuis (KNAW); Amsterdam, NL

2. Teaching

Student intern supervision

- Sep 2016 - Feb 2017 Supervised HBO student Philip van Doeselaar on a project of USP40
- Fall 2014 Supervised student Rik Poot on a 'teachers of science in science' project
- Feb-Jul 2013 Supervised bachelor student Sonja Brouwers on the project "Characterization of BRCC36 containing complexes"

Demonstrations

- 20-24 Nov 2017 Instructor at iNext Biophysical Characterisation course; Amsterdam, NL

Country codes refer to; CZ: Czech Republic; IT: Italy; NL: the Netherlands; UK: United Kingdom

Addendum. F. List of Publications

F. List of Publications

- Kim, R.Q.**, Geurink, P.P., Mulder, M.P.C., Fish, A., Ekkebus R., El Oualid, F., van Dijk, W.J., van Dalen, D., Ovaa, H., van Ingen H. and Sixma, T.K. Kinetic analysis of multistep USP7 mechanism shows critical role for target protein in activity. *Nature Communications* (*in press*). <https://doi.org/10.1038/s41467-018-08231-5>
- Kim, R.Q.** and Sixma, T.K. Regulation of USP7: A High Incidence of E3 Complexes. *Journal of Molecular Biology* 429 2017, 3395–408. <https://doi.org/10.1016/j.jmb.2017.05.028>
- Kim, R.Q.**, van Dijk, W.J. and Sixma, T.K. Structure of USP7 catalytic domain and three Ubl-domains reveals a connector α -helix with regulatory role. *Journal of Structural Biology* 195 2016, 11–8. <https://doi.org/10.1016/j.jsb.2016.05.005>
- Kim, R.Q.**, Offen, W.A., Davies, G.J. and Stubbs, K.A. Structural enzymology of *Helicobacter pylori* methylthioadenosine nucleosidase in the futasine pathway. *Acta Crystallographica Section D, Biological Crystallography* 70 2014, 177–85. <https://doi.org/10.1107/S1399004713026655>
- Hemsworth, G.R., Taylor, E.J., **Kim, R.Q.**, Gregory, R.C., Lewis, S.J., Turkenburg, J.P., Parkin, A., Davies, G.J. and Walton, P.H. The copper active site of CBM33 polysaccharide oxygenases. *Journal of the American Chemical Society* 135 2013, 6069–77. <https://doi.org/10.1021/ja402106e>
- Roy, S., Planken, K.L., **Kim, R.**, v. d. Mandele, D. and Kegel, W.K. Direct Evidence on the Existence of [Mo 132] Keplerate-Type Species in Aqueous Solution. *Inorganic Chemistry* 46 2007, 8469–71. <https://doi.org/10.1021/ic701076s>

G. Acknowledgements

All things come to an end, just like this thesis. Funnily, for theses, the ending gets read the most: does your name get mentioned? Scout for your name in bold, or read the whole bit with all acknowledged people (in no particular order).

First of all, **Titia**, thank you for your guidance during these six years of my PhD. Your thoroughness and drive really have shaped my scientific career and I'm pretty sure we will meet again.

Then to **Pim**, my other co-author on all the preceding chapters. None of this would be possible without your help, protein preps, motorcycle talk and your lab management!

I would also like to extend scientific acknowledgements to my other co-authors. **Sasha**, thank you for the training in all these biophysical techniques and your help in all the data modelling, I am pretty sure I will contact you again for advice in this! **Hugo**, your positive attitude is a real inspiration. Thank you for teaching me NMR and the best of luck back in Utrecht. **Paul**, **Monique**, **Farid** and **Huib**, thank you for this collaboration on USP7, where will the combination of chemistry and biochemistry take us next?

My paranympths, **Tatjana** and **Shreya**, thank you for standing by me during the defence, and all the other 'paranympthing'. **Tati**, the lab is a more happy and upbeat place with you, keep it up! **Shrey**, I thoroughly enjoyed our time inside and outside the lab (rap sessions, food, cricket, Warung Aji, Mumbai, food), keep going and you can write a similar piece very soon! This makes an easy bridge to my other office mates ('Oficina de Frustração'): **Luca**, **Nassos**, **Elisa**. Thank you for enjoying drop and tosti's just as much as I do and for the dinners shared at various foreign restaurants (these thanks also extend to **Mayuri**, **Martha**, Tati and **Andrea**). When selecting a new singer in the lab, my vote is still on Nassos ;-).

My other colleagues at the Sixma group; **Doreth**, **Susanne**, **Xiaohu**, **Roy** and **Yvette**, but also former members **Herrie**, **Michael**, **Flora**, **Danny**, **Judith**, **Francesca**, **Marcel**, **Marcello** and **Thanga**. Thank you all for making the lab environment the way it is, combining scientific discussion with the occasional drink, helping me survive these all-night synchrotron sessions or sharing a great part of our PhD-journey together.

These thanks I would also like to extend to our neighbours from the Perrakis group: **Tassos**, **Yoshi**, **Robbie**, **Bart**, **Willem-Jan**, **George**, **Fernando** and **Misbha**. It is great to have such neighbours to share the lab space with. **Patrick**, **Magda** and **John**, also known as the **Protein Facility**, thank you for showing everybody how protein purification really should be done. I will try and do my best to reach that level...

Addendum. G. Acknowledgements

Then the rest of our floor. Thank you Brummelkamp group (**Thijn, Lisa, Abdel, Markus, Lucas, Vincent, Joppe** and **Jacqueline**), for showing us cell biology and for our inter-group gossiping. Thanks **Mirna**, for taking care of all the packages and NKI bureaucracy. Thanks to the computer guys (**Torben** and **Ismail**) for still allowing me to touch the work stations.

Work luckily is more than just time in the lab. I would like to thank my former colleagues from the **borrelcommittee** for the countless borrels, the **NKI football** group for supplying me with at least some physical exercise and my fellow punk-connoisseurs **Torben, Markus, and Tiemen** for pulling me out of the pit when necessary. I may still have omitted some colleagues, so if you read this, thank you!

Special thanks go out to my friends outside of work. Thank you for putting life in perspective, your friendship and your support: **Thijs, Marjanne, Eva, Gruson, Aldo, Elze, Mark, Maartje, Tiemen, Winnie, Remi, Robin, Jan Peke, Elisa, Maarten, Zonne** and everybody I accidentally omitted here...

My thanks also extend to my family (in-law) for discussions about science and life in general. **Moeder, Pa, Patrick** en **Oma** dank voor jullie onvoorwaardelijke steun!

Finally, **Hedwich**, thank you for the wonderful cover around this book and all your support during its fabrication. Whether scientific or regarding everyday life, I value your help and I am looking forward to our future together.



